

Generating biomarkers of human Nek8 kinase activity

Thesis submitted for the degree of
Doctor of Philosophy
at the University of Leicester

by

Karolin Kroese BSc MSc (University of Leicester)
Department of Molecular and Cell Biology
University of Leicester

October 2017

Declaration

The accompanying thesis submitted for the degree of Doctor of Philosophy, entitled “Generating biomarkers of human Nek8 kinase activity” is based on work conducted by the author in the Department of Molecular and Cell Biology at the University of Leicester mainly during the period between April 2014 and October 2017. All work recorded in this thesis is original unless otherwise acknowledged in the text or by references. None of the work has been submitted for another degree in this or any other University.

Signed:

Date:

Department of Molecular and Cell Biology
University of Leicester
Lancaster Road
Leicester
LE1 9HN

Generating biomarkers of human Nek8 kinase activity

Karolin Kroese

ABSTRACT

Nek8 is a member of the human NIMA-related serine/threonine protein kinase family that has roles in cell cycle progression, primary cilia function and the DNA damage response. Mutations in the human *nek8* gene cause Nephronophthisis (NPHP), an autosomal recessive polycystic kidney disease in which defects in primary cilia lead to a broad range of often severe symptoms that affect many organs of the body. In the kidneys, NPHP causes the development of cortico-medullary cysts that impair kidney function and ultimately lead to kidney failure. Nek8 localises to the primary cilium where it interacts with Inversin and PC-2, products of genes that are also mutated in inherited cystic kidney diseases. Nek8 also plays a role in the intra-S phase DNA damage checkpoint where it contributes to cell cycle arrest by inhibiting CDK2 activity to allow time for repair of stalled replication forks. The purpose of this study was to generate novel biomarkers of Nek8 kinase activity that could be used to shed light on its role at the primary cilium and in the replication stress response. Our aim was therefore to identify phosphosites of Nek8 in its potential substrate proteins, Inversin and PC-2, and to generate phospho-specific antibodies against these sites. We chose three sites in the Inversin N-terminus for phospho-specific antibody generation and showed that these were capable of detecting purified, phosphorylated Inversin upon incubation with Nek8. Second, we characterised a phospho-Nek8 antibody that recognises a phosphorylation site in the activation loop of the kinase. This antibody was capable of detecting auto-phosphorylated Nek8 by Western blot and immunofluorescence microscopy as confirmed using two, newly identified chemical inhibitors of Nek8. Localisation studies with this antibody revealed novel data on the presence of active Nek8 at centrosomes, cilia and sites of DNA damage. Finally, we found that Nek8 inhibition was associated with generation of enlarged multinucleated cells and accumulation of DNA damage foci. Together, these data support a role for Nek8 in linking ciliary signalling pathways and the DNA damage response, while the phospho-specific antibodies represent a new set of tools that can be used to explore Nek8 function in normal and pathological states.

Acknowledgements

I would like to start by saying a huge thank you to my supervisor, Professor Andrew Fry, for giving me this unique opportunity. Andrew is one of the most knowledgeable people I have ever met and a real expert in his field. Thank you for your support and guidance that have made this PhD become a reality. Many thanks also to my second supervisor, Dr Sue Shackleton, and my committee members, Dr Steven Foster and Professor Richard Bayliss, for helpful ideas and interesting discussions throughout my PhD.

Next, I would like to thank all past and present members of the Fry lab for a great work environment. Especially Josephina, Jess, Sarah, Tammy and Rozi for endless discussions and support through the ups and downs of this PhD. The past 3.5 years would not have been the same without your friendship and I am grateful for having had you around.

To Mattia, thank you for the endless hours of listening to me going on and on about this PhD and the constant encouragement and positive reinforcement. You kept me sane throughout the last 6 months of this journey!

Last but not least, I would like to thank my family and friends for their encouragement and support! In particular, I would like to thank my Mum for always lending me an open ear and believing in me even when I started to doubt myself. Mama, wie du immer sagst, es wird sich alles finden! Special thanks also to my Dad, who is no longer with us, for opening so many doors for me and supporting each and every decision without questioning it, as well as to my brother, Fabian, who I can count on no matter what. I would have not made it to where I am now without you and am more than grateful to have such an amazing family around me!

Statement of contributions

All the experiments were performed by myself in the Fry laboratory, if not otherwise stated. Throughout this thesis, we worked closely with the Bayliss laboratory at the University of Leicester. Prof Richard Bayliss was my second supervisor until his lab moved to Leeds in 2016.

1. Generation of Inversin and Nek8 constructs

The cloning, sequencing and mutagenesis primers for the used Inversin and Nek8 constructs for cell studies and protein purifications were designed by myself. However, the primers were then generated by Eurofins Genomics and delivered to us in lyophilised form. Once the primers were received, I diluted them in the appropriate amount of dH₂O and submitted these as well as a DNA sample for Nek8 or Inversin to the University of Leicester's PROTEX facilities to undertake cloning into the appropriate vectors or mutagenesis for me. PROTEX provided me with bacteria colonies of the constructs, which I used to miniprep and maxiprep the plasmid DNA from that was then used for all further experiments.

2. Expression and purification of the Nek8 and Inversin proteins

The purified, active Nek8 kinase for the kinase assays was provided by the Bayliss laboratory.

The His-Inversin 1-553 protein was designed, expressed and purified by myself. After several unsuccessful attempts in purifying also the C-terminal Inversin proteins, the GST-Inversin 554-1065, GST-Inversin 899-1065 and GST-Inversin 950-1065 proteins were expressed and purified by Sophie Millett in the Bayliss laboratory at the University of Leicester. We provided DNA samples of the cloned plasmid DNA of these constructs, as well as a full-length genomic DNA sample for Inversin. Sophie Millett was successful in expressing the above-mentioned proteins from newly cloned constructs using our genomic DNA and provided me with proteins bound to beads to perform further experiments.

3. Phosphomapping

Samples from kinase assays were submitted to the University of Leicester's Proteomics facilities, where MALDI-ToF-ToF analysis was performed to map individual phospho-sites on the Inversin proteins.

4. Generating phosho-Inversin antibodies

The sequences for the phospho-Inversin antibodies were designed by myself after knowing the location of the Nek8 phospho-sites along the Inversin protein. The amino acid sequence was then submitted to Amsbio for generation of the antigens and production of the antibodies in rabbits. Amsbio provided us with two batches of lyophilised phospho-specific and non-phospho-specific antibodies.

5. Generation of the RPE1 CRISPR cell line for Nek8

Koji Kobayashi from Prof Kouji Hirota's research group at Tokyo Metropolitan University spent three months with us in Leicester to generate an RPE1 CRISPR cell line for Nek8. Under my supervision, Koji learnt how to use the cell culture facilities and how to look after RPE1 cells. He then generated the CRISPR cell line using the vectors and transfection reagents he brought with him from Tokyo. After generating a KO cell line, he performed an initial growth curve assay comparing proliferation rates of Nek8 WT and KO cells. He further stained these cells with antibodies against the proliferation marker Ki67. Analysis of the percentages of Ki67 positive cells in two independent experiments using the confocal microscope was performed by myself. Also, the PCR to investigate the knockdown of Nek8 was performed by myself, using Koji Kobayashi's primers.

6. Reagents that were supplied by other research groups

The PC-2 protein was provided by Prof Albert Ong.

The custom made pNek8 antibody and the two commercial Nek8 inhibitors, CCT32 and CCT90, were provided by Prof Richard Bayliss and his research group.

Contents

| | |
|---|------|
| Declaration..... | ii |
| Abstract..... | iii |
| Acknowledgements | iv |
| Statement of contributions | v |
| List of Abbreviations | xiii |
| Table of Figures..... | 0 |
| Table of Tables | 2 |
| CHAPTER 1 INTRODUCTION | 3 |
| 1.1. The eukaryotic cell cycle | 3 |
| 1.1.1 Cell cycle checkpoints | 5 |
| 1.1.2 The centrosome cycle | 8 |
| 1.1.3 The DNA damage response | 8 |
| 1.1.3.1 Causes of DNA damage..... | 10 |
| 1.1.3.2 The DNA damage signalling cascades..... | 12 |
| 1.1.3.3 DNA repair pathways..... | 12 |
| 1.1.3.4 Replication stress response | 13 |
| 1.1.3.4.1 Causes of replication stress | 14 |
| 1.1.3.4.2 Replication stress signalling..... | 15 |
| 1.2. Cilia..... | 17 |
| 1.2.1 Ciliogenesis and cilia structure | 17 |
| 1.2.2 The importance of the primary cilium | 19 |
| 1.3. Ciliopathies..... | 21 |
| 1.3.1 Polycystic kidney disease | 21 |
| 1.3.1.1 Nephronophthisis | 23 |
| 1.3.2 Signalling defects as a cause of ciliopathies | 25 |

| | |
|---|----|
| 1.3.2.1 The hedgehog pathway | 25 |
| 1.3.2.2 The canonical and non-canonical Wnt in ciliopathies | 27 |
| 1.4. NPHP9/Nek8 | 29 |
| 1.4.1 The NIMA-related kinase family | 31 |
| 1.4.2 Nek8 in polycystic kidney disease..... | 33 |
| 1.4.3 Nek8 and the DNA damage response..... | 36 |
| 1.5. Aims and objectives | 39 |
| CHAPTER 2 MATERIALS AND METHODS..... | 40 |
| 2.1 Materials | 40 |
| 2.1.1 Chemical suppliers | 40 |
| 2.1.2 Mammalian and bacterial constructs | 41 |
| 2.1.3 Oligonucleotides | 41 |
| 2.1.3.1 Cloning primers for Inversin and Nek8 constructs | 41 |
| 2.1.3.2 Mutagenesis primers for HA-Inversin..... | 42 |
| 2.1.3.3 PCR primers for genomic DNA amplification..... | 43 |
| 2.1.3.4 GuideRNAs | 43 |
| 2.1.3.5 siRNAs | 43 |
| 2.1.4 Antibodies..... | 43 |
| 2.1.4.1 Primary antibodies..... | 43 |
| 2.1.4.2 Phospho-Inversin antibodies | 44 |
| 2.1.4.3 Secondary antibodies | 45 |
| 2.1.5 Cell lines | 46 |
| 2.1.6 Radioisotopes..... | 47 |
| 2.1.7 Kinases | 47 |
| 2.1.8 Small molecule inhibitors | 47 |
| 2.2 Methods..... | 48 |

| | |
|--|----|
| 2.2.1 Molecular biology | 48 |
| 2.2.1.1 Plasmid construction | 48 |
| 2.2.1.2 Transformation of plasmid DNA into bacteria | 48 |
| 2.2.1.3 Generation of plasmid DNA by Maxiprep..... | 49 |
| 2.2.1.4 Sequencing of plasmid DNA..... | 49 |
| 2.2.1.5 Site-directed mutagenesis | 49 |
| 2.2.2 Cell biology techniques | 50 |
| 2.2.2.1 Maintenance of cell lines..... | 50 |
| 2.2.2.2 Long term storage of cell line stocks | 50 |
| 2.2.2.3 Serum starvation of cells | 51 |
| 2.2.2.4 Transient transfection of mammalian cells | 51 |
| 2.2.2.5 Transient transfection of siRNA oligonucleotides | 51 |
| 2.2.2.6 Drug treatments of cells | 52 |
| 2.2.2.7 Immunofluorescence microscopy | 52 |
| 2.2.2.8 Proximity ligation assay | 52 |
| 2.2.2.9 3D cell culture | 53 |
| 2.2.2.10 Flow cytometry | 54 |
| 2.2.2.11 Generation of a CRISPR cell line | 55 |
| 2.2.2.12 qRT-PCR and agarose gel electrophoresis | 55 |
| 2.2.2.13 Cell proliferation curve | 57 |
| 2.2.3 Biochemistry techniques | 58 |
| 2.2.3.1 Preparation of cell lysates | 58 |
| 2.2.3.2 BCA protein assay | 58 |
| 2.2.3.3 SDS-PAGE | 58 |
| 2.2.3.4 Coomassie Blue staining | 59 |
| 2.2.3.5 Western blotting..... | 59 |

| | |
|--|----|
| 2.2.3.6 Immunoprecipitation from cell lysates..... | 60 |
| 2.2.3.7 In vitro translation and pulldown assay | 60 |
| 2.2.3.8 Purification of the His-Inversin 1-553 protein | 61 |
| 2.2.3.9 Expression and purification of the GST-Inversin proteins | 62 |
| 2.2.3.10 In vitro kinase assays | 63 |
| 2.2.3.11 Phosphosite mapping | 64 |
| 2.2.3.12 Generation of phospho-specific antibodies | 64 |
| CHAPTER 3 NEK8 AND INVERSIN CONTAIN MULTIPLE SITES OF INTERACTION | 65 |
| 3.1 Introduction | 65 |
| 3.2 Results..... | 67 |
| 3.2.1 RPE1 cells exit the cell cycle upon serum starvation in media containing 0% FBS..... | 67 |
| 3.2.2 Inversin localises to cilia in 2D and 3D cell models | 67 |
| 3.2.3 Generation of mammalian Inversin and Nek8 constructs..... | 70 |
| 3.2.4 Inversin localises to centrosomes through its C-terminal domain..... | 73 |
| 3.2.5 Co-immunoprecipitation studies of Inversin fragments with Nek8 suggests multiple sites of interaction..... | 73 |
| 3.3 Discussion | 82 |
| 3.3.1 Subcellular localisation of Nek8 and Inversin..... | 82 |
| 3.3.2 Interaction studies of Nek8 with Inversin..... | 83 |
| CHAPTER 4 THE CILIARY POLYCYSTIC KIDNEY DISEASE PROTEINS, INVERSIN AND PC-2, ARE SUBSTRATES FOR NEK8 KINASE ACTIVITY | 87 |
| 4.1 Introduction | 87 |
| 4.2 Results..... | 89 |
| 4.2.1 Purification of Nek8 and Inversin proteins for in vitro kinase assays | 89 |
| 4.2.2 Identification of multiple sites of Nek8 phosphorylation in Inversin | 93 |

| | |
|--|-----|
| 4.2.3 Generation of phospho-Inversin antibodies..... | 99 |
| stream of the phosphorylated Threonine or Serine. Hydrophilic amino acids are shown in blue, neutral amino acids in green, and hydrophobic amino acids in black, with the most common amino acid indicated at the top. | 102 |
| 4.2.4 Characterisation of phospho-Inversin antibodies by Western blot | 102 |
| 4.2.5 Characterisation of phospho-Inversin antibodies by immunofluorescence microscopy..... | 105 |
| 4.2.6 Validation of Inversin siRNA oligonucleotides..... | 106 |
| mice. In summary, to use the Inversin siRNA as a reliable approach to validate the Inversin antibodies, further conditions have to be tested. | 109 |
| 4.2.7 Generation of Inversin mutants..... | 109 |
| 4.2.8 The PC-2 C-terminus is a substrate for Nek8 kinase activity in vitro..... | 109 |
| 4.3 Discussion | 114 |
| 4.3.1 Inversin as a substrate for Nek8 kinase activity | 114 |
| 4.3.2 PC-2 is a substrate for Nek8 kinase activity..... | 116 |
| CHAPTER 5 THE pNEK8 ANTIBODY AS A BIOMARKER FOR NEK8 ACTIVITY IN CELL CYCLE PROGRESSION, THE DNA DAMAGE RESPONSE AND CILIOGENESIS | 119 |
| 5.1 Introduction | 119 |
| 5.2 Results..... | 120 |
| 5.2.1 The pNek8 antibody detects active Nek8 kinase domain protein..... | 120 |
| 5.2.2 CCT32 and CCT90 inhibit Nek8 kinase activity in vitro | 120 |
| buffer. Analysis with the Inv-pT359 antibody showed strong phosphorylation of Inversin by both kinases that was reduced upon treatment with either CCT32 or CCT90. This reduction was more pronounced for the CCT32 inhibitor than the CCT90 inhibitor, especially for the in-house kinase, although both blocked sufficient phosphorylation of the substrate by Nek8. Hence, taken together these data show that both compounds are good inhibitors of Nek8 kinase activity in vitro..... | 126 |
| 5.2.3 Localisation of active Nek8 throughout the cell cycle | 126 |

| | |
|--|-----|
| 5.2.4 Localisation of active Nek8 to sites of DNA damage | 126 |
| 5.2.5 Consequences of Nek8 inhibition on cell cycle progression, ciliogenesis and DNA damage | 130 |
| 5.2.6 Generation of a gene-edited Nek8 knockout cell lines | 135 |
| 5.3 Discussion | 143 |
| 5.3.1 Validating the pNek8 antibody | 143 |
| 5.3.2 Investigation of Nek8's role in the cell | 143 |
| CHAPTER 6 DISCUSSION..... | 146 |
| 6.1 Identifying biomarkers of Nek8 kinase activity | 146 |
| 6.1.1 Designing Inversin phospho-antibodies as biomarkers of Nek8 kinase activity | 146 |
| 6.1.2 Investigating PC-2 as a substrate for Nek8 kinase activity | 147 |
| 6.1.3 Validation of the pNek8 antibody as a biomarker of Nek8 kinase activity . | 148 |
| 6.2 Analysis of the role of Nek8 in the cell | 149 |
| 6.2.1 A role for Nek8 at the primary cilium | 149 |
| 6.2.2 A role for Nek8 in cell cycle progression | 150 |
| 6.3 A model for the role of Nek8 in the cell | 151 |
| 6.4 Concluding remarks | 152 |
| CHAPTER 7 BIBLIOGRAPHY | 155 |

List of Abbreviations

| | |
|--------------|--------------------------------------|
| 3D | three-dimensional |
| μg | microgram |
| μl | microlitre |
| μM | micromolar |
| a | alanine |
| aa | amino acid |
| ab | antibody |
| AD | autosomal dominant |
| AR | autosomal recessive |
| ATM | ataxia-telangiectasia mutated |
| ATP | adenosine triphosphate |
| ATR | ATM- and Rad3-related |
| BSA | bovine serum albumin |
| APC/C | anaphase promoting complex/cyclosome |
| BER | base-excision repair |
| bim | blocked in mitosis |
| C- | carboxy- |
| CDK | cyclin-dependent kinase |
| cDNA | complementary deoxyribonucleic acid |
| CHK | checkpoint kinase |
| CKI | cyclin-dependent kinase inhibitor |
| cm | centimetre |
| CV | ciliary vesicle |
| ds | double strand |
| DBS | double strand breaks |
| DMEM | Dulbecco's modified eagle medium |
| DMSO | dimethylsulfoxide |
| DNA | deoxyribonucleic acid |
| DDR | DNA damage response |
| Dvl | Dishevelled |
| E | glutamic acid |
| ESRD | end stage renal disease |
| ESRF | end stage renal failure |

| | |
|-------------|---|
| FL | full-length |
| FBS | fetal bovine serum |
| G0 | quiescence |
| G1/G2-phase | growth phase 1/2 |
| h | hour |
| HR | homologous repair |
| IF | immunofluorescence microscopy |
| IFT | intraflagellar transport |
| IVT | <i>in vitro</i> translation |
| <i>jck</i> | juvenile cystic kidney |
| kDa | kilo Dalton |
| KO | knockout |
| L | litre |
| M | molar |
| mg | milligram |
| min | minute/s |
| ml | millilitre |
| mM | millimolar |
| ng | nanogram |
| nM | nanomolar |
| M-phase | mitosis |
| N- | amino- |
| NER | nucleotide-excision repair |
| NHEJ | non-homologous end joining |
| NIMA | never in mitosis gene A |
| NLS | nuclear localisation sequence |
| NPHP | Nephronophthisis |
| NTP | nucleotide triphosphate |
| PC-1/2 | Polycystin 1/2 |
| PCP | planar cell polarity |
| PCR | polymerase chain reaction |
| PKD | polycystic kidney disease |
| PKHD1 | polycystic kidney and hepatic disease 1 |
| PLK | Polo-like kinase |

| | |
|----------|---|
| qRT | quantitative real time |
| R | restriction checkpoint |
| Rb | Retinoblastoma |
| RCC1 | regulator of chromatin condensation |
| RNA | ribonucleic acid |
| ROS | reactive oxygen species |
| S | serine |
| SAP | spindle assembly checkpoint |
| SDS-PAGE | sodium dodecyl sulphate- polyacrylamide gel electrophoresis |
| sec | seconds |
| siRNA | small interfering ribonucleic acid |
| S-phase | synthesis phase |
| ss | single strand |
| SSB | single strand breaks |
| T | threonine |
| TF | transition fibres |
| TRP | transient receptor potential |
| TZ | transition zone |
| v/v | volume per volume ratio |
| WB | Western blot |
| WT | wildtype |
| w/v | weight per volume ratio |

Table of Figures

| | |
|---|----|
| Figure 1.1: The eukaryotic cell cycle | 4 |
| Figure 1.2: Regulation of cell cycle progression | 7 |
| Figure 1.3 The centrosome cycle | 9 |
| Figure 1.3: The DNA damage response | 11 |
| Figure 1.4: Replication stress signalling..... | 16 |
| Figure 1.5 Ciliogenesis | 18 |
| Figure 1.6 Cilia structure..... | 20 |
| Figure 1.7 Clinical phenotype of NPHP | 22 |
| Figure 1.8 Interaction of ciliopathy proteins at the cilia | 26 |
| Figure 1.9 The canonical and non-canonical Wnt pathway in the kidney tubules..... | 28 |
| Figure 1.10 A role for non-canonical Wnt signalling in preventing polycystic kidney disease | 30 |
| Figure 1.11 Domain organisation of the human Nek kinases..... | 32 |
| Figure 1.12 Nek kinase functions through the cell cycle | 35 |
| Figure 1.13 A role for Nek8 in coordinating ciliary signalling with DDR control | 38 |
| Figure 2.1 Schematic of the insertion of resistance markers into the CRISPR gene locus | 56 |
| Figure 3.1 RPE1 cells exit the cell cycle upon 48 h serum starvation..... | 68 |
| Figure 3.2 Inversin localises with acetylated tubulin in dividing HeLa and quiescent RPE1 cells | 69 |
| Figure 3.3 Inversin localises to cilia in serum starved IMCD3 spheroids..... | 71 |
| Figure 3.4 Schematic of Nek8 and Inversin constructs used to examine subcellular localisation and interaction | 72 |
| Figure 3.5 The Inversin C-terminus harbours a centrosome-targeting motif | 74 |
| Figure 3.6 Nek8 constructs localise predominantly in the cytoplasm in cycling RPE1 cells | 75 |

| | |
|---|-----|
| Figure 3.7 Nek8 interacts with the N-terminus of Inversin in serum starved RPE1 cells | 77 |
| Figure 3.8 Nek8 interacts with the C-terminus of Inversin in HEK293T cells | 78 |
| Figure 3.9 <i>In vitro</i> translated Nek8 interacts predominantly with the Inversin N-terminus | 80 |
| Figure 3.10 HA-Inversin interacts with the catalytic and non-catalytic domain of Nek8 | 81 |
| Figure 3.11 Model of Nek8 and Inversin interaction | 86 |
| Figure 4.1 Generation of active Nek8 kinase | 91 |
| Figure 4.2 Schematic of Inversin constructs used for phosphorylation assays | 92 |
| Figure 4.3 Purification of GST-tagged Inversin C-terminal constructs | 94 |
| Figure 4.4 Purification of the N-terminal His-Inversin 1-553 protein | 95 |
| Figure 4.5 Inversin is a substrate for Nek8 <i>in vitro</i> | 96 |
| Figure 4.6 Time course of phosphorylation of the Inversin N-terminus by Nek8 | 98 |
| Figure 4.7 Identification of Nek8 phosphorylation sites in the Inversin protein | 100 |
| Figure 4.8 Peptide design for generation of Inversin phosphoantibodies | 101 |
| Figure 4.9 Validation of Inversin phosphoantibodies on purified Inversin proteins.... | 103 |
| Figure 4.10 Analysis of Inversin antibodies by Western blot of transfected cell lysates | 104 |
| Figure 4.11 Analysis of Inversin antibodies by immunofluorescence microscopy of RPE1 cells | 107 |
| Figure 4.12 Analysis of Inversin phosphoantibodies by immunofluorescence microscopy | 108 |
| Figure 4.13 Validation of Inversin siRNA oligonucleotides in cells | 111 |
| Figure 4.14 Generation of disease and phosphorylation site mutants of Inversin | 112 |
| Figure 4.15 The PC-2 C-terminus is a substrate for Nek8 <i>in vitro</i> | 113 |
| Figure 5.1 Validation of pNek8 antibodies using <i>in vitro</i> kinase assays | 121 |
| Figure 5.2 Small molecule inhibitors of Nek8 | 123 |

| | |
|--|-----|
| Figure 5.3 Chemical inhibition of Nek8 kinase activity..... | 124 |
| Figure 5.4 Validation of CCT32 and CCT90 as chemical inhibitors of Nek8..... | 125 |
| Figure 5.5 Active Nek8 localises to centrosomes, spindle poles and the midbody in cycling RPE1 cells | 127 |
| Figure 5.6 Active Nek8 localises to the basal body in serum starved RPE1 cells | 128 |
| Figure 5.7 Active Nek8 localises to sites of DNA damage..... | 129 |
| Figure 5.8 PLA assay reveals close association of active Nek8 with γ H2AX foci | 132 |
| Figure 5.9 CCT90 treatment inhibits Nek8 kinase activity..... | 133 |
| Figure 5.10 CCT90 treatment does not affect ciliogenesis..... | 134 |
| Figure 5.11 CCT90 treatment causes formation of multinucleated cells..... | 136 |
| Figure 5.12 CCT32 treatment causes multinucleated cells with supernumerary centrosomes | 137 |
| Figure 5.13 CCT90 treatment reduces proliferation in RPE1 cells..... | 138 |
| Figure 5.14 CCT90 treatment leads to enlarged DNA damage foci in RPE1 cells..... | 140 |
| Figure 5.15 Attempting to generate RPE1 KO cells by gene editing | 141 |
| Figure 5.16 Growth studies on gene-edited RPE1 Nek8 KO cells..... | 142 |

Table of Tables

| | |
|---|-----|
| Table 1.1 Summary of NPHP disease genes and proteins | 24 |
| Table 1.2 Summary of Nek kinases and their associated human diseases | 34 |
| Table 4.1 A summary of the activity of the phospho-specific and non-phospho-specific Inversin antibodies..... | 118 |

CHAPTER 1 INTRODUCTION

1.1. The eukaryotic cell cycle

The cell cycle is a tightly regulated series of conserved events responsible for the error-free duplication and distribution of genetic material from one cell generation to the next. In eukaryotic cells, the cell cycle is divided into two main phases, mitosis and interphase, with the latter consisting of the S-phase for DNA replication, where the genetic content of the cell is duplicated, sandwiched between two growth phases (G1 and G2), where cells obtain mass, integrate growth signals and prepare for cell division. During G1 phase, the cell can also exit the cell cycle if growth factors or nutrients are not sufficient for the cell to divide further, and enter quiescence (G0 phase), where it remains in a dormant state until re-entering the cell cycle.

Mitosis is the separation of the chromosomes into the two daughter cells and is followed by cytokinesis, which is the physical division of those two cells. Mitosis consists of five phases: prophase, prometaphase, metaphase, anaphase, and telophase (Fig. 1.1). In prophase, the DNA condenses so that individual chromosomes can be separated and centrosomes migrate to opposite sides of the nucleus ready to form the mitotic spindle (Salaun et al., 2008). In prometaphase, the nuclear envelope is broken down and the kinetochores of each chromosome pair attach to microtubules of the mitotic spindle. In metaphase, all chromosomes are aligned along the metaphase plate in the centre of the cell, before the separation of the sister chromatids towards the two opposite poles of the spindle in anaphase. This leads to the creation of two identical gene pools, which are then enclosed in two newly formed nuclear envelopes in telophase (Nigg, 2001). Finally, the cytoplasm is physically separated during cytokinesis by formation of a contractile ring of myosin and actin, which constricts the plasma membrane to the point of abscission when two identical daughter cells are generated (Salaun et al., 2008).

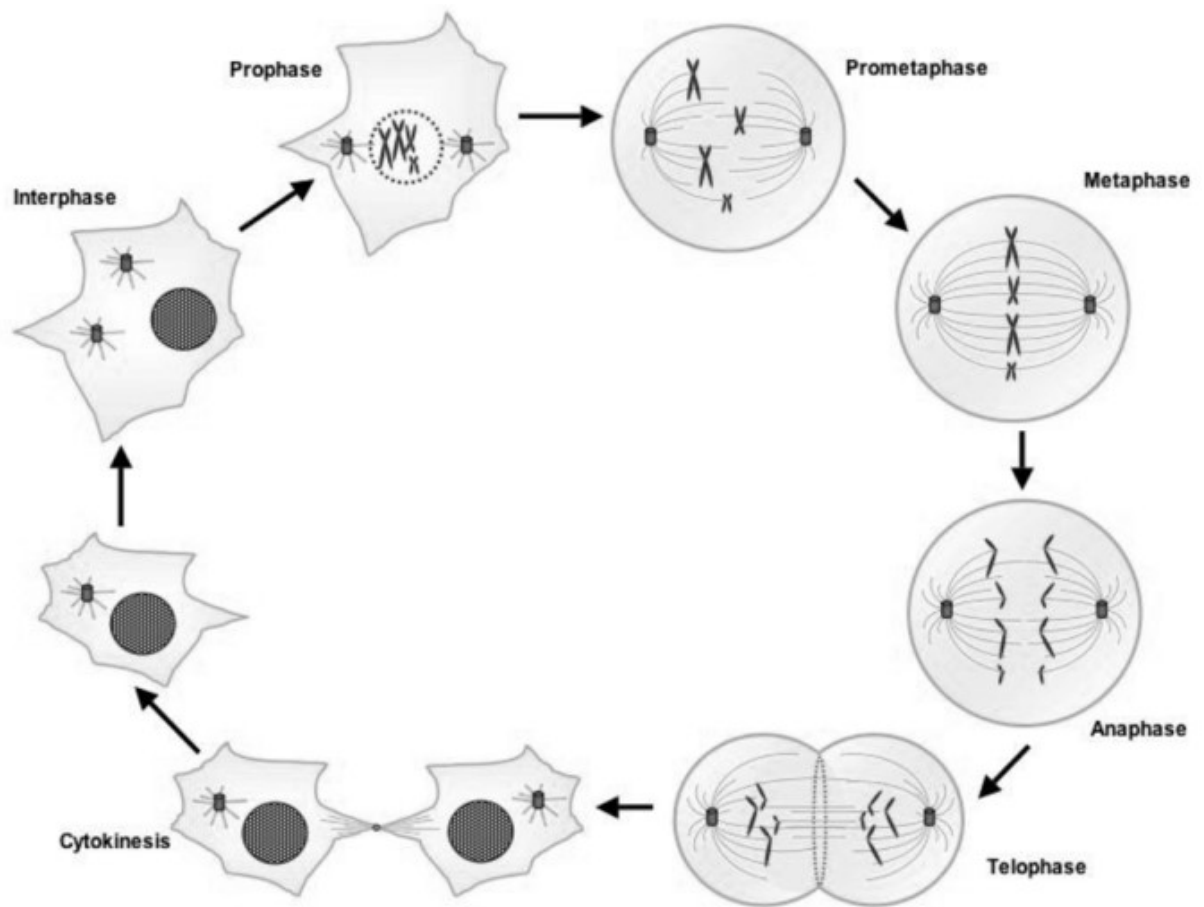


Figure 1.1: The eukaryotic cell cycle

The eukaryotic cell cycle is divided into interphase and mitosis. Mitosis consists of prophase, prometaphase, metaphase, anaphase, telophase and cytokinesis and leads to the separation of the duplicated DNA into two newly formed daughter cells. In prophase, chromosomes condense and the nuclear envelope disintegrates, in prometaphase, spindle microtubule form from the two spindle poles and chromosomes attach, in metaphase, chromosomes are aligned along the metaphase plate, and sister chromatids will be separated in anaphase. In telophase, a contractile ring divides the mother cell into two newly formed daughter cells with physical restriction during cytokinesis (taken from Salaun et al., 2008).

1.1.1 Cell cycle checkpoints

Progression through the cell cycle is under tight control of a complex network of signalling pathways that guarantees the accurate duplication and separation of the genetic material into two identical daughter cells. Eukaryotes have developed four major cell cycle checkpoints where the cell acts upon internal and external stimuli and stops progression if necessary. This prevents uncontrolled cell division and the accumulation of genetic damage and therefore maintains genome stability and avoids the development of diseases such as cancer.

These checkpoints are tightly regulated through the cyclin-dependent kinases (CDKs), a serine/threonine kinase family that phosphorylates its substrates to promote cell cycle progression (Barnum and O'Connell, 2014). Humans express more than 21 CDK proteins, of which only CDK1, CDK2, CDK4 and CDK6 have been described to play an essential role in cell cycle progression. All four are expressed throughout the entire cell cycle, but only become catalytically active upon heterodimerisation with specific members of the cyclin protein family (Connell-Crowley et al., 1993). As their name indicates, cyclins are expressed and degraded in a cyclic manner at different stages of the cell cycle, which in turn allows control over which CDK kinase is active. Additional to this regulation, CDKs are also negatively regulated by binding to inhibitory proteins, the so-called cyclin dependent kinase inhibitors (CKIs).

The first checkpoint, known as the restriction checkpoint (R), is located at the end of G1 phase and allows for scanning of resources needed in S-phase, such as sufficient nutrients and growth factors. The cell then decides to either commit to mitosis or to enter quiescence. In order to proceed through the cell cycle in G1 phase, Cyclin D is expressed and forms a heterodimer with CDK4 and CDK6. These active complexes then phosphorylate the tumour suppressor protein, Retinoblastoma (Rb), which, in its unphosphorylated state, inhibits the transcription of cell cycle progression favouring genes by binding to transcription factors like HDACs, chromatin remodelling factors and E2F family members. The release of E2F transcription factors leads to an increase in Cyclin E expression, which forms a complex with CDK2, needed for late G1 progression

and initiation of DNA replication in S-phase (Malumbres and Barbacid, 2005). During S-phase, Cyclin E is rapidly degraded to prevent initiation of excessive DNA replication, and Cyclin A expression gets activated. The CDK2/Cyclin A complex then phosphorylates various proteins involved in S-phase progression (Hwang and Clurman, 2005). The second checkpoint is located mid S-phase and scans for stalled replication forks during DNA synthesis to guarantee that all genetic material is copied properly before proceeding into G2-phase. Once the cell has transitioned into G2-phase, Cyclin A expression leads to its binding of CDK1. However, this complex remains inactive by being phosphorylated at certain residues of CDK1 until the G2/M checkpoint has been passed, where the cell assesses if DNA replication has been completed and resolves all DNA damage. If this is the case, Cdc25A phosphatases remove the inhibitory phosphorylation on CDK1 and progression into mitosis is initiated. The fourth checkpoint is located at the metaphase to anaphase transition, where spindle assembly is assessed (spindle assembly checkpoint) and progression into anaphase is inhibited, if kinetochores are not correctly attached to spindle microtubule. Thus, ensuring prevention of aneuploidy and genetic instability. Upon checkpoint activation, the APC/C (anaphase-promoting complex/cyclosome) remains in an inactive state, resulting in Cyclin B abundance in the cell and arrests the cell in early mitosis until all chromosomes are attached properly. Once APC/C gets activated, Cyclin B levels in the cell increase and Cyclin A gets replaced in the heterodimer with CDK1 to favour progression through mitosis (Davis et al., 2013; Bertoli et al., 2013; Lim and Kaldis, 2013). A summary of this is shown in Figure 1.2.

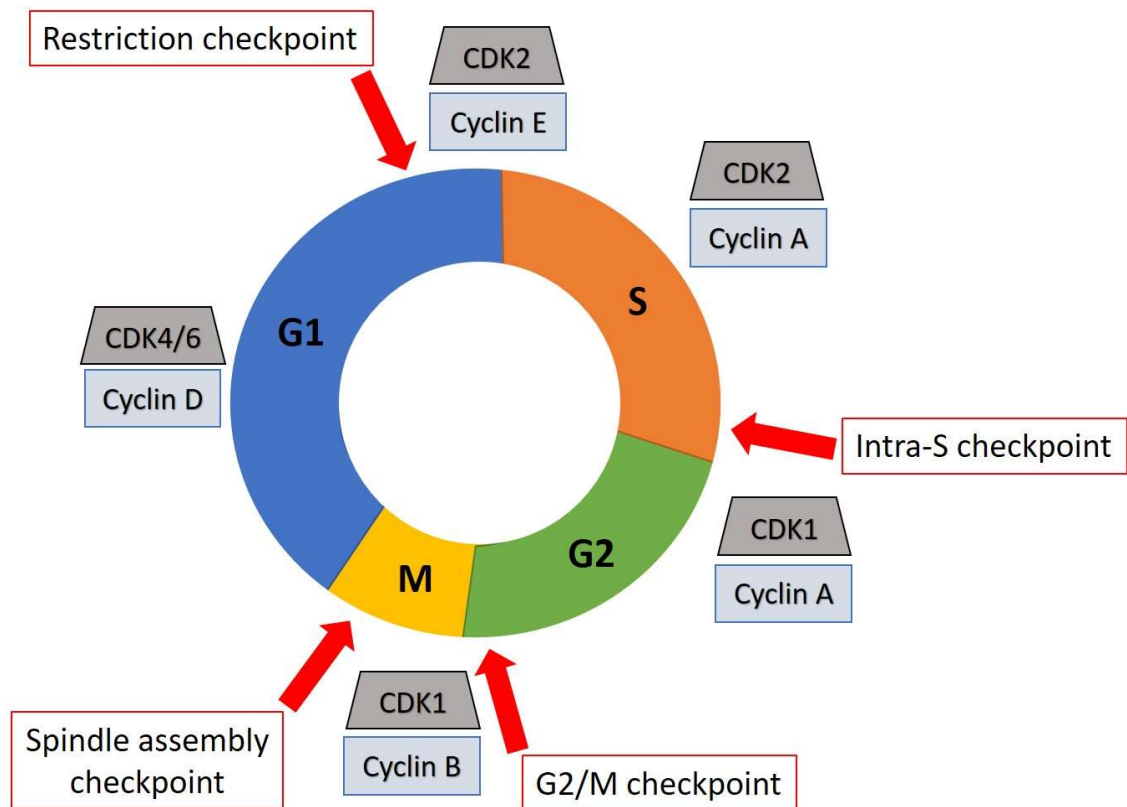


Figure 1.2: Regulation of cell cycle progression

Heterodimers of CDKs and their activating Cyclin counterparts tightly regulate and promote cell cycle progression. Also shown are the four eukaryotic cell cycle checkpoints in G1 phase (Restriction point), intra-S phase as a DNA damage checkpoint, at the transition from G2- to M-phase, and between metaphase and anaphase in mitosis (spindle assembly checkpoint).

1.1.2 The centrosome cycle

The centrosome plays a key role in the cell cycle as it acts as the primary microtubule organising centre in most eukaryotic cells. As such it has a major role in mitotic spindle assembly and ciliogenesis (Debec et al., 2010). The centrosome consists of two centrioles, each built of nine microtubule triplets in a 9-fold symmetry (Fig. 1.3A) (Bettencourt-Dias and Glover, 2007; Bornens, 2002). Centrosomes are surrounded by the so-called PCM (pericentriolar material), a distinct set of proteins involved in microtubule nucleation and anchoring. The centrosome duplication cycle is tightly coupled to the progression of the cell cycle and consists of four consecutive steps: centriole disengagement, nucleation of the daughter centrioles, or so-called procentrioles, elongation of the procentrioles, and separation of the centrosomes (Fig. 1.3B) (Bettencourt-Dias and Glover, 2007).

Newly formed cells that have just exited mitosis have two centrioles, that are connected on their proximal ends through a tether of filamentous protein, the so-called inter-centriolar linker. Centriolar disengagement appears in G1 phase with the centrioles still remaining loosely connected by the inter-centriolar linker. The duplication of each centriole is tightly linked to DNA replication and is initiated by the CDK2/Cyclin E complex. The Polo-like kinase 4 (PLK4) then promotes centrosome duplication by recruiting and phosphorylating a number of substrates, including SAS-6, a core regulator of this pathway (Fong et al., 2014). Centriole maturation during G2 phase is initiated by the Aurora A kinase via Plk-1. Once the daughter centrioles have grown to full size at the G2/M transition, the inter-centriolar linker is disrupted by Nek2 and phosphorylation of its downstream substrates, the linker components C-Nap1 and rootletin (Fry et al., 2012; Bahe et al., 2005; Faragher and Fry, 2003; Fry et al., 1998; Yang et al., 2006). The two centrosomes then migrate to opposite sides of the cell and act as spindle poles for the emerging bipolar spindle (Fu et al., 2015).

1.1.3 The DNA damage response

The role of the DNA damage response (DDR) is to detect, mediate and erase DNA lesions

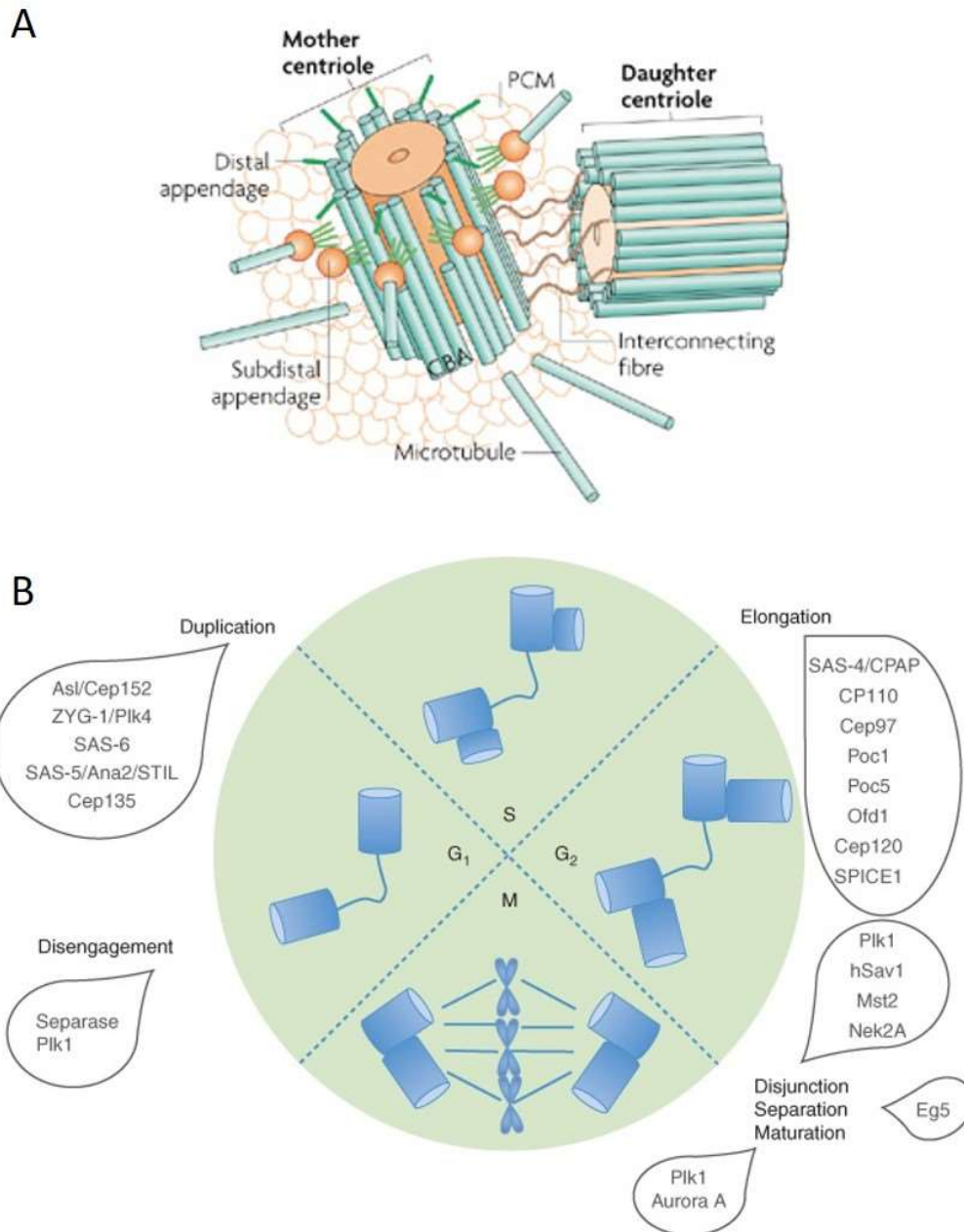


Figure 1.3 The centrosome cycle

A. Structure of the mother and daughter centriole connected by fibres. Both consist of nine microtubule triplets and are surrounded by the PCM. The mother centriole exhibits a distinct set of distal and subdistal appendages (modified from Bettencourt-Dias and Glover, 2007). **B.** The centrosome cycle is divided into four stages of disengagement of the tightly bound centrioles in G₁ phase, duplication of the mature centrioles and nucleation of the newly formed procentrioles in S-phase, elongation of the procentrioles during G₂ phase and finally, disjunction and separation of the matured centrosomes at the G₂/M transition, where they migrate to opposite sides of the cell to form the mitotic spindle. These processes are tightly regulated by the recruitment and activation of distinct sets of proteins at each stage (modified from Fu et al., 2015).

by activating signalling pathways that alert the cell of their presence and promote their repair to maintain genome stability (Fig. 1.3). Detected lesions activate a complex network of pathways that inhibit CDK activity and arrest cell cycle progression at the G1/S transition, intra S and G2/M transition checkpoints to allow time for DNA repair. If DNA repair is not possible, cells will enter apoptosis to avoid accumulation of DNA lesions (Jackson and Bartek, 2009). DDR pathway proteins are generally separated into three groups: (a) sensor proteins that recognise DNA lesions; (b) transducer proteins, usually kinases that amplify the signal by phosphorylating multiple substrates; and (c) effector proteins that mediate the cellular response and inhibit cell cycle progression (Nyberg et al., 2002).

1.1.3.1 Causes of DNA damage

DNA damage can be caused by both intrinsic and extrinsic factors. The most harmful intrinsic factors are reactive oxygen species (ROS) that escape the site of oxidative metabolism. These ROS are often free radicals with unpaired electrons, such as the superoxide anion and hydroxyl radical, as well as the non-radical, hydrogen peroxide. They can form covalent bonds with the DNA backbone leading to the development of modified bases, which are not able to pair with their counterparts, thus destroying the pairing of the DNA double helix (Bridge et al., 2014). Further intrinsic sources of DNA damage are errors in DNA synthesis, abortive topoisomerase activity and reactive molecules released during inflammatory responses (Jackson and Bartek, 2009). Additionally, spontaneous DNA changes can occur, where bases are not paired properly or modifications of bases occur stochastically, leading to changes in the structure and code of the DNA (Hoeijmakers, 2001).

Extrinsic DNA damaging agents come from the environment. The most common cause is UV irradiation from sunlight, which can cause as many as 100,000 lesions per cell per hour (Jackson and Bartek, 2009). Further common factors that lead to harmful DNA modifications are ionising radiation, such as X-rays, which induces oxidation of DNA

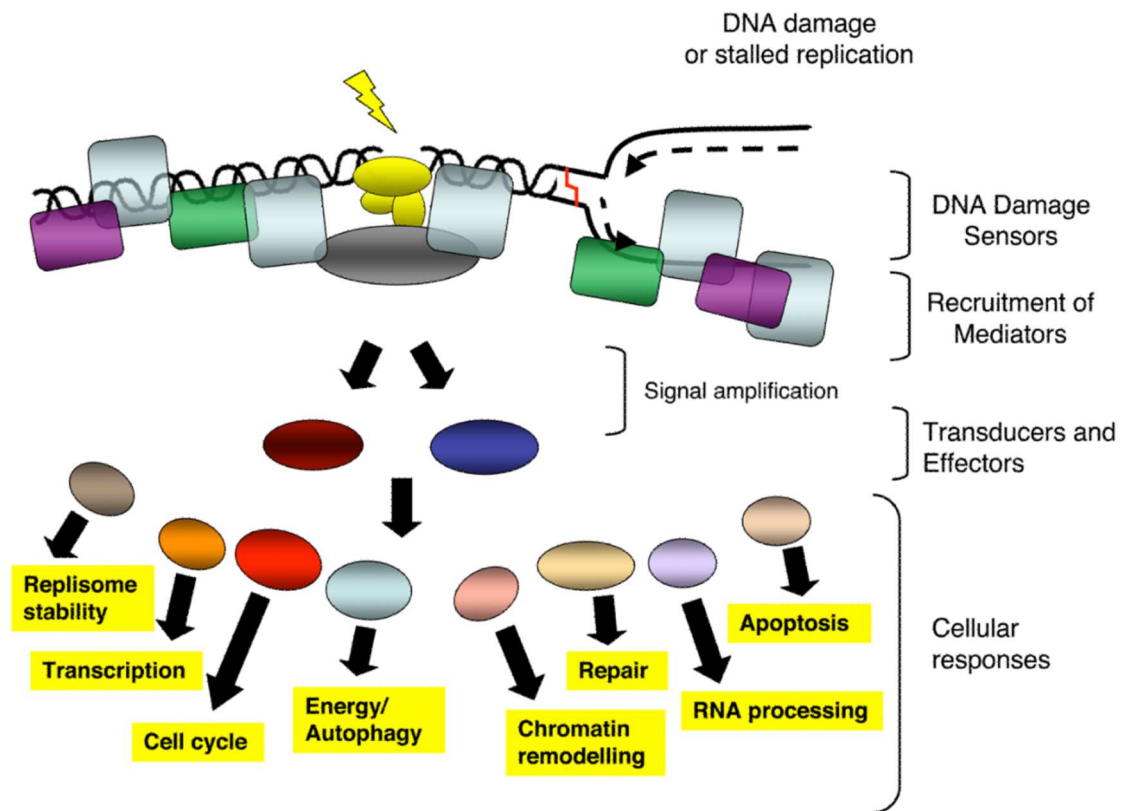


Figure 1.3: The DNA damage response

The DNA damage response proteins can be separated into three categories of DNA damage sensors, signal transducers such as kinases, and effectors that mediate cellular responses such as DNA repair, cell cycle progression or apoptosis. Sometimes mediators are also recruited to sites of DNA damage to amplify the signal (taken from Jackson and Bartek, 2009).

bases, and mutagenic chemicals introduced to the body such as tobacco smoke or aflatoxins in foods (Wogan et al., 2004). Chemotherapeutic drugs also act by damaging DNA, for example by acting as crosslinking agents that form covalent bonds between DNA strands, introducing single or double strand breaks, or by leading to alkyl attachments to DNA bases (Ciccio and Elledge, 2010).

1.1.3.2 The DNA damage signalling cascades

Once DNA lesions have been detected by proteins of the sensor category, signals are transduced by members of the PIKK (phosphatidylinositol 3-kinase-like protein kinase) family, Ataxia telangiectasia mutated (ATM), Ataxia telangiectasia related (ATR) and DNA-dependent protein kinase (DNA-PK). These three kinases are the main regulators of the DDR. ATM and DNA-PK get recruited for double strand breaks (DSBs), whereas ATR mainly works on single strand breaks (SSBs) and stalled replication forks in S-phase (Harper and Elledge, 2007; Meek et al., 2008). They either phosphorylate mediator proteins, like CHK1 (Checkpoint kinase 1) and CHK2 (Checkpoint kinase 2), which amplify the signal, or go on to phosphorylate effector proteins directly (Zhou and Elledge, 2000). Together, these mediate a fast response of cell cycle arrest, and slower responses that allow DNA repair.

1.1.3.3 DNA repair pathways

To handle the variety of DNA lesions caused by different types of damage, complex DNA repair pathways have been developed early in evolution and are conserved across the prokaryotic and eukaryotic kingdom. These partly overlapping pathways are mismatch repair (MMR), nucleotide-excision repair (NER), base-excision repair (BER), homologous recombination (HR) and non-homologous end joining (NHEJ) (Lindahl and Wood, 1999).

Which pathway gets activated depends on the type of the lesion, including distinguishing between SSBs and DSBs. NER, BER and MMR usually deal with SSBs and other types of base damage, with MMR working on repairing mismatched bases, whereas more

complex SSBs, where the affected area of the DNA strand has to be cut and the intact complementary strand used as a template for repair, are usually dealt with by NER and BER. NER gets activated by helix-distorting lesions that affect base-pairing and therefore replication of the DNA and are generally caused by exogenous factors. The NER pathway is divided into two sub-pathways, the so called global genome NER scanning the entire genome for lesions, and transcription-coupled repair NER, which scans for errors in regions of active transcription (Tornaletti and Hanawalt, 1999). In contrast, BER gets activated when bases exhibit chemical alterations, mainly as a result of intrinsic DNA damaging sources, such as ROS, methylation, deamination and hydroxylation. These alterations do not necessarily affect DNA replication, but often lead to faults in transcription.

DSBs have many sources, such as ionizing radiation, X-rays, free radicals or chemicals, and are more difficult to repair. Here, the decision which pathway will be activated depends on the stage of the cell cycle. HR is favoured in S and G2 phase, where the sister chromatid of the chromosome can be used as a template for DNA repair following DNA replication. NHEJ steps in in G1 phase, when there is no template to align with. This makes this pathway less accurate and mistake prone (Hoeijmakers, 2001).

1.1.3.4 Replication stress response

The replication stress response is a specialised pathway of the DNA damage response that gets activated when cells detect stalled replication forks and alteration in fork structure during DNA replication. Replication forks are complex structures where the double strand (ds) parental DNA helix is unwound to form a single strand (ss) template for DNA replication and a docking point for the DNA polymerases (Johnson and O'Donnell, 2005). Causing replication fork stalling and alteration of its structure is called 'replication stress' and plays a major role in the formation of genome instability (Bartek et al., 2007), due to the generation of extensive areas of unstable ssDNA and collapsed replication forks. This makes the DNA prone to breaking (Branzei and Foiani, 2010) and can lead to chromosome rearrangements and translocations which not only affect site-specific, but also genome-wide, stability (Kastan and Bartek, 2004) – a crucial hallmark

of cancer development (Vogelstain and Kinzler, 2004). Next to cancer, several other diseases can arise because of defects in replication stress response proteins (Zeman and Cimprich, 2014), mainly in those involved in detecting or repairing lesions. For example, loss or reduced expression of the key regulator of the replication stress response, ATR, or its interaction partner, ATRIP, causes Seckel syndrome, a disease characterised by developmental delay, microcephaly and mental retardation (Ogi et al., 2012).

To avoid this, cells stop cell cycle progression at the intra-S checkpoint (see above) to allow additional time to re-start fork progression and finish error-free replication (Paulovich and Harwell, 1995; Boddy and Russell, 2001; Nyberg et al., 2002; Osborn et al., 2002).

1.1.3.4.1 Causes of replication stress

Replication fork initiation, assembly and progression are highly complex processes that are tightly controlled in a timely fashion and can be perturbed by a variety of causes that usually lead to nicks and gaps in the DNA, or long stretches of unstable ssDNA (Zeman and Cimprich, 2014).

The number of initiated replication forks is tightly controlled to avoid over-firing of replication origins that might lead to a lack of resources for DNA synthesis due to limited dNTP pools. Overexpression of oncogenes such as HRAS, MYC or Cyclin E, as often found in cancers, can shift this balance and ultimately, lead to genome instability (Bester et al., 2011). However, if not enough origins are formed, there is a risk of not duplicating the whole genome in time (Beck et al., 2012).

Unrepaired DNA lesions caused by intrinsic or extrinsic sources as mentioned in 1.1.3.1 can affect replication fork progression by leading, for example, to the development of DNA-topoisomerase adducts, intra-strand crosslinks or bulky DNA adducts. These create

physical barriers that cannot be overcome by helicases that unwind the double helix for DNA replication and DNA polymerases that are transcribing the unwound ssDNA. They therefore often result in stalled DNA synthesis and the accumulation of long stretches of unstable ssDNA (Branzei and Foiani, 2010; Zegerman and Diffley, 2010; Chaudhuri et al., 2012). Other physical barriers can result from trinucleotide sequences that form hairpin structures (McMurray, 2010).

Other sources of replication stress are misincorporation of ribonucleotides instead of deoxyribonucleotides (Delgaard, 2012), the blocking of the replication machinery by the transcription machinery of the gene (Bermejo et al., 2012), or problems of chromatin accessibility due to chromatin condensation (Lambert and Carr, 2013).

1.1.3.4.2 Replication stress signalling

The replication stress checkpoint is activated upon detection of long stretches of ssDNA originating from a faulty replication fork (You et al., 2002; Zou and Elledge, 2003). It varies depending on the detected damage, but generally operates in four stages: (i) inhibiting origin firing; (ii) slowing elongation; (iii) stabilising stalled replication forks; and (iv) stopping progression through the cell cycle until the replication forks are repaired (Nyberg et al., 2002). The signalling cascade is activated by the excessive accumulation of the ssDNA binding protein RPA, which recruits the main activator of the signalling cascade, the ATR/ATRIP complex to the site by directly interacting with ATRIP (Zou and Elledge, 2003). RPA also recruits and activates the RAD17-RFC2-5 clamp loader, which then binds a complex consisting of RAD9, HUS1 and RAD1 (termed 9-1-1) bound to the ATR-activating TOPBP1 protein. This acts as a feedback loop to stimulate ATR kinase activity (Cimprich and Cortez, 2008; Ellison and Stillman, 2003; Kumagai et al., 2006; Mordes et al., 2008; Zou et al., 2003) and phosphorylation of its downstream mediators, CHK1 and CHK2, which then continue to phosphorylate further downstream effector proteins involved in promoting fork stability and restarting of stalled forks to complete DNA replication before progression of the cell cycle (Fig. 1.4) (Cimprich and Cortez, 2008).

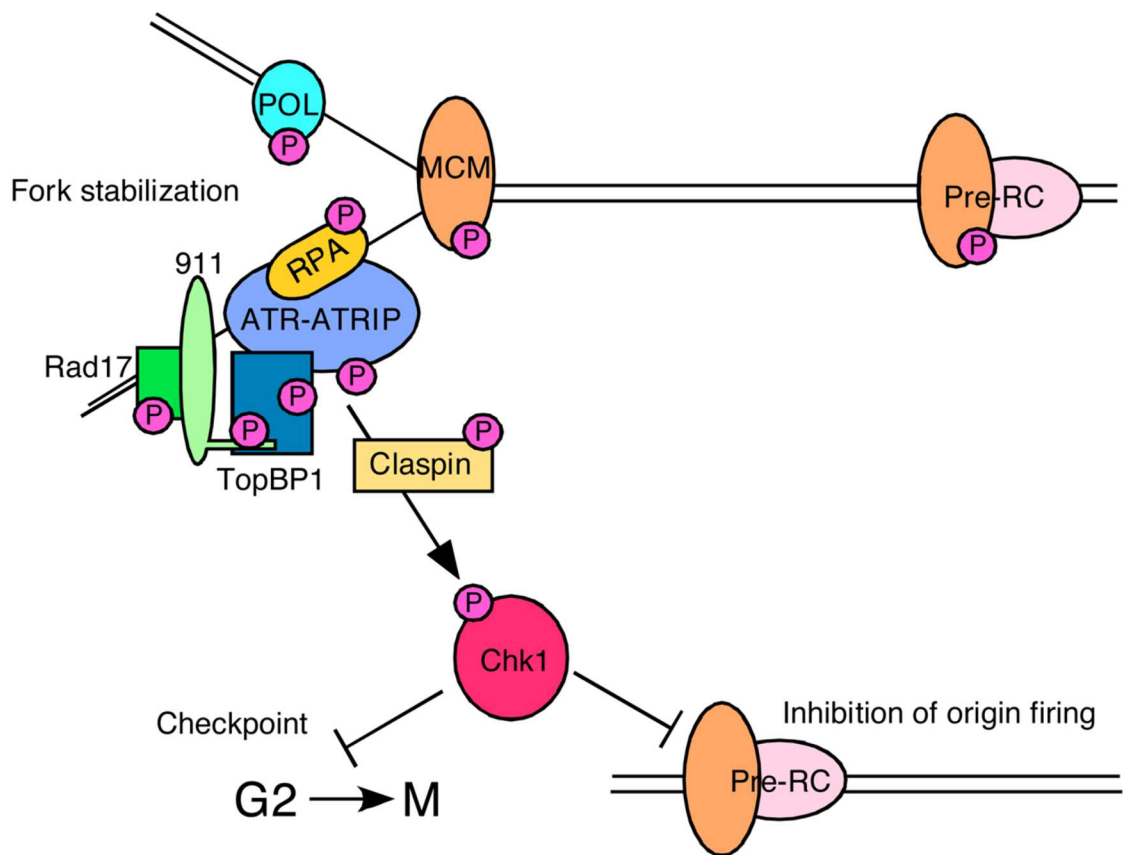


Figure 1.4: Replication stress signalling

RPA binds to ssDNA and recruits the ATR-ATRIP complex alongside other ATR activating proteins such as the 911 complex and Rad 17 and TopBP1. ATR then activates downstream DNA repair mediators by phosphorylating Chk1, which leads to G2/M checkpoint activation and inhibition of origin firing (taken from Cimprich and Cortez, 2008).

1.2. Cilia

Cilia are microtubule-based organelles that extend from the surface of almost all eukaryotic cells. Depending on their structure, they can be divided into motile cilia and non-motile sensory cilia, which are called primary cilia. The rhythmic beating or propelling of motile cilia helps to move fluids within the body, which is why they are found in vast numbers on the apical surfaces of epithelial cells, i.e. of the trachea or the ependymal cells of brain ventricles (Berbary et al., 2009). Conversely, the single, primary cilium of a cell is motionless and extends like an antenna from the cell surface, where it acts as a mechano-, photo- and olfactory sensor and allows the cell to receive stimuli from its surroundings and transduce these into signalling pathways that control proliferation and differentiation (Eggenschwiler and Anderson, 2007; Singla and Reiter, 2006).

1.2.1 Ciliogenesis and cilia structure

Ciliogenesis is a highly complex, conserved mechanism that allows the growth of cilia in a manner that is coordinated with the cell cycle and centrosome duplication cycle. The mother centriole of the centrosome gives rise to the cilium in G1 or G0 phase, while resorption occurs in S-phase prior to complete disassembly before the cell enters mitosis (Ishikawa and Marshall, 2011). As shown in Figure 1.5, ciliogenesis is initiated by docking of a ciliary vesicle to the distal end of the mother centriole, which is now referred to as a basal body. This then migrates towards the cell surface where the basal body anchors to the cell membrane via transition fibres (Sorokin, 1962; Sorokin, 1968). The vesicle extends to form the main body of the cilium, the so-called axoneme, which consists of nine peripheral microtubule doublets (9+0), which surround a tenth, central pair in motile cilia (9+2). (Davenport and Yoder, 2005). Each microtubule doublet consists of an A tubule and an incomplete B tubule attached to the A tubule (Kikkawa et al., 1994) (Fig. 1.6). These elongating microtubule pairs are nucleated directly from the A and B tubule of the basal body (Deane et al., 2001). Small dynein arms are attached to the A tubule in a precise geometry that generate force and allow the cilium to bend and move (Smith and Yang, 2004). Axoneme assembly and disassembly at the tip is driven

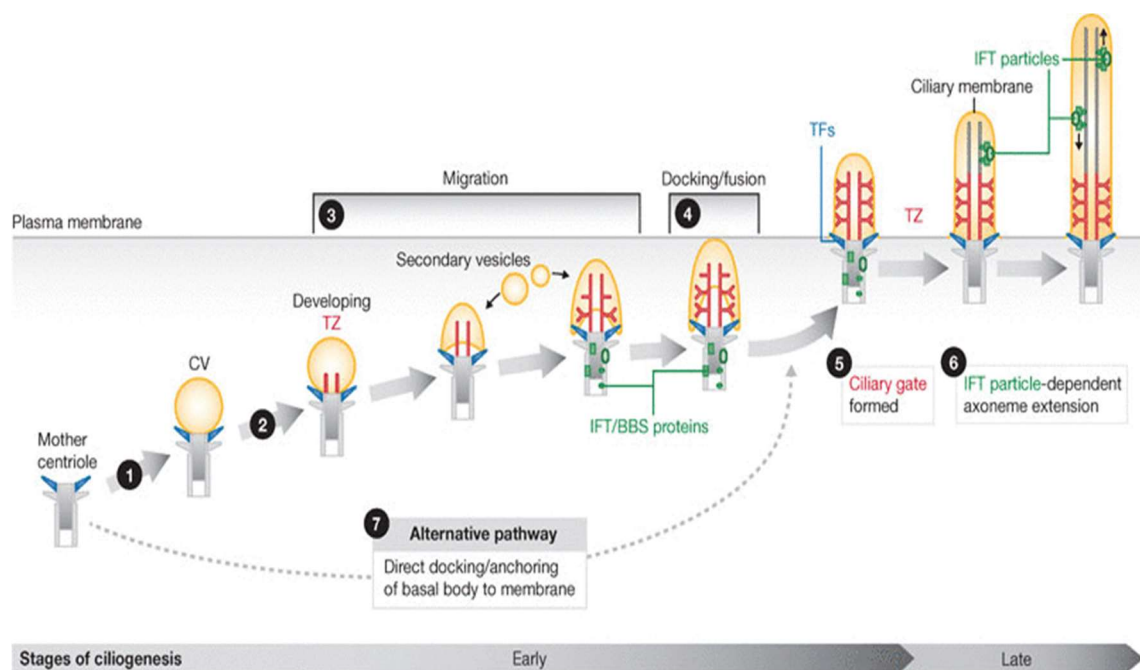


Figure 1.5 Ciliogenesis

Ciliogenesis is initiated by docking of a ciliary vesicle (CV) to the mother centriole. This complex migrates to the cell surface while the vesicle extends into the proximal part of the axoneme. Secondary vesicles attach to the newly formed axoneme and the IFT machinery gets recruited to the base of the cilium, allowing cargo transport into the extending axoneme. The mother centriole attaches to the cell membrane with transition fibres (TF), forming the ciliary gate in the region known as the transition zone (TZ). The IFT machinery helps extending the axoneme further by delivering cargo to the tip (modified after Reiter et al., 2012).

by a cargo transport machinery, called the intraflagellar transport (IFT) in both motile and primary cilia (Pazour et al., 2002; Scholey, 2003). IFT is driven by two counteracting complexes, with complex A being responsible for anterograde transport of proteins from the base of the cilia to the tip, and complex B for the retrograde transport from the tip to the basal body (Pederson and Rosenbaum, 2008). Once the cilium has reached its final length, tubulin assembly at the tip by complex A does not stop, but gets counter balanced by disassembly by complex B (Stephens, 1997; Wallace et al., 2001). The movement of these cargo carrying complexes along the microtubules of the axoneme is powered by ciliary kinesin and dynein motor proteins that move specifically either towards the tip (plus end) or the base (minus end) respectively. Meanwhile, membrane proteins needed for cilia assembly are carried from the cytoplasm to the basal body in vesicles arising from the Golgi apparatus (Follit et al., 2006).

The axoneme is covered by the ciliary membrane which shows distinct features from the cell membrane by exhibiting several cilia-specific receptors and channels that are necessary for ciliary signalling. The most proximal part of the axoneme that connects to the basal body is called the transition zone and consists of a specific set of proteins (Ringo, 1967) that help stabilise the basal body, as well as act as a 'gatekeeper' by regulating protein migration to and from the cytoplasm (Spencer et al., 1988).

1.2.2 The importance of the primary cilium

Primary cilia are able to sense a variety of different signals due to the concentration of a vast number of receptors that enable photosensation (in the eye), mechanosensation (e.g. urine flow in the kidney), osmosensation, thermosensation, hormone sensation, and olfactory sensation. Downstream signalling pathways activated by the receptors include sonic hedgehog (Shh) and the canonical and non-canonical Wnt pathways that are involved in embryo development, proliferation, polarity, nerve growth, differentiation and tissue maintenance (Hildebrandt et al., 2011). As a correspondence, interruption of either the structure or function of primary cilia leads to a series of severe diseases, commonly termed ciliopathies.

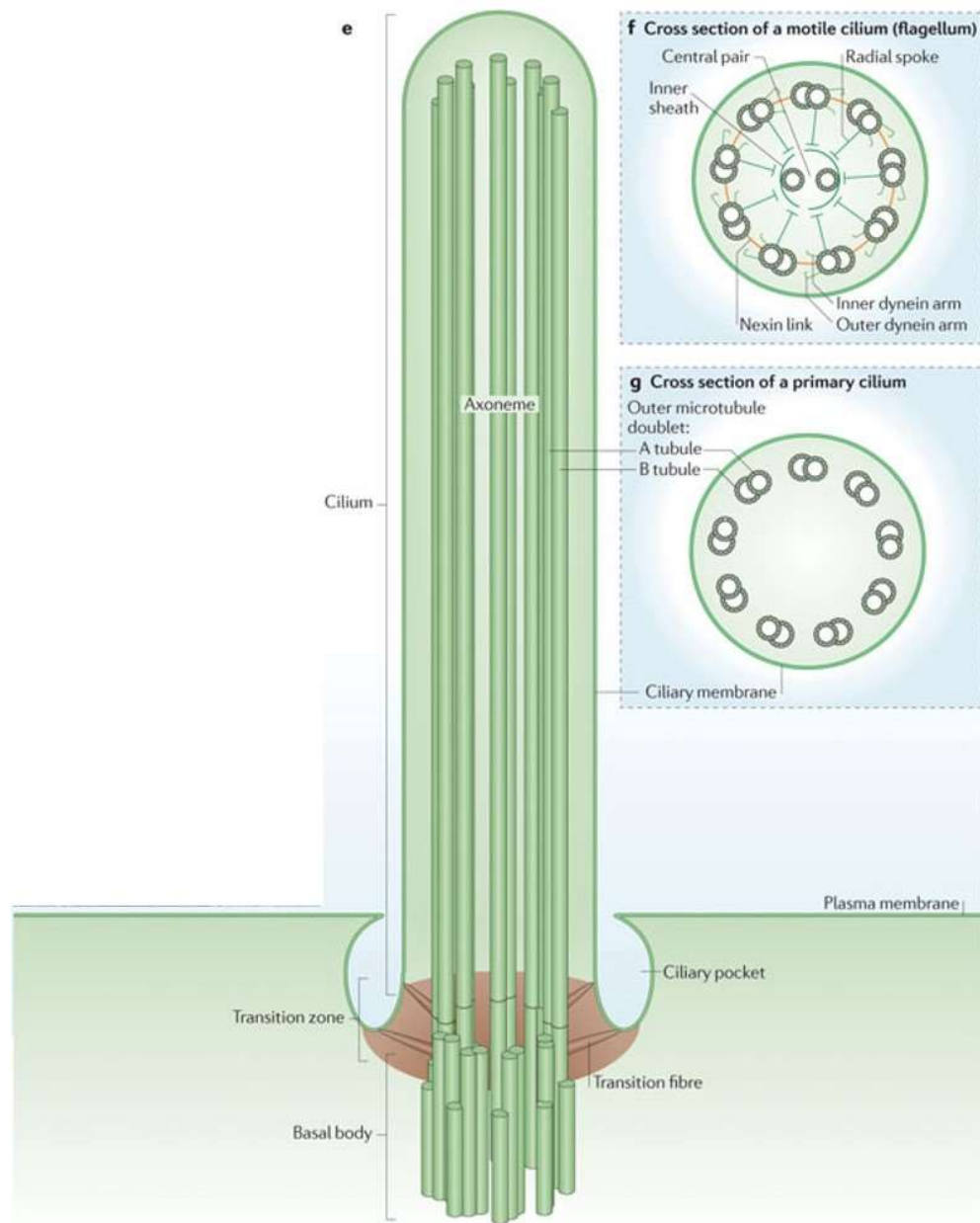


Figure 1.6 Cilia structure

The fully formed cilium consists of an axoneme extending from the basal body. The axoneme consists of nine microtubule pairs, formed on an A tubule and a B tubule. Primary cilia exhibit a 9+0 microtubule pair structure, whereas motile cilia have a central tenth pair (9+2), as well as inner and outer dynein arms that connect the outer microtubule doublets (modified after Ishikawa and Marshall, 2011).

1.3. Ciliopathies

Ciliopathies are a group of heterogeneous diseases whose underlying defects are thought to reside in the structure or function of the cilium. Due to the roles of primary cilia as sensory organelles in almost all epithelial cells, ciliopathies can affect a wide range of organs with disease phenotypes ranging from renal cysts, to retinal degradation, polydactyly, mental retardation, and obesity (Hildebrandt et al., 2009; Zaghloul and Katsanis, 2009).

1.3.1 Polycystic kidney disease

Polycystic kidney disease (PKD) is the most common ciliopathy (Marshall and Nonaka, 2006) and can be divided into autosomal dominant (ADPKD) and autosomal recessive polycystic kidney disease (ARPKD). ADPKD exists with a frequency of 1 in 1000 people in the USA and Europe and is considered one of the most common potentially lethal autosomal dominant diseases (Torres et al., 2007). Symptoms at early stages include hypertension, abdominal pain, a palpable abdominal mass, haematuria, urinary tract infections, cerebral aneurysms, and intestinal diverticulosis. End-stage renal disease (ESRD) develops at the age of 55 to 75, leading to complete loss of kidney function.

Loss-of-function mutations in two genes are responsible for ADPKD, with 80-85% of patients exhibiting mutations in the *PKD1* gene, encoding the protein polycystin-1 (PC-1), and 15-20% of patients showing mutations in *PKD2*, encoding polycystin-2 (PC-2) (Ong and Harris, 2015). Both proteins are transmembrane channels in the primary cilium that regulate calcium influx and efflux and activate downstream signalling cascades involved in renal tubular differentiation and maintenance, assumingly maintaining the cell's differentiated state (Torres et al., 2007; Kim and Walz, 2007).

ARPKD is a less frequent disease with only 1 in 20,000 people affected. However, end-stage renal disease (ESRD) can manifest at any time during the neonatal period, infancy, childhood or adulthood. The most prominent symptoms are bilateral cysts in the kidney,

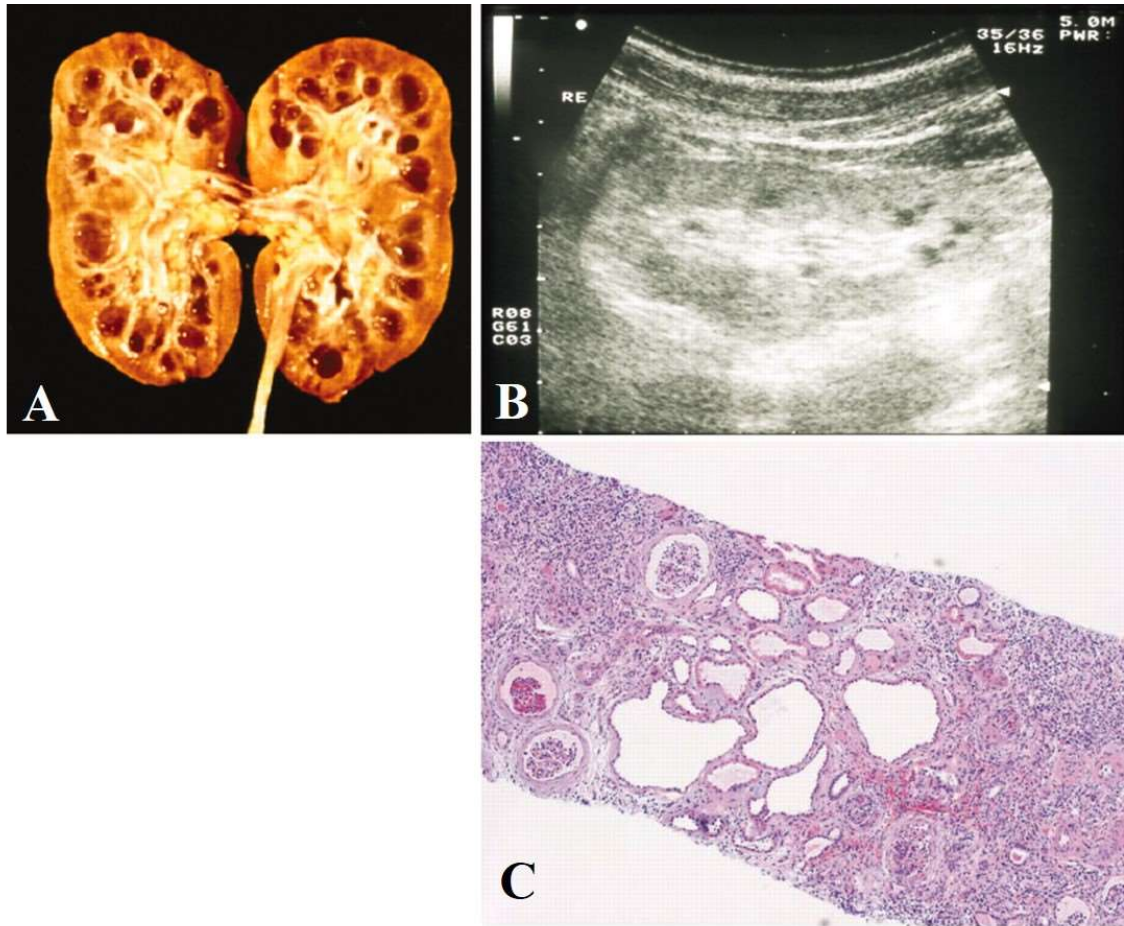


Figure 1.7 Clinical phenotype of NPHP

Cysts in NPHP patients arise from the cortico-medullary junction of normal-sized kidneys as shown in macroscopic pathology of a patient kidney (**A**), renal ultrasound (**B**) and histology of renal tubular cysts (**C**). This also reveals tubular membrane disruption and interstitial fibrosis (modified after Hildebrandt and Zhou, 2007).

inhibiting their function, as well as liver fibrosis. Recessive mutations in the *PKHD1* (polycystic kidney and hepatic disease type 1) gene are responsible for the development of this disease (Adeva et al., 2006). *PKHD1* encodes the membrane-associated receptor-like protein fibrocystin, which is expressed in primary cilia of renal epithelial cells and co-localises with PC-2, where it plays a role in terminal differentiation of the collecting duct and biliary systems (Kim et al., 2008). However, a large number of other recessive diseases have been diagnosed that also affect ciliary function in the kidneys, additionally to multiple other tissues and have therefore been categorised as syndromic in nature.

1.3.1.1 Nephronophthisis

Nephronophthisis (NPHP) is a syndromic autosomal recessive polycystic kidney disease and the most frequent genetic cause for end-stage renal failure (ESRF) in young people (Otto et al., 2008). Depending on the time of onset of ESRD, three forms of NPHP can be distinguished. The juvenile, or type 1, NPHP has an onset of ESRD at an average age of 13 years, the infantile, or type 2, NPHP prior to 4 years, and adolescent, or type 3, NPHP at an average of 19 years (Hildebrandt et al., 1997). NPHP symptoms are subtle at the beginning and are almost undetectable by renal ultrasound. However, symptoms later on are severe and include polyuria, polydipsia, secondary enuresis and anemia that are caused by the development of smaller, hyperechogenic kidneys with cortico-medullary cysts and poor cortico-medullary differentiation (Fig. 1.7). Histopathologically, NPHP can be characterised by tubulo-interstitial alterations such as tubular atrophy, thickening or thinning of the tubular membrane, interstitial fibrosis and inflammation. These symptoms ultimately develop into ESRD with severe anemia, growth retardation and hypertension (reviewed by Wolf, 2015). Due to NPHP being a syndromic ciliopathy, extra-renal manifestations in other organs that rely on cilia function can be found. 10-15% of NPHP patients demonstrate disease of the eyes, such as oculomotor apraxia type Cogan, which describes an impairment of the horizontal gaze and nystagmus (Betz et al., 2000), or retinis pigmentosa, which can cause vision loss and night blindness (Ronquillo et al., 2012). NPHP in combination with retinis pigmentosa is called Senior-Loken syndrome. Other organs that can be affected with NPHP development are the liver, the

| Gene (protein) | Phenotype (average age at ESRD) | Extrarenal symptoms |
|---|---------------------------------|--|
| NPHP1 (Nephrocystin-1) | NPHP (13yrs) | RP (10%), OMA (2%), JBTS (rarely) |
| NPHP2/INVS (Inversin) | Infantile NPHP (<4yrs) | RP (10%), LF, situs inversus, CHD |
| NPHP3 (Nephrocystin-3) | Infantile and adolescent NPHP | LF, RP (10%), situs inversus, MKS, CHD |
| NPHP4 (Nephrocystin-4) | NPHP (21 yrs) | RP (10%), OMA, LF |
| NPHP5/IQCB1 (Nephrocystin-5) | NPHP (13 years) | Early-onset RP |
| NPHP6/CEP290 (Nephrocystin-6/CEP290) | NPHP | JBTS, MKS |
| NPHP7/GLIS2 (Nephrocystin-7/GLIS2) | NPHP | — |
| NPHP8/RPGRIP1L (Nephrocystin-8/RPGRIP1L) | NPHP | JBTS, MKS |
| NPHP9/NEK8 (Nephrocystin-9/NEK8) | Infantile NPHP | — |
| NPHP10/SDCCAG8 (Nephrocystin-10/SDCCAG8) | Juvenile NPHP | RP (SLS), BBS-like |
| TMEM67/MKS3/NPHP11 (Nephrocystin-11/Meckelin) | NPHP | JBTS, MKS, LF |
| TTC21B/JBTS11/NPHP12 (Nephrocystin-12/IFT139) | Early onset NPHP, juvenile NPHP | JATD, MKS, JBTS, BBS- like |
| WDR19/NPHP13 (Nephrocystin-13/IFT144) | NPHP | JATD, SBS, CED, RP, Caroli, BBS-like |
| ZNF423/NPHP14 (Nephrocystin-14/ZNF423) | Infantile NPHP, PKD | JBTS, situs inversus |
| CEP164/NPHP15 (Nephrocystin-15 centrosomal protein 164 kDa) | NPHP (8 years) | RP, JBTS, LF, obesity |
| ANKS6/NPHP16 (Nephrocystin-16/ANKS6) | NPHP, PKD | LF, situs inversus, cardiovascular abnorm. |
| IFT172/NPHP17 (Nephrocystin-17/IFT172) | NPHP | JATD, MZSDS, JBTS |
| CEP83/NPHP18 (Nephrocystin-18/centrosomal protein 83 kDa) | Early-onset NPHP (3 years) | learning disability, hydrocephalus, LF |
| NPHP1L/XPNPEP3 (nephrocystin-1L/XPNPEP3) | NPHP | Cardiomyopathy, seizures |
| NPHP2L/SLC41A1 (nephrocystin-2L/SLC41A1) | NPHP | bronchiectasis |

Table 1.1 Summary of NPHP disease genes and proteins

Shown is a summary of the known NPHP disease genes and their encoded proteins, the form of NPHP they cause and the associated syndromes. CAD, Cranioectodermal dysplasia; CHD, congenital heart disease; JATD, Jeune asphyxiating thoracic dysplasia; JBTS, Joubert syndrome; LF, liver fibrosis; MKS, Meckel-Gruber syndrome; NPHP, nephronophthisis; OMA, oculomotor apraxia; PTK2B, protein tyrosine kinase 2B; RP, retinitis pigmentosa; RPGR, retinitis pigmentosa GTPase regulator; SBS, Sensenbrenner syndrome (modified from Wolf, 2015).

heart and the skeleton, leading to the classification of further NPHP-related ciliopathies, such as Meckel-Gruber or Joubert Syndrome (JBTS). So far, 18 *NPHP* genes have been identified by positional cloning. These partly overlap with associated syndromes as shown in table 1.1. Mutations in these genes can be compound heterozygous or homozygous in nature. The most common mutation is a heterozygous deletion of the *NPHP1* gene, which causes NPHP in 20% of patients. However, the genes known to date are only responsible for NPHP in about one third of patients, while the rest still remain unknown. The encoded proteins of all these genes are described to localise to the primary cilium, with many specifically concentrating near the transition zone towards the proximal end of the cilia. Proteomic studies suggest they interact at least in three distinct networks (Fig. 1.8) (Sang et al., 2011).

1.3.2 Signalling defects as a cause of ciliopathies

Primary cilia act to transduce signals from the environment into biochemical cascades inside the cell. Extensive research has been undertaken into the exact molecular mechanisms involved and how these are perturbed in ciliopathy patients.

1.3.2.1 The hedgehog pathway

The hedgehog pathway plays a major role in embryonic tissue development (Rohatgi and Scott, 2007). A connection between this pathway and ciliopathies was identified in a mutagenesis screen in mice, where mutations in the IFT machinery were found to cause hedgehog mutant phenotypes (Huangfu et al., 2003; Corbit et al., 2005). The Hedgehog pathway receptor Patched 1 (Ptch1) is located in the cilia membrane. Without hedgehog signalling, the Ptch1 receptor inhibits the function of the Smoothened (Smo) receptor and a truncated protein of the Gli family of transcription factors is produced, called Gli repressor (GliR) that translocates to the nucleus and represses transcription of hedgehog target genes (Hammerschmidt et al., 1996). When the hedgehog pathway is activated by ligands such as sonic hedgehog (Shh), the PTCH1 receptor is translocated from the cilia membrane to allow for Smo accumulation (Corbit et al., 2005). Smo

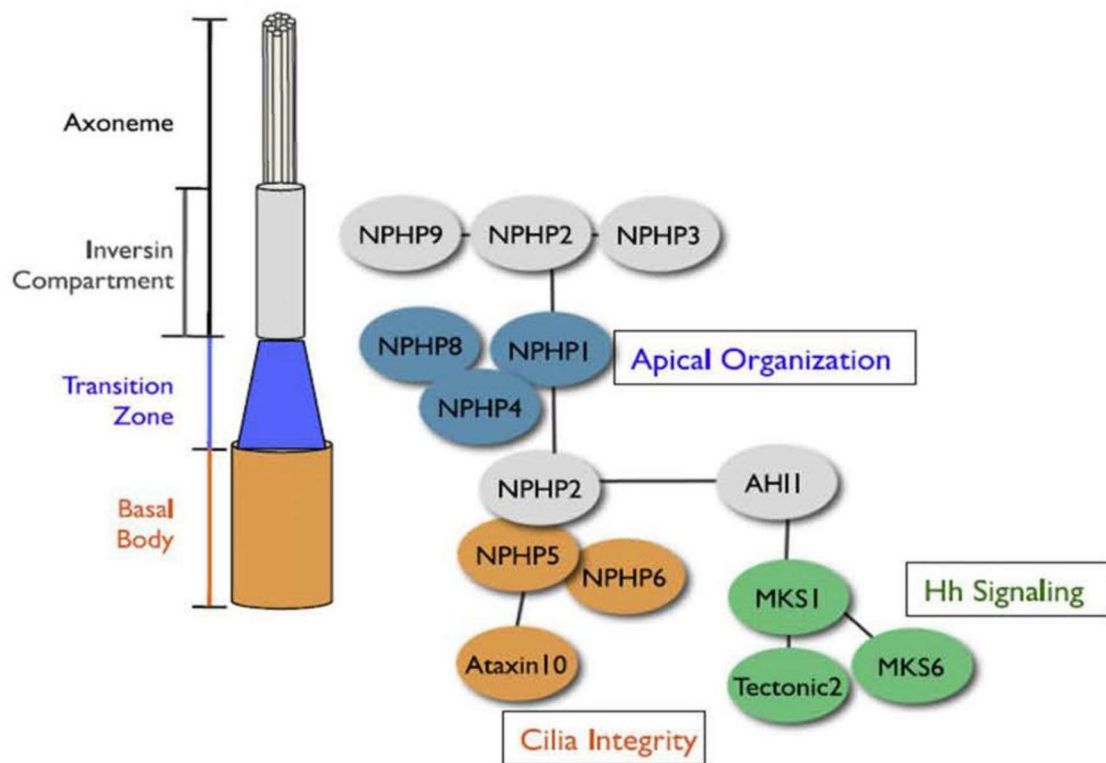


Figure 1.8 Interaction of ciliopathy proteins at the cilia

The ciliopathy proteins involved in the development of NPHP and related syndromes interact in multiple complexes along the proximal end of the primary cilium and are involved in cilia integrity, apical organisation and Hedgehog (Hh) signalling. Orange demonstrates interactions at the basal body, blue at the transition zone and grey at an area called the Inversin compartment (Wolf, 2015).

accumulation and activation by ligands then leads to expression of the full-length protein of the Gli family of transcription factors, that migrate into the nucleus and activate transcription of target genes, such as Cyclin D and FOXM involved in proliferation (Haycraft et al., 2005).

1.3.2.2 The canonical and non-canonical Wnt in ciliopathies

Evidence that defects in the canonical and non-canonical Wnt pathways might play a crucial role in ciliopathy disease progression, and specifically in NPHP, came from findings on the *nphp2/inv*s gene product, Inversin (Inversion of embryonic turning). *inv*s mutants cause an infantile form of NPHP (Otto et al., 2003), as well as *situs inversus*, a condition in which the arrangement of organs in the body is reversed to varying extents along the body's vertical axis, and kidney cysts in mice. However, the underlying molecular mechanisms were unclear, until Simons et al. (2005) found that Inversin acts as a regulator of the canonical Wnt (β -catenin dependent) and non-canonical Wnt/PCP (β -catenin independent) pathways. These act downstream of primary cilia and are involved in regulating cell proliferation, as well as determining cell polarity within the plane of the tissue (Fig. 1.9). The Wnt receptor is a member of the Frizzled family and is found on the ciliary membrane where it gets activated upon ligand binding. In the canonical Wnt pathway, cytoplasmic Dishevelled (Dvl) attaches to the Frizzled receptor and binds to Axin, a protein of the β -catenin destruction complex, therefore inhibiting this complex from forming and allowing accumulation of β -catenin in the cytoplasm. Once a certain threshold of β -catenin concentration is reached, β -catenin enters the nucleus and acts as a transcriptional co-activator for genes such as C-Myc, involved in cell proliferation. In contrast, upon detection of fluid movement in the kidney tubules, mechano-stimulated channels in the ciliary membrane, such as PC-2, open and allow for Calcium influx. This somehow enhances Inversin expression or activation in the cilia, where it binds to cytoplasmic Dvl and either targets it for proteasomal degradation or promotes its re-localisation into the cell membrane. This allows the Axin/Apc/GSK3 β complex to form and target β -catenin for proteasomal degradation, thus, inhibiting the canonical Wnt proliferation pathway, but activating cytoskeletal proteins involved in cell

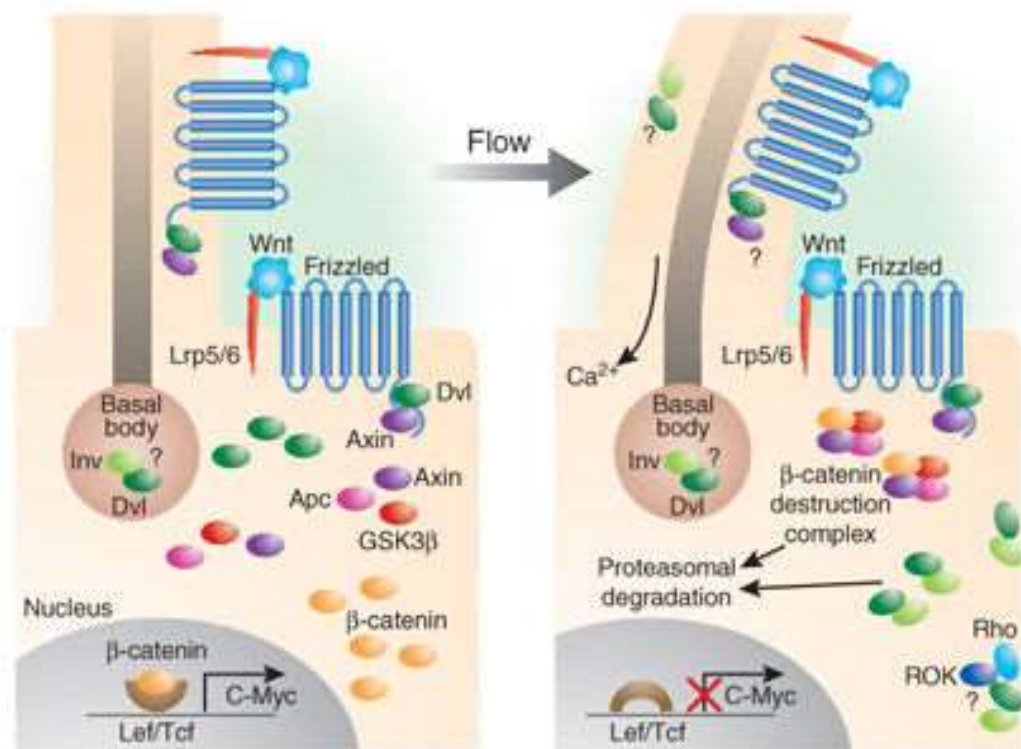


Figure 1.9 The canonical and non-canonical Wnt pathway in the kidney tubules

Canonical Wnt signalling leads to the disassembly of the β -catenin destruction complex by Dvl binding to Axin and accumulation of cytoplasmic β -catenin. β -catenin then migrates into the nucleus and activates the transcription of target genes such as C-Myc, that promote proliferation. Flow in the kidney tubules activates the non-canonical Wnt pathway involved in planar cell polarity by complex formation of Inversin and Dvl, leading to proteasomal degradation of Dvl. This allows the β -catenin destruction complex to form, which targets β -catenin for proteasomal degradation and leads to the inhibition of transcription of target genes involved in proliferation (Germino, 2005).

polarity (Simons et al., 2008). Defects in maintaining this balance between cell proliferation and planar cell polarity can lead to overproliferation of cells, or division in the wrong plane, either of which may be the cause of cyst formation (Fig. 1.10) (Hildebrandt et al., 2011).

1.4. NPHP9/Nek8

The *NPHP9* gene encodes the serine/threonine kinase Nek8 that belongs to the NIMA – or Nek-family of protein kinases with functions in mitosis, signal transduction, and the DNA damage response (Fry et al., 2012). The Nek8 protein consists of an N-terminal catalytic domain and a C-terminal RCC1 domain (regulator of chromatin condensation 1) that is predicted to allow protein-protein interactions with substrates and coregulators (Fry et al., 2012). Nek8 gets activated upon exit from the cell cycle when it localises to a specific region near the proximal end of the primary cilium (Zalli et al., 2011). This region does not immediately seem to differ morphologically from the rest of the axoneme, but harbours a docking point for a complex network of interaction proteins, mediated by the NPHP2 disease protein, Inversin. Hence, this region has been called the ‘Inversin or Inv-compartment’ (Shiba et al., 2010). Studies have shown that Inversin anchors several NPHP disease proteins in the Inv compartment, including Nek8. Cells expressing an Inversin protein that is lacking amino acids 1- 741 exhibit loss of Nek8 localisation to the cilium (Shiba et al., 2010), emphasising the importance of Inversin for Nek8 recruitment. Moreover, these studies suggest a role for Nek8 downstream of Inversin in cilia signalling. However, its specific role in cilia organisation or function is still unknown.

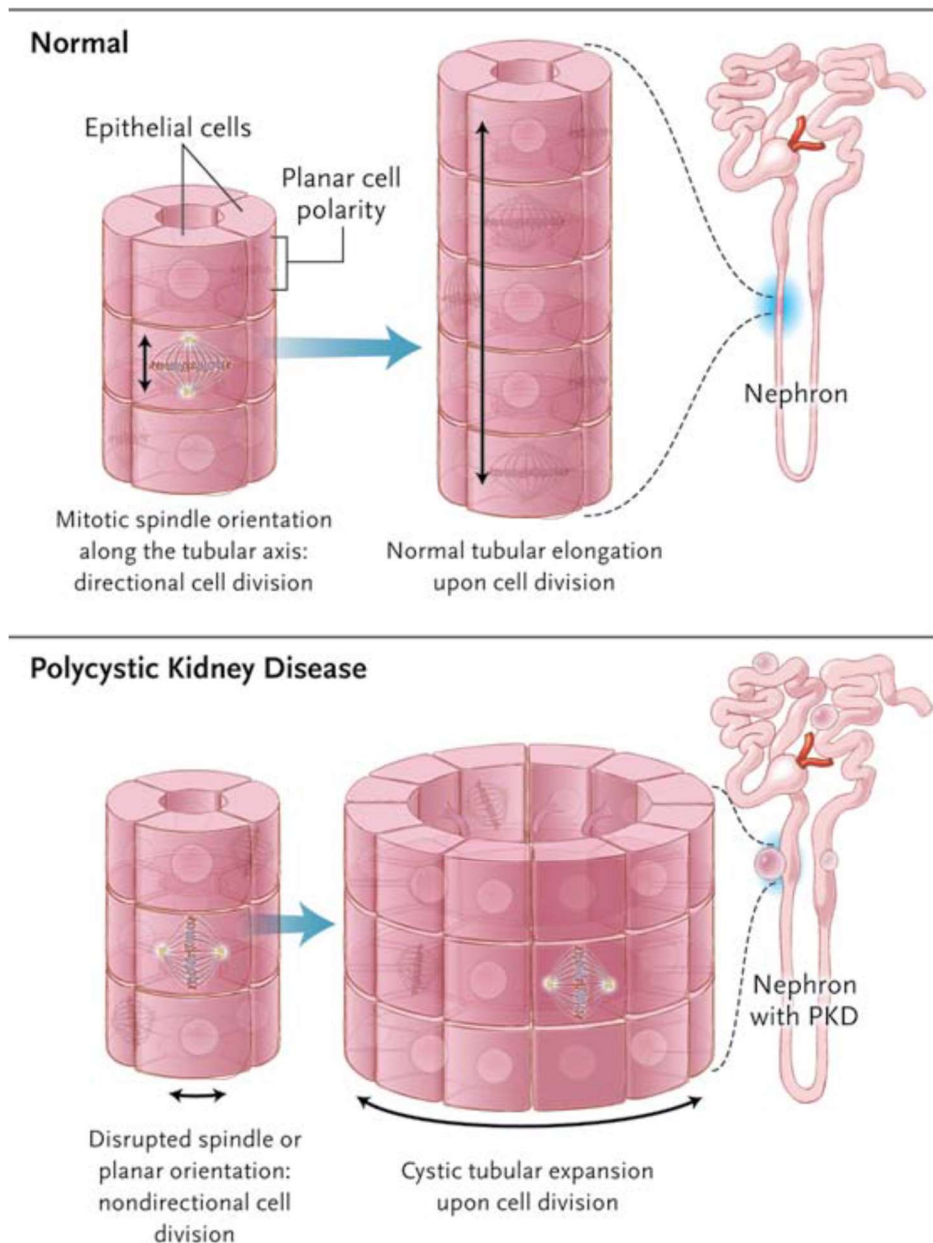


Figure 1.10 A role for non-canonical Wnt signalling in preventing polycystic kidney disease

The non-canonical Wnt/PCP pathway is responsible for directed cell division in the plane of a tissue such as the kidney nephron. Centrosome and spindle alignment are crucial. In polycystic kidney disease, misdirected alignment of the spindle poles might cause cell division along the wrong axis, leading to tubular expansion and the development of cysts (Hildebrandt et al., 2011).

1.4.1 The NIMA-related kinase family

The NIMA-related kinase, or Nek, family was first discovered in the filamentous fungus *Aspergillus nidulans* during a temperature-sensitive genetic screen for cell cycle mutants (Oakley and Morris, 1983). Mutants that failed to exit mitosis were termed *bim* (*blocked in mitosis*) and mutants that never entered mitosis were termed *nim* (*never in mitosis*). Characterisation of the first one of the *nim* mutants, *nimA* (*never in mitosis gene A*) revealed a serine/threonine protein kinase that was called NIMA. Loss of function mutations of *nimA* led to G2 arrest of the cell cycle, whereas overexpression caused premature entry to mitosis (Osmani et al., 1991; Osmani et al., 1988). When NIMA was ectopically expressed in other organisms, including fission yeast, *Xenopus* oocytes or human cells, characteristics of mitotic entry could be observed, leading to the conclusion that NIMA orthologs may play roles in cell cycle control in other eukaryotes (Lu and Hunter, 1995; O'Connell et al., 1994).

Genome sequencing, as well as functional studies, have revealed that Nek kinases are conserved across eukaryotic species from protists, such as *Chlamydomonas* and *Plasmodium*, to yeasts (i.e. *Saccharomyces cerevisiae* and *Schizosaccharomyces pombe*), as well as *Drosophila*, *Xenopus*, mice and humans. Even though Nek kinases do not always have functions that are essential for cell survival in these organisms, they play key roles in cell cycle related processes, such as spindle assembly, chromatin condensation and cytokinesis (De Souza et al., 2000; Grallert and Hagen, 2002; Grallert et al., 2004; Krien et al., 1998; Wu et al., 1998).

In humans, eleven *nek* genes were identified, expressing Nek kinases 1 to 11 (Fig.1.11). Nek2 is the closest related human proteolytic sequence to the ancestor NIMA in *Aspergillus nidulans*. Structurally, all human Nek kinases, apart from Nek10, have an N-terminal catalytic domain harbouring all the features of serine/threonine kinases and share approximately 40-50% conservation with NIMA and each other. They all contain a His-Arg-Asp (HRD) motif within the catalytic domain, suggesting positive regulation by phosphorylation in the activation loop (Johnson et al., 1996). Consistent with this, they contain a serine or threonine residue within their activation loop that can either be

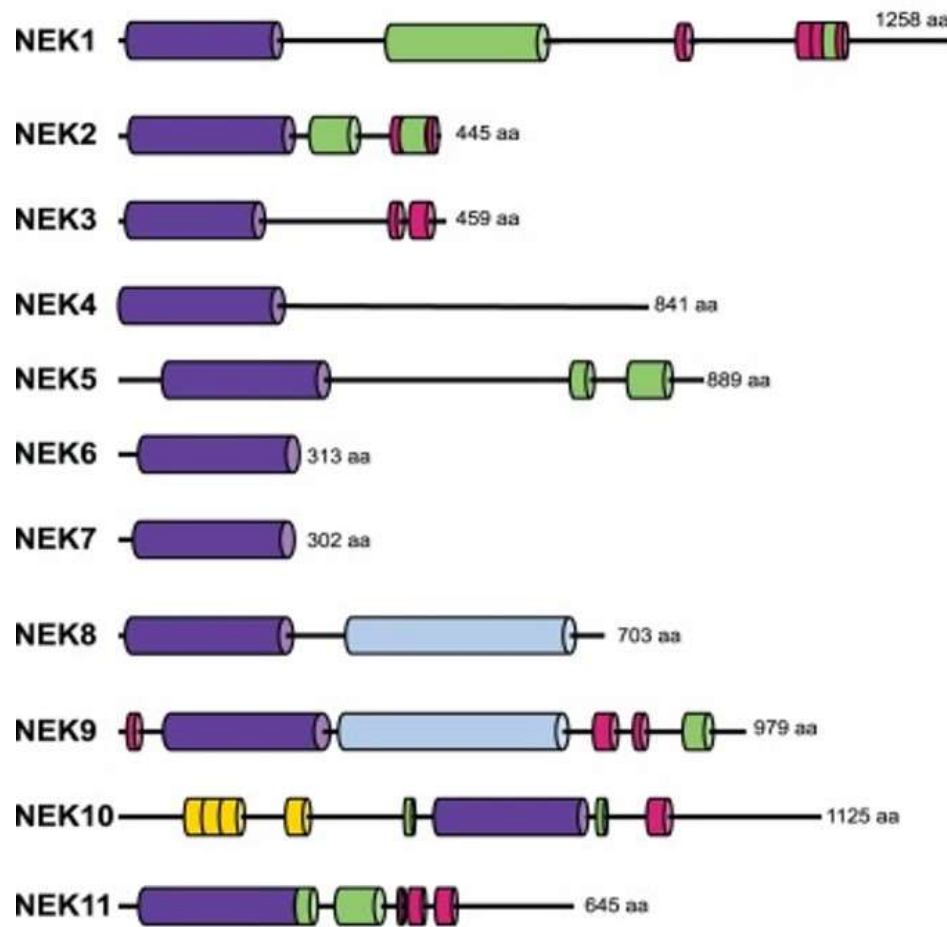


Figure 1.11 Domain organisation of the human Nek kinases

The 11 human Nek kinases have an N-terminal catalytic domain (purple), followed by a less well conserved C-terminal domain that can include coiled-coils (green), degradation motifs (red), an RCC1 (regulator of chromatin condensation 1) domain (light blue) and armadillo repeats (yellow) (modified from Fry et al., 2012).

autophosphorylated or phosphorylated by upstream kinases (Belham et al., 2003; Bertran et al., 2011; Rellos et al., 2007; Roig et al., 2002). However, the C-terminus of Nek kinases is less well conserved and varies in amino acid sequence, length and structure suggesting a variety of roles for the different proteins. One common feature within the C-terminus of most Nek kinases is a coiled-coil motif that promotes oligomerisation, autophosphorylation and activation. Human Nek kinases play roles in mitosis (Nek2, 6, 7, 9), signalling pathways (Nek3, 5), DNA damage response (Nek1, 8, 10, 11) and at the cilia (Nek1, 4, 8) (Fig. 1.12) (Fry et al., 2012) and are linked to a variety of human disease, such as ciliopathies and cancers (Table 1.2).

1.4.2 Nek8 in polycystic kidney disease

The involvement of Nek8 in polycystic kidney disease was first discovered in the *jck* (juvenile cystic kidney) mouse model, where a homozygous G488V substitution in the non-catalytic RCC1 domain of Nek8 was detected (Liu et al., 2002). Cells in the kidneys of these mice had significantly elongated cilia, suggesting a role for Nek8 in ciliogenesis (Smith et al., 2006; Sohara et al., 2008). Furthermore, mice expressing a homozygous *nek8* null allele die in utero and exhibit left-right asymmetry defects (Manning et al., 2013). Knockdown of Nek8 in zebrafish embryos led to the formation of pronephric cysts and also exhibit left-right asymmetry defects (Fukui et al., 2012). On this basis, Otto et al. (2008) performed a mutational screen of the human *nek8* gene in 188 NPHP patients and discovered three missense mutations in patients of individual families: a heterozygous L330F substitution, a heterozygous A497P substitution and a homozygous H425Y substitution. These mutations are located in the Nek8 RCC1 domain and are well conserved across human, mouse, *Xenopus*, and zebrafish. Experiments with transiently transfected GFP-tagged mouse orthologs into murine IMCD3 cells showed localisation defects of the H425Y and L330F proteins to cilia (Otto et al., 2008). However, overexpression of these three disease proteins had no effect on ciliogenesis in IMCD3 cells, although it did lead to the formation of multinucleated cells, suggesting additional roles in cell cycle control. Indeed, this phenotype was also observed in *in vitro* studies upon knockdown of Nek8 (Liu et al., 2002). Further studies on the human Nek8 mutants

| Kinase | Disease | Reference |
|--------|--|---|
| Nek1 | Skeletal ciliopathies, such as Axial spondyloepiphyseal dysplasia and short rib thoracic dystrophy | Wang et al., 2017B |
| | Oral-facial-digital (OFD) ciliopathies, such as Mohr syndrome | Monroe et al., 2016 |
| | Amyotrophic lateral sclerosis | Kenna et al., 2016 |
| Nek2 | Cancers, e.g. liver cancer (Hepatocellular carcinoma) | Wu et al., 2017 Li et al., 2017 |
| | Potentially breast cancer | Wang et al., 2017A |
| Nek3 | Breast cancer | Miller et al., 2007 Harrington and Clevenger, 2016 |
| Nek4 | - | - |
| Nek5 | - | - |
| Nek6 | Cancers, e.g. Hepatic cell cancer | Jee et al., 2013 Cao et al., 2012 |
| Nek7 | Hepatocellular carcinoma | Zhou et al., 2016 |
| Nek8 | Nephronophthisis | Otto et al., 2008 |
| | Breast cancer | Bowers and Boylan, 2003 |
| Nek9 | Cancer | Kurioka et al., 2014 |
| | Ciliopathy lethal skeletal dysplasia | Casey et al., 2016 |
| | Nevus Comedonicus | Levinsohn et al., 2016 |
| Nek10 | Breast cancer | Ahmed et al., 2009 |
| Nek11 | Cancers, such as ovarian cancer and colorectal cancer | Liu et al., 2014 Sabir et al., 2015 |

Table 1.2 Summary of Nek kinases and their associated human diseases

Shown is a summary of the 11 human Nek kinases and their known associated diseases. References are stated in the table.

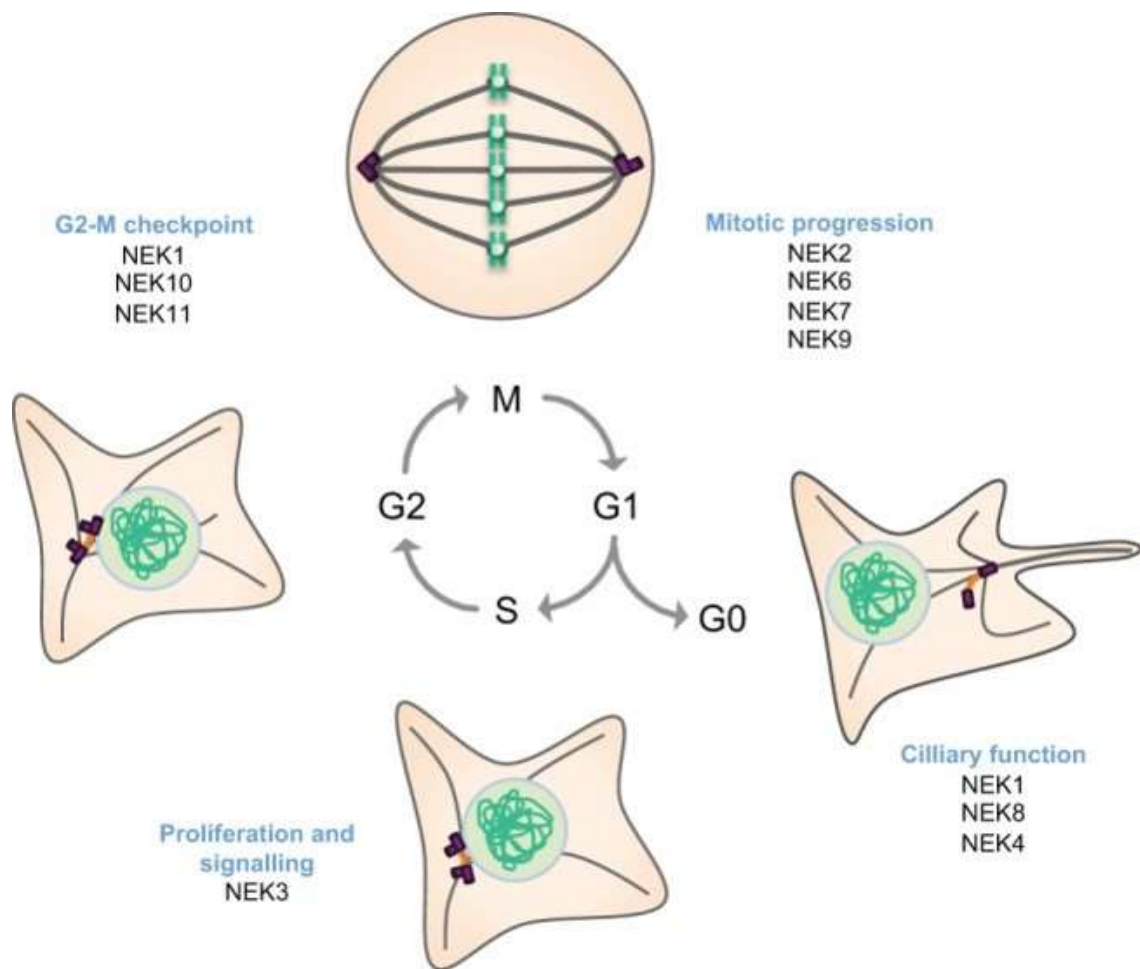


Figure 1.12 Nek kinase functions through the cell cycle

Nek kinases can be clustered into functional complexes, with Nek1, 10 and 11 being involved in the DNA damage response at the G2/M checkpoint, Nek2, 6, 7 and 9 having roles in mitotic progression, Nek1, 4 and 8 being involved in ciliogenesis, and Nek3 playing a role in signalling transduction in S-phase (Fry et al., 2012).

following transfection into RPE1 cells revealed no perturbation of kinase activity, but loss of localisation of the H425Y mutant to the primary cilium and centrosomes (Zalli et al., 2011). Recent studies have shown a role for Nek8 in the Hippo pathway with important roles in regulating proliferation rates, organ size development and tumourigenesis (Waleras and Wrana, 2012; Pan, 2012; Benhamouche et al., 2010). The involvement of the Hippo pathway in cilia structure of function, however, still remains unclear. However, the ciliary NPHP disease protein NPHP4 has been shown to play a key inhibitor role of this pathway, suggesting some ciliary involvement in its regulation. Nek8 acts to stabilise the Hippo pathway effector protein TAZ (transcriptional co-activator with PDZ-binding motif), an oncogene that has been described to be overexpressed in non-small cell lung cancer and breast cancer (Habbig et al., 2012; Zhou et al., 2010; Chan et al., 2011; Chan et al., 2009). NPHP4 promotes nuclear localisation of the Nek8/TAZ complex, where TAZ then acts as a transcription factor. Interestingly, all three Nek8 mutants failed to activate TAZ-mediated gene transcription in HEK293T cells, leading to decreased proliferation levels (Habbig et al., 2012).

1.4.3 Nek8 and the DNA damage response

Unexpectedly, an involvement of Nek8 in the replication stress response has also been discovered. siRNA knockdown of the *nek8* gene led to hypersensitivity of fibroblasts to aphidicolin, an inhibitor of the DNA polymerase. Treated cells still arrested at the intra-S checkpoint, but failed to repair DNA DSBs. Moreover, Nek8 depleted cells exhibited increased levels of CDK2 kinase activity, a crucial mediator of the intra-S phase checkpoint. DNA damage accumulation by loss of Nek8 was rescued with CDK inhibitors, suggesting an inhibitory function for Nek8 in checkpoint progression (Choi et al., 2013). Nek8 was also shown to physically interact with core components of the DDR pathway, including the replication stress response signal transducer ATR, its interaction partner ATRIP, and the downstream mediator kinase Chk1. In a separate approach, Nek8 has been shown to be involved in the DSB repair pathway of homologous recombination, a pathway activated in S-phase upon DSB formation (Abeyta et al., 2017). Here, Nek8 was identified as a regulator of RAD51 foci formation, a core component of replication fork protection in the HR pathway that localises to DSBs and modulates DNA replication and

fork protection through CHK1 (Parplys et al., 2015). These findings suggest a new role for Nek8 in the DNA damage response that would be separate from its role at the primary cilium. Nek8 is involved in maintaining genome integrity by inhibiting cell cycle progression at the intra-S checkpoint by mediating the replication stress response (Fig. 1.13).

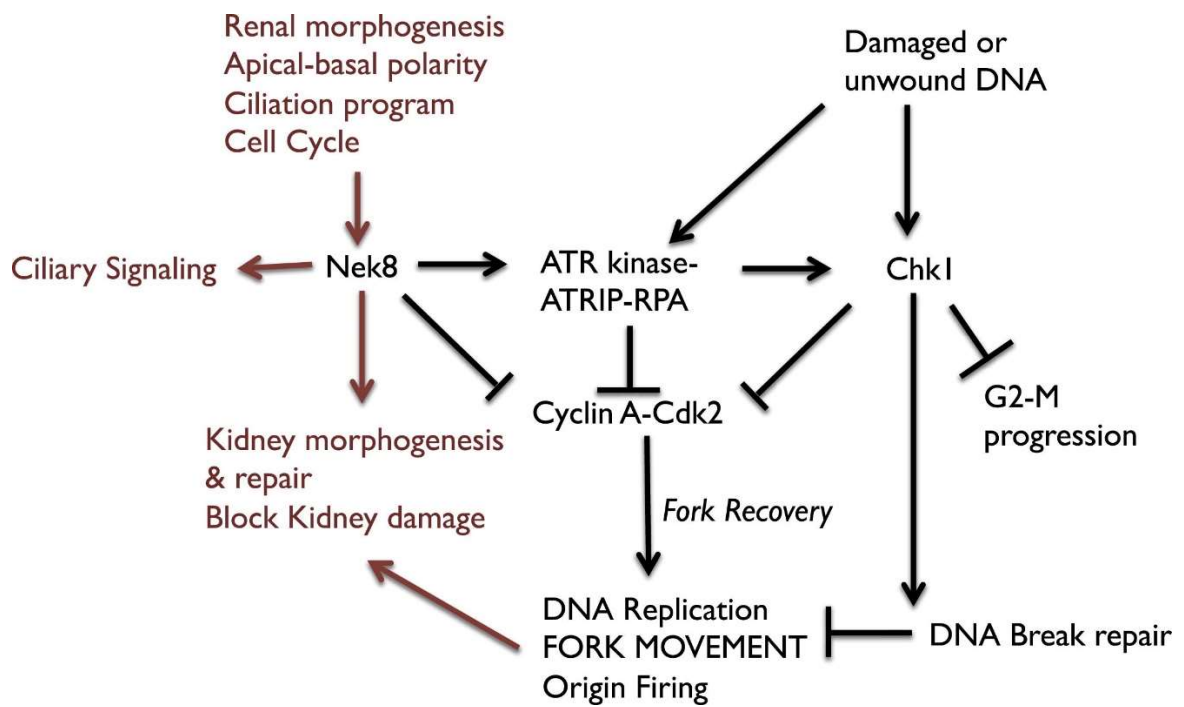


Figure 1.13 A role for Nek8 in coordinating ciliary signalling with DDR control

Nek8 works within a complex network, receiving stimuli from the cell cycle and cilia and transforming these into response pathways by interacting with Inversin at the cilium, and ATR and Chk1 in the DDR pathway. It is plausible that both functions are required to maintain Kidney integrity (Jackson, 2013).

1.5. Aims and objectives

The aim of this project was to generate biomarkers of Nek8 kinase activity that could be used for *in vitro* assays, including screening of small molecule inhibitors, and for cell-based studies that would shed light on its role in normal cell cycle progression and explain why mutations should lead to phenotypes associated with NPHP.

To achieve this aim, the following specific objectives were pursued:

1. To set up *in vitro* and cell-based systems for assessing Nek8 interaction sites with its ciliary interaction partner, Inversin. This was done using a variety of human cell lines to investigate interaction between Nek8 and Inversin under cycling and serum starved conditions. For this, mammalian Inversin and Nek8 constructs were generated, transfected into cells and their interactions were analysed using *in vitro* co-immunoprecipitation assays.
2. To map sites of phosphorylation in the Nek8 substrates, Inversin and PC-2, and generate phospho-specific antibodies against some of these sites. This was done by performing *in vitro* kinase assays with Nek8 and purified Inversin and PC-2 domain proteins. Phospho-sites in these proteins were then mapped by MALDI-TOF analysis. Phospho-specific antibodies were generated against some of these sites to investigate these as biomarkers for Nek8 kinase activity and validation of their specificity took place *in vitro* in kinase assays and *in vivo* in RPE1 cells by immunofluorescence microscopy.
3. To validate a phospho-Nek8 antibody that was generated against the threonine 162 residue in the Nek8 activation loop as a biomarker of Nek8 activity and investigate the phenotype of Nek8 inhibition with respect to ciliogenesis, cell cycle progression and the DNA damage response. This was done by validating the phospho-Nek8 antibody in *in vitro* kinase assays and investigating the localisation pattern of active Nek8 in RPE1 cells. Two small molecule inhibitors were tested for their ability to inhibit Nek8 kinase activity *in vitro* using kinase assays with Nek8 and Inversin as a substrate, before validating phenotypes of Nek8 inhibition in RPE1 cells by immunofluorescence microscopy.

CHAPTER 2 MATERIALS AND METHODS

2.1 Materials

2.1.1 Chemical suppliers

All chemicals were of analytical grade purity or higher and supplied by Sigma (Poole, UK) or Roche (Lewis, UK) if not otherwise stated in the table below. All cell culture solutions and plastic ware were supplied by Invitrogen Life Sciences (Paisley, UK), if not otherwise stated.

| Chemicals | Supplier |
|--|--|
| Penicillin RNase A Streptomycin | Invitrogen, Part of Life Sciences, Paisley, UK |
| PMSF | Fluka, Gillingham, UK |
| HEPES NaHCO ₃ SDS | Melford, Suffolk, UK |
| Agar Tryptone Yeast extract | Oxoid, Basingstoke, UK |
| EDTA Glycerol KCl KH ₂ PO ₄ Methanol MgCl ₂ MnCl ₂ NaCl Na ₂ HPO ₄ ProtoFlowgel Tween-20 | Thermo Fisher, Loughborough, UK |

2.1.2 Mammalian and bacterial constructs

| Name | Vector | Resistance | Supplier |
|-----------------------|-------------------------|------------|---------------------------------------|
| His-Inversin 1-553 | pLEICS-01, bacterial | Amp | PROTEX, University of Leicester |
| GST-Inversin 554-1065 | pLEICS-02, bacterial | Amp | |
| GST-Inversin 899-1065 | | | |
| GST-Inversin 950-1065 | | | |
| HA-Inversin FL | pLEICS-19, mammalian | Amp | |
| HA-Inversin 1-553 | | | |
| HA-Inversin 554-1065 | | | |
| Flag-Inversin 1-603 | pLEICS-12, mammalian | Amp/Neo | |
| Flag-Nek8 FL | | | |
| Flag-Nek8 Kinase | | | |
| Flag-Nek8 RCC1 | | | |

2.1.3 Oligonucleotides

All primers were provided by Eurofins Genomics (Louisville, USA).

2.1.3.1 Cloning primers for Inversin and Nek8 constructs

| Name | Forward primer | Reverse primer |
|--------------------|--|---|
| His-Inversin 1-553 | GTATTTTCAGGGCGCCAACAAGTC AGAGAACCTGCT | GACGGAGCTCGAATTCAGGCTGC GATGGACAGGGC |

| | | |
|--------------------------|--|---|
| GST-Inversin 1-600 | TACTTCCAATCCATGAACAAGTCA GAGAACCTGCT | TATCCACCTTTACTGTCTTCTCCTCT CGCTTTTTGGCAG |
| GST-Inversin 899-1065 | TACTTCCAATCCATGCGACTGCAG ATAATTCAGA | TATCCACCTTTACTGTCAATCAAGGT TTTGTTTTGTTTTTGGC |
| GST-Inversin 601-1065 | TACTTCCAATCCATGAACAAACGA AAAGAGGCAGAA | TATCCACCTTTACTGTCAATCAAGGT TTTGTTTTGTTTTTGGC |
| HA-Inversin FL | GTATTTTCAGGGCGCCAACAAGTC AGAGAACCTGCT | GACGGAGCTCGAATTCATCAAGGT TTTGTTTTGTTTTTGGC |
| HA-Inversin 1-553 | GTATTTTCAGGGCGCCAACAAGTC AGAGAACCTGCT | GACGGAGCTCGAATTCAGGCTGC GATGGACAGGGC |
| HA-Inversin 554-1065 | GTATTTTCAGGGCGCCATACAAGA CATCGCCGCC | GACGGAGCTCGAATTCATCAAGGT TTTGTTTTGTTTTTGGC |
| Flag-Inversin 1-603 | GTATTTTCAGGGCGCCAACAAGTC AGAGAACCTGCT | GACGGAGCTCGAATTCATCGTTTG TTTTCTCCTCTCGCT |
| Flag-Nek8 FL | GTATTTTCAGGGCGCCAGTGGTG GGGAGAGGTGCCTTC | GACGGAGCTCGAATTCAGGGGGG GACCGGCTCA |
| Flag-Nek8 Kinase | GTATTTTCAGGGCGCCAGTGGTG GGGAGAGGTGCCTTC | GACGGAGCTCGAATTCAGCAGAG GGGCTGTGCCATGA |
| Flag-Nek8 RCC1 | GTATTTTCAGGGCGCCATCCGTGC CCTCCTCA | GACGGAGCTCGAATTCAGGGGGG GACCGGCTCA |

2.1.3.2 Mutagenesis primers for HA-Inversin

| Name | Forward primer | Reverse primer |
|-------|-----------------------|-----------------------|
| L493S | AGAACAGCTTCGCATTGGTCC | GGACCAATGCGAAGCTGTTCT |

| | | |
|--------|--|--|
| T359A | GCTGACAAATATGGAGGTGCA GCTTTGCATGCTGCTGCTC | GAGCAGCAGCATGCAAAGCTG CACCTCCATATTTGTCAGC |
| T866A | GAGACATCTGCCCTGTCCGAG | CTCGGACAGGGAAGATGTCTC |
| T1032A | AACTCAGTGGCCAACCTACAG | CTGTAGGTTGGCCACTGATTG |
| T1057A | CAATCAGCTGCTCAGCCAAAA | TTTGGCTGAGCAGCTGATTG |

2.1.3.3 PCR primers for genomic DNA amplification

| Name | Forward primer | Reverse primer |
|-----------|--------------------------|----------------------------|
| Nek8 | TGGAGAAGTACGAGCGGATCCGAG | GCCACTCATGATCTTCAGCACCAGTG |
| knock-out | TGGTGG | CTGG |
| GAPDH | GAGTCAACGGATTTGGTCGT | TTGATTTTGGAGGGATCTCG |

2.1.3.4 GuideRNAs

| gRNA | Sequence (with PAM) |
|-----------|-------------------------|
| gRNA Nek8 | ACAAGGCTTGGCGACTAAGCAGG |

2.1.3.5 siRNAs

| siRNA | Sequence | Supplier |
|-------------------|----------------------|---|
| Human GAPDH | Not available | Ambion |
| Human Inversin 05 | GCACUGGGCAGCUUUUUAUA | LQ-012523-00-0002, 2 nmol, Dharmacon |
| Human Inversin 06 | GAGAACACCACUUAUGUAU | |
| Human Inversin 07 | GAGCAAGGGUAGAUCUAGU | |
| Human Inversin 06 | GCAAGAGUCUACAGCAUUG | |

2.1.4 Antibodies

2.1.4.1 Primary antibodies

Where known, final antibody concentrations are shown in brackets behind dilutions.

| Antibody | Species | Dilution | Supplier |
|-------------------------|---------|------------------------------|-----------------------------------|
| α -tubulin | mouse | IF 1:1,000 (0.2 μ g/ml) | T5168, Sigma-Aldrich |
| Acetylated-tubulin | mouse | IF 1: 1,000 | T6793, Sigma Aldrich |
| CenpA | mouse | IF 1: 1,000 (0.5 μ g/ml) | ab13939, Abcam |
| Flag M2 | mouse | WB 1: 1,000 IF 1: 1,000 | F3165, Sigma-Aldrich |
| γ H2AX (pSer139) | mouse | IF 1,000 (0.5 μ g/ml) | Abcam |
| γ -tubulin | mouse | IF 1: 1,000 | T6557, Sigma Aldrich |
| γ -tubulin | rabbit | IF 1:500 | T3559, Sigma-Aldrich |
| γ -tubulin | goat | IF 1: 200 | sc-7396, Santa Cruz |
| GAPDH | rabbit | WB 1: 1,000 | 14C10, Cell Signalling Technology |
| HA-tag | rabbit | WB 1: 1,000 IF 1: 500 | C29F4, Cell Signalling |
| His | mouse | WB 1: 1,000 | H1029, Sigma Aldrich |
| Inversin | goat | WB 1:500 IF 1:250 | sc-8719, Santa Cruz |
| Ki67 | mouse | IF 1:1,000 | clone MIB-1, Dako |
| pNek8 | rabbit | WB 1:500 IF 1: 500 | Prof Richard Bayliss |
| p-Rb (Ser807/811) | rabbit | WB 1: 1,000 | 9308, Cell Signalling |
| 53BP1 | rabbit | IF 1: 500 | ab21083, Abcam |

2.1.4.2 Phospho-Inversin antibodies

| Antibody | Rabbit | Concentration after dilution | Supplier |
|--------------|--------|------------------------------|----------|
| T121 batch 1 | | 0.32 μ g/ μ l | |

| | | | |
|---------------|---|------------|--------|
| | | | |
| pT121 batch 1 | | 0.39 µg/µl | |
| T324 batch 1 | | 0.2 µg/µl | |
| pT324 batch 1 | 1 | 0.18 µg/µl | |
| T359 batch 1 | | 0.44 µg/µl | |
| pT359 batch | | 0.35 µg/µl | |
| T121 batch 2 | | 0.23 µg/µl | |
| pT121 batch 2 | | 0.3 µg/µl | |
| T324 batch 2 | | 0.2 µg/µl | |
| pT324 batch 2 | | 0.2 µg/µl | |
| T359 batch 2 | 2 | 0.32 µg/µl | |
| pT359 batch 2 | | 0.3 µg/µl | |
| | | | AMSBIO |

2.1.4.3 Secondary antibodies

Where known, final antibody dilutions are shown in brackets behind dilutions.

| Antibody | Dilution | Supplier |
|--|------------------|------------|
| Donkey anti-mouse IgG Alexa 594 | 1:200 (10 µg/ml) | Invitrogen |
| Donkey anti-rabbit IgG Alexa 488 | | |
| Donkey anti-goat Alexa IgG 647 | | |
| Goat anti-mouse horseradish peroxidase conjugate (HRP) | 1: 1000 | Sigma |
| Goat anti-rabbit HRP | | |
| Donkey anti-goat HRP | | |

2.1.5 Cell lines

Growth media was supplied by Invitrogen Life Sciences (Paisley, UK).

| Cell line | Growth Media | Freezing media |
|--|---|---|
| HeLa (immortalised Henrietta Lacks cervical cancer cells) | DMEM (Dulbecco's Modified Eagle Medium) 10% v/v FBS 1% v/v Pen/Strep (100 IU/ml penicillin and 100 µg/ml streptomycin) | Growth media + 40% v/v FBS + 10% v/v DMSO |
| hTERT-RPE1 (hTERT immortalised retina pigmented epithelium cells) | DMEM-Ham's F12 (1:1) (L-Glutamate 15mM HEPES) 10% v/v FBS 1% v/v Pen/Strep (100 IU/ml penicillin and 100 µg/ml streptomycin) 7.5% NaHCO ₃ | Growth media + 50% v/v FBS + 20% v/v DMSO |
| mIMCD3 (mouse inner medullary collecting duct cells) | DMEM-Ham's F12 (1:1) (L-Glutamate 15mM HEPES) 10% v/v FBS 1% v/v Pen/Strep (100 IU/ml penicillin and 100 µg/ml streptomycin) | Growth media + 40% v/v FBS + 10% v/v DMSO |
| HK2 (human kidney cells) | DMEM-Ham's F12 (1:1) 10% v/v FBS 1% v/v Pen/Strep (100 IU/ml penicillin and 100 µg/ml streptomycin) | Growth media + 40% v/v FBS + 5% v/v DMSO |
| HEK293T cells (Human embryonic kidney cells 293T) | DMEM (Dulbecco's Modified Eagle Medium) 10% v/v FBS | Growth media + 40% v/v FBS + 10% v/v DMSO |

| | | |
|--|--|--|
| | 1% v/v Pen/Strep (100 IU/ml penicillin and 100 µg/ml streptomycin) | |
|--|--|--|

2.1.6 Radioisotopes

| Isotope/ Activity | Specific activity | Supplier |
|-----------------------------------|-------------------|----------------------------|
| [γ - ³² P]-ATP | 111 TBq/mmol | Perkin Elmer, Waltham, USA |

2.1.7 Kinases

| Kinase | Supplier |
|---------------|---|
| Nek3 | 14-694, Merck Millipore |
| Nek5 | SRP5328, Sigma |
| Nek6 | 14-578, Merck Millipore |
| Nek8 | N10-11G, SignalChem |
| In-house Nek8 | Provided by the Bayliss lab (University of Leicester) |

2.1.8 Small molecule inhibitors

| Inhibitor | Supplier |
|-----------|---|
| CCT137690 | 15552, Cayman Chemical |
| CCT129932 | Provided by the Bayliss lab (University of Leicester) |

2.2 Methods

2.2.1 Molecular biology

2.2.1.1 Plasmid construction

Nek8 and Inversin constructs were generated in bacterial expression vectors for protein purification or mammalian expression vectors for transfection into eukaryotic cells. Vectors were provided by the Protein Expression Laboratory (PROTEX) at the University of Leicester (2.1.2).

Forward and reverse primers were designed to have a 5' pLEICS vector homology region and a 3' insert homology region of 18-24 nucleotides with a GC:AT ratio of approximately 50% to ensure an annealing temperature $\sim 74^{\circ}\text{C}$. Primer sequences for the different constructs are shown in 2.1.3.

Cloning was performed by PROTEX using the PCR primers and the pLEICS vectors. Nek8 was sub-cloned from an existing in-house clone (originally cloned from the German cDNA Consortium (RZPD), clone DKFZp434NO419), whereas an Inversin clone was ordered from GE Healthcare (MGC Human Inversin isoform 1, BC111761). Briefly, standard PCR reactions were performed, followed by transformation of the DNA into DH5 α *E. coli* cells, and minipreps of plasmid DNA.

2.2.1.2 Transformation of plasmid DNA into bacteria

For protein purification, bacterial expression vectors were transformed into competent Arctic Express (DE3) RIL *E. coli* cells (Agilent Technologies). For mammalian transfections, eukaryotic expression vectors were transformed into competent DH5 α *E. coli* cells. 2 μg of plasmid DNA and 30 μl bacteria were mixed by carefully flicking the side of the Eppendorf tube and incubated on ice for 30 min, followed by a heat shock at 42°C for 1 min to induce DNA uptake and a second incubation on ice for 2 min. Under sterile conditions, 450 μl of SOC media (Invitrogen) was added and the tube was incubated in a shaking incubator at 37°C and 225 rpm for 1 h. Under sterile conditions, 250 μl was streaked out on Luria Broth (LB) agar plates (17 mM NaCl, 0.5% w/v yeast extract, 1% w/v tryptone, 10 mM Tris pH 7.5, plus 2% w/v agar) containing the appropriate antibiotics (ampicillin at 100 $\mu\text{g}/\text{ml}$, kanamycin at 50 $\mu\text{g}/\text{ml}$, chloramphenicol at 100

µg/ml). After allowing the bacteria suspension to dry into the agar at RT, plates were incubated upside down at 37°C over night.

2.2.1.3 Generation of plasmid DNA by Maxiprep

For purification of large quantities of plasmid DNA, maxipreps were performed using the QIAfilter Plasmid Maxi kit (Qiagen). Briefly, single colonies were picked from LB agar plates and incubated in 5 ml of LB media containing the appropriate antibiotics for 5 h at 37°C and 225 rpm. This starter culture was then used to inoculate 100 ml of LB with the appropriate antibiotics and incubated at 37°C and 225 rpm overnight. After collecting cells by centrifugation at 6000x g for 15 min at 4°C, maxipreps were performed according to the manufacturer's protocol. Purified plasmid DNA was resuspended in dH₂O and the DNA content was determined by measuring the absorbance at 260 nm of 1 µl of DNA in 49 µl of dH₂O against a blank containing only dH₂O using the BioPhotometer Plus (Eppendorf). Plasmid stocks were diluted to 1 µg/µl and stored at -20°C for further use.

2.2.1.4 Sequencing of plasmid DNA

To validate sequence integrity of plasmid DNA, Sanger-based sequencing was performed by the Protein Nucleic Acid Chemistry Laboratory (PNACL) at the University of Leicester using their in-house vector specific primers. DNA was submitted and automated sequencing was performed. The data were analysed using the CLC free workbench viewer 6 (CLCbio).

2.2.1.5 Site-directed mutagenesis

Oligonucleotides were designed to introduce mutations into the mammalian and bacterial expression constructs. Primer sequences are shown in 2.1.3.2. The PCR reaction was set up using the GoTaq Green Master Mix (Promega) containing 1 U GoTaq DNA Polymerase in reaction buffer at pH 8.5, 400 µM dNTP mix, 3 mM MgCl₂ and yellow and blue loading dyes. 200 nM forward primer, 200 nM reverse primer and 200 ng DNA template were added to the reaction. Mutagenesis PCR cycles consisted of an initial denaturation step at 94°C for 2 min, followed by 30 cycles of denaturation at 94°C for 1.5 min, annealing at the T_m of the primer minus 5°C for 2 min, and extension at 68°C

for 1 min per kb of the PCR product. This was followed by a final step of extension at 68°C for 10 min. DNA was then transformed into XL 10-Gold Ultracompetent *E. coli* cells (Agilent Technologies) following the manufacturer's instructions.

2.2.2 Cell biology techniques

2.2.2.1 Maintenance of cell lines

Adherent human and mouse cell lines were cultured in 10 cm dishes in 10 ml growth media as indicated in 2.1.5. Media was supplemented with 10% v/v heat inactivated foetal bovine serum (FBS) (Invitrogen) and penicillin-streptomycin (Pen/Strep) (100 U/ml and 100 µg/ml, respectively) (Invitrogen). Cell lines were kept in an incubator at 37°C and 5% CO₂ and passaged when they reached approximately 80% confluency. For this, media was aspirated, and cells were washed once with 2.5 ml of phosphate buffered saline (PBS) (137 mM NaCl, 2.7 mM KCl, 8.1 mM Na₂HPO₄, 1.5 mM KH₂PO₄, pH 7.4). Cells were then detached by adding 2.5 ml of 0.05% Trypsin/EDTA (Invitrogen) for 5 min at 37°C and 5% CO₂. After incubation, cells were washed off the plates by adding 7.5 ml of fresh pre-warmed media, seeded in appropriate dishes with fresh, pre-warmed media, and cultured at 37°C and 5% CO₂.

2.2.2.2 Long term storage of cell line stocks

For long term storage, cells were cryopreserved in liquid nitrogen. After trypsinising, cells were collected by centrifugation at 1,100 rpm for 5 min. The cell pellet was then re-suspended in freezing media indicated in 2.1.5 and 1 ml of cell suspension was transferred to cryotubes (TPP Helena Biosciences). Tubes were then incubated at -20°C for 24 h, before being transferred to -80°C for another 24 h, and storage in liquid nitrogen.

To culture cells, a cryotube was thawed in a warm water bath at 37°C and added to a 10-cm dish containing 10 ml of fresh, pre-warmed growth media. The media was changed the next day by aspirating the old media, washing cells once with PBS and adding fresh, pre-warmed growth media.

2.2.2.3 Serum starvation of cells

For experiments under serum starved conditions, cells were cultured in media containing 0% FBS for 48 h if not otherwise stated. For this purpose, growth media was aspirated, cells were washed twice with PBS, and then fresh pre-warmed media without FBS was added. Cells were then incubated at 37°C and 5% CO₂.

2.2.2.4 Transient transfection of mammalian cells

Cultured cells were transiently transfected with eukaryotic expression constructs using Lipofectamine2000 (Invitrogen). Cells were seeded in appropriate dishes to reach 80% confluency on the day of transfection. If cells were to be transfected under serum starved conditions, media was changed to growth media without FBS 24 h prior to transfection. On the day, growth media was changed by washing cells twice with PBS and adding growth media without FBS or Pen/Strep. Two Eppendorf tubes containing appropriate amounts of Opti-MEM (Invitrogen) were prepared and plasmid DNA was added to one tube, whereas Lipofectamine2000 was added to the second tube in a 1 µg: 4 µl ratio. For transfection of cells in 6-well plates, 1 µg of DNA was used, and for transfection of cells on 10 cm dishes, 4 µg of DNA was used. Eppendorf tubes were incubated for 5 min at RT, before gently being mixed together and incubated for another 20 min at RT. The transfection mix was then added drop-wise to cells in media without FBS or Pen/Strep and incubated at 37°C and 5% CO₂ for 4 h before adding 10% FBS to cells (except where serum starvation was performed) and a further 20 h incubation at 37°C and 5% CO₂. Cells were then processed for further studies as required.

2.2.2.5 Transient transfection of siRNA oligonucleotides

RPE1, HeLa and IMCD3 cells were seeded in growth media containing 10% FBS and incubated over night at 37°C and 5% CO₂ until 50% confluency was reached. Prior to performing the transfections, the workplace was cleaned with RNaseZap (Sigma Aldrich). Cells were then transfected using Lipofectamine as described in 2.2.2.4 using 100 nM of siRNA oligonucleotide for a 10 cm plate. Cells were incubated for 48 h before whole cell lysates were generated.

2.2.2.6 Drug treatments of cells

RPE1 cells were treated with small molecule inhibitors of Nek8 kinase activity at doses stated in the text. 24 h prior to fixing and processing for immunofluorescence microscopy. If cells were treated under serum starved conditions, media without FBS was added 24 h prior to treatment with the inhibitors. For DNA damage studies, cells were treated with the inhibitor 4h prior DNA damage induction with 1.6 nM Aphidicolin (A0781, Sigma) in complete media for 20 h.

2.2.2.7 Immunofluorescence microscopy

Cells were grown on acid-etched glass coverslips in 6-well plates. For cilia staining, plates were transferred from the incubator straight onto ice for 25 min to disrupt the microtubule background. Cells were then washed twice with PBS (except phospho-specific antibodies) or TBS (only phospho-specific antibodies) (Tris buffered saline, 50 mM Tris- HCl pH 7.5, 150 mM NaCl, dH₂O), before being fixed in ice-cold methanol for at least 30 min at -20°. Cells were washed again three times in PBS or TBS (as above) and blocked for 30 min in either PBS or TBS containing 2% w/v BSA (bovine serum albumin, Fisher Scientific), 0.2% v/v Triton and 0.1% v/v Tween. After blocking, cells were incubated with the primary antibody in blocking solution for 1 h at RT. Cells were then washed again three times in PBS or TBS and incubated with appropriate secondary antibodies and 0.8 µg/ml Hoechst 33258 (Calbiochem) in blocking solution for another hour in the dark and washed again three times in PBS/TBS. Coverslips were then mounted upside down on glass microscope slides (VWR) with a drop of mounting solution (80% v/v glycerol, 3% w/v n-propyl gallate, PBS) and were sealed with nail varnish. Fluorescence microscopy was performed using the Leica TCS SP5 laser scanning confocal microscope equipped with a Leica DMI 6000B inverted microscope using a Plan Apo 63x oil objective (NA 1.4). Single z-stacks were taken to create merged images, which were processed using the Leica LAS AF software and PowerPoint.

2.2.2.8 Proximity ligation assay

To determine whether two proteins localise within close proximity in the cell, a proximity ligation assay (PLA) was performed using the Duolink In Situ Fluorescence

proximity ligation assay kit. Briefly, cells were seeded on acid-etched glass coverslips in a 24-well plate and treated as required. Cells were then fixed in ice-cold Methanol as above and incubated with primary antibodies for 1h in a humidity chamber at 37°C. After three washes in PBS, cells were incubated with PLA probes in the humidity chamber for 1h at 37°C. PLA probes bind the species-specific part of the primary antibody and contain either a minus or plus strand oligonucleotide that form a ring and act as a primer for rolling circle DNA amplification. PLA probes were diluted 1:5 in blocking buffer (as above) and incubated at RT for 20 min before use. Cells were washed two times for 5 min at RT in Wash Buffer A (part of the kit), before being incubated with a ligase (diluted 1:5 in high purity water) for 30 min in the humidity chamber at 37°C to ligate minus and plus strands of the PLA probes. Cells were then washed twice for 2 min in Wash Buffer A at RT, before being incubated with the Polymerase (diluted 1:5 in high purity water) for 100 min in the humidity chamber at 37°C to amplify PLA probe strands in a rolling circle reaction. Cells were then washed twice in Wash Buffer A for 10 min at RT and once in 0.01% Wash Buffer B for 1 min, before mounting on microscope slides.

2.2.2.9 3D cell culture

Mouse IMCD3 and human HK2 cells were grown in Matrigel (BD Biosciences) as 3D spheroids to better mimic organ structures. Briefly, cells were trypsinised and diluted to 10,000 cells in 165 µl of full growth media. Matrigel was thawed on ice and 165 µl were gently pipetted and mixed with the 165 µl cell suspension in one well of an 8-well chamber slide (Thermo Fisher). The Matrigel-cell-mix was allowed to settle for 15 - 30 min at RT, before drop-wise adding 500 µl of full media. The chambers were then incubated at 37°C and 5% CO₂. The following day, media was changed by carefully pipetting the old media from one corner of the chamber, and adding 500 µl fresh media drop wise, before a further incubation at 37°C and 5% CO₂ over night. On Day 3 and 4, media was changed as above to media without FBS, and cells were incubated until spheroid formation could be observed under the light microscope. Cells were then fixed by washing them twice in 500 µl DPBS (Sigma), before adding 500 µl 4% PFA (paraformaldehyde) for at least 30 min to digest the Matrigel and fix the spheroids to the bottom of the chamber. PFA was changed every 30 min until all Matrigel was

digested. Cells were then washed three times quickly, and twice for 5 min on a rocker in DPBS, before adding 250 µl permeabilisation buffer (7 mg/ml gelatine, 0.5% v/v Triton-X100, DPBS) for 30 min at RT. 500 µl primary antibody solution in permeabilisation buffer were then added overnight at 4°C. The following day, cells were washed once quickly and three times for 10 min in 500 µl permeabilisation buffer, before incubation overnight with 500 µl secondary antibody in permeabilisation buffer at 4°C in the dark. The following day, cells were washed again once quickly and three times for 10 min in permeabilisation buffer, before incubation with 1 drop of DAPI (NucBlue Fixed Cell ReadyProbes Reagent, Thermo Fisher) for 15 min in the dark. Cells were then washed three times for 10 min in permeabilisation buffer, and incubated twice for 5 min in DPBS. After carefully taking off all the liquid, chambers were sealed with one drop of Fluoromount (Sigma) overnight at RT in the dark. Cells were then ready to be analysed by fluorescence microscopy using the Leica TCS SP5 laser scanning confocal microscope equipped with a Leica DMI 6000B inverted microscope using a Plan Apo 63x oil objective (NA 1.4). Obtained images of single and merged z-stacks were processed using the Leica LAS AF software.

2.2.2.10 Flow cytometry

To determine the population of cells in different stages of the cell cycle, cells were prepared for propidium iodide (PI) staining. Briefly, cells were harvested by trypsinising and centrifugation at 1,100 rpm for 5 min. Cell pellets were washed once in PBS, centrifuged, and re-suspended in 200 µl PBS. To fix cells, ice-cold 70% ethanol was added drop-wise while vortexing the cell suspension carefully to avoid cells clumping together. Cells were then stored at -20°C for a minimum of 30 min. Cells were centrifuged at 3,000 rpm and 4°C for 5 min and washed twice with PBS to remove residual ethanol. The washed cell pellet was resuspended in PI solution (50 µg/ml PI, 100 µg/ml RNase A, PBS), transferred to FACS tubes (Corning Science), and incubated at 4°C over night. The next day, the DNA content of 10,000 cells was measured using the BD FACSCanto™ II flow cytometer and data were analysed using the FACSDiva™ 6.0 software (Becton Dickinson).

2.2.2.11 Generation of a CRISPR cell line

RPE1 knock out cell lines for Nek8 were generated by Prof Kouji Hirota and Koji Kobayashi from the Tokyo Metropolitan University. To generate RPE1 knock out cell lines with CRISPR, Prof Hirota's group designed three vectors (see Fig. 2.1). The first one is the CRISPR vector (pX330) that carries the Cas9 nickase and the guide RNA (gRNA). The gRNA is specifically designed as a homologue to the Nek8 gene. Specificity of it was tested using the CRISPR web tool. The gRNA also carries a PAM sequence (NGG) which once aligned with the genomic DNA at the Nek8 gene locus, acts as a docking point for Cas9 to nick the genomic DNA. Two KO vectors were designed to insert resistance gene into the nicked NEK8 gene locus in the genomic DNA by homology directed repair. KO vector number one carries a neomycin resistance gene that inserts into the first allele and KO vector number 2 carries a puromycin resistance gene that inserts into the second allele. The following was performed by Koji Kobayashi under my supervision in the Fry laboratory. Briefly, RPE1 cells were transfected using electroporation in growth media without Pen/Strep and FBS with all three vectors using the Neon transfection system (Thermo Fisher) according to the manufacturer's protocol. Cells were then incubated for 24 h at 37°C and 5% CO₂ and treated with 2 µg/ml Puromycin and 1 mg/ml Neomycin to select for cell clones that had both Nek8 alleles replaced with the resistance genes. Cells were incubated and observed for another five to seven days until single cell colonies could be observed. These cells were separated and grown in growth media up to full confluency before being seeded for experiments.

2.2.2.12 qRT-PCR and agarose gel electrophoresis

To test the success of the Nek8 CRISPR cell line generation, quantitative reverse transcription (qRT) - Polymerase chain reaction (PCR) was performed using primers that amplified the KO gene locus, as well as a control gene locus for the housekeeping gene GAPDH. RNA was extracted from RPE1 WT and KO cells by adding 1 ml TRI reagent (Sigma) to a pre-washed 10 cm plate. Cells were scraped into an Eppendorf tube and incubated for 5 min at RT. 200 µl chloroform were added and the cell suspension was mixed by vigorously shaking the tube for 15 sec, before incubating it for 10 min at RT and centrifugation at 12,000xg for 15 min at 4°C. The upper phase containing the RNA

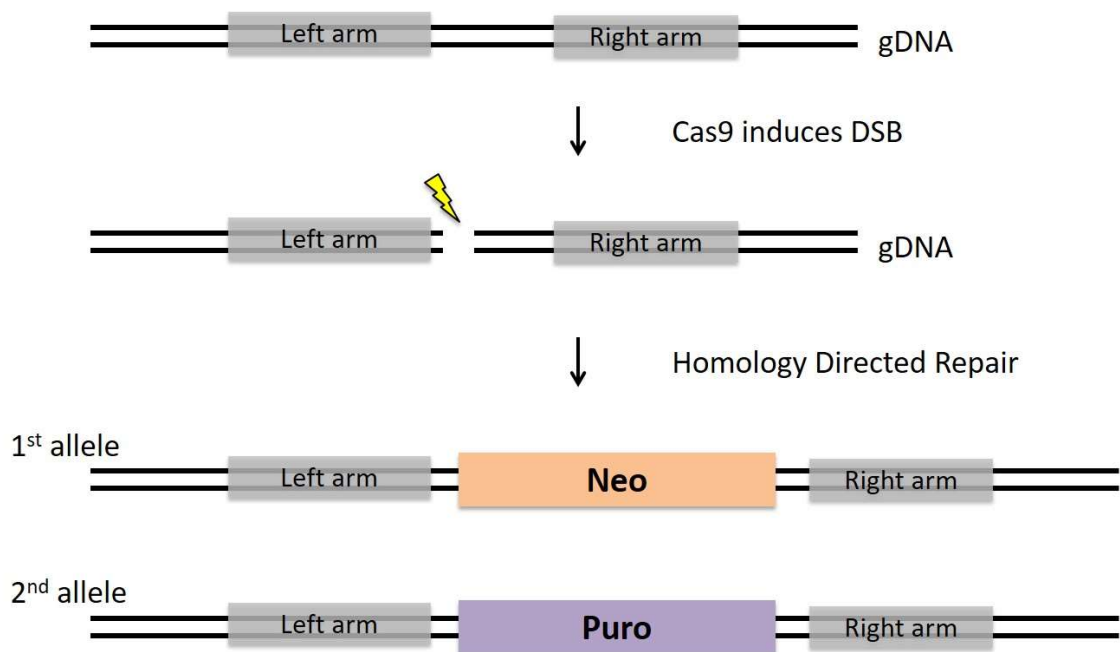


Figure 2.1 Schematic of the insertion of resistance markers into the CRISPR gene locus

The CRISPR vector introduces a double strand break of the genomic DNA (gDNA) at the Nek8 gene locus. Two KO vectors introduce the marker genes neomycin and puromycin into the two alleles of the nicked Nek8 gene for selection purposes.

was collected and mixed with 500 µl isopropanol. Samples were incubated for 5 min at RT, before being centrifuged at 12,000xg for 10 min at 4°C. The pellet was then washed in 1 ml 75% ethanol, centrifuged at 7,500xg for 10 min at 4°C, and dried at RT. Dried RNA was then resuspended in 20 µl dH₂O for 10 min at 55°C and RNA content was measured using a Spectrometer at 260 nm. Reverse transcription of the RNA into cDNA was performed using the Superscript III reverse transcriptase kit (Invitrogen). Briefly, between 2 µg and 5 µg of RNA were incubated with 1 µl of 10 mM dNTP, 1 µl Oligo dt 500 ng and up to 13 µl dH₂O to provide a reaction volume of 20 µl. Samples were then incubated at 65°C for 5 min and on ice for 1 min, before adding 4 µl 5x Buffer, 1 µl 0.1M DTT, 1 µl RNase Out, and 1µl Superscript III reverse transcriptase. Reverse transcription was performed for 1 h at 50°C, before inactivating the enzyme at 70°C for 15 min. cDNA was stored at -20°C or used directly for PCR analysis. Per sample 5 µl of cDNA were used in a reaction mix containing 2 µl 10x Polymerase Buffer (Invitrogen), 0.5 µl MgCl₂, 1 µl 20 µM forward primer, 1 µl 20 µM reverse primer, 2 µl 10 mM dNTP, 0.2 µl Taq Polymerase (Invitrogen), 14.8 µl dH₂O. PCR cycles consisted of an initial denaturation step at 94°C for 2 min, followed by 35 cycles of denaturation at 94°C for 1.5 min, annealing at 50°C for 2 min, and extension at 72°C for 2 min. This was followed by a final step of extension at 72°C for 10 min. 15 µl of samples were then analysed on a 10% agarose gel (10% agarose in 1x TBE buffer (0.1 M Tris, 0.1 M Boric Acid, 2 mM EDTA, dH₂O, 1 drop EtBr) in TBE buffer next to a 1 kb DNA ladder (Thermo Fisher). Gel electrophoresis was performed at 80 mA for 1 h and gel bands were analysed under UV light.

2.2.2.13 Cell proliferation curve

RPE1 cells were detached from a 10 cm plate as described in 2.2.2.1 and transferred to a 15 ml falcon tube. Cells were then collected by centrifugation at 1,100 rpm for 5 min and the pellet was resuspended in 1 ml PBS. The cell number per millilitre was calculated by pipetting 5 µl of cell suspension onto a Haemocytometer and estimating the average number of cells in four squares and multiplying it by 10⁶. 100,000 cells were then seeded on 6 cm plates and their cell number was calculated as above after 24, 48, 72, 96 and

120 h. If cell numbers were observed under serum starved conditions, media without FBS was added after 48 h and data were normalised against control, untreated cells.

2.2.3 Biochemistry techniques

2.2.3.1 Preparation of cell lysates

Whole cell lysates were prepared for analysis by SDS-PAGE or interaction studies. Cells were trypsinised and collected by centrifugation at 1,100 rpm for 5 min. Cell pellets were then washed in PBS, before being re-suspended in appropriate amounts of ice-cold RIPA lysis buffer (50 mM Tris-HCl pH 8, 150 mM NaCl, 1% v/v Nonidet P-40, 0.1% w/v SDS, 0.5% w/v sodium deoxycholate) supplemented with 5 mM NaF, 5 mM β -glycerophosphate, 30 μ g/ml RNase A, 30 μ g/ml DNase I, 1x Protease Inhibitor cocktail (PIC), and 1 mM PMSF immediately before use. The cell suspension was incubated on ice for 30 min before being passed 10 times through a 27G needle (Becton Dickinson) to lyse cells. The lysates were then subjected to centrifugation at 13,000 rpm for 10 min at 4°C to remove cell debris. Supernatants were then either processed directly for SDS-PAGE analysis or interaction studies, or snap frozen in liquid nitrogen and stored at -80°C to avoid degradation of proteins.

2.2.3.2 BCA protein assay

Protein concentrations of samples were determined using the BCA protein assay (Bio-RAD). 5 μ l of sample were diluted in 45 μ l of dH₂O. BCA reagents were generated following the manufacturer's instructions and 1 ml was added to the diluted lysate sample. Samples were incubated at 37°C for 30 min and the absorbance was measured at 550 nm against a blank containing dH₂O only. Several different concentrations of bovine serum albumin (BSA) were measured alongside to generate a standard curve from which the protein concentrations of samples could be determined.

2.2.3.3 SDS-PAGE

Protein samples were separated by sodium dodecyl sulphate (SDS)- polyacrylamide gel electrophoresis (PAGE). 10% Resolving gel (40% ProtoFlowgel (30% w/v acrylamide), 375

mM Tris-HCl pH 8.8, 0.1% w/v SDS, 0.13% w/v APS, 0.08% v/v TEMED) and stacking gel (13% ProtoFlowgel (30% w/v acrylamide), 126 mM Tris-HCl pH 6.8, 0.1% w/v SDS, 0.15% w/v APS, 0.1% v/v TEMED) were prepared and pipetted into the Bio-Rad gel electrophoresis system. Samples were boiled in sample buffer (Laemmli buffer, 62.5 mM Tris-HCl pH 6.8, 10% v/v glycerol, 2% w/v SDS, 5% v/v β -mercaptoethanol, 0.01% w/v bromophenol blue) in a 1:1 ratio at 95°C for 10 min. Appropriate amounts of samples in buffer were then loaded on the SDS-PAGE and separated alongside Precision Plus twocolour protein standards (Biorad) at 160 – 180 V for 45 – 60 min in SDS-based running buffer ((0.1% w/v SDS, 25 mM Tris, 192 mM Glycine).

2.2.3.4 Coomassie Blue staining

To visualise the separated proteins following SDS-PAGE, gels were stained with Coomassie Blue (0.25% w/v Brilliant Blue R, 40% v/v IMS, 10% acetic acid) for at least 60 min at RT. This was followed by several incubations in destain (7.5% v/v acetic acid, 25% IMS), which was exchanged every 30 min until bands were clearly visible.

For gels submitted for mass spectrometry, the Coomassie Blue stain and destain were prepared fresh to avoid contamination.

2.2.3.5 Western blotting

For detection of specific proteins following SDS-PAGE, proteins were transferred onto a nitrocellulose membrane via semi-dry electrophoretic blotting. The SDS-polyacrylamide gel, a 0.45 μ m pore size nitrocellulose membrane (Schleicher and Schuell), and six pieces of Whatman 3 MM chromatography paper were soaked in blotting buffer (25 mM Tris, 192 mM glycine, 10 % v/v methanol) and stacked on a TE 77 semi-dry transfer unit (Amersham). Three blotting papers built the base for the nitrocellulose membrane, followed by the SDS-polyacrylamide gel and another three blotting papers. Transfer was carried out for 1 h at 1 mA/cm².

Membranes were then blocked for 30 min at RT in PBST (0.1% v/v Tween-20, PBS) with 5% w/v milk (Skimmed milk powder, Premier Beverages). Membranes incubated with phospho-antibodies were blocked in TBST (0.1% v/v Tween-20, TBS) with 5% w/v BSA (bovine serum albumin, Thermo Fisher) before being incubated with the primary

antibody solution (PBST and milk, or TBST and BSA plus antibodies) for 1 h at RT or overnight at 4°C. Membranes were then washed three times for 10 min at RT in PBST or TBST and incubated with the secondary antibody solution for 1h at RT, before being washed another three times with PBST or TBST. Membranes were then incubated for 1 min with 1 ml of enhanced chemiluminescence (ECL) Western blotting detection solution (Pierce), prepared according to the manufacturer's instructions. In the dark room, X-ray films (Super RX X-ray films, Fuji photo film) were used to visualise the signal emitted by the ECL solution. The X4 X-ray film processor (Xograph imaging system) was used to develop the X-ray films.

2.2.3.6 Immunoprecipitation from cell lysates

24 h after co-transfection or single transfection of cells in 10 cm dishes, cells were lysed and the protein content was measured as described in 2.2.3.2. A 20 µl input sample was then taken and boiled in sample buffer at 95°C for 10 min. The rest of the lysate was incubated overnight at 4°C with a primary antibody generated in mouse and Protein G beads (Sigma), or a primary antibody generated in rabbits and Protein A beads (Sigma). Briefly, depending on the type of antibody, 80 µl of Protein G or A beads were washed three times in 100 µl ice-cold RIPA lysis buffer and centrifuged at 1,000 rpm for 1 min in between washes to pellet the beads, before re-suspending them in 50 µl of RIPA buffer. Primary antibodies were added at 1:500 for 30 min on ice while flicking the Eppendorf tube gently every 10 min. Meanwhile, whole cell lysates were equalised for their protein content and added to the beads/antibody mix. RIPA buffer was added to make up a minimum of 500 µl per sample before incubating them on a rotator at 4°C over night. The following day, beads were collected by centrifugation at 1,000 rpm for 2 min and washed three times with 200 µl ice-cold RIPA buffer and either boiled 1:1 in sample buffer for 10 min at 95°C or used with *in vitro* translated protein.

2.2.3.7 *In vitro* translation and pulldown assay

Flag-Nek8 proteins were *in vitro* translated using the T7 promoter of the pLEICS-13 vector. Briefly, the TNT T7 Quick Master Mix (Promega) was thawed on ice and 8 µl were added to an Eppendorf tube containing 1 µg of the template Flag-Nek8 plasmid and 1 µl

of 1 mM Methionine. The mix was then incubated at 30°C for 90 min. A 2 µl sample was boiled in sample buffer and analysed by SDS-PAGE and Western blotting to confirm expression of the protein. Immunoprecipitates bound to beads were collected by centrifugation at 1,000 rpm and 4°C for 5 min and re-suspended in 500 µl lysis buffer containing 5 µl of IVT protein. Following incubation on a rotator at 4°C for 1-2 h, beads were pelleted by centrifuging them at 1,000 rpm for 5 min at 4°C and washed three times in 100 µl lysis buffer, before re-suspending in 50 µl sample buffer and boiling at 95°C for 10 min. IP samples were then analysed by SDS-PAGE and Western blotting.

2.2.3.8 Purification of the His-Inversin 1-553 protein

His-Inversin 1-553 protein was generated for use as a substrate for *in vitro* kinase assays. To express and purify the His-Inversin 1-553 protein, starter cultures of 50 ml LB media with the appropriate antibiotics were inoculated with a single colony of transformed Arctic express (DE3) RIL *E. coli* cells. After incubation, overnight at 37°C and 225 rpm, a 1 L culture containing the appropriate antibiotics was inoculated with 25 ml of the starter culture and incubated at 37°C and 225 rpm until O.D.₆₀₀ of 0.5-0.8 was reached. Cultures were cooled to RT and then induced with 0.6 mM IPTG and incubated at 18°C and 225 rpm over night. The next day, bacteria were collected by centrifugation at 4,000 rpm at 4°C for 15 min. The bacterial pellet was then stored at -80°C for at least 30 min. The bacterial pellet was then thawed on ice and re-suspended in 15 ml lysis buffer (50 mM HEPES pH 7.5, 300 mM NaCl, 20 mM Imidazole, 5% v/v Glycerol, 0.2 mM MnCl₂, 1 mM MgCl₂, 0.03% v/v DNase, dH₂O). Cells were lysed by sonicating eight times for 10 sec on and 10 sec off on ice before centrifugation at 15,000 rpm at 4°C for 40 min. Samples of the pellet (insoluble fraction) and supernatant (soluble fraction) were taken and boiled in sample buffer for 5 min at 95°C and stored at -20°C. Nickel-NTA Agarose beads (Invitrogen) were washed three times in dH₂O and three times in Buffer A (50 mM HEPES pH 7.5, 300 mM NaCl, 20 mM Imidazole, 5% v/v Glycerol, dH₂O). The supernatant was then incubated with 2 ml of washed Ni-NTA Agarose beads in filter columns (BIO-RAD) at 4°C. The following steps were undertaken at 4°C. The column was placed in an upright position to allow the Nickel-NTA Agarose beads to settle onto the filter and the

lysate to drip through the beads by gravity. A sample of the flowthrough was taken, mixed with sample buffer, boiled and stored at -20°C. The beads were then washed 5 times with 3 ml Buffer A and samples of each wash as well as the beads were collected. Following the washes, the protein was eluted off the beads with 25%, 50%, 75% and 100% of Buffer B (50 mM HEPES pH 7.5, 300 mM NaCl, 250 mM Imidazole, 5% v/v Glycerol, dH₂O) in Buffer A and samples of each elution step were taken. Flowthrough, washes and elutions were stored at 4°C, while 15 µl of the corresponding samples were analysed by 10% SDS-PAGE and Coomassie Blue staining. Where clear bands were detected in the elution fractions, these fractions were pooled and pipetted into a pre-activated dialysis cassette (Slide-A-Lyzer 5 kDa cut-off, Thermo Fisher) using a 26G needle and suspended in dialysis buffer (20 mM HEPES, 5% v/v Glycerol, 5 µM DTT) overnight at 4°C. Prior to use cassettes were activated by incubating them in dialysis buffer for 20 min at 4°C. The following day, concentrating columns (Sartorius stedim biotech, Vivaspin20, 10 kDa cut-off) were pre-cleaned with 20 ml dH₂O and centrifuging at 3,500 rpm at 4°C for 15 min. After taking out a 50 µl aliquot, the dialysed protein was pipetted into the pre-cleaned concentration columns and centrifuged at 3,500 rpm at 4°C for 30 min. This step was repeated until the protein was sufficiently concentrated. After each 30-min spin, the absorbance of the concentrated protein was measured at 280 nm (A₂₈₀) using a Spectrometer to determine the protein concentration by comparing the amino acid sequence with the A₂₈₀ reading (<http://www.mrc-lmb.cam.ac.uk/ms/methods/proteincalculator.html>). The concentrated protein was aliquoted into 50 µl samples, snap frozen and stored at -80°C.

2.2.3.9 Expression and purification of the GST-Inversin proteins

Expression and purification of the GST-tagged C-terminal Inversin proteins was performed by Sophie Millett (University of Leicester). Briefly, Inversin constructs were transformed into BL21 (DE3) RIL *E. coli* cells (Agilent Technologies) and starter cultures were grown at 37°C overnight with appropriate antibiotics. Each starter culture was used to induce two 1 L cultures that were grown to OD₆₀₀ of 0.6 to 0.8 and then induced with 0.5 mM IPTG at 18°C overnight. Bacteria cells were collected by centrifugation at 6,000 rpm for 30 min and the pellet was re-suspended in equilibration buffer (50 mM

Tris-HCl pH 8, 300 mM NaCl, 5 mM DTT, 0.02% v/v NaN₃, 50 μ M EDTA, 100 μ M AEBSF). Cells were lysed on ice by sonication for two times 2 min with 10 sec on and 20 sec off and centrifuged at 15,000 rpm and 4°C for 40 min to clear the supernatant from cell debris. The lysate was then added to 1 ml glutathione beads and incubated at 4°C overnight. The following day, glutathione beads were washed three times with 5 ml equilibration buffer and samples of the flowthrough, washes and beads were analysed by SDS-PAGE and Coomassie blue staining.

2.2.3.10 *In vitro* kinase assays

5 μ g of substrates either bound to beads or in solution were incubated with 40 μ l kinase buffer (50 mM Hepes-KOH pH 7.4, 50 mM MnCl₂, 50 mM β -glycerophosphate, 50 mM NaF, 4 μ M ATP, 1 mM DTT), 1 μ Ci γ -32P-ATP and 100 ng of kinase. Both, the in-house and commercial Nek8 kinase, were pre-incubated in kinase buffer at 30°C for 15 min. Substrates were then added for another 30 min and incorporation of radioactivity was analysed by SDS-PAGE, Coomassie Blue staining, and autoradiography. Non-radioactive kinase assays were performed in buffer containing an additional 6 μ M of ATP. The CCT32 and CCT90 small molecule inhibitors were added at concentrations indicated to the pre-incubation mix of the kinases.

The extent of phosphorylation of substrates at different time points was determined by scintillation count. After autoradiography, corresponding bands were cut out of the Coomassie Blue stained gel and incubated in a cocktail of liquid scintillators that emit photons proportionally to the radioactivity of the sample. This emission is detected by a liquid scintillation counter. Samples were normalised against control substrates.

100 ng of commercial Nek3 (14-694, Merck Millipore), Nek5 (NO7-11G, SignalChem), Nek6 (14-578, Merck Millipore), or in-house Nek8 kinase and 1 μ Ci radioactive γ -32P-ATP as described above. Incorporation of radioactivity was analysed by SDS-PAGE, Coomassie Blue staining and destaining, and autoradiography. Phosphomapping was then performed as described in 2.2.3.12 with the in-house Nek8 kinase.

2.2.3.11 Phosphosite mapping

Mapping of phosphorylated sites in substrate proteins was performed by the University of Leicester Proteomics Facility. Briefly, kinase assays were performed without radiolabeled ATP and the products separated by SDS-PAGE. Following Coomassie Blue staining, relevant protein bands were excised from the gel and submitted for tryptic digestion and MALDI-ToF analysis by the Proteomics Facility. Detected peptides were matched against their amino acid sequence and their detected molecular weight was compared to an estimated molecular weight to locate sites of phosphorylation.

2.2.3.12 Generation of phospho-specific antibodies

Phospho-specific antibodies were designed as 11 amino acid long sequences with 5 amino acids on either side of the phosphorylation site. Sequences were submitted to AMSBIO for peptide synthesis and antibody generation. Briefly, two rabbits were immunised per peptide to generate phospho-specific and non-phospho-specific antibodies. Rabbits were immunised with 250 µg antigen in weeks 0, 2, 5, 6 and 10 and tested for antibody generation in week 6 by ELISA. Production bleeds were then taken in weeks 7, 8, 9, 10 and 11 and Protein G purification was performed, followed by peptide purification for the non-phospho peptide first, followed by incubation with the phospho-peptide. Purity was established by ELISA, Western blotting and dot blots and antibodies were provided in lyophilised form with 0.02% sodium azide for preservation. On arrival antibodies were resuspended in dH₂O and stored at -80°C.

CHAPTER 3 NEK8 AND INVERSIN CONTAIN MULTIPLE SITES OF INTERACTION

3.1 Introduction

Primary cilia are antenna-like structures usually present as a single copy on the surface of almost all eukaryotic cells. They act as mechano-, photo- and olfactory sensors that receive stimuli from the cell's surroundings and transduce these into signalling pathways (Eggenchwiler and Anderson, 2007; Singla and Reiter, 2006). Cilia are microtubule-based structures that harbour a specific set of proteins that is distinct from the cytoplasm (Ringo, 1967). Faulty cilia assembly or cilia signalling can lead to the development of a series of diseases, the so-called ciliopathies (Hildebrandt et al., 2009; Zaghoul and Katsanis, 2009). One of these ciliopathies is the autosomal recessive polycystic kidney disease nephronophthisis (NPHP). NPHP is a heterogenous disease leading to the development of cortico-medullary cysts in the kidney tubules and collecting ducts which eventually lead to kidney failure. NPHP disease proteins have been described to localise to primary cilia and are involved in downstream signalling cascades (Wolf et al., 2015). One of these proteins is NPHP9/Nek8 (Otto et al., 2008).

Nek8 is a member of the NIMA or Nek kinase family of serine/threonine kinases. The *nek8* gene encodes a 692-amino acid long protein with an N-terminal catalytic domain (1-258) and a C-terminal RCC1 (regulator of chromatin condensation) domain (312-692) that folds into a seven-bladed propeller made of β -strands, as well as a coiled-coil domain thought to be involved in protein-protein interactions (Holland et al., 2001). Nek8 has been described to localise to centrosomes and the nucleus in cycling cells, and primary cilia in quiescent cells (Zalli et al., 2011). At the cilia, Nek8 is anchored at the Inversin compartment, a proximal region of the cilium, described to be involved in a complex network of interactions, by direct interaction with Inversin (Shiba et al., 2010).

The *invs* gene encodes four different mammalian splice variants of Inversin, with isoform 1 being a 1065 amino acid long protein that consists of 16 helix-loop-helix ankyrin repeats in the N-terminus (amino acids 1-553) involved in protein-protein interactions

(Lienkamp et al., 2011), and a C-terminus consisting of two IQ domains (amino acids 554-603 and 899-950) that are involved in calmodulin binding (Morgan et al., 2002). A ninein-homology region towards the end of the C-terminus is required for ciliary targeting (Lienkamp et al., 2011). Inversin also contains two D-boxes for potential interaction with the APC/C complex (Lienkamp et al., 2011, Morgan et al., 2002), and a nuclear localisation sequence in the C-terminus (Lienkamp et al., 2011, Nurnberger et al., 2002). Inversin is a key regulator of the canonical Wnt and non-canonical Wnt/PCP (planar cell polarity) pathway, which are downstream cilia signalling pathways involved in proliferation and cell polarity (Simons et al., 2005). Here, Inversin interacts with cytoplasmic Dvl and targets it for APC/C-dependent degradation. In cycling cells, Inversin localises to leading cell edges in a cell cycle dependent manner as part of its function in the PCP pathway (Veland et al., 2013), as well as the nucleus, centrosomes and spindle microtubules in mitotic cells (Nurnberger et al., 2004) and the midbody during cytokinesis (Otto et al., 2002). Inversin has been described to cause NPHP type 2 in humans, an NPHP disease variant with extra-renal manifestations, such as *situs inversus*.

In this chapter, we have generated mammalian Inversin and Nek8 constructs to investigate which regions of these proteins are important for their specific localisation in cycling and quiescent cells. Furthermore, we have performed interaction studies with transfected Inversin and Nek8 constructs to map key interaction sites.

3.2 Results

3.2.1 RPE1 cells exit the cell cycle upon serum starvation in media containing 0% FBS

To investigate the role of Nek8 in cilia-dependent processes, model cell systems would need to be established. Human retinal pigmented epithelial (RPE1) cells that had been immortalised with the human telomerase (hTERT) gene were analysed as these are known to efficiently grow a primary cilium and activate cilia-dependent signalling pathways. To analyse ciliogenesis, RPE1 cells need to exit the cell cycle and enter quiescent, which is achieved by depriving them off nutrients. To confirm this behaviour in our batch, flow cytometry was performed on RPE1 cells grown in media with 10% FBS, as well as cells grown in media containing either 1%, 0.1%, or 0% FBS for 48h (Fig. 3.1A). Media with 0% FBS caused the biggest population of cells to exit the cell cycle, as indicated by the largest increase in the fraction of cells in G1/G0 phase of the cell cycle, increasing from 73.9% in 10% FBS to 94.4% in 0% FBS. Cells grown in media containing 1% and 0.1% FBS had 82.1% and 85.6% of cells in G1/G0 phase, respectively. Exit from the cell cycle upon serum starvation with media containing 0% FBS was confirmed by performing immunofluorescence microscopy with the proliferation marker Ki67. This showed a significant reduction in the population of Ki67 positive cells in the absence of FBS (Fig. 3.1B). Western blotting using an antibody against phosphorylated retinoblastoma protein (p-Rb) as another proliferation marker showed loss of p-Rb expression upon serum starvation with 0% FBS (Fig. 3.1C). Cells were therefore serum starved for 48h in media containing 0% FBS for all further experiments in which we wanted to analyse cells in quiescence.

3.2.2 Inversin localises to cilia in 2D and 3D cell models

Initially, fluorescence microscopy was performed in cycling HeLa cells. This showed localisation of Inversin to stabilised microtubules, as visualised using an acetylated tubulin antibody, including the mitotic spindle and midbody in dividing cells (Fig. 3.2B). RPE1 cells were then used to investigate the localisation of Inversin under serum starved conditions. In these cells, Inversin was found to localise to the primary cilium as visualised by acetylated tubulin staining (Fig. 3.2C).

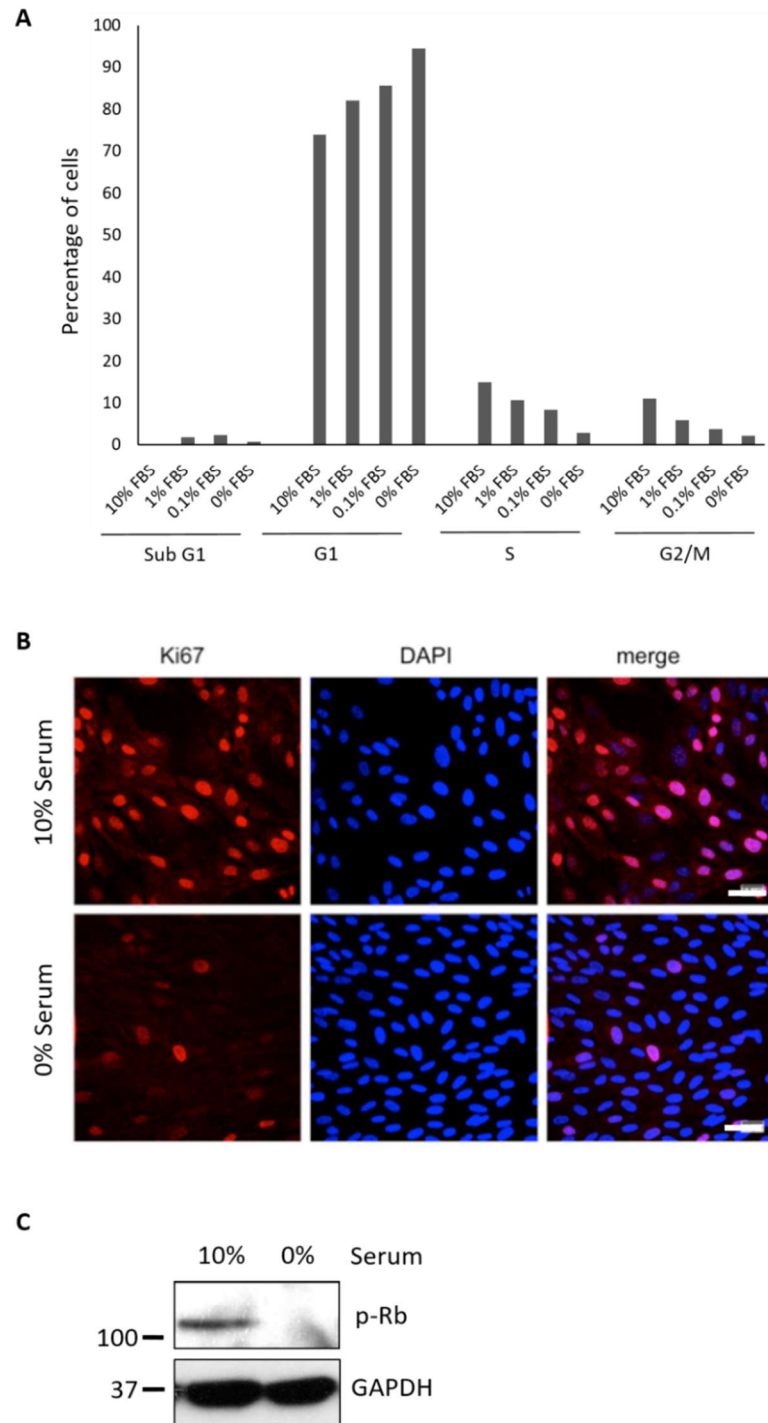


Figure 3.1 RPE1 cells exit the cell cycle upon 48 h serum starvation

A. Cell cycle analysis by flow cytometry of RPE1 cells incubated with media containing 10%, 1%, 0.1%, and 0% FBS for 48h as indicated. **B.** Immunofluorescence microscopy of cycling (10% serum) and serum starved (0% serum) RPE1 cells stained with antibodies against Ki67 (red). DNA was stained with DAPI (blue). Scale bars, 100 μ m. **C.** Western blot analysis with the p-Rb and GAPDH antibodies of lysates prepared from cycling (10% serum) and serum starved (0% serum) RPE1 cells. Molecular weights (kDa) are indicated on the left.

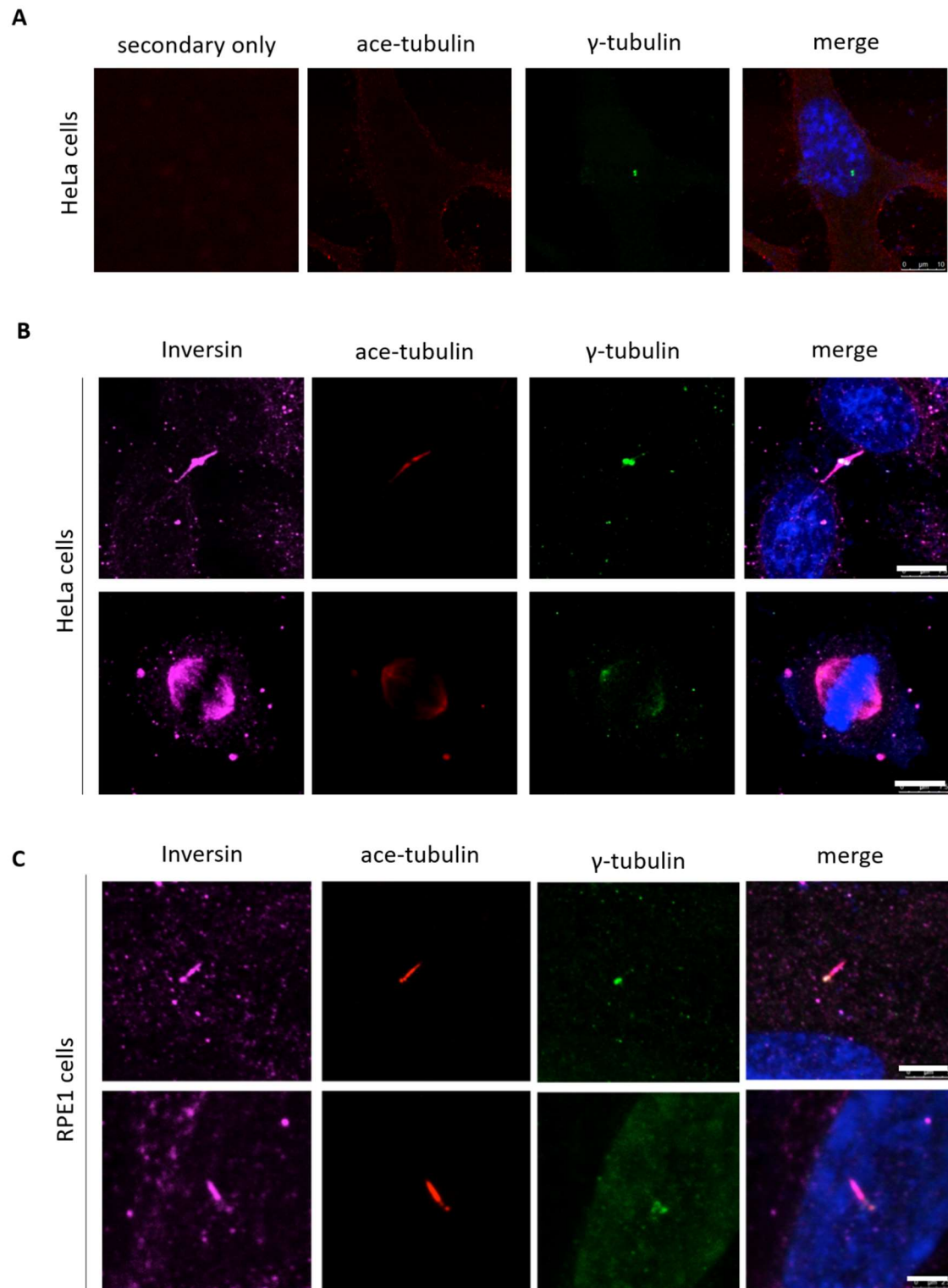


Figure 3.2 Inversin localises with acetylated tubulin in dividing HeLa and quiescent RPE1 cells

Immunofluorescence microscopy of cycling HeLa cells (**A**, **B**) and serum starved RPE1 cells (**C**) stained with antibodies against Inversin (purple, in B, C) or the secondary anti-goat antibody only as a control (**A**), acetylated-tubulin (red) and γ -tubulin (green). DNA was stained with DAPI (blue). Scale bars, 10 μ m (**A**), 7.5 μ m (**B**), and 5 μ m in top row and 2.5 μ m in bottom row of **C**.

As a more complex model system, mouse inner medullary collecting duct (IMCD3) cells were grown in a 3D matrix to form spheroids. IMCD3 spheroids have been previously validated as a good model system for ciliopathies due to mimicking the collecting duct structure (Sang et al., 2011). Cells were seeded in Matrigel and incubated at 37°C and 5% CO₂ for two to three days in full media and then media containing 0% FBS to initiate ciliogenesis until spheroid formation could be observed. Spheroids form around a lumen with cilia pointing inside as shown in Figure 3.3. Immunofluorescence microscopy was performed with antibodies against Inversin and acetylated tubulin to visualise cilia. Whereas an anti-goat secondary antibody only control for the Inversin antibody revealed non-specific staining around the spheroid and along the outline of single cells within the spheroid (Fig. 3.3A), staining with the commercial Inversin antibody revealed specific localisation of the protein with primary cilia within the spheroids, as well as the cell edges. .

These cell models can be used for studies of the role of Nek8 in cilia organisation and cilia-regulated signalling pathways, as well as studying the consequences of NPHP disease or phospho-specific mutants.

3.2.3 Generation of mammalian Inversin and Nek8 constructs

Studies have shown that Inversin anchors Nek8 at the primary cilium (Shiba et al., 2010). To investigate the molecular mechanisms underlying this, subcellular localisation and interaction, constructs were generated for expression in mammalian cells. A construct of the full-length Nek8 protein, a kinase domain construct encoding amino acids 1 to 258 and a C-terminal RCC1 domain construct encoding amino acids 258 to 692 were generated in the pLEICS-12 vector that contains an N-terminal tag consisting of ten Histidine residues and three Flag proteins (Fig. 3.4A). Inversin was divided into an N-terminal Ankyrin repeat construct encoding amino acid 1 to 553 and a C-terminal construct encoding amino acids 554 to 1065. These constructs, as well as full-length Inversin, were sub-cloned into the pLEICS-19 vector with an N-terminal HA-tag (Fig. 3.4B).

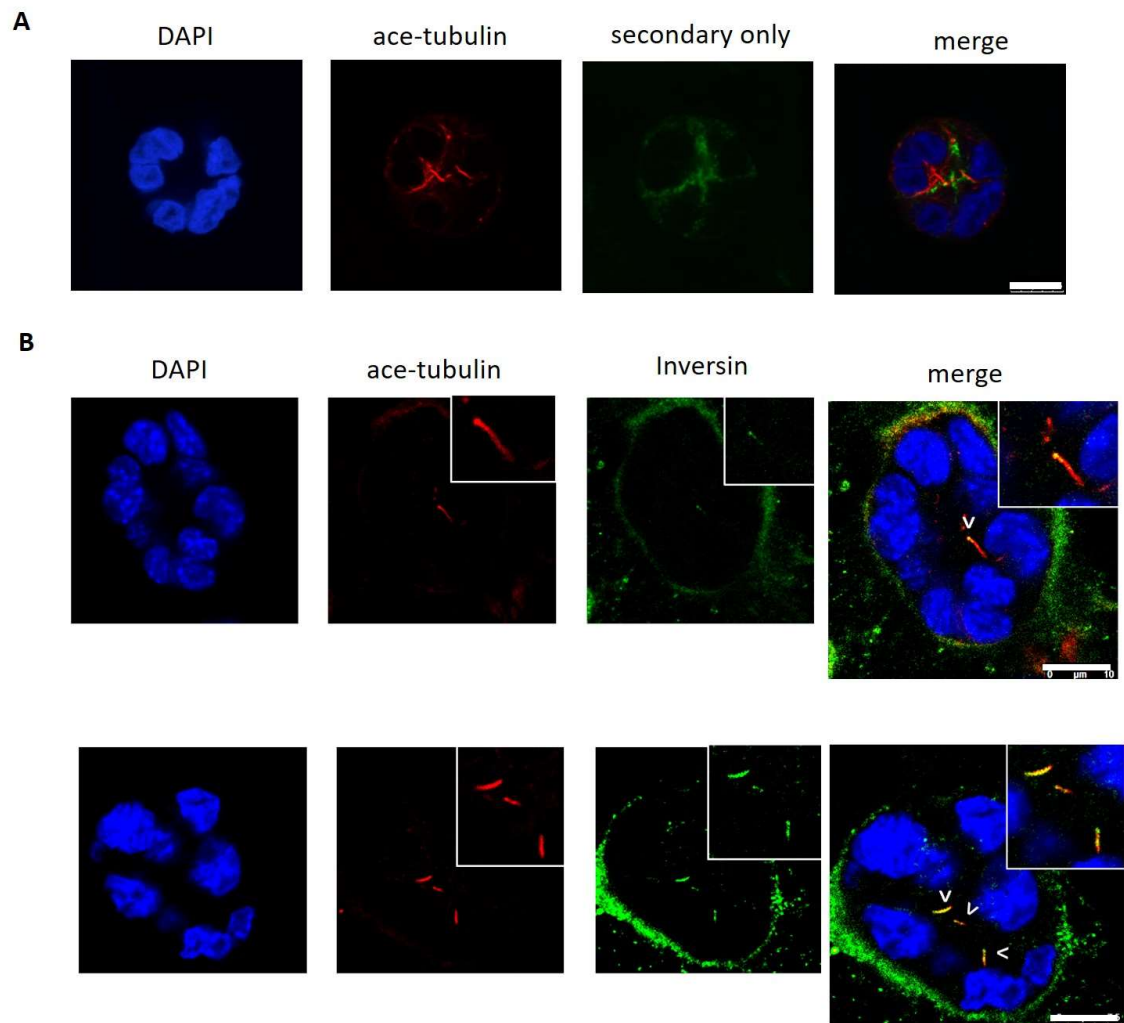


Figure 3.3 Inversin localises to cilia in serum starved IMCD3 spheroids

Immunofluorescence microscopy of serum starved IMCD3 spheroids stained with antibodies against acetylated tubulin (red) and Inversin (green) in **B** or acetylated tubulin (red) and the secondary anti-rabbit only as a control (**A**). Shown are single z-sections of spheroids. Insets show magnified views of representative cilia and arrows are indicating co-localisation of Inversin with acetylated tubulin. DNA was stained with DAPI (blue). Scale bars, 10 μm in top row of **B** and 7.5 μm in bottom row of **B**.

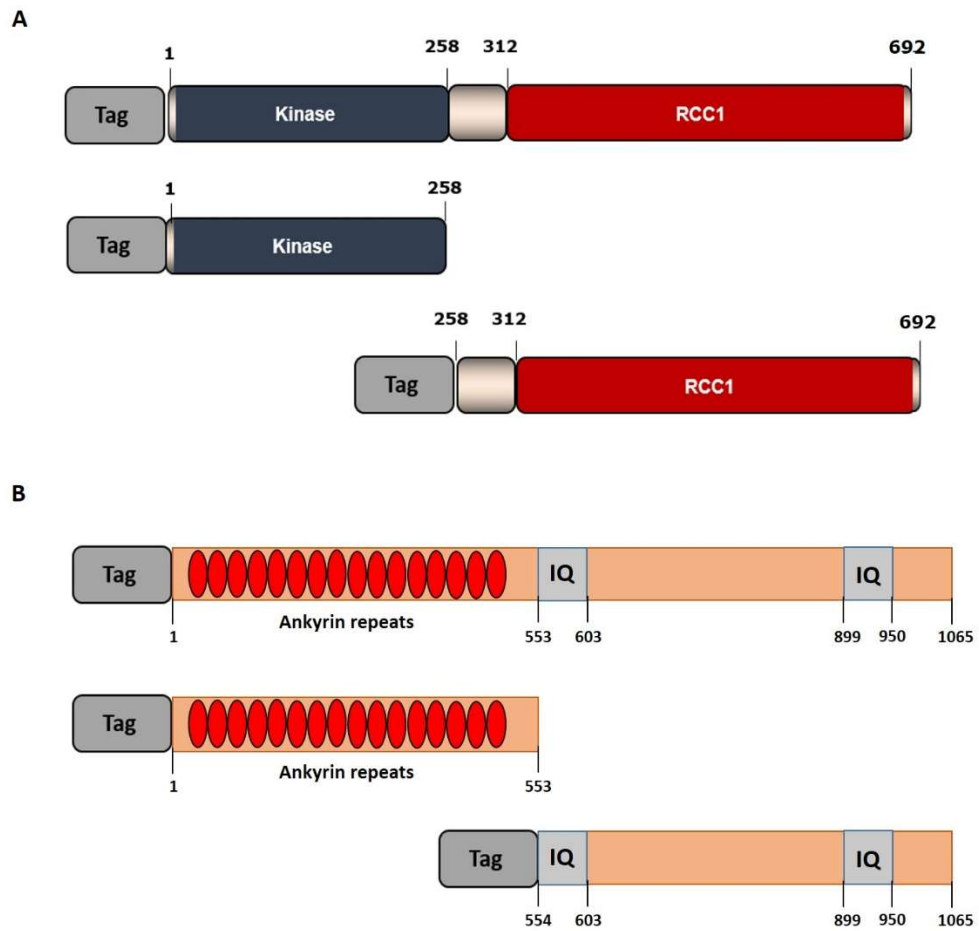


Figure 3.4 Schematic of Nek8 and Inversin constructs used to examine subcellular localisation and interaction

A. Cartoon shows N-terminal tagged versions of full-length Nek8, the N-terminal kinase domain encoding amino acids 1-258 (blue), and a C-terminal RCC1 domain encoding amino acids 258-692 (red). **B.** Cartoon shows N-terminal tagged versions of full-length Inversin, an N-terminal Ankyrin repeat construct encoding amino acids 1-553 (red), and a C-terminal construct encoding amino acids 554-1065 (grey), including the IQ domains (green).

3.2.4 Inversin localises to centrosomes through its C-terminal domain

To investigate subcellular localisation of the Inversin constructs, HA-Inversin FL, HA-Inversin 1-553, and HA-Inversin 554-1065 were transfected into RPE1 cells and analysed by immunofluorescence microscopy with antibodies against the HA-tag and γ -tubulin to visualise centrosomes (Fig. 3.5A). Interestingly, the Inversin FL and C-terminal 554-1065 domain localised to centrosomes, whereas the N-terminal 1-553 domain showed only general cytoplasmic localisation. Counts of 20 cells in three independent transfection experiments showed that the Inversin FL construct localised to centrosomes in 80% of cells, and 100% of cells expressing the 554-1065 construct, whereas 0% of cells expressing the 1-553 construct showed co-localisation with centrosomes (Fig. 3.5B). Thus, we conclude that the active localisation motif is located in the C-terminal 554-1065 domain of Inversin.

To investigate the subcellular localisation of Nek8, RPE1 cells were transfected with Flag-Nek8 FL, kinase domain, and RCC1 domain constructs, before analysis by immunofluorescence microscopy using a Flag-tag antibody (Fig. 3.6). All three constructs localised to the cytoplasm of cycling RPE1 cells, although there was no obvious localisation to the centrosome for any construct. In addition, the Nek8 FL protein and the Nek8 RCC1 domain also localised to the nucleus, whereas the Nek8 kinase domain showed no nuclear staining. Thus, we conclude that the RCC1 domain of Nek8 either harbours a nuclear localisation sequence (NLS) itself or it associates with another protein with an NLS.

3.2.5 Co-immunoprecipitation studies of Inversin fragments with Nek8 suggests multiple sites of interaction

To investigate the sites of interaction of Nek8 with Inversin, several different experimental approaches were undertaken. Representative data for these approaches are shown and discussed in this results section. The first approach was to co-transfect Flag-tagged full-length Nek8 with HA-tagged Inversin constructs encoding the N-

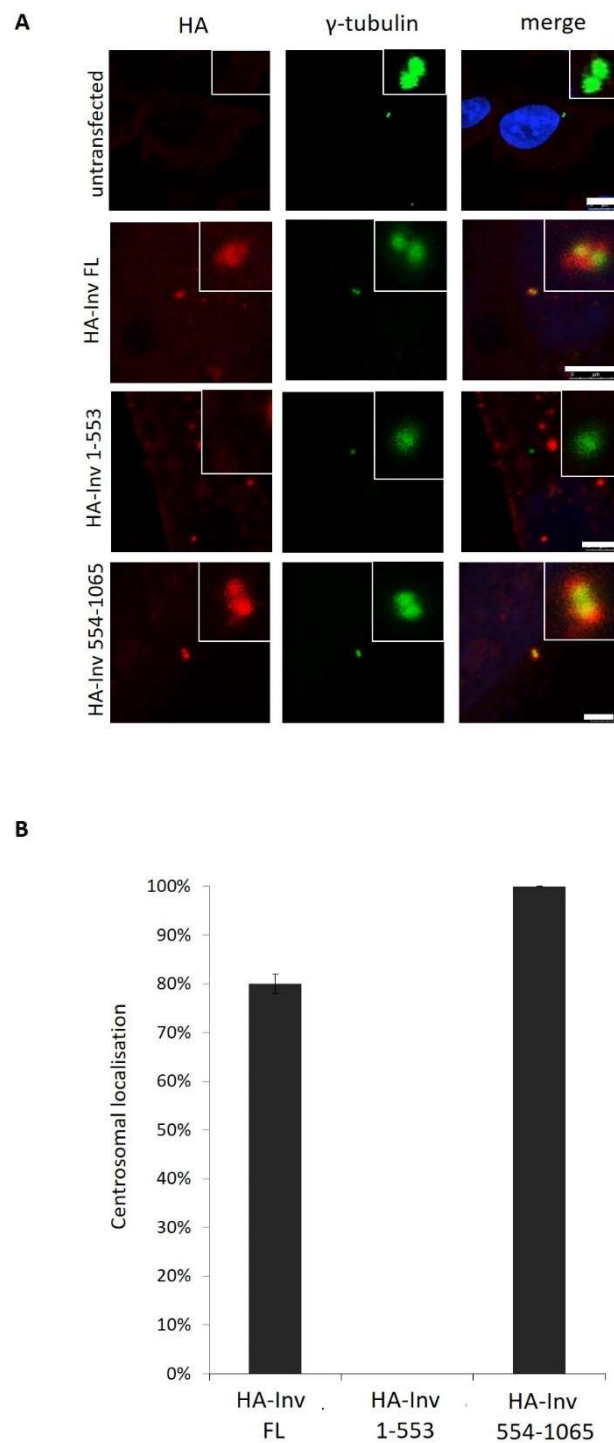


Figure 3.5 The Inversin C-terminus harbours a centrosome-targeting motif

A. Immunofluorescence microscopy of cycling RPE1 cells transfected with the HA-Inversin FL, HA-Inversin 1-553, and HA-Inversin 554-1065 constructs. Untransfected cells were used as controls. Cells were stained with antibodies against the HA-tag (red) and γ -tubulin (green) for centrosomes. DNA was stained with DAPI (blue). Scale bars, 5 μ m in upper row and 2.5 μ m in bottom row. **B.** The presence or absence of the Inversin constructs at centrosomes was scored in three independent experiments, counting 20 transfected cells each.

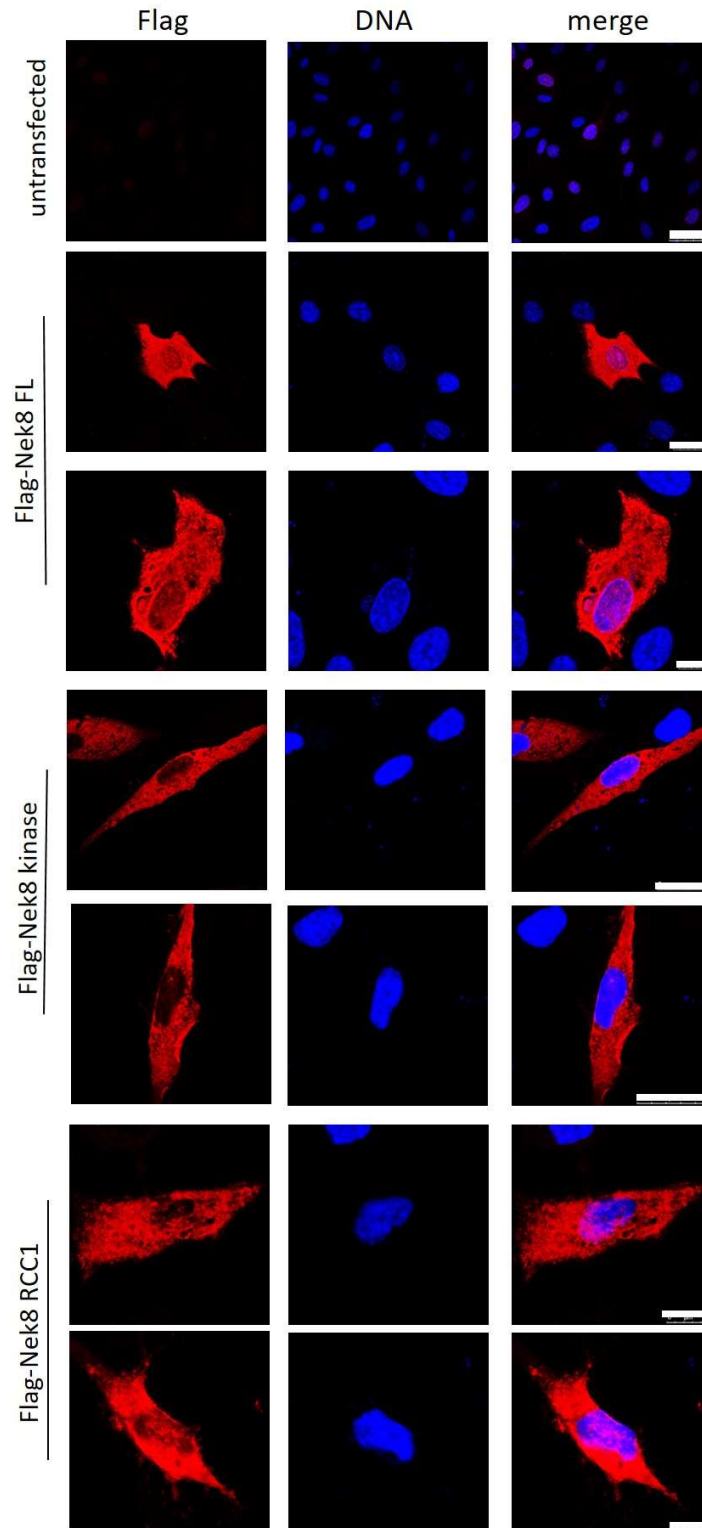


Figure 3.6 Nek8 constructs localise predominantly in the cytoplasm in cycling RPE1 cells

Immunofluorescence microscopy of untransfected, cycling RPE1 cells and RPE1 cells transfected with the Flag-Nek8 FL, Flag-Nek8 kinase domain, and Flag-Nek8 RCC1 domain constructs as indicated were stained with antibodies against the Flag-tag (red). DNA was stained with DAPI (blue). Scale bars, 50 μm in row 1, 25 μm in rows 2, 4, and 5, and 10 μm in rows 3, 6, and 7. Experiments were performed in triplicate, counting 10 transfected cells each time.

terminal 1-553 or the C-terminal 554-1065 domain. This was initially done in serum starved RPE1 cells on the basis that the proteins are known to associate at the primary cilium. Immunoprecipitates were generated using a Flag-tag antibody and were then analysed alongside input samples by SDS-PAGE and Western blotting using Flag-tag and HA-tag antibodies (Fig. 3.7). All three constructs were expressed at the expected size and Flag-Nek8 was efficiently immunoprecipitated. Importantly, the HA-Inversin 1-553 protein associated more strongly with Flag-Nek8 than the HA-Inversin 554-1065 construct, although both Inversin proteins were detected in the Flag-Nek8 immunoprecipitates. This suggests that Nek8 can interact with both the Inversin N- and C-terminal regions, albeit more strongly with the N-terminal ankyrin-repeat domain.

As the efficiency of transfections in RPE1 cells proved to be inconsistent, a second approach was adopted, using cycling and serum starved HEK293T cells, which generally exhibit high transfection efficiencies (Fig. 3.8). Upon co-transfection, expression of the Flag-Nek8 and HA-Inversin 554-1065 constructs worked well; however, the HA-Inversin 1-553 construct was poorly expressed. Following immunoprecipitation with Flag antibodies, only a small fraction of bound HA-Inversin 1-553 could be detected in the immunoprecipitates. However, the C-terminal Inversin 554-1065 construct was clearly detected in the Flag-Nek8 immunoprecipitates. There was no difference in preference of interaction between cycling and serum starved HEK293T cells. Hence, we conclude that Nek8 is capable of interacting independently with both the N- and C-terminal domains of Inversin.

As a third approach to test the interaction of Nek8 and Inversin, it was decided to express Flag-Nek8 by *in vitro* translation and to then mix the protein with HA-tagged Inversin immunoprecipitates prepared from transfected RPE1 cells using a HA-tag antibody (Fig. 3.9). SDS-PAGE and Western blot analysis confirmed the presence of the HA-Inversin 1-553 and HA-Inversin 554-1065 proteins in whole cell lysates and immunoprecipitates. *In vitro* translated Flag-Nek8 was separately detected using a Flag-tag antibody (Fig. 3.9A). Samples were then mixed and incubated over night before binding of Nek8 to the Inversin proteins was analysed using a Flag-tag antibody. The

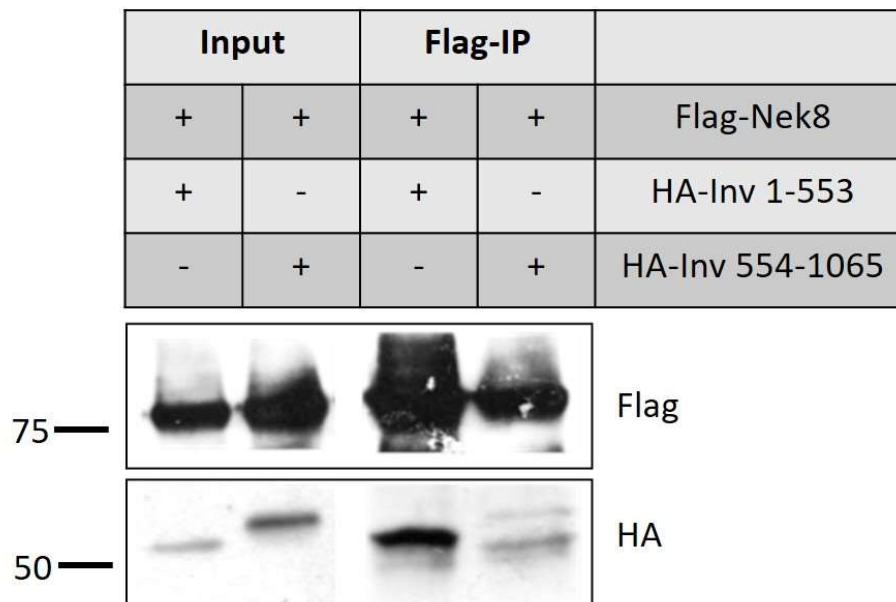


Figure 3.7 Nek8 interacts with the N-terminus of Inversin in serum starved RPE1 cells

RPE1 cells were serum starved for 24 h and transiently transfected with Flag-Nek8 FL and either HA-Inversin 1-553 or HA-Inversin 554-1065 as indicated for a further 24 h. Lysates (input) and Flag- immunoprecipitates were analysed by Western blotting with the antibodies indicated. Representative data from five independent experiments are shown. Molecular weights (kDa) are indicated on the left.

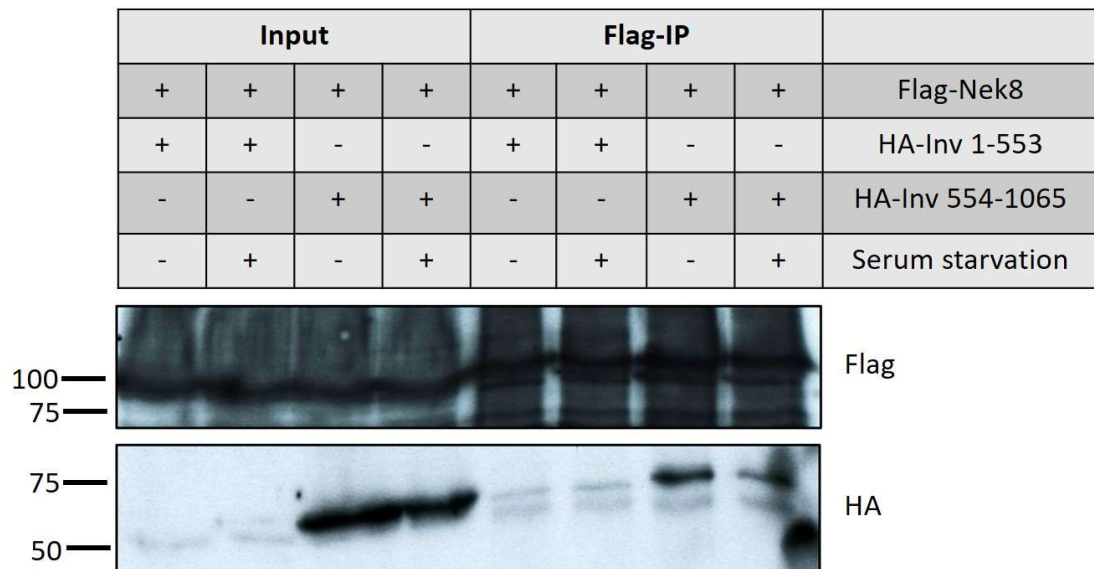


Figure 3.8 Nek8 interacts with the C-terminus of Inversin in HEK293T cells

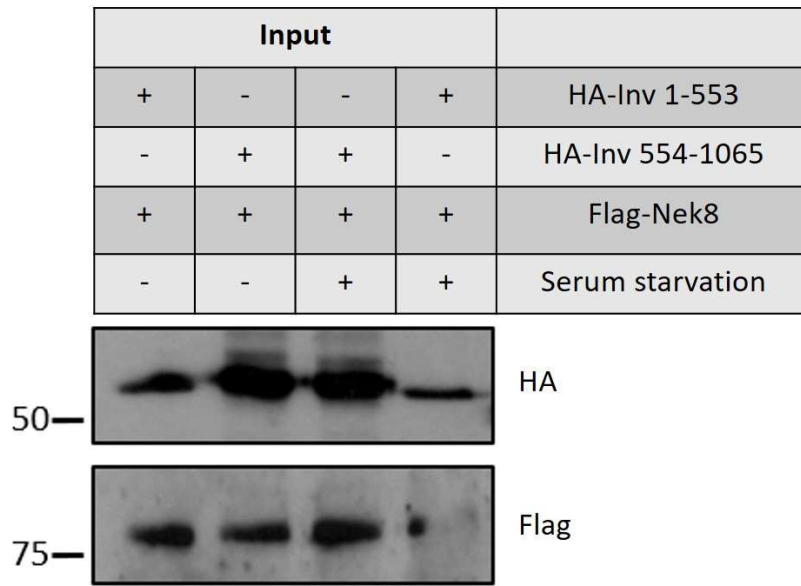
Cycling and serum starved HEK293T cells were transiently transfected with Flag-Nek8 FL and either HA-Inversin 1-553 or HA-Inversin 554-1065 as indicated. Lysates (input) and Flag co-immunoprecipitates were analysed by Western blotting with the antibodies indicated. Representative data from two independent experiments are shown. Molecular weights (kDa) are indicated on the left.

results confirmed interaction of Nek8 with the N-terminal Inversin 1-553 protein isolated from cycling RPE1 cells. However, a small fraction of Nek8 could also be detected with the Inversin C-terminal 554-1065 construct, supporting the notion of weak interaction. Interestingly, a second upshifted band was detected in the Nek8 blot, suggesting potential phosphorylation of Nek8 upon interaction with the Inversin C-terminus (Fig. 3.9B).

To investigate which domain of Nek8 interacts with Inversin, *in vitro* translations of the Flag-Nek8 kinase and Flag-Nek8 RCC1 domains were performed. SDS-PAGE and Western blotting with a Flag-tag antibody demonstrated successful translation of both constructs (Fig. 3.10B). Meanwhile, HA-Inversin 1-553 and 54-1065 proteins were immunoprecipitated from transfected RPE1 cells using a HA-tag antibody as before. Whole cell lysates (Fig. 3.10A) and immunoprecipitated samples were analysed by SDS-PAGE and Western blotting using a HA-tag antibody to confirm expression and immunoprecipitation of the Inversin proteins (Fig. 3.10C). The HA-Inversin proteins were then mixed with the *in vitro* translated Flag-Nek8 domains. Analysis of bound Nek8 proteins to the Inversin immunoprecipitates by SDS-PAGE and Western blotting revealed strong binding of the Nek8 kinase domain to the N-terminal Inversin 1-553 protein isolated from cycling or serum starved cells. The Nek8-RCC1 domain seemed to interact with both the N-terminal Inversin 1-553 and C-terminal Inversin 554-1065 domains isolated from cycling as well as serum starved cells.

Taken together, these studies reveal the likelihood of multiple binding sites between the Nek8 and Inversin proteins. They show that Nek8 interacts strongly with the Inversin N-terminal ankyrin-repeat domain containing amino acids 1 to 553. This is likely to occur mainly through the Nek8 kinase domain. However, the Nek8 RCC1 domain was capable of interaction with both the N-terminal Inversin 1-553 and C-terminal 554-1065 domains. Based on the experiments undertaken here, no consistent differences were detected in the Nek8-Inversin interactions between cycling and serum starved cells.

A



B

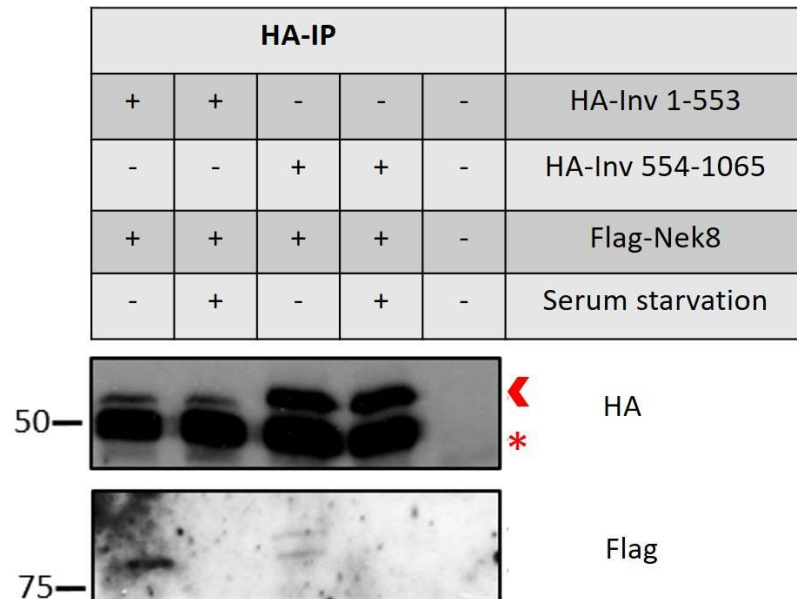


Figure 3.9 *In vitro* translated Nek8 interacts predominantly with the Inversin N-terminus

A. Cycling and serum starved RPE1 cells were transfected with HA-Inversin 1-553 or HA-Inversin 554-1065 as indicated. Lysates (input) were analysed by Western blotting using a HA-tag antibody. Full-length Flag-Nek8 was *in vitro* translated and input samples were analysed by SDS-PAGE and western blotting using a Flag-tag antibody. **B.** Immunoprecipitations performed with a HA antibody of the HA-Inversin domains mixed with Flag-Nek8 were analysed by Western blotting with the antibodies indicated. A control with beads only was included. Red arrow head indicates HA-Inversin constructs and red asterisk indicates the IgG heavy chain. Representative data of three independent experiments. Molecular weights (kDa) are indicated on the left.

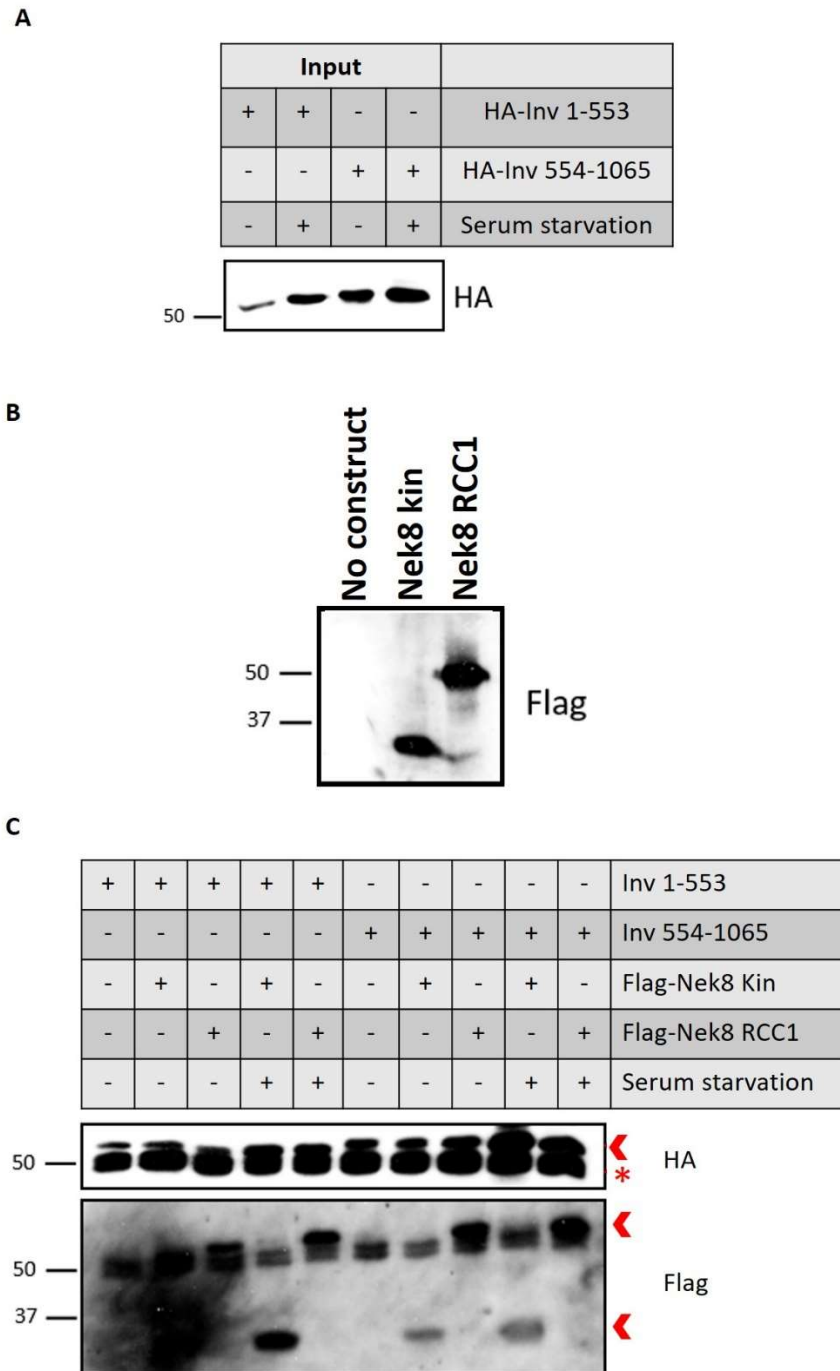


Figure 3.10 HA-Inversin interacts with the catalytic and non-catalytic domain of Nek8

A. Cycling and serum starved RPE1 cells were transiently transfected with HA-Inversin 1-553 or HA-Inversin 554-1065 as indicated. Lysates (input) were analysed by Western blotting using a HA-tag antibody. **B.** Flag-Nek8 kinase domain and RCC1 domain constructs were *in vitro* translated and analysed by Western blotting using a Flag-tag antibody. **C.** The *in vitro* translated Nek8 fragments were mixed with HA-Inversin 1-553 or HA-Inversin 554-1065 immunoprecipitates and analysed by Western blotting with the antibodies indicated. Red arrows indicate the HA-tagged and Flag-tagged proteins of interest. Red asterisk indicates the IgG heavy chain. Representative data of three independent experiments. Molecular weights (kDa) are indicated on the left.

3.3 Discussion

3.3.1 Subcellular localisation of Nek8 and Inversin

In this chapter, we investigated the localisation patterns of mammalian Inversin and Nek8 proteins in cells. In dividing cells, Inversin has been described to localise to the leading cell edges in a cell cycle dependent manner as part of its function in the PCP pathway (Veland et al., 2013), as well as centrosomes and spindle microtubules and the midbody in mitotic cells (Nürnberg et al., 2004). In quiescent cells, Inversin localises to a proximal region of the primary cilium, the so-called Inversin compartment, where it acts as a key regulator of the canonical Wnt and non-canonical Wnt/PCP pathway (Simons et al., 2005). Our data on the localisation of endogenous Inversin supported these findings, showing that Inversin localised to spindle microtubule and the midbody in HeLa cells, as well as the primary cilium in quiescent RPE1 cells and IMCD3 spheroids. In IMCD3 cells, Inversin also localised to the basal membrane. However, localisation to cilia in RPE1 cells seemed to be less defined and was not restricted to the proximal region of the Inversin compartment. This has also been reported upon overexpression of Inversin and so may well rely on expression levels (Veland et al., 2013). However, in our experiments the observed cilia were very short and might have not been fully assembled. For localisation studies of Inversin domains, we designed Inversin constructs harbouring either the N-terminal ankyrin-rich domain (amino acids 1-553) or the C-terminal domain (amino acids 554-1065). The Inversin FL, as well as the C-terminus localised to centrosomes in cycling RPE1 cells, whereas the N-terminal construct did not. Inversin has been shown to localise to stabilised microtubule such as centrosomes, spindle poles, the mitotic spindle and primary cilia (Nürnberg et al., 2004). Since the N-terminus did not localise to centrosomes, we conclude that the ciliary and centrosomal targeting motif is located in the C-terminus. This is consistent with previous results on the ciliary targeting motif being located in the C-terminus of Inversin at the ninein-homology domain (Shiba et al., 2009).

Nek8 has been described to localise to centrosomes, the Inversin compartment of cilia, and the nucleus. However, the Nek8 antibodies that were used in this study did not show any specific staining, so we investigated the localisation pattern of transfected Nek8

constructs. We divided the Nek8 protein into its N-terminal catalytic domain (amino acids 1-258) and its C-terminal RCC1 domain (amino acids 258-692). It has been previously shown that mutations at H425 and A497 interfere with its localisation to cilia and centrosomes, therefore suggesting a targeting motif in the C-terminus (Zalli et al., 2011). However, it was also shown that Nek8 needs to be active to localise correctly, as phospho-null mutants of a key residue in the activation loop at position T162 (T162A) inhibited correct localisation. It was hypothesised that active Nek8 is auto-phosphorylated in the C-terminus leading to a conformational change that allowed interaction with centrosomal binding proteins. However, our constructs did not localise to centrosomes, but accumulated mainly in the cytoplasm, which could be due to the fact that the transfected constructs were heavily overexpressed in the cell making it difficult to spot specific localisation. It could also be that the endogenous Nek8 had already saturated the binding sites at the centrosomes, so the transfected protein was not able to exhibit centrosomal localisation. However, we detected nuclear localisation of the FL and the RCC1 domain construct, but not of the kinase domain construct, suggesting a nuclear localisation sequence (NLS) in the C-terminus, or interaction of the C-terminus with a NLS containing protein. Nek8 has been described to form homodimers and undergo autophosphorylation to activate itself. If kinase activity and autophosphorylation is required for Nek8 localisation, this could explain why the individual domains could not localise effectively when expressed as isolated fragments. However, the C-terminal fragment exhibited nuclear localisation, suggesting that this fragment is capable of dimerising with and being phosphorylated by endogenous Nek8 protein. Homo-dimerisation and autophosphorylation has also been described for other kinases of the Nek family, such as Nek2 via coiled-coil domains in the C-terminus (Holland et al., 2001; Rellos et al., 2007).

3.3.2 Interaction studies of Nek8 with Inversin

Co-immunoprecipitation of Inversin and Nek8 showed interaction of these proteins with preference of the full-length Nek8 for the Inversin N-terminus in both cycling and quiescent RPE1 cells. However, in HEK293T cells, Nek8 also interacted with the Inversin C-terminus in cycling and quiescent cells. This suggests that this interaction might be cell

type specific. When Nek8 was divided into its catalytic N-terminus and the C-terminal RCC1 domain, our data show that the RCC1 domain interacts with both the Inversin N- and C-terminal fragments in RPE1 cells, whereas the kinase domain interacts more strongly with the Inversin N-terminus. The N-terminus of Inversin harbours 16 ankyrin-repeats known to be involved in protein-protein interactions. More specifically, amino acids 1 to 741 of the Inversin protein, harbouring the ankyrin repeats, a D-box and the first IQ domain, have been described to be required for Nek8 localisation to cilia (Shiba et al., 2010). Hence, this is consistent with the N-terminus of Inversin harbouring the interaction domain. This also fits with the interaction of Nek8 with ANKS6, a protein that also localises to the Inversin compartment of primary cilia and harbours nine ankyrin repeats (Hoff et al., 2013). Interaction with ANKS6 also leads to activation of Nek8. Interestingly, we detected an upshift of Nek8 on a Coomassie stained gel upon interaction with the Inversin C-terminus, which suggests that this interaction may also cause Nek8 autophosphorylation and activation. However, our data only show weak interaction of Nek8 with the C-terminal Inversin 554-1065 protein. Some domains of the C-terminus of Inversin are also involved in interactions with proteins, such as the D-box domain at position 909-917, which has been described to potentially regulate Inversin's interaction with the APC/C complex, and a calmodulin-binding IQ domain (Morgan et al., 2002). The serine/threonine kinase Akt, involved in cell cycle progression and proliferation, has also been described to directly interact with the Inversin C-terminus, as well as phosphorylating it (Suizu et al., 2016). Weak interaction of Nek8 with these structures is possible, however, to further investigate this, interaction studies with smaller C-terminal Inversin fragments need to be undertaken to accurately map interaction sites.

While our data suggest equal amounts of interaction of the Nek8 C-terminal RCC1 domain with the Inversin N- and C-terminus, it seems that the kinase domain interacts more strongly with the Inversin N-terminus (Fig. 3.11). Inversin might therefore be a substrate for Nek8 kinase activity, as well as a binding partner. This supports a model of Nek8 and Inversin binding through their C-termini and a more mobile Nek8 catalytic domain, phosphorylating the Inversin N-terminus. Furthermore, our data show that the RCC1 domain is needed for nuclear localisation of the Nek8 protein, potentially by

interacting with a protein harbouring an NLS sequence. Inversin exhibits an NLS sequence in the C-terminus. Hence, a Nek8 and Inversin interaction could also be important for nuclear localisation and function of these proteins in cycling cells.

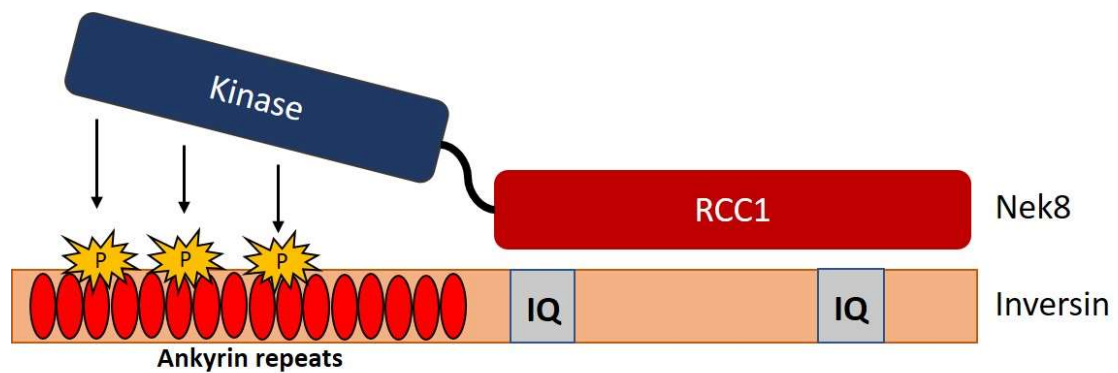


Figure 3.11 Model of Nek8 and Inversin interaction

Nek8 and Inversin interact via their C-terminal domains, allowing for a flexible catalytic domain of Nek8 (blue) that interacts mainly with the Inversin N-terminal ankyrin repeats domain and potentially uses this domain as a substrate.

CHAPTER 4 THE CILIARY POLYCYSTIC KIDNEY DISEASE PROTEINS, INVERSIN AND PC-2, ARE SUBSTRATES FOR NEK8 KINASE ACTIVITY

4.1 Introduction

Mutations in the serine/threonine kinase Nek8 cause nephronophthisis type 9 (NPHP9), an autosomal recessive polycystic kidney disease that - amongst other symptoms - leads to cyst formation and left-right asymmetry defects. However, the exact role of Nek8 in the development of NPHP has yet to be understood. It is known, however, that Nek8 is activated upon cell cycle exit and localises to primary cilia where it is recruited and anchored by Inversin, another NPHP disease protein, causing NPHP type 2 (Shiba et al., 2010; Zalli et al., 2011). Several recessive mutations have been found in Inversin in a screen performed by Otto et al. (2002) with seven truncating mutations (R899X, Q485fsX509, R603X, R396X, E970fsX971, R907X, K916fsX1002), and two missense mutations (P482R, L493S) leading to similar phenotypes as NPHP9, with and without *situs inversus*, an inversion of organs within the body axis (Otto et al., 2003). This supports a functional connection between Nek8 and Inversin.

Both proteins are part of a broader, complex network of interacting proteins at primary cilia, with Nek8 being the only described kinase (Mahjoub et al., 2005; Shiba et al., 2010; Sang et al., 2011). In kidney tubules and ducts, primary cilia act as mechanosensors and transduce fluid flow-induced ciliary shear stress into calcium-dependent signalling cascades. This is thought to keep the cell in a differentiated, dormant state (Manning et al., 2012; Zhou, 2009). The two calcium-channels in the ciliary membrane are PC-1 and PC-2 that allow calcium influx or efflux (Manning et al., 2012; Pennekamp et al., 2002). Controlled calcium influx is particularly important in embryo development as asymmetric calcium concentrations determine left-right asymmetry (Field et al., 2011; Kamura et al., 2011). Mutations in either the *pkd1* or *pkd2* genes that encode PC-1 and PC-2, respectively, cause autosomal dominant polycystic kidney disease (ADPKD) (Ong and Harris, 2015; Ong and Harris, 2005), which shows many similar symptoms to NPHP, including left-right asymmetry defects.

PC-2 is a member of the transient receptor potential (TRP) channel family whose members localise to the membranes of cilia, the endoplasmic reticulum, and the plasma membrane where they act as calcium channels that sense intracellular calcium levels. PC-2 consists of six putative transmembrane helices and a pore-forming loop. The C-terminal cytoplasmic domain consists of a calcium-binding EF-hand (Ong and Harris, 2015) and a coiled-coil domain (amino acids 830-872) known to be involved in channel assembly and hetero-oligomerisation with other proteins (Yang et al., 2015). A connection between PC-2 and Nek8 was established by Sohara et al. (2008), who showed that PC-2 expression and recruitment to the ciliary membrane is dependent on complex formation with Nek8. Furthermore, *jck* mice, which express a Nek8 protein with a G488V substitution in the RCC1 domain, showed PC-2 enrichment at the cilia and enhanced phosphorylation, leading to the hypothesis that PC-2 might be a substrate for Nek8 kinase activity.

Given the interaction of Nek8 with Inversin and PC-2, and the similar phenotypes caused by their mutations, we wanted to investigate whether Inversin and PC-2 are substrates for Nek8 kinase activity and if so, identify the sites of phosphorylation. These could then provide biomarkers of Nek8 activity that could ultimately lead to a better understanding of NPHP progression.

4.2 Results

4.2.1 Purification of Nek8 and Inversin proteins for *in vitro* kinase assays

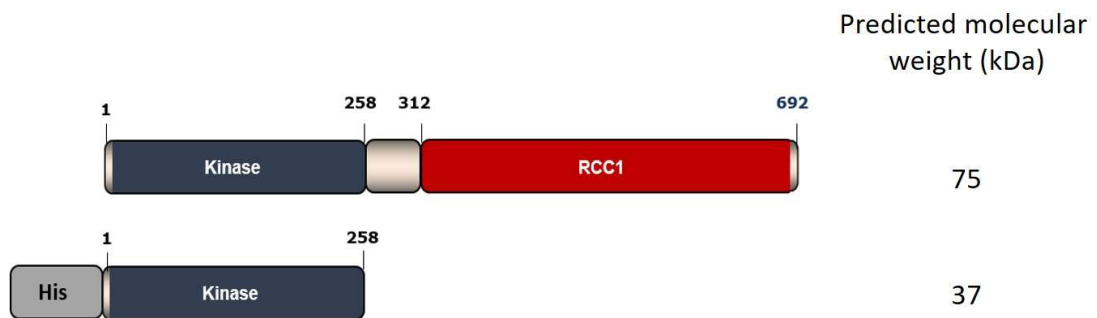
Having shown interaction between the Nek8 kinase domain and Inversin, we next investigated whether Inversin is a substrate for Nek8 kinase activity. For this purpose, we first generated an active Nek8 catalytic domain fragment in collaboration with the Bayliss laboratory at the University of Leicester. A construct with the N-terminal amino acids 1 to 258 of Nek8 with an N-terminal His-tag was expressed in *E. coli* by Dr Sharon Yeoh and purified using Nickel affinity chromatography and gel filtration. The purity of this sample was confirmed by SDS-PAGE and Coomassie Blue staining with the major band detected at the predicted molecular weight of 37 kDa (Fig. 4.1). This kinase domain preparation was used for *in vitro* kinase assays using purified Inversin proteins as substrates.

Meanwhile, Inversin constructs were cloned into bacterial vectors for expression in bacteria cells and used as substrates in Nek8 kinases assays. The Inversin protein was divided into two N-terminal constructs. The first construct encodes amino acids 1 to 553 and harbours the ankyrin-repeat domain, known to be involved in protein-protein interactions. The second construct contains amino acids 1 to 600, which includes the first IQ domain, believed to be involved in Calmodulin binding. The three C-terminal fragments, one encoding the entire C-terminus (residues 554 to 1065) that encompassed the two IQ domains, and two smaller constructs, encoding amino acids 899 to 1065, and amino acids 950 to 1065. The smallest of the C-terminal constructs contains what has previously been reported as the ciliary localisation motif (Fig. 4.2). Whereas the N-terminal Inversin constructs were cloned into the bacterial pLEICS-01 vector containing an N-terminal His-tag, the C-terminal constructs were cloned into the pLEICS-02 vector containing an N-terminal GST-tag.

Initial experiments to purify the GST-tagged C-terminal Inversin proteins in BL21 (DE3) RIL *E. coli* cells were unsuccessful (Fig. 4.3 A and B). Expression induction of the GST-

Inversin 554-1065 construct did not work using either 0.6 mM or 1 mM IPTG with incubation of the culture at 18°C over night. The GST-Inversin 601-1065 and GST-Inversin 899-1065 constructs, however, were induced successfully (Fig. 3.4A). Following induction with 0.6 mM IPTG, purification in lysis buffer containing 50 mM Tris-HCl (pH 8.0), 50 mM NaCl, 5 mM EDTA, 0.15 mM PMSF, 1 mM β -mercaptoethanol and 0.1 mM protease inhibitor cocktail, and sonication for 10 sec with 10 sec internals for 5 times, showed that both proteins were insoluble and only a small fraction of the GST-Inversin 601-1065 protein bound to glutathione beads (Fig. 3.4B). However, this fraction did not elute from the beads using 50 mM Tris-HCl (pH 8.0) and 10 mM reduced glutathione. After finding that the proteins were insoluble, sonication was increased to 5 times 20 sec with 20 sec internals, however, the GST-Inversin 601-1065 and 899-1065 proteins did not accumulate sufficiently in the soluble fraction to purify a good amount for further studies. The C-terminal constructs were therefore passed on to Sophie Millett (University of Leicester) for troubleshooting in a structural biology laboratory. They were expressed again in BL21 (DE3) RIL *E. coli* cells and purified using glutathione agarose beads as described in 2.2.3.9. The GST-Inversin 554-1065, GST-Inversin 899-1065 and GST-Inversin 950-1065 proteins were induced and expressed successfully in these cells, however, to reach a good amount of protein, they remained bound to glutathione beads for further studies. Analysis of the purified products by SDS-PAGE and Coomassie Blue staining revealed clear bands of protein bound to beads at the correct estimated molecular weights (Fig. 4.3C). Breakdown products could be detected in all samples. A purified GST protein bound to beads was analysed alongside, showing a single band at 26 kDa.

A



B

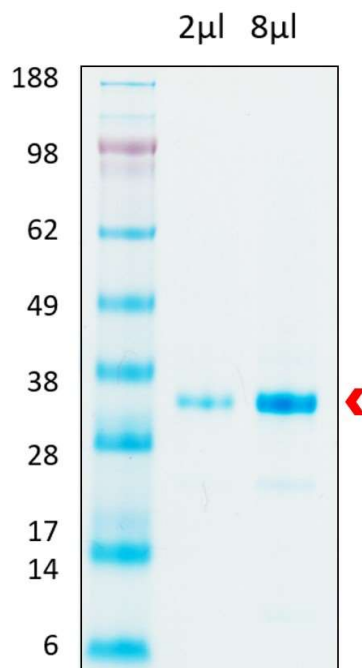


Figure 4.1 Generation of active Nek8 kinase

A. Schematic of the Nek8 full-length protein with the kinase domain in blue and RCC1 domain in red and the His-tagged catalytic domain fragment encoding amino acids 1-258. Predicted molecular weights of proteins are indicated. **B.** The His-tagged Nek8 kinase domain fragment was expressed in *E. coli* and purified by Nickel affinity chromatography and gel filtration by Dr Sharon Yeoh. The concentration and purity were assessed by analysing 2 µl and 8 µl of purified protein by SDS-PAGE and staining with Coomassie Blue (red arrow head). The stained molecular weight markers (kDa) are indicated on the left.

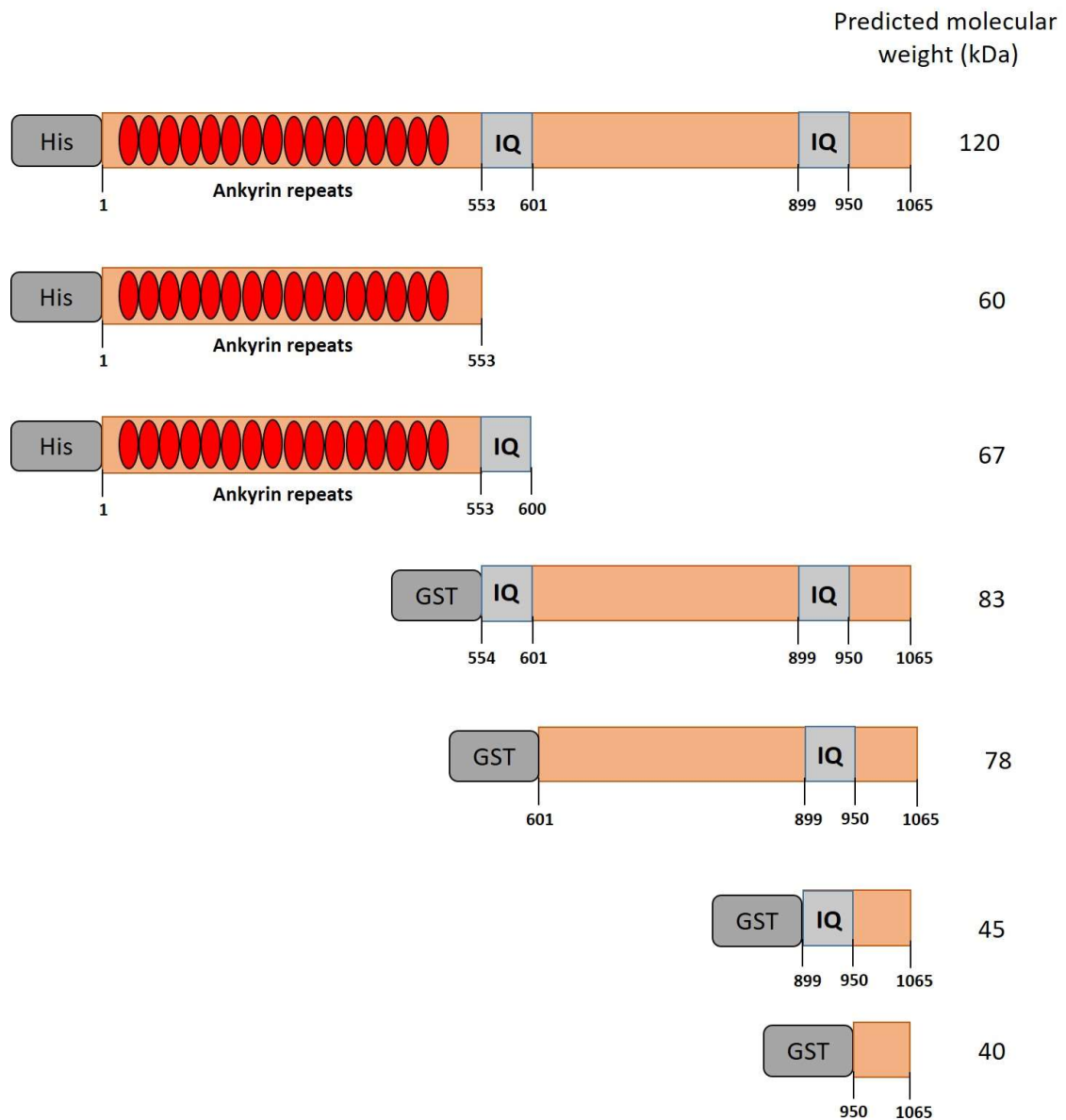


Figure 4.2 Schematic of Inversin constructs used for phosphorylation assays

Inversin constructs for protein expression and purification were cloned into bacterial expression vectors. The His-tagged N-terminal 1-553 construct contains the 16 Ankyrin repeats (red), and the His-Inversin 1-600 construct contains the ankyrin repeats and the first IQ domain (grey). C-terminal constructs were generated as GST-tagged proteins. The 554-1065 construct contains the C-terminus of the Inversin protein (grey), including two IQ domains (green), whereas the 601-1065 construct starts after the first IQ domain. Two smaller constructs containing amino acids 899-1065 and 950-1065 were also generated. Predicted molecular weights of tagged proteins are indicated.

Expressions of the N-terminal His-Inversin 1-553 and 1-601 proteins were performed in BL21 (DE3) RIL *E. coli* cells. Cells were induced with 0.6 mM IPTG at 18°C over night and bound to Nickel beads. Analysis of samples by SDS-PAGE and Coomassie Blue staining revealed a clear band bound to the Nickel beads at the predicted molecular weight of 60 kDa for the His-Inversin 1-553 protein and at 67 kDa for the His-Inversin 1-600 protein (Fig. 4.4A). Western blotting analysis using a His-tag antibody was performed to compare the amount of bound protein to the beads. This revealed a much higher amount in the His-Inversin 1-553 sample, as well as clearly detectable induction of this protein with IPTG (Fig. 4.4B). The His-Inversin 1-553 protein was therefore eluted from the beads with increasing concentrations of imidazole and samples analysed by SDS-PAGE and Coomassie Blue staining revealing successful elution of the His-Inversin protein with 135 mM (elution 2) and 192.5 mM imidazole (elution 3, Fig. 4.4B). These elutions were then pooled and dialysed into HEPES buffer and concentrated to 1 mg/ml (Fig. 4.4C). The overall yield of the His-Inversin 1-553 protein from a 1 L bacterial culture was 2 mg protein. This was used alongside the GST-tagged C-terminal Inversin proteins as putative substrates in Nek8 kinase assays.

4.2.2 Identification of multiple sites of Nek8 phosphorylation in Inversin

In vitro kinase assays were performed with the active Nek8 kinase domain and the purified Inversin proteins. The soluble His-Inversin 1-553 protein and the C-terminal GST-tagged Inversin proteins bound to beads were used as substrates. Protein bound to beads was used in similar amounts to the His-Inversin 1-553 protein as judged by the intensity of the Coomassie stained band. Myelin basic protein (MBP) and GST were used as control substrates, while glutathione beads without bound protein were used as negative controls. Samples of substrates incubated with and without active Nek8 in the presence of radiolabelled ATP were analysed by SDS-PAGE and Coomassie Blue staining to confirm presence of the proteins. Gels were then dried onto blotting paper and phosphorylation of the proteins was analysed by autoradiography (Fig. 4.5). MBP was strongly phosphorylated by Nek8, confirming activity of the kinase, whereas neither GST alone nor the glutathione beads sample exhibited significant phosphorylation. Interestingly, all four of the Inversin proteins were phosphorylated, showing that

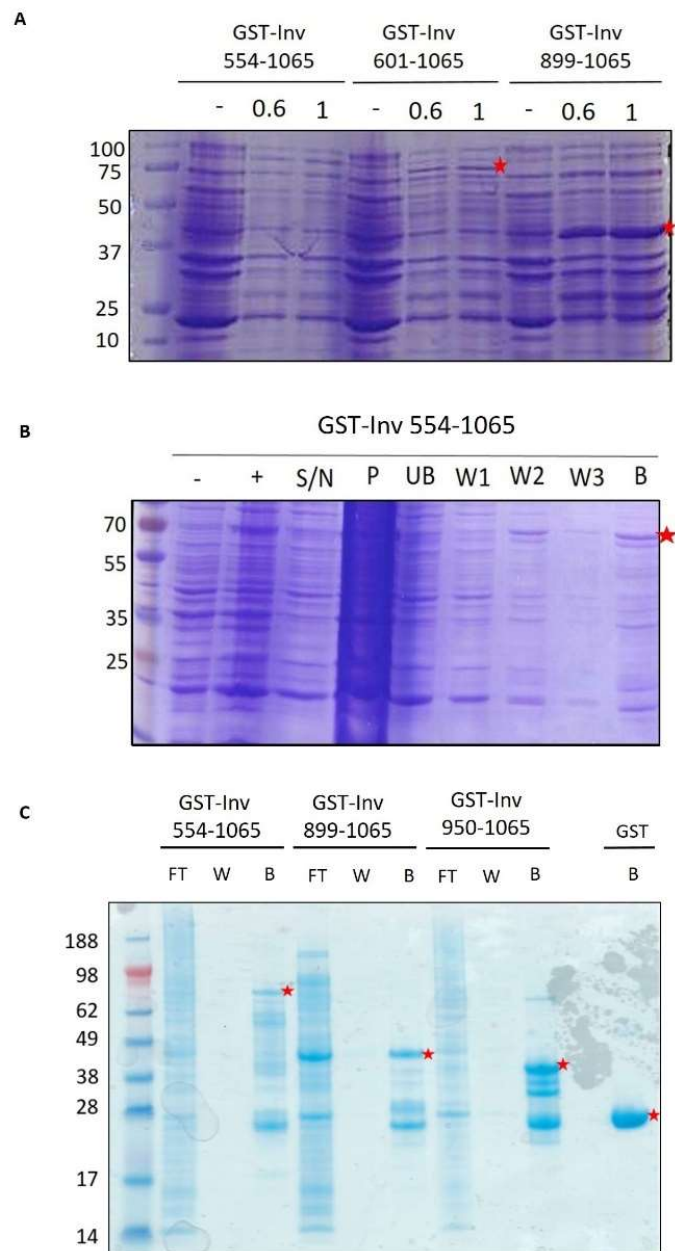


Figure 4.3 Purification of GST-tagged Inversin C-terminal constructs

A. Test induction of GST-tagged C-terminal Inversin constructs in bacteria cells with either 0.6 mM or 1 mM IPTG as indicated. Induced proteins are indicated by asterisks. Molecular weights (kDa) are indicated on the left. **B.** Test purification of GST-Inv 601-1065 glutathione beads. Samples prior to induction (-), after IPTG induction (+), from the supernatant (S/N), pellet (P), unbound protein (UB), washes (W1-3), and protein bound to beads (B) were analysed by SDS-PAGE and Coomassie Blue stain. Asterisks indicate the GST-Inversin protein. Molecular weights (kDa) are indicated on the left. **C.** GST-tagged Inversin C-terminal constructs 554-1065, 899-1065 and 950-1065 were expressed and purified by Sophie Millet (University of Leicester). After binding to glutathione beads, samples from the flow-through (FT), washes (W), and beads (B) were analysed by SDS-PAGE and Coomassie Blue stain. Protein bound to beads is indicated by red asterisks. Molecular weights (kDa) are indicated on the left.

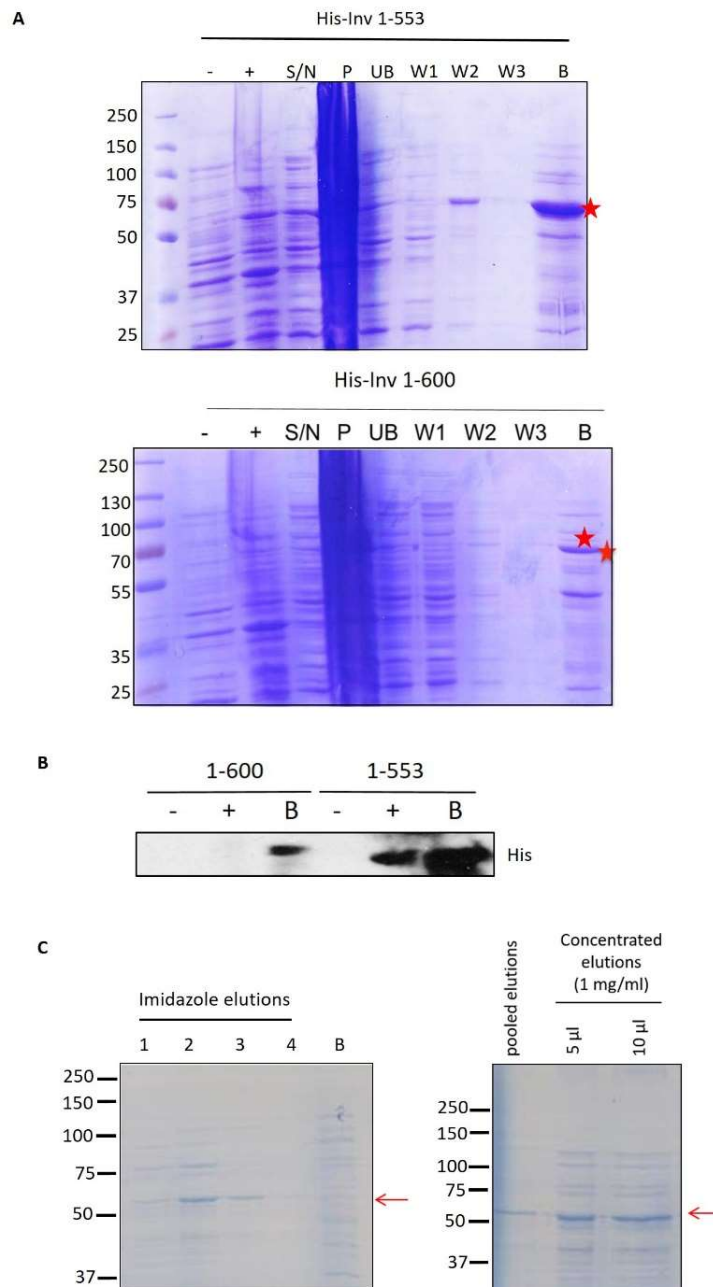


Figure 4.4 Purification of the N-terminal His-Inversin 1-553 protein

A. The N-terminal His-tagged Inversin 1-553 and 1-600 proteins were expressed in bacteria and purified using Nickel affinity chromatography. Samples prior to induction (-), after IPTG induction (+), from the supernatant (S/N), pellet (P), unbound protein (UB), washes (W1-3), and protein bound to Nickel beads (B) were analysed by SDS-PAGE and Coomassie Blue stain. Asterisks indicate the His-Inversin proteins. Molecular weights (kDa) are indicated on the left. **B.** Western blotting analysis was performed using a His-tag antibody to compare the amount of protein bound to beads in the His-Inv 1-553 and 1-600 purification. **C.** His-Inv 1-553 elutions with increasing imidazole concentration (1-4) of the His-Inversin 1-553 protein and protein remaining bound to Nickel beads after elution steps (B) were analysed by SDS-PAGE and Coomassie Blue stain (on the left). Elutions 2 and 3 were pooled and analysed alongside concentrated protein at indicated volumes on an SDS-PAGE and by Coomassie Blue stain (on the right). Red arrows indicate the His-Inversin 1-553 protein. Molecular weights (kDa) are indicated on the left.

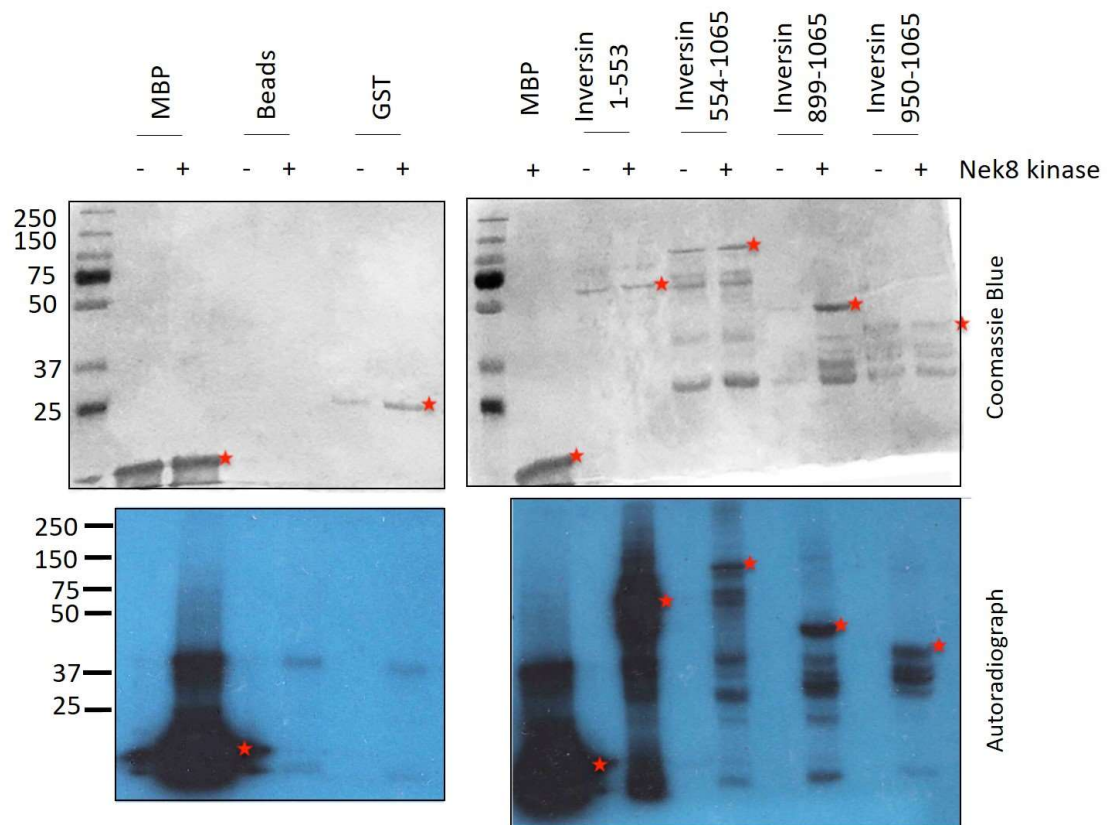


Figure 4.5 Inversin is a substrate for Nek8 *in vitro*

Kinase assays were performed using the purified Inversin proteins as substrates. MBP, glutathione beads (Beads) and GST were incubated as controls as indicated. Samples were incubated in kinase buffer containing radio-labelled ATP with and without Nek8 kinase (-/+). Samples were analysed by SDS-PAGE, Coomassie Blue stain (top panel) and autoradiograph (bottom panel). Phosphorylated proteins are indicated (red asterisks). Representative data of three independent experiments. Molecular weights (kDa) are indicated on the left.

Inversin contains multiple sites of phosphorylation for Nek8 kinase activity *in vitro*. The Inversin N-terminus showed a stronger signal on the autoradiograph compared to the C-terminal proteins suggesting a higher level of phosphorylation. Nek8 autophosphorylation was also detected at 37 kDa.

Having shown that Inversin is a substrate for Nek8 kinase activity *in vitro*, the next step was to map the phosphorylation sites as a first step to testing their significance. Firstly, a time course at 15, 30, 60 and 120 min was performed to determine the point at which phosphorylation reached maximum levels. The His-Inversin 1-553 protein was used for this experiment as it was a soluble protein that had been eluted off the beads. Samples from the different time points were separated by SDS-PAGE, stained with Coomassie Blue and analysed by autoradiography (Fig. 4.6A). The MBP and His-Inversin 1-553 bands were then cut from the gel and processed for scintillation counting. The incorporation of radiolabel was normalised against MBP that had been incubated with Nek8 for 30 min. This showed that near maximum levels of phosphorylation of His-Inversin 1-553 were reached after 15 min of incubation with Nek8 with only minimal increase after that time (Fig. 4.6B). Nevertheless, to ensure maximal phosphorylation, kinase assays were performed for 120 min with unlabelled ATP for phosphomapping by mass spectrometry.

The His-Inversin 1-553 protein was incubated with the Nek8 kinase domain in three separate experiments and submitted for phosphomapping by mass spectrometry, whereas the GST-Inversin 554-1065 and GST-Inversin 899-1065 proteins were both submitted twice for phosphomapping. MALDI-ToF analysis was performed at the University of Leicester Proteomics Laboratory. Protein sequences for all constructs were submitted alongside and peptides matched against them. A summary of the 20 phosphosites identified is listed in Fig. 4.7A and B. The 12 phosphosites that were identified in all three experiments with the His-Inversin 1-553 protein and in both experiments with the GST-Inversin 554-1065 protein, as well as in a minimum of three out of four experiments with the GST-Inversin 554-1065 and GST-Inversin 899-1065 proteins combined are shown in red. These sites were then highlighted on an Inversin schematic to visualise their location with respect to the Inversin protein domains (Fig. 4.7C). The three sites consistently identified in the N-terminus were T121, T324 and

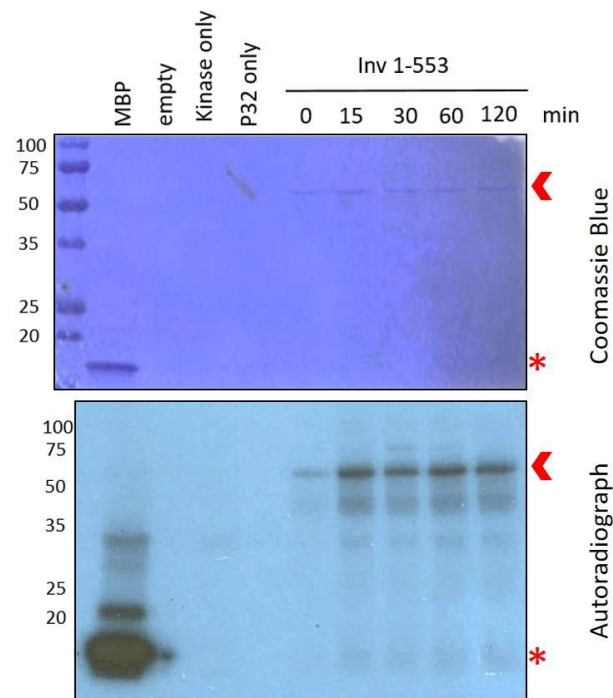
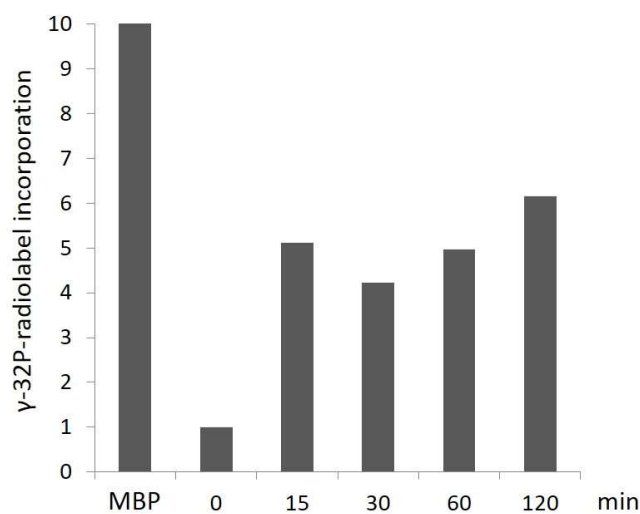
A**B**

Figure 4.6 Time course of phosphorylation of the Inversin N-terminus by Nek8

A. Nek8 kinase assays were performed with MBP and His-Inversin 1-553 in kinase buffer with radiolabelled ATP at 30°C for times indicated. MBP was incubated with Nek8 for 30 min. Kinase buffer without radiolabelled ATP without Nek8 (empty) and with Nek8 (Kinase only), and buffer with radiolabelled ATP (P32 only) were analysed as controls. Molecular weights (kDa) are indicated on the left. **B.** The His-Inversin 1-553 samples as well as MBP were cut out of the Coomassie Blue stained gel and analysed by scintillation counting. The amount of γ -³²P incorporated is indicated.

T359. Sites in the C-terminus were spread over three areas. One site was mapped at position T683, whereas four sites cluster near the second IQ domain: T841, T864, T865, and T866. A second cluster was located near the extreme C-terminus of the protein, at T958, S1032, S1043 and T1057. The WebLogo 3.5.0 programme was used for sequence comparison of all 12 sites comparing sequences from position -10 to +8 relative to the phosphorylated threonine or serine to show the probability of a certain amino acid within that sequence (Fig. 4.7D). The output revealed preference of Nek8 for phosphorylation of threonine rather than serine and indicates a high probability of leucine at position -3, -4, and +2. It was also more common to have a leucine at positions -9 and +7. Furthermore, arginine seems to be preferred at positions -5 and +4.

4.2.3 Generation of phospho-Inversin antibodies

To investigate the importance of individual phosphorylation sites, phospho-Inversin antibodies were generated against the three sites in the N-terminal ankyrin-repeat domain (Fig. 4.8A). These sites were chosen due to the strong interaction of Nek8, and here specifically the Nek8 catalytic domain, with the N-terminal Inversin fragment and the high level of phosphorylation in the N-terminus compared to the C-terminus. Phosphoantibodies were generated against 11 amino acid long peptides with five amino acids upstream and downstream of the phosphorylated site (Fig. 4.8B). Peptide sequences were submitted to AMSBIO for antibody generation. Briefly, these peptides were synthesised with an N-terminal KLH conjugated cysteine and a C-terminal NH₂ group for stability. Two Japanese White Rabbits were immunised three times with 250 µg of antigen over the course of five weeks and the first serum was extracted in week 6 to test antibody titre by ELISA and Western blotting on appropriate cells. Further bleeds were taken in weeks 7, 8, 9, 10 and 11 and antibodies were purified by peptide affinity purification with the non-phospho-peptide first, followed by incubation of the flow through with a column containing the phospho-peptide. This generated two separate batches of non-phospho-specific and phospho-specific antibodies per immunised rabbit, which were analysed by ELISA, Western blotting and dot blot before being delivered in lyophilised form and re-suspended in dH₂O.

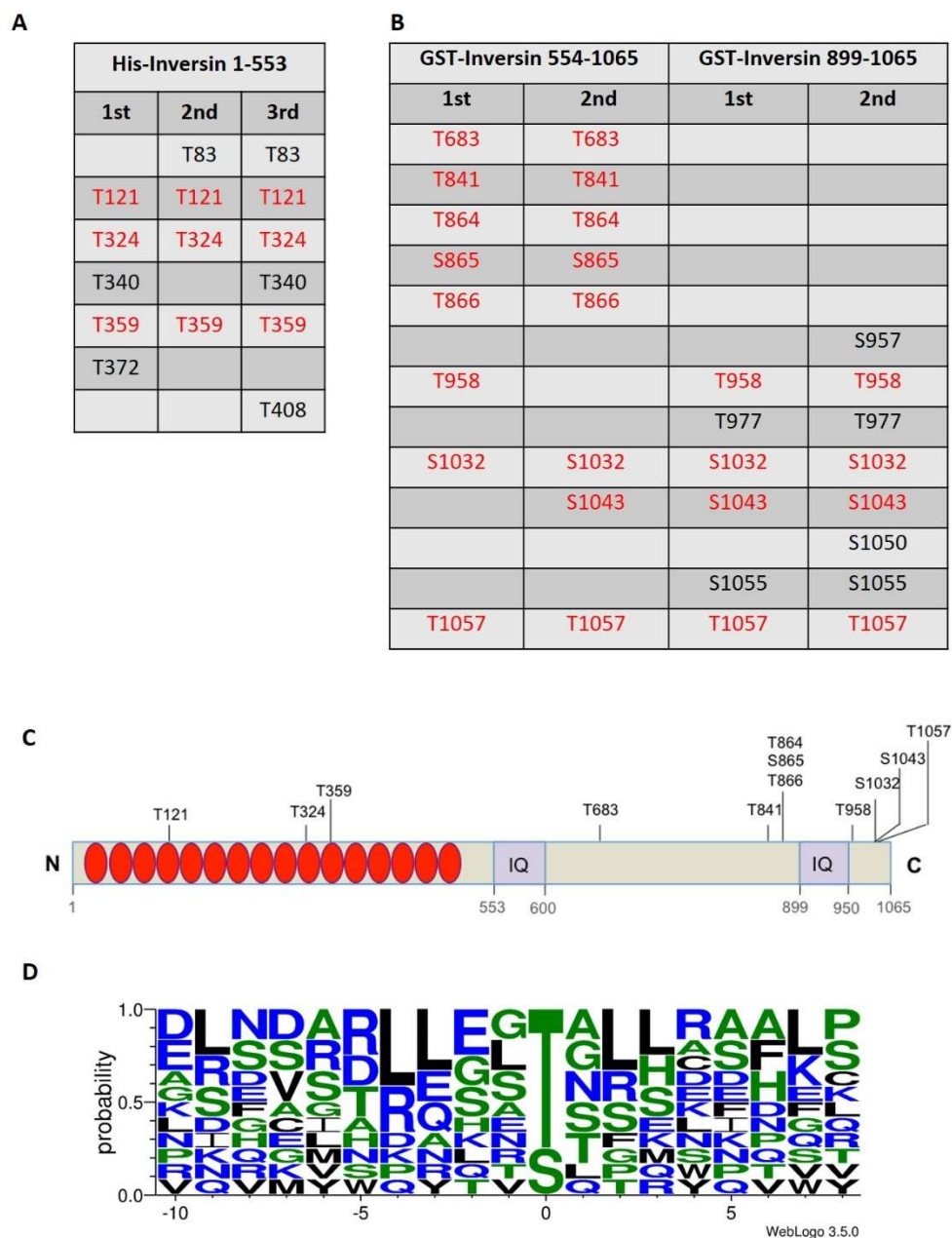
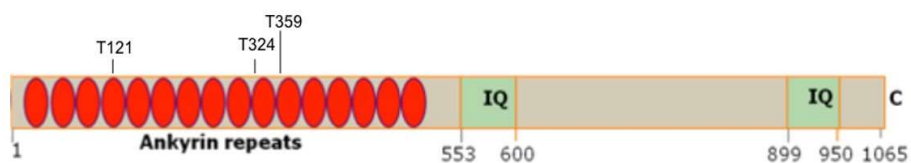


Figure 4.7 Identification of Nek8 phosphorylation sites in the Inversin protein

Mass spectrometry performed after *in vitro* kinase assays with Nek8 revealed several phosphorylation sites within the Inversin protein. The sites in the N-terminal His-Inversin 1-553 protein from three independent experiments is shown in **(A)**, and the sites from two independent experiments with the C-terminal GST-Inversin 554-1065 and GST-Inversin 899-1065 proteins are shown in **(B)**. The 12 phosphosites that were identified in either all three submissions in **(A)** or three out of four in **(B)** are indicated in red and their localisation along the Inversin protein is shown in **(C)**. **D**. A sequence preference was created using the WebLogo 3.5.0 programme to analyse sequence conservation across the 12 phosphosites. Probability of the occurrence of a certain amino acid was plotted against the position of this residue up- and down-

A



B

| Phosphosite | Peptide sequence |
|-------------|-----------------------|
| T121 | TPLHL p TTRHRS |
| T324 | DLEGR p TSFMWA |
| T359 | DKYGG p TALHAA |

Figure 4.8 Peptide design for generation of Inversin phosphoantibodies

A. Phosphoantibodies were generated against the three Nek8 phosphorylated sites indicated in the N-terminus of the Inversin protein. **B.** For phosphoantibody generation, 11-aminoacid-long peptides with five amino acids upstream and downstream of the site of interest (bold) were synthesised and used for immunisation and purification by AMSBIO.

stream of the phosphorylated Threonine or Serine. Hydrophilic amino acids are shown in blue, neutral amino acids in green, and hydrophobic amino acids in black, with the most common amino acid indicated at the top.

4.2.4 Characterisation of phospho-Inversin antibodies by Western blot

To determine the reactivity of the phospho-Inversin antibodies, they were first assessed by Western blot on purified His-Inversin 1-553 protein. For this, 2, 5 and 10 µg of purified His-Inversin 1-553 protein were separated by SDS-PAGE and analysed with a His-tag antibody by Western blotting to confirm presence of the protein (Fig. 4.9A). As 2 µg of protein was sufficient to detect a clear band after 30 sec of ECL exposure, it was decided to perform further experiments using 1 µg of His-Inversin 1-553 protein per lane. His-Inversin 1-553 was incubated in kinase buffer with and without Nek8 for 120 min at 30°C. A Coomassie Blue stained gel showed a small upshift for the His-Inversin 1-553 protein incubated with Nek8 suggestive of phosphorylation (Fig. 4.9B). Western blotting was then performed using a His-tag antibody to validate equal amounts of unphosphorylated and phosphorylated sample. Subsequently, the purified Inversin antibodies from both rabbits were tested on both, unphosphorylated and phosphorylated His-Inversin 1-553 protein. All non-phospho specific antibodies were able to detect the purified phosphorylated and unphosphorylated His-Inversin 1-553 protein. However, the phospho-specific antibodies varied in their reactivity. Both pT121 antibodies detected the phosphorylated protein; however, pT121 from rabbit two also weakly detected the unphosphorylated protein. The pT324 antibody from both rabbits was less specific as it detected equal amounts of unphosphorylated and phosphorylated protein. However, the pT359 antibody from both rabbits mainly detected the phosphorylated protein and only weakly detected the unphosphorylated protein (Fig. 4.9C). In summary, the T121, T324, and T359 antibodies were able to detect purified His-Inversin 1-553 protein by Western blot, but only the pT121 and pT359 antibodies, but not the pT324 antibody, could distinguish between the phosphorylated and unphosphorylated Inversin protein.

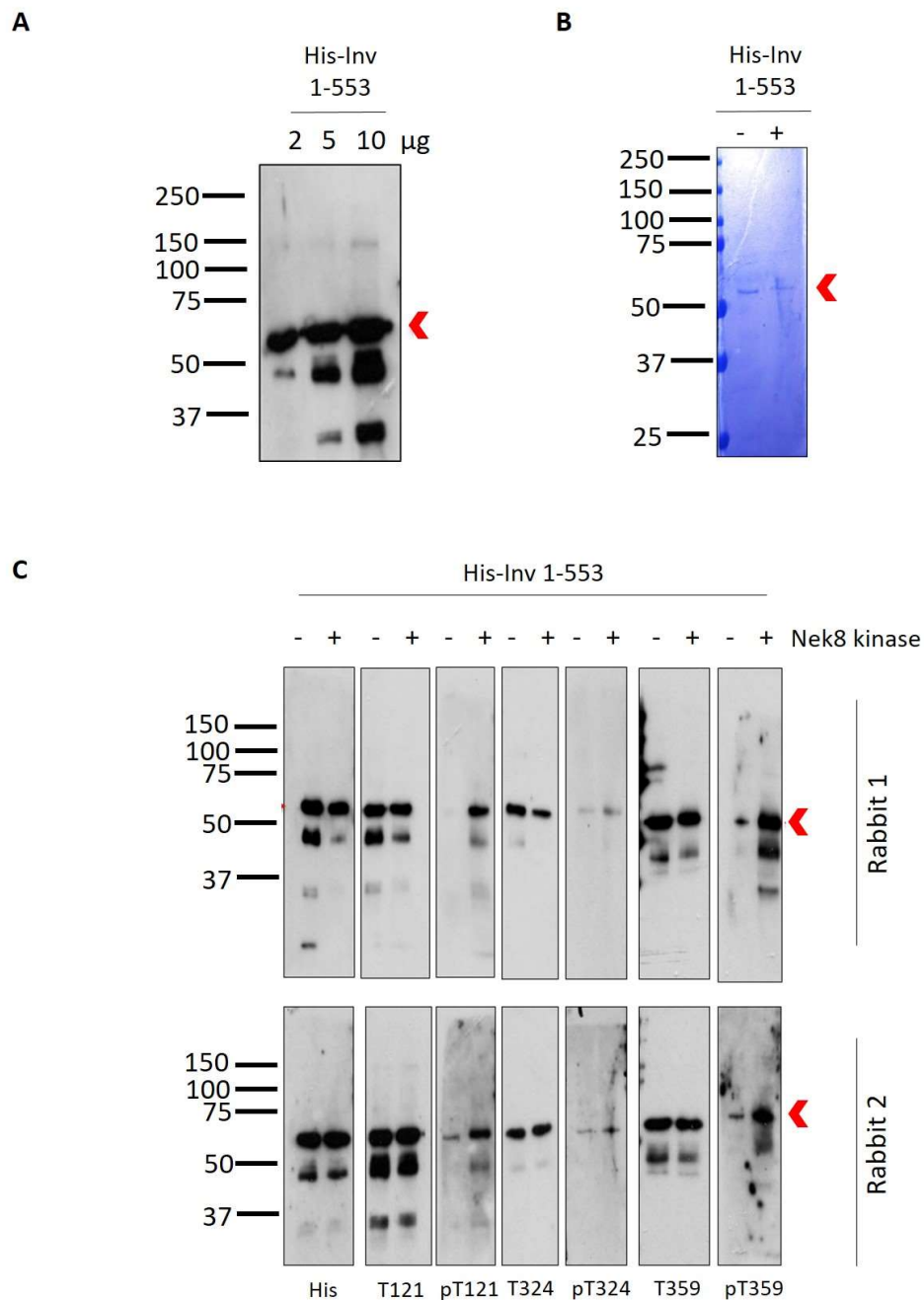


Figure 4.9 Validation of Inversin phosphoantibodies on purified Inversin proteins

A. 2, 5, and 10 µg of the purified His-Inversin 1-553 protein were analysed by Western blotting using a His-tag antibody. Arrow head indicates the expected band at 60 kDa. **B.** Coomassie blue staining following SDS-PAGE was performed on the His-Inversin 1-553 protein that had been incubated with (+) or without (-) Nek8 and ATP for 1h. Arrow head indicates the His-Inversin 1-553 protein at 60 kDa. **C.** Western blot analysis of the His-Inversin 1-553 protein incubated with (+) or without (-) Nek8 and ATP using a His-tag, T121, pT121, T324, pT324, T359, and pT359 antibody as indicated. The peptide-specific antibodies from two rabbits were tested. Representative data of two independent experiments. Molecular weights (kDa) are indicated on the left.

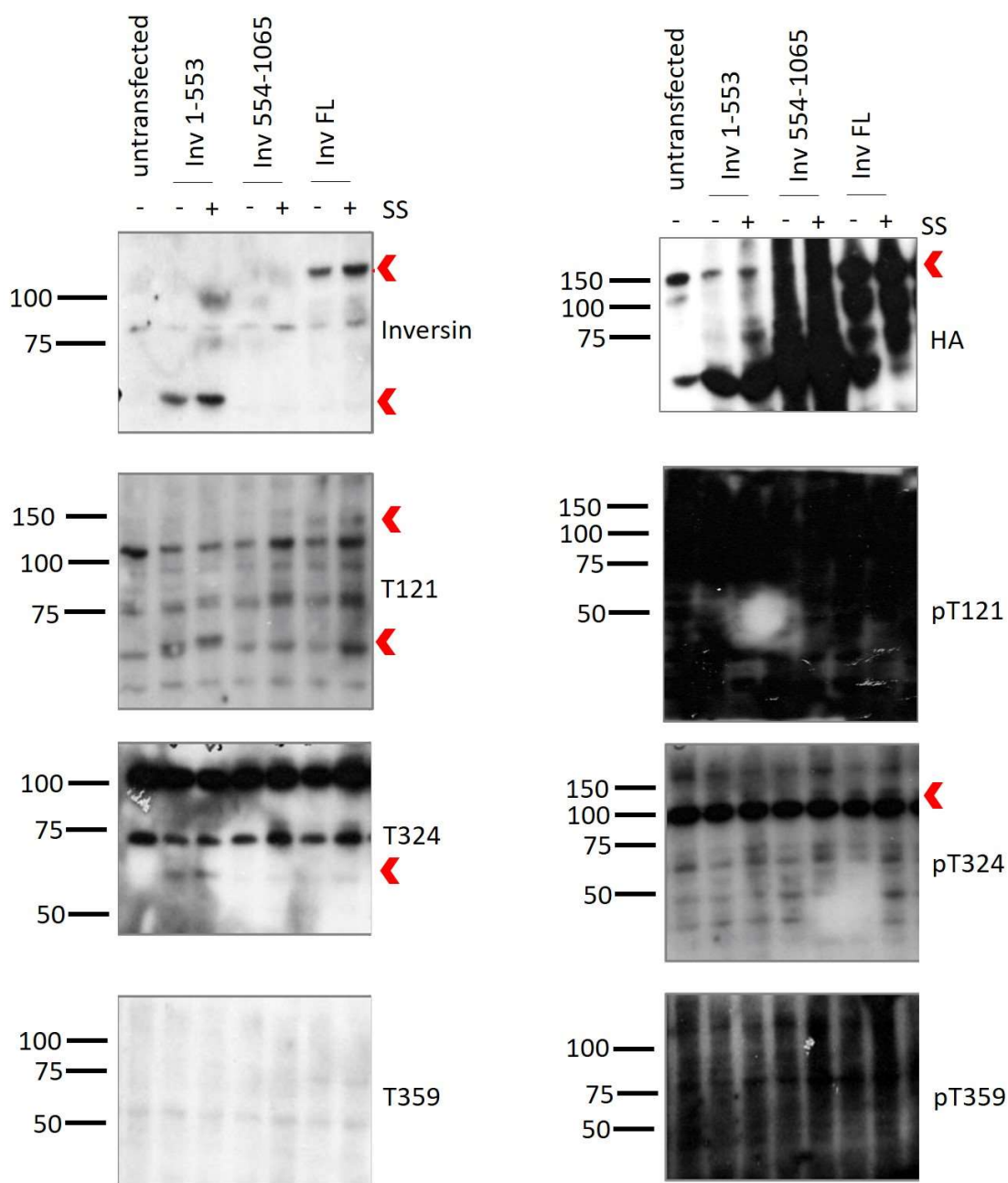


Figure 4.10 Analysis of Inversin antibodies by Western blot of transfected cell lysates

Cycling (-SS) and serum starved (+SS) RPE1 cells were transfected with HA-tagged Inversin 1-553, Inversin 554-1065, and Inversin full-length (FL) for 24 h. 10 µg of whole cell lysates of transfected cells or an untransfected sample were analysed by SDS-PAGE and Western blotting using a commercial Inversin antibody raised against the N-terminus, a HA-tag antibody and the T121, pT121, T324, pT324, T359, and pT359 antibodies. Arrowheads indicate transfected protein. Molecular weights (kDa) are indicated on the left.

Antibodies from the first batch were then tested by Western blotting of lysates from transfected cycling and serum starved RPE1 cells and representative data of experiments using different antibody concentrations, buffers, and exposure times of the autoradiograph are shown in Figure 4.10. Cells were transfected with HA-Inversin 1-553 and HA-Inversin FL which contained the peptide against which the antibodies were raised and HA-Inversin 554-1065 which did not. The HA-tag antibody confirmed transfection of all three constructs with all three proteins migrating at their estimated molecular weights. A commercial Inversin antibody was also tested. This antibody was raised against a peptide in the N-terminus and therefore only detected the HA-Inversin 1-553 and HA-Inversin FL proteins. Testing the Inversin antibodies against the non-phosphorylated protein, the T121 and T324 antibodies weakly detected the transfected HA-Inversin 1-553 and FL proteins. However, the T359 antibody did not detect the transfected proteins. Testing the antibodies raised against the phosphorylated protein revealed no detectable bands and showed a generally very dark blot. The data shown in Figure 4.10 were performed using the Inversin antibodies in TBST buffer and 5% BSA at a dilution of 1:500. Membranes were washed three times for 15 min each after incubation with the primary and secondary antibody for 1h each. These data are representative of experiments performed two times at the stated conditions as well as under further conditions with these primary antibodies at dilutions of 1:1000 and 1:200, both times incubated for 1h, as well as experiments performed at a dilution of 1:500, but with washed of five times 15 min each. The results suggest that either the antibodies are not good enough to detect the protein in cell extracts or that the Inversin protein is not phosphorylated in transfected cells.

4.2.5 Characterisation of phospho-Inversin antibodies by immunofluorescence microscopy

To test the Inversin antibodies by immunofluorescence microscopy, cycling and serum starved RPE1 cells were co-stained with the Inversin antibodies. The centrosomal marker, γ -tubulin, was also stained in cycling cells, and γ -tubulin and the primary cilium marker, acetylated-tubulin, in serum starved cells. Whereas the T359 and pT359 antibodies did not show any staining (data not shown), the T121 and T324 antibodies

showed punctuate nuclear staining in both, cycling and serum starved, cells (Fig 4.11A and B). Moreover, the T324 antibody showed co-localisation with centrosomes in cycling cells and the basal body of primary cilia in serum starved cells (Fig. 4.11B). Localisation to centrosomes and the nucleus could also be detected with the pT121 (Fig. 4.12A) and pT324 (Fig. 4.12B) antibodies in cycling cells.

Summarising, the T121 and T324 proteins detected transfected Inversin 1-553 and FL protein in cell lysates by Western blot, whereas by immunofluorescence microscopy the T324, pT121 and pT324 antibodies are potentially able to detect Inversin protein.

4.2.6 Validation of Inversin siRNA oligonucleotides

To test the specificity of the newly generated Inversin antibodies, human Inversin siRNA oligonucleotides were validated in RPE1, HeLa, and IMCD3 cells (Fig. 4.13). Experiments were performed using lipofectamine transfections and cells were incubated with the oligonucleotides for 48 h in the shown experiments. However, beforehand siRNA experiments were also performed using oligofectamine (Invitrogen) and the manufacturer's instructions, but no knockdown of Inversin could be observed.

Using lipofectamine and 100 nM of siRNA in 10 cm dishes, HeLa cells showed a small reduction of Inversin protein after 48 h of treatment with oligonucleotide 05, as well as the pool, containing 25 nM of each of the four Inversin oligonucleotides. GAPDH knockdown was performed as a control, showing complete loss of the GAPDH protein in HeLa cells. In RPE1 cells, siRNA transfection led to reduction of GAPDH protein levels by roughly 50%. Inversin knockdown of both visible human Inversin isoforms at 120 kDa and 100 kDa occurred using the Inversin siRNA oligonucleotide 08. However, when the Inversin oligonucleotide 08 and the pool of oligonucleotides were transfected into RPE1 cells a second time, as well as IMCD3 cells, neither one reduced the protein levels of both Inversin isoforms in RPE1 cells, and one detectable isoform in IMCD3 cells. Also the GAPDH oligonucleotide did not reduce the protein levels as well as in the previous experiments. In IMCD3 cells, this could be the case because of these oligonucleotides being designed against the human sequence, whereas IMCD3 cells are derived from

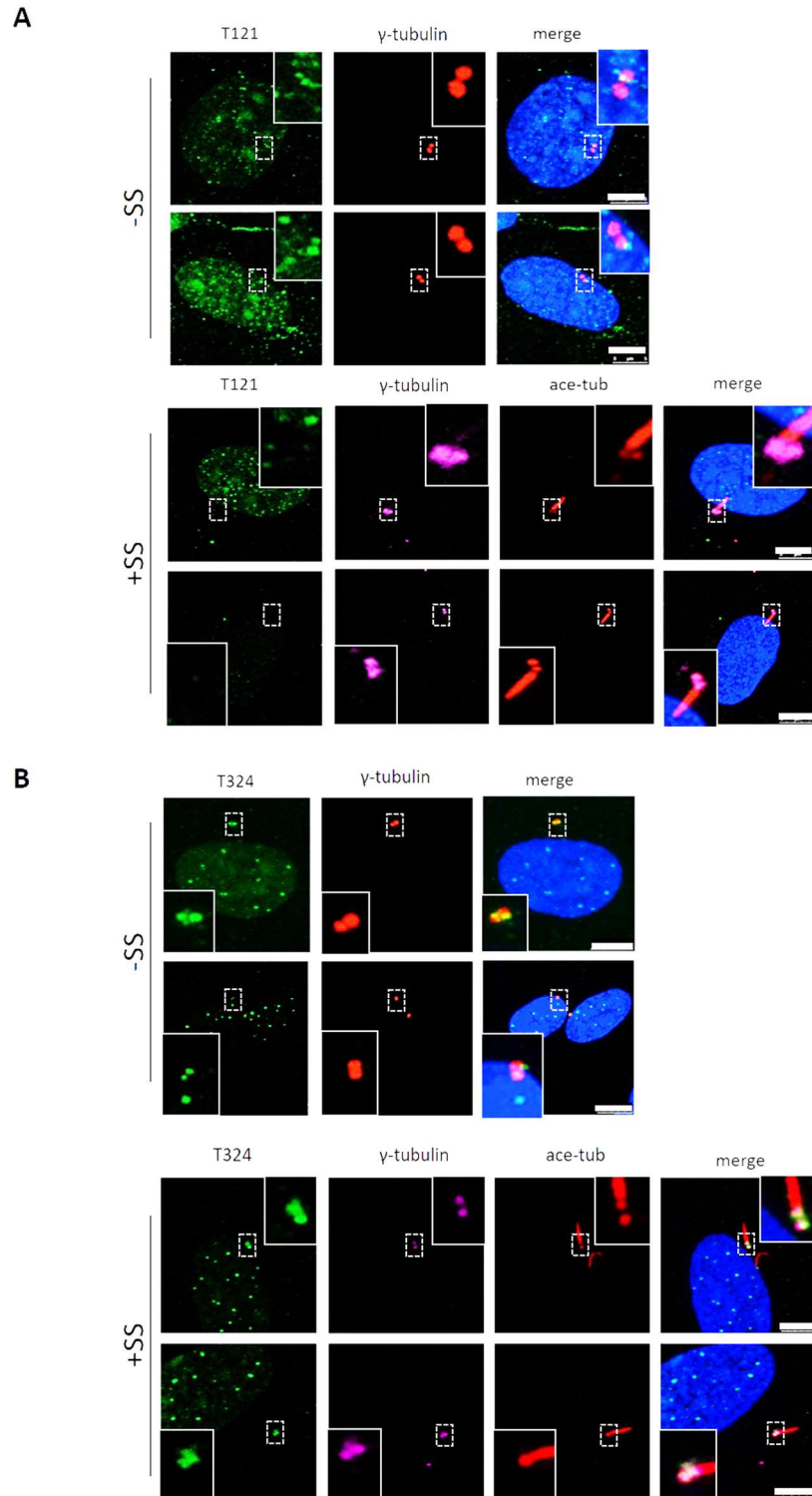


Figure 4.11 Analysis of Inversin antibodies by immunofluorescence microscopy of RPE1 cells

Immunofluorescence microscopy of cycling (-SS) and serum staved (+SS) RPE1 cells stained with antibodies raised against Inversin T121 (green, **A**), or T324 (green, **B**) together with γ -tubulin for centrosomes (red or purple as indicated) and acetylated tubulin (red). DNA was stained with DAPI (blue). Magnified images show localisation of Inversin to centrosomes or cilia. Images show representative data from three independent experiments. Scale bars, 5 μ m, apart from last row in **A** and second in **B**, 7.5 μ m.

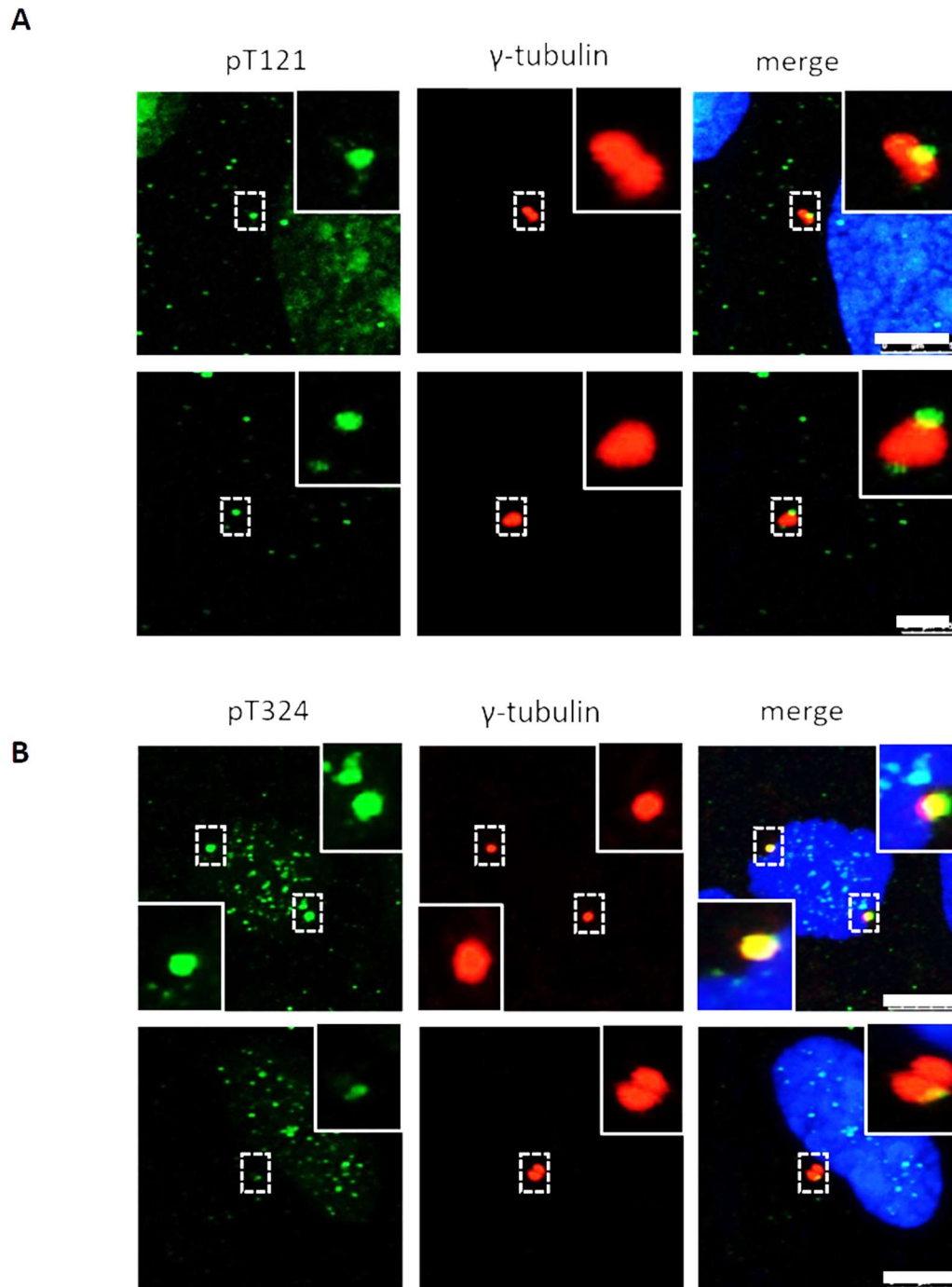


Figure 4.12 Analysis of Inversin phosphoantibodies by immunofluorescence microscopy

Immunofluorescence microscopy of cycling RPE1 cells stained with antibodies against phosphorylated Inversin, pT121 (**green, A**) or pT324 (**green, B**) together with γ -tubulin (red) for centrosomes. Magnified images show localisation of Inversin to centrosomes. DNA stained with DAPI (blue). Images show representative data from three independent experiments. Scale bars, 5 μ m in top row in **A** and bottom row in **B**, 2.5 μ m in bottom row in **A**, and 7.5 μ m in bottom row in **B**.

mice. In summary, to use the Inversin siRNA as a reliable approach to validate the Inversin antibodies, further conditions have to be tested.

4.2.7 Generation of Inversin mutants

To further explore the importance of Inversin phosphorylation by Nek8 in cells, a set of phosphomutants was generated. Initially, generation of phospho-mimetic (threonine to glutamic acid or serine to aspartic acid) and phospho-null (threonine or serine to alanine) mutants of all 12 mapped phosphosites was planned. Primers were designed and mutagenesis was performed in the HA-tagged Inversin FL mammalian expression construct. Mutagenesis of the three phosphosites in the N-terminus (T121, T324, T359) in the bacterial His-Inversin 1-553 construct was also planned to validate phosphorylation in kinase assays with purified proteins. In parallel, known mammalian NPHP disease mutants were designed for generation in the mammalian expression construct. However, mutagenesis was only partially successful. DNA sequencing confirmed that phospho-null mutants of T1032, T359, T1057, and T866 were successfully generated, as well as the NPHP disease-associated mutants representing the L493S substitution and a prematurely truncated protein of 603 amino acids. The localisation of these mutations in the Inversin protein is shown in Figure 4.14A. All generated constructs were transfected into RPE1 cells in one initial experiment to confirm estimated proteins sizes by SDS-PAGE and Western blotting using a HA-tag antibody (Fig. 4.14B). Whereas the L439S, T1032A, T359A, T1057A, and T866A mutants were generated in the full-length Inversin vector and ran at an estimated molecular weight of 140 kDa, the re-cloned, truncated R603* protein ran at an estimated molecular weight of 50 kDa. These constructs can now be used in further cell-based assays.

4.2.8 The PC-2 C-terminus is a substrate for Nek8 kinase activity *in vitro*

A further potential substrate for Nek8 is the ciliary membrane Calcium channel, PC-2. To test this, a purified, N-terminally His-tagged PC-2 fragment encoding the C-terminal

cytoplasmic domain (amino acids 680 to 968) was kindly provided by Prof Albert Ong (University of Sheffield). Radiolabelled kinase assays were performed using the His-Nek8 active kinase domain protein, as well as commercially obtained Nek3, Nek5, and Nek6 kinases to validate specificity (Fig. 4.15A). MBP was used as a control substrate. Incubation of the PC-2 C-terminus with Nek8 led to an upshift of the His-PC-2 680-968 protein as visualised by SDS-PAGE and Coomassie Blue stain, suggesting the presence of multiple phosphorylation sites. An autoradiograph showed phosphorylation of both, the MBP and PC-2 proteins, by all four kinases to varying extents. Indeed, it was clear that while PC-2 was a good substrate for Nek3 and Nek6, it was an excellent substrate for Nek8.

Kinase assays were therefore performed with Nek8 and unlabelled ATP and phosphorylation sites mapped by MALDI-ToF analysis at the University of Leicester Proteomics Facility. Mapped sites within the purified cytoplasmic C-terminus of PC-2 are highlighted in Fig. 4.15B. 21 phosphorylation sites for Nek8 were mapped at the following positions according to the full-length PC-2 protein sequence (isoform 1): T683, S658, S698, S701, T721, S726, S728, T751, T771, S794, S795, S812, S492, S898, S914, S917, T931, S951, T952, S963 and S964. WebLogo analysis of all sites and the 10 amino acids up- and downstream of the sites revealed a preference for serine at position -4 and -8, and for aspartic acid at -7. Furthermore, glutamine seemed preferable at position +6, and arginine at positions -9, +4 and +9, as well as lysine at position -10 (Fig. 4.15C).

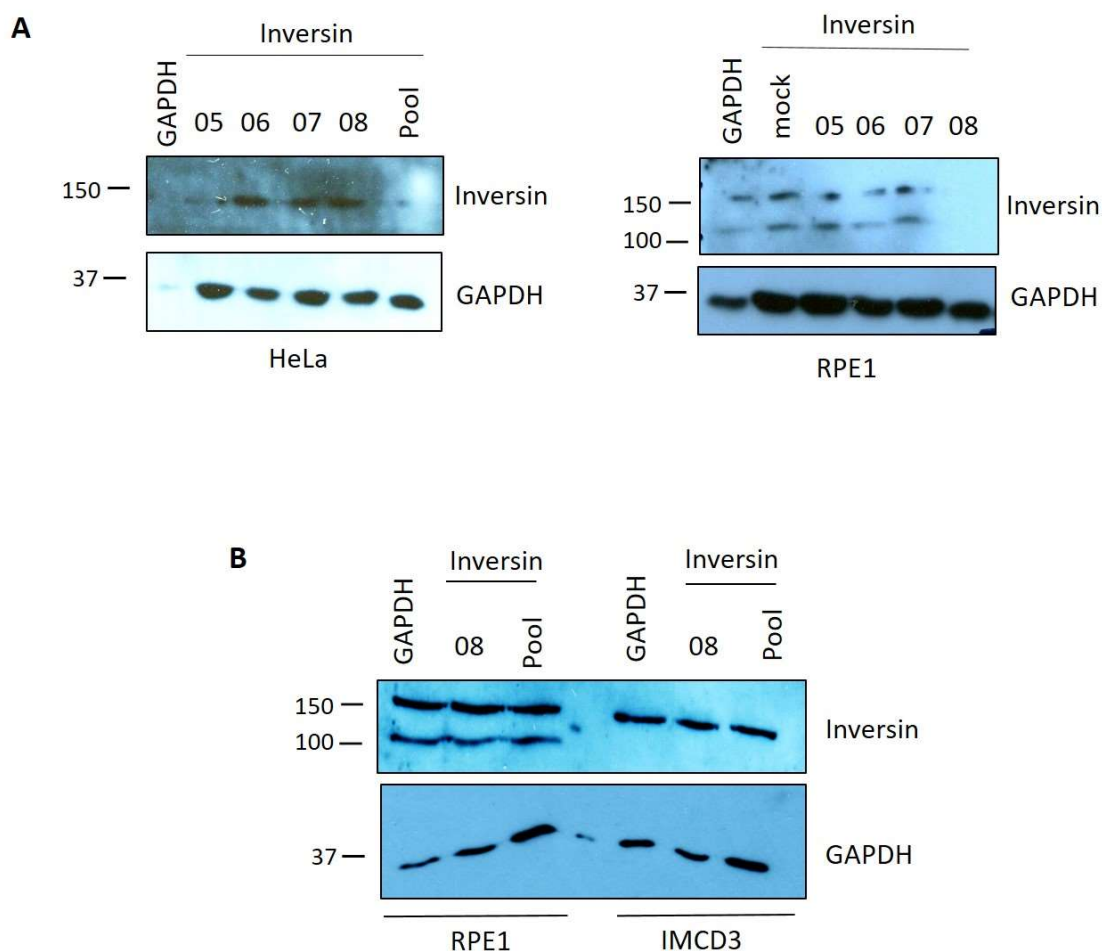
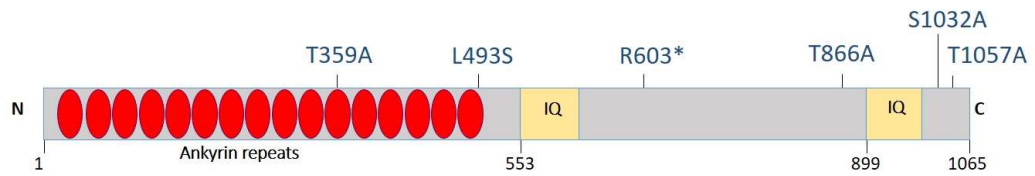


Figure 4.13 Validation of Inversin siRNA oligonucleotides in cells

A. HeLa and RPE1 cells were transfected with GAPDH and Inversin siRNA oligonucleotides as indicated and incubated for 48 h. Whole cell lysates were analysed by Western blotting using Inversin and GAPDH antibodies. Molecular weights are indicated on the left (kDa). **B.** PPE1 and IMCD3 cells were transfected with Inversin siRNA oligonucleotide 08, the pooled oligonucleotides, or the GAPDH oligonucleotide and incubated for 48 h. Whole cell lysates were analysed by Western blotting using Inversin and GAPDH antibodies. Molecular weights are indicated on the left (kDa).

A



B

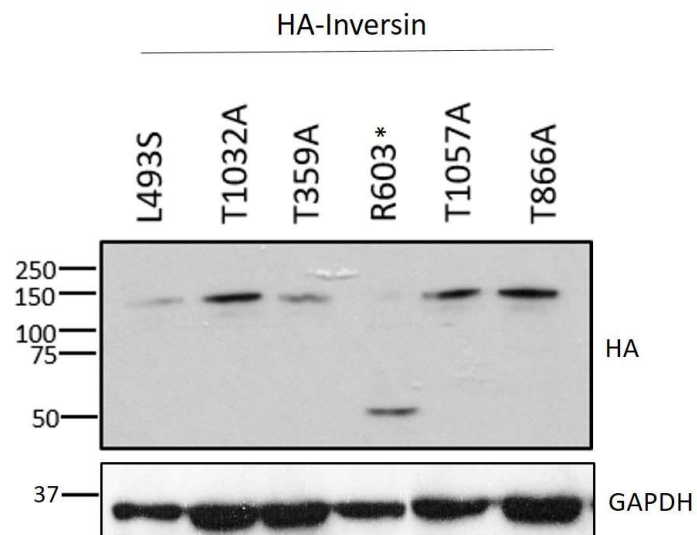


Figure 4.14 Generation of disease and phosphorylation site mutants of Inversin

(A) Schematic of Inversin showing position of mutations relative to the domain structure. **(B)** RPE1 cells were transfected with HA-Inversin mutants (as indicated) and whole cell lysates were analysed by Western blotting using a HA-tag and a GAPDH antibody as indicated. Molecular weights (kDa) are indicated on the left.

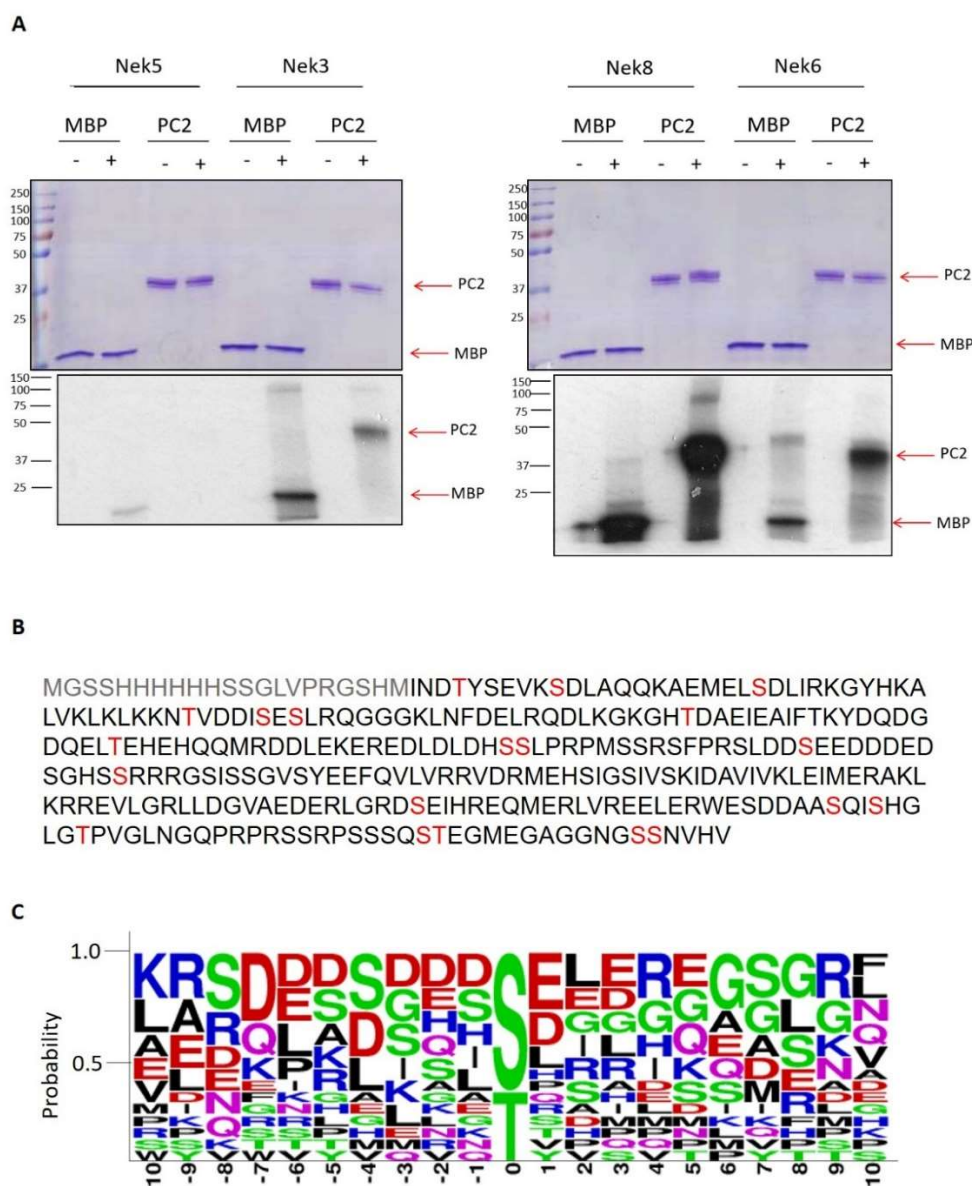


Figure 4.15 The PC-2 C-terminus is a substrate for Nek8 *in vitro*

A. Kinase assays were performed using the purified PC-2 C-terminal domain and MBP as indicated as substrates. Samples were incubated in kinase buffer containing radio-labelled ATP with and without (-/+) Nek3, Nek5, Nek6 or Nek8 kinase as indicated. Samples were analysed by SDS-PAGE, Coomassie Blue stain and autoradiography. Phosphorylated proteins are indicated (red arrows). Shown are representative data from three independent experiments. Molecular weights (kDa) are indicated on the left. **B.** The His-PC2 680-968 protein was submitted for mass spectrometry analysis after incubating with Nek8 kinase and ATP for 120 min. The His-PC2 protein sequence, including tag and linker (grey), and the C-terminal amino acids 600 to 968 is shown with phosphorylation sites identified highlighted in red. **C.** A sequence preference was created using the WebLogo 3.5.0 programme to analyse sequence conservation across the phosphosites. Probability of the occurrence of a certain amino acid was plotted against the position of the residue up- and down-stream of the phosphorylated Threonine or Serine. Polar amino acids are green, hydrophobic amino acids are black, basic amino acids are blue, and acidic amino acids are red, with the most common amino acid indicated at the top.

4.3 Discussion

4.3.1 Inversin as a substrate for Nek8 kinase activity

Our data show that Inversin is an excellent substrate for Nek8 kinase activity *in vitro*. Using mass spectrometry, we mapped 20 phosphorylation sites in Inversin, of which 12 could be confidently stated as Nek8 phosphosites. Sequence comparison of the 12 confidently assigned sites with the WebLogo 3.5.0 programme revealed a strong preference for leucine at position -3, -4 and +2, as well as a preference for leucine at positions -9 and +7. A leucine or phenylalanine at position -3 has also been shown to be of preference for Nek2, with both Nek2 and Nek6 generally preferring hydrophobic residues in the peptide sequence surrounding a phosphosite (Fry et al., 2012, Alexander et al., 2011).

Three sites of phosphorylation are located in the Inversin N-terminus at positions T121, T324 and T359, and nine are located in three clusters in the C-terminus (see Fig. 4.7C). Even though only a quarter of the identified sites are located in the N-terminus, this fragment was phosphorylated much more efficiently than the Inversin C-terminus. This leads to the conclusion that these sites might be more important for regulation of Inversin by Nek8 within the cell. This is also consistent with the fact that Nek8, and more specifically the Nek8 kinase domain, interacts more strongly with the Inversin N-terminus, indicating a tighter affinity of these protein domains. Phosphorylation at these residues, or maybe only one of these residues, might be a key regulator of Inversin function and might mediate Inversin's interaction with other proteins. However, the phosphosites in the C-terminus seem to cluster in areas of functional importance for Inversin. The sites at the far end of the C-terminus (T1032, T1043 and T1059) are located in the ciliary targeting motif, suggesting a role for Inversin phosphorylation by Nek8 in its localisation to cilia. Furthermore, T841, T864, S865 and T866 are located near the NLS (amino acids 778-796) (Lienkamp et al., 2011), potentially changing the conformation of the protein when phosphorylated and making the NLS either accessible or inaccessible. T864, S865 and T866 have also been described to be phosphorylated by the serine/threonine kinase Akt that localises to the basal body of primary cilia and mediates ciliogenesis and well as processes involved in cell cycle progression, proliferation and

spindle axis determination. Akt-dependent phosphorylation of these Inversin residues is required for cilia growth, cell proliferation and the cell polarity (Suizo et al., 2016). This suggests that Akt and Nek8 might be phosphorylating these particular residues at different times throughout the cell cycle, with Nek8 potentially regulating Inversin function in cycling cells in the nucleus and at spindle poles.

Due to the preference of the Nek8 kinase for the Inversin N-terminus and the substantial phosphorylation in this region, we decided to generate phospho-antibodies against these three sites, T121, T324 and T359, as potential biomarkers for Nek8 kinase activity. AMSBIO were commissioned to generate phospho-specific and non-phospho-specific antibodies that we tested against recombinant Inversin. A summary of the data is shown in table 4.1. Analysis of these antibodies revealed that all of them, apart from the Inv-pT359 antibody, were able to detect purified Inversin *in vitro* by Western blot, but only T121 and T324 detected transfected Inversin protein in cell lysates. By IF, the T324, pT121 and pT324 antibodies were able to detect a signal in the nucleus and at centrosomes in cycling cells and the basal body in serum starved cells. Although we cannot be certain that this is phosphorylated Inversin protein, these are the main structures to which Inversin has been described to localise (Otto et al., 2002; Nurnberger et al., 2004). The fact that neither the T359, nor the pT359 antibody can detect the Inversin protein in cells, leads to the assumption that this residue might be buried on the inside of the Inversin protein or within a complex of Inversin and binding partners, and therefore only available for antibody binding under denatured conditions, such as by Western blot. The T359 site might also not be phosphorylated *in vivo*. Surprisingly, the T121 antibody only detected Inversin in the nucleus, but did not show obvious centrosomal staining, thus suggesting that binding of Inversin to centrosomal proteins might block antibody accessibility.

The residues T121 and T324 are both phosphorylated *in vivo* in the nucleus and at the centrosomes. This supports a role for Nek8 and Inversin as a complex at these structures. However, it should be kept in mind that Inversin may be phosphorylated at the same sites by other kinases. Hence, to validate this specificity, Nek8 inhibitors or depletion approaches could be used. In addition, to further validate if these antibodies specifically

detect Inversin, the Inversin siRNA oligonucleotides have to be further validated and different conditions have to be tested to reach consistent knockout of the protein. Furthermore, if knockdown cannot be detected by Western blot analysis, qRT-PCR can be performed.

Overall, we conclude that the T121 and T324 antibodies are excellent for detecting purified Inversin protein and transfected protein in cell lysates by Western blot and work well in immunofluorescence microscopy. The pT121 and pT324 antibodies are excellent for immunofluorescence microscopy, while the pT121 and pT359 antibodies work well on purified Inversin protein by Western blot. Hence, these antibodies are excellent biomarkers of Nek8 activity.

4.3.2 PC-2 is a substrate for Nek8 kinase activity

PC-2 is a transmembrane calcium channel located in the membrane of the endoplasmic reticulum and cilia. It's C-terminal cytoplasmic domain consists of a calcium-binding EF-hand (amino acids 719-798) (Ong and Harris, 2015) and a coiled-coil domain (amino acids 830-872) that contributes to oligomerisation, protein regulation and channel assembly (Yang et al., 2015). The localisation of PC-2 to the cilium has been described to be Nek8-dependent (Sohara et al., 2008). It has also been proposed that PC-2 might be a substrate for Nek8 kinase activity, as murine PC-2 proteins in *jck* mice exhibit an upshift by SDS-PAGE, suggesting excessive post-translational modification. To test this hypothesis, we performed kinase assays with Nek8 and the C-terminal domain (amino acids 680-968) of the human PC-2 protein and showed that the PC-2 C-terminus is an excellent substrate for Nek8 kinase activity *in vitro*. We were able to map the following 21 sites by MALDI-ToF analysis: T683, S658, S698, S701, T721, S726, S728, T751, T771, S794, S795, S812, S492, S898, S914, S917, T931, S951, T952, S963 and S964. Sequence analysis of these sites with the WebLogo tool revealed no similarity to the preferred sequence of Nek8 in Inversin, or the described preference of other Nek kinases in the literature. However, Nek kinases do not always have strong sequence preferences (Fry et al., 2012). Phosphorylation of PC-2 has previously been described to mediate its localisation. *Jck* mice not only exhibit elevated levels of PC-2 phosphorylation, but also

show accumulation of the protein at the cilia. Sohara et al. (2008) therefore proposed a gain-of-function mutation of Nek8 in *jck* mice, which leads to over-phosphorylation of its substrate, PC-2, and affects its localisation to cilia. Furthermore, studies in *C. elegans* have shown that a phospho-null mutant of PC-2 at position S534 (serine substitution to alanine) prevents ciliary localisation (Sohara et al., 2008, Hu et al., 2006). To further investigate the importance of these mapped phosphorylated sites, phospho-mutants will need to be generated and localisation studies performed.

| Antibody | Detects purified protein by WB | Detects transfected protein by WB | Localisation by IF |
|--------------|--------------------------------|-----------------------------------|---------------------------------------|
| T121 | Yes | Yes | Nucleus |
| T324 | Yes | Yes | Nucleus Centrosomes Basal body |
| T359 | Yes | No | None |
| pT121 | Yes | No | Nucleus Centrosomes Basal body? |
| pT324 | No | No | Nucleus Centrosomes Basal body? |
| pT359 | Yes | No | None |

Table 4.1 A summary of the activity of the phospho-specific and non-phospho-specific Inversin antibodies

Shown are the antibodies generated against Nek8 phospho-sites in the Inversin N-terminus and their ability to detect phosphorylated Inversin *in vitro* by Western blot (WB), by Western blot from cell lysates and by immunofluorescence microscopy (IF).

CHAPTER 5 THE pNEK8 ANTIBODY AS A BIOMARKER FOR NEK8 ACTIVITY IN CELL CYCLE PROGRESSION, THE DNA DAMAGE RESPONSE AND CILIOGENESIS

5.1 Introduction

The NPHP disease protein Nek8 is a cell cycle dependent serine/threonine kinase of the NIMA (Never in Mitosis Gene A) kinase family. As described earlier, Nek8 localises to centrosomes in cycling cells and to cilia in quiescent cells, where it is anchored by Inversin (Shiba et al., 2010). It has also been reported that Nek8 has to be active to localise to these structures, suggesting a role for kinase activity in localisation (Zalli et al., 2011). Nek8 has also been described to play a role in the DNA damage response by controlling replication fork dynamics and progression through S-phase by inhibiting CDK1 activity (Choi et al., 2013). However, it remains unclear exactly how Nek8 activity is involved in cell cycle arrest.

In this chapter, we have characterised a customised phospho-Nek8 antibody raised against the threonine 162 residue in the activation loop of the kinase domain. This residue is often subject to phosphorylation in protein kinases and is thought to be a key positive regulator of Nek8 kinase activity. A phospho-null mutation at this residue, substituting the threonine with an alanine, leads to a catalytically-inactive protein, whereas a phospho-mimetic mutation, exchanging the threonine to glutamic acid, causes the protein to behave as if it may be constitutively active (Zalli et al., 2011). We have focused mainly on localisation of active Nek8 to centrosomes, cilia and sites of DNA damage and validated the specificity of the antibody using chemical inhibitors of Nek8.

The Nek8 inhibitors were also used to investigate the cellular consequences of loss of Nek8 kinase activity and consider how the phenotypes relate to known Nek8 NPHP disease phenotypes. For this work, two inhibitors, CCT137690 and CCT129932, were used that were found to inhibit Nek8 kinase activity in biochemical assays. However, caution is required in interpreting cellular phenotypes as both inhibitors were initially

discovered as very potent Aurora A inhibitors, another serine/threonine kinase with roles in mitotic progression (Bavetsias et al., 2012).

5.2 Results

5.2.1 The pNek8 antibody detects active Nek8 kinase domain protein

To explore the spatial and temporal pattern of Nek8 activity in cells, we decided to make use of a phospho-specific antibody that had been raised against the threonine 162 residue in the activation loop of the catalytic domain of Nek8 by the Bayliss laboratory (University of Leicester) (Fig 5.1A).

To validate the pNek8 antibody, *in vitro* kinase assays were performed with purified Nek8 kinase domain protein and non- radiolabelled ATP (Fig. 5.1B). The Nek8 kinase was pre-incubated in buffer containing ATP for 15 min at 30°C and then incubated for another 60 min with the His-Inversin 1-553 substrate. Buffers without ATP or the substrate served as negative controls. After separation of samples by SDS-PAGE, Western blotting was performed with a His-tag antibody. The pNek8 antibody was then used to determine Nek8 phosphorylation at the T162 activation site and the Inv-pT121 antibody was used to determine the activity of Nek8 against its physiological substrate, Inversin. The pNek8 antibody detected Nek8 kinase more strongly when it had been pre-incubated with ATP than when it was not pre-incubated. This suggests that the kinase was not phosphorylated or active before addition of ATP. The Inv-pT121 antibody detected the Inversin protein weakly in the absence of ATP, but much more strongly after it had been incubated with active Nek8 and ATP. This confirms that the Nek8 kinase was active and able to phosphorylate Inversin in the presence of ATP and that the pNek8 antibody is able to selectively detect activated Nek8.

5.2.2 CCT32 and CCT90 inhibit Nek8 kinase activity *in vitro*

Having established that the pNek8 antibody was capable of detecting phosphorylated, active Nek8, it was used to validate the ability of two small molecule inhibitors,

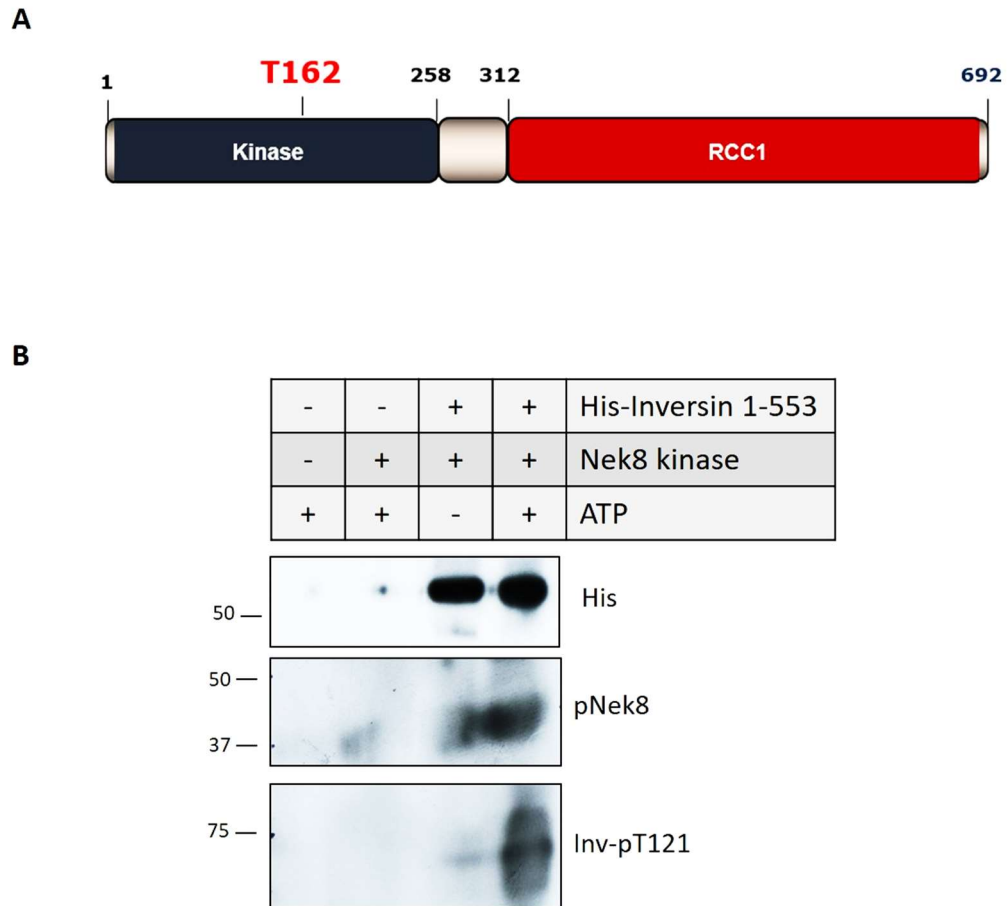


Figure 5.1 Validation of pNek8 antibodies using *in vitro* kinase assays

A. The phospho-Nek8 (pNek8) antibody was raised against the phosphorylated Threonine 162 in the activation loop of the kinase domain. **B.** *In vitro* kinase assays were performed with the purified, recombinant Nek8 kinase following pre-incubation in kinase buffer with or without ATP as indicated for 15 min at 30°C. His-Inversin 1-553 and ATP were added where indicated for another 60 min. Samples were analysed by Western blotting using a His-tag, pNek8, and Inv-pT121 antibody. Shown are representative data of three independent experiments. Molecular weights (kDa) are indicated on the left.

CCT129932 (CCT32) and CCT137690 (CCT90), to inhibit Nek8 kinase activity. Both inhibitors were previously discovered as Aurora A inhibitors with CCT90 binding the catalytic domain of the Aurora kinases and having an IC₅₀ of 15 nM against Aurora A, 25 nM against Aurora B and 19 nM against Aurora C (Bavetsias et al., 2012). They had been subsequently tested for their ability to inhibit Nek8 in biochemical assays by Dr Sharon Yeoh (University of Leicester) prior to these studies. The IC₅₀ against Nek8 of the CCT32 inhibitor had been calculated to be 3.206 μ M and the IC₅₀ of CCT90 was 14.09 μ M using a fluorescent peptide substrate (Fig. 5.2).

First, kinase assays were performed to confirm the ability of CCT32 to inhibit Nek8 kinase activity *in vitro* (Fig. 5.3). After pre-incubation of the Nek8 kinase with buffer containing ATP for 15 min, samples were incubated for another 60 min in buffer with and without the substrate, purified His-Inversin 1-553, and with and without ATP and CCT32 at 3 μ M (Fig. 5.3A). Western blot analysis using a His-tag antibody confirmed the presence of the His-Inversin 1-553 protein. Phosphorylation of the Nek8 kinase in the presence of ATP was confirmed using the pNek8 antibody, and the activity of the Nek8 kinase against Inversin was determined using two antibodies, pT121 and pT359. Both showed phosphorylation of the substrate in the presence of Nek8 and ATP, but not when the CCT32 compound was also present, demonstrating the ability of this compound to inhibit Nek8 activity against Inversin (Fig. 5.3B).

Since the in house Nek8 kinase used in previous experiments was provided by the Bayliss lab in limited quantity, a commercial Nek8 kinase was bought in to eventually replace the in-house protein. To compare the activity of this commercial kinase with the in-house protein, as well as to validate the specificity of the second Nek8 inhibitor, further kinase assays were performed using both kinases and both inhibitors alongside each other and the results were analysed by Western blotting (Fig. 5.4). The pNek8 antibody showed phosphorylation of both the in-house and the commercial Nek8 kinase upon addition of ATP. This was slightly reduced in samples that did not contain ATP, stating that parts of the Nek8 kinase are already phosphorylated during the generation process of the protein. Fluctuation in the phosphorylation levels of the Nek8 kinase as detected with the pNek8 antibody probably stem from inconsistency in pipetting when mixing the

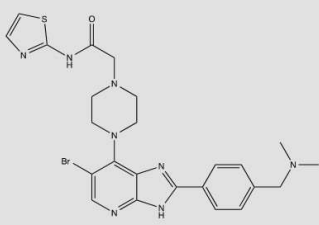
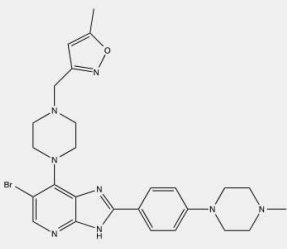
| Inhibitor | Structure | IC ₅₀ against Nek8 | Working concentration |
|----------------------|--|-------------------------------|---|
| CCT129932 (CCT32) |  | 3.206 μ M | <i>in vitro</i> : 3.2 μ M <i>in vivo</i> : 3.2 μ M |
| CCT137690 (CCT90) |  | 14.09 μ M | <i>in vitro</i> : 14 μ M <i>in vivo</i> : 3 μ M |

Figure 5.2 Small molecule inhibitors of Nek8

The chemical structures, IC₅₀ for Nek8 and working concentrations of the CCT129932 and CCT137690 inhibitors are shown.

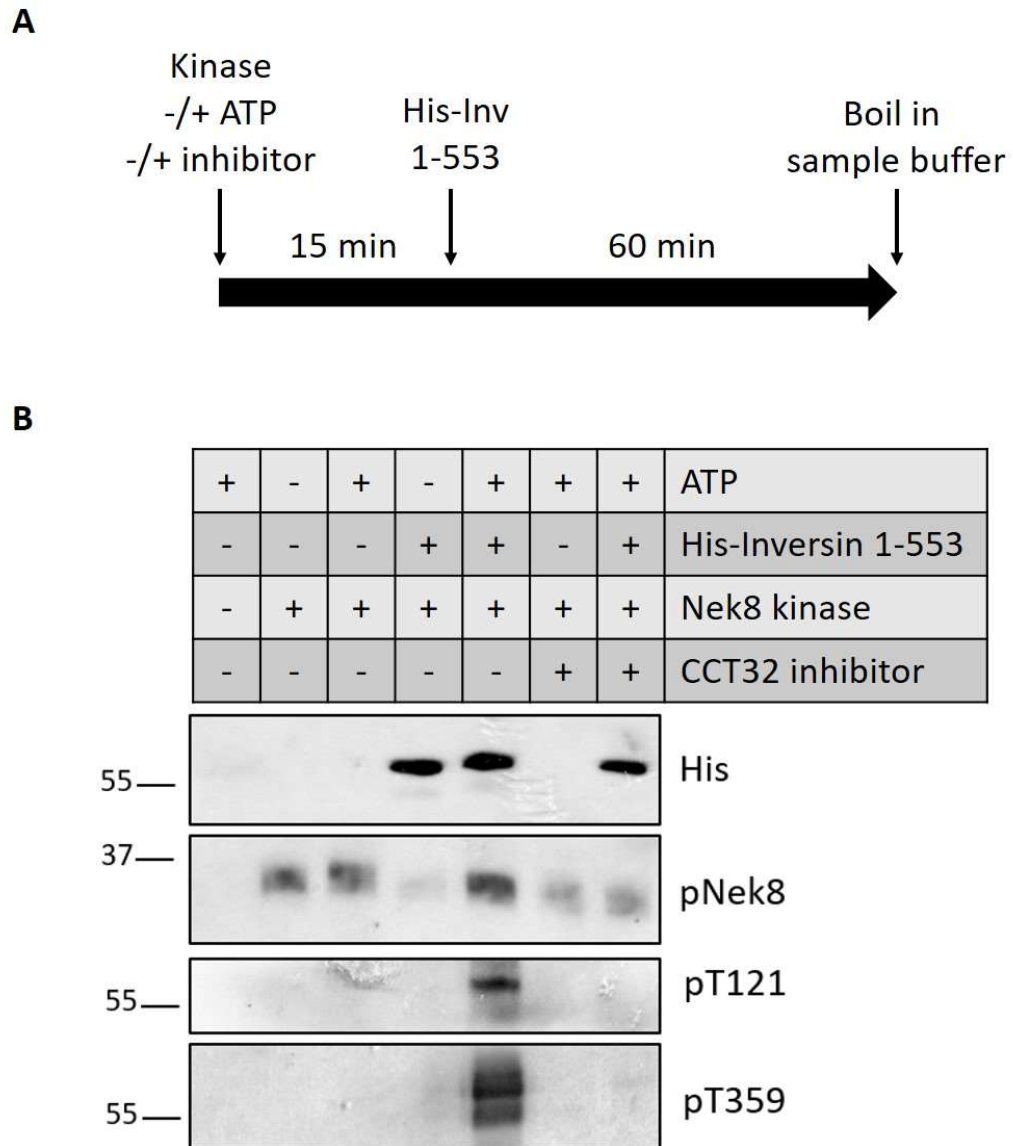
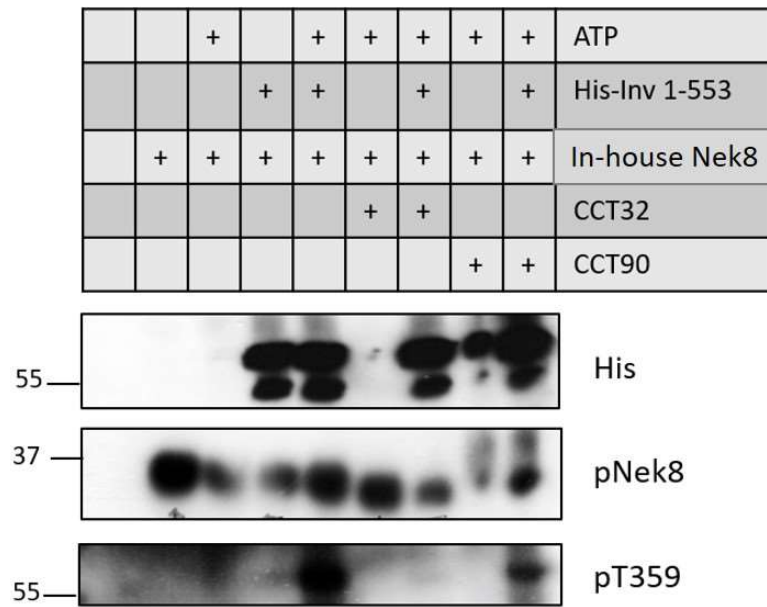
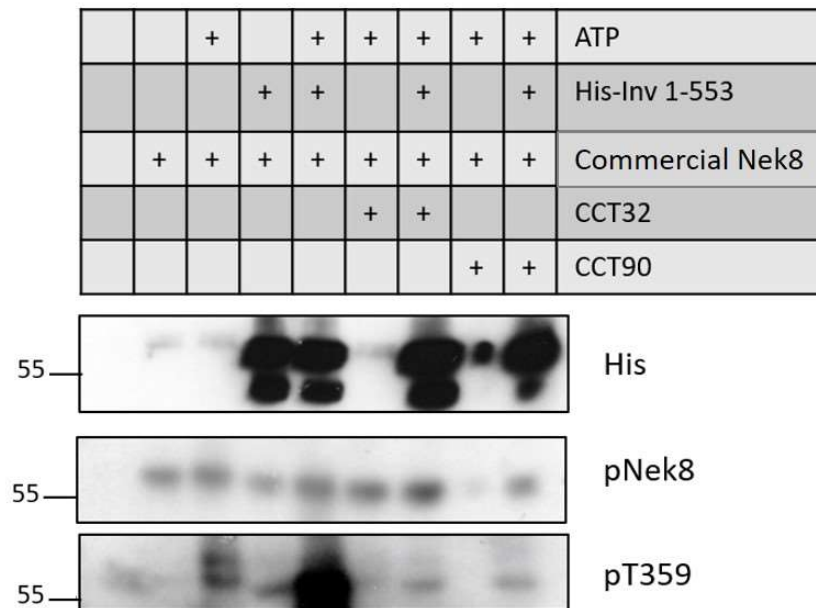


Figure 5.3 Chemical inhibition of Nek8 kinase activity

A. *In vitro* kinase assays were performed with the purified, recombinant Nek8 kinase following pre-incubation in kinase buffer with and without ATP and the CCT32 inhibitor as indicated for 15 min at 30°C. His-Inversin 1-553 was added as indicated for another 60 min. **B.** Samples were analysed by Western blotting using His-tag, pNek8, Inv-pT121, and Inv-pT359 antibodies. Shown are representative data of four independent experiments. Molecular weights (kDa) are indicated on the left.

A**B****Figure 5.4 Validation of CCT32 and CCT90 as chemical inhibitors of Nek8**

In vitro kinase assays were performed with the purified, recombinant in house Nek8 kinase (**A**) or a commercial Nek8 kinase (**B**) following pre-incubation in kinase buffer with ATP and either the CCT32 or CCT90 inhibitor as indicated for 15 min at 30°C. His-Inversin 1-553 was added as a substrate as indicated for another 60 min. Samples were analysed by Western blotting using His-tag, pNek8, and pInvT359 antibodies. Shown are representative data of three independent experiments. Molecular weights (kDa) are indicated on the left.

buffer. Analysis with the Inv-pT359 antibody showed strong phosphorylation of Inversin by both kinases that was reduced upon treatment with either CCT32 or CCT90. This reduction was more pronounced for the CCT32 inhibitor than the CCT90 inhibitor, especially for the in-house kinase, although both blocked sufficient phosphorylation of the substrate by Nek8. Hence, taken together these data show that both compounds are good inhibitors of Nek8 kinase activity *in vitro*.

5.2.3 Localisation of active Nek8 throughout the cell cycle

The pNek8 antibody was used for immunofluorescence microscopy in cycling and serum starved RPE1 cells to explore the localisation of active Nek8 throughout the cell cycle. In interphase cells the pNek8 antibody weakly stained both, centrosomes, visualised by γ -tubulin staining, and the nucleus. In mitotic cells, pNek8 was more obviously detected at spindle poles in prophase, prometaphase and metaphase. In telophase, pNek8 was detected predominantly at the midbody as shown by co-localisation with α -tubulin (Fig. 5.5). Meanwhile, in serum starved RPE1 cells that had entered quiescence, pNek8 localised to the nucleus as well as to the basal body, as visualised by co-localisation with γ -tubulin and acetylated tubulin staining (Fig. 5.6). Hence, these data suggest that a population of active Nek8 is present at centrosomes in interphase, spindle poles in mitosis and the basal body in ciliated cells. A fraction is also present in the nucleus.

5.2.4 Localisation of active Nek8 to sites of DNA damage

To specifically investigate the potential function of Nek8 in the DNA damage response (Choi et al., 2013), the localisation of pNek8 in the nucleus was investigated. For this purpose, DNA damage was induced by treatment of cycling RPE1 cells with 1.6 nM Aphidicolin for 24h. DNA damage foci were visualised using an antibody against 53BP1. Immunofluorescence microscopy after Aphidicolin treatment revealed that 53BP1 foci were more distinct compared to untreated cells which showed a more diffuse nuclear staining (Fig. 5.7A). Immunofluorescence microscopy was then performed in untreated and Aphidicolin-treated RPE1 cells with antibodies against pNek8 and γ H2AX as a DNA

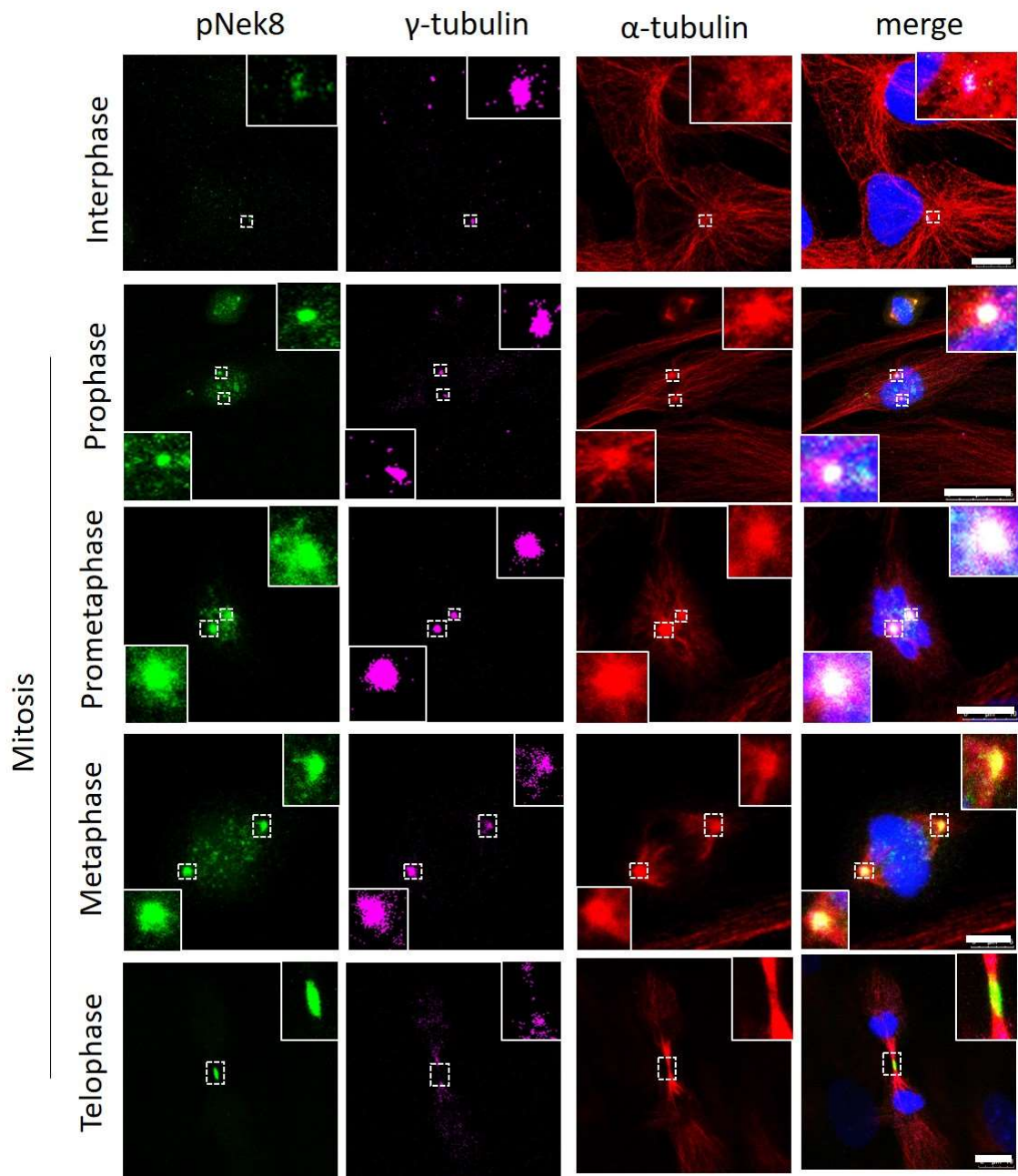


Figure 5.5 Active Nek8 localises to centrosomes, spindle poles and the midbody in cycling RPE1 cells

Immunofluorescence microscopy of cycling RPE1 cells stained with antibodies against pNek8 (green), γ -tubulin (purple), and α -tubulin (red). Cells at different stages of the cell cycle are indicated and magnified images show localisation of pNek8 to centrosomes, spindle poles, or the midbody. Merge includes DNA stained with DAPI (blue). Shown are representative data of seven independent experiments, analysing 20 cells each. Scale bars, 10 μ m in top, third and bottom row, 25 μ m in second row, and 5 μ m in fourth row.

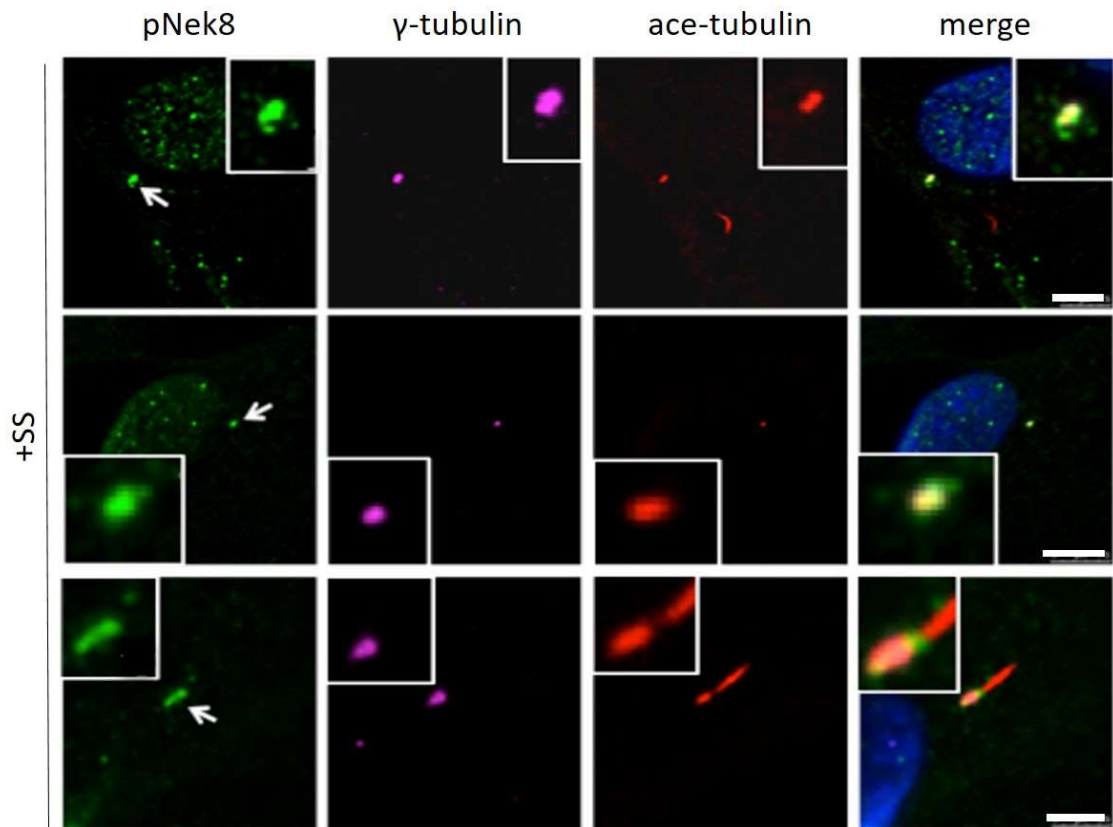


Figure 5.6 Active Nek8 localises to the basal body in serum starved RPE1 cells

Immunofluorescence microscopy of serum starved (+SS) RPE1 cells stained with antibodies against pNek8 (green), γ -tubulin (purple), and acetylated-tubulin (red). Magnified images show localisation of pNek8 to the basal body of the primary cilium. Merge includes DNA stained with DAPI (blue). Shown are representative data of ten independent experiments, analysing 5-20 cells each. Scale bars, 7.5 μ m.

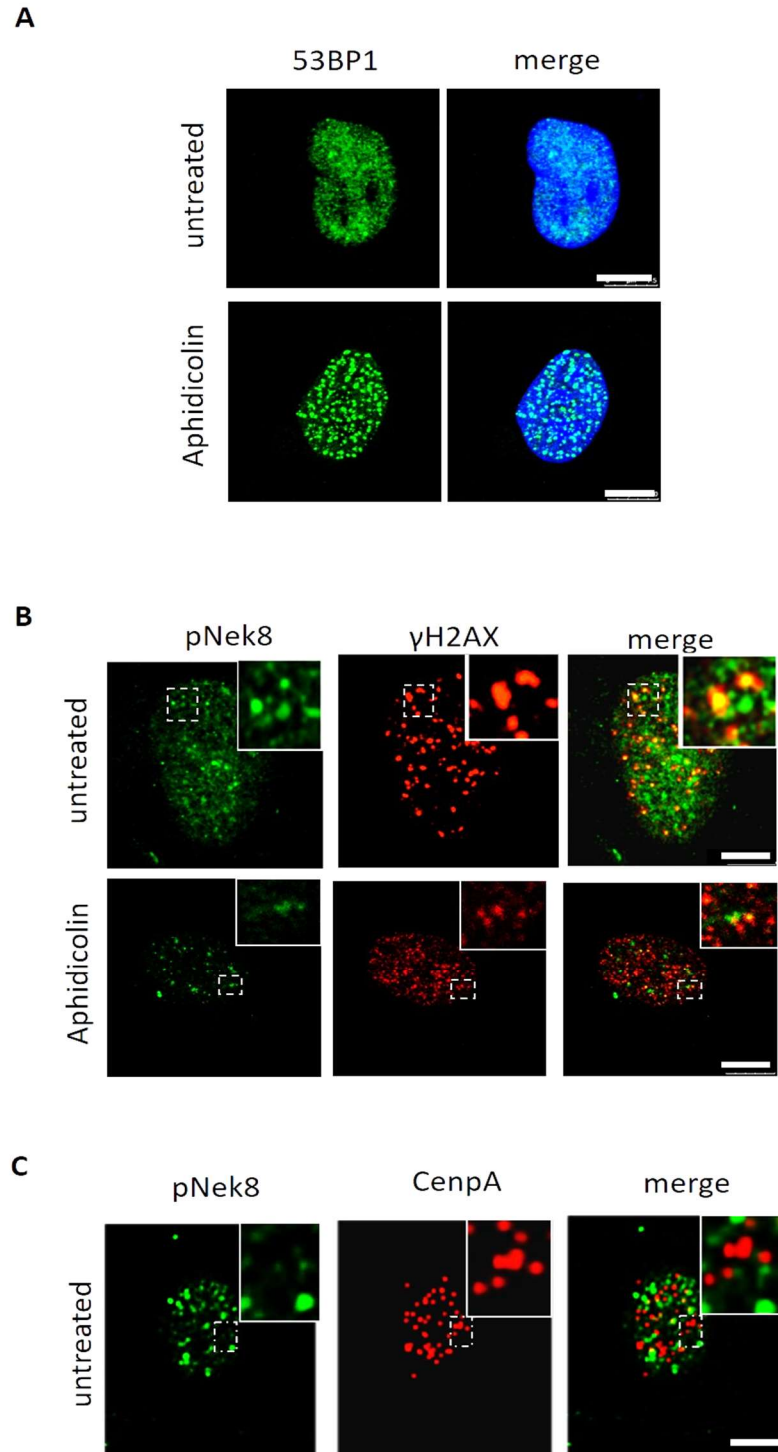


Figure 5.7 Active Nek8 localises to sites of DNA damage

Immunofluorescence microscopy of untreated and Aphidicolin treated RPE1 cells stained with antibodies against pNek8 (green) and either the DNA damage markers 53BP1 (red, **A**), and γ H2AX (red, **B**), or the centromere marker CenpA (red, **C**). Magnified images show localisation of pNek8 to DNA damage foci (**A**, **B**), but not to centromeres (**C**). Shown are representative data of one experiment, investigating 25 nuclei (**A**), and three experiments, analysing 25 nuclei each (**B**, **C**). Scale bars, 10 μ m in bottom rows of **A** and **B**, and in **C**, 7.5 μ m in top rows of **A** and **B**.

damage marker. The results showed more defined γ H2AX foci in Aphidicolin-treated compared to untreated cells and an accumulation of pNek8 in the nucleus and partial co-localisation with γ H2AX foci under both conditions (Fig. 5.7B). In contrast, there was no co-localisation of nuclear pNek8 foci with centromeres stained with antibodies against CenpA (Fig. 5.7C).

To confirm association of pNek8 with DNA damage foci, proximity ligation assays (PLA) were performed. This technique uses secondary antibodies that are attached to oligonucleotides (PLA probes) that hybridise when in close proximity to each other and form a complete circle after DNA ligation. One of the oligonucleotides then acts as a primer for rolling circle amplification, which can be visualised by a fluorescent probe. Primary antibodies were used against pNek8, γ H2AX, 53BP1 and CenpA. γ H2AX and 53BP1 were used as a positive control for the assay showing an average of 3.75 foci of co-localisation per nucleus in three independent experiments, analysing 10 nuclei each (Fig. 5.8B). γ H2AX and CenpA were used as a negative control to validate specificity of the assay and showed no foci of co-localisation for these two proteins in three independent experiments, analysing 10 nuclei each (Fig. 5.8A). When co-localisation of pNek8 with γ H2AX was analysed, an average of 2.5 foci per nucleus was observed after analysing 10 nuclei each in three independent experiments (Fig. 5.8C). The results confirm co-localisation of pNek8 with γ H2AX foci supporting a role for Nek8 kinase activity in the DNA damage response.

5.2.5 Consequences of Nek8 inhibition on cell cycle progression, ciliogenesis and DNA damage

To investigate the effect of Nek8 inhibition on cell cycle progression, ciliogenesis and the DNA damage response, RPE1 cells were treated with CCT32 or CCT90 for 20h, if not otherwise stated. At the IC₅₀ for CCT32 (3.2 μ M), the majority of cells was alive after treatment, whereas at the IC₅₀ for the CCT90 inhibitor (14 μ M), the majority of cells died. Hence, CCT90 was used at 3 μ M, which did not cause substantial cell death.

When the CCT90 inhibitor was validated in immunofluorescence microscopy, treatment of serum starved RPE1 cells showed loss of active Nek8 (pNek8 antibody) and potential reduction of γ -tubulin at the basal body of cilia (Fig. 5.9). This adds weight to the conclusion that this antibody is specific for active Nek8. However, loss of Nek8 did not lead to ciliogenesis defects as shown by statistical analysis of ciliogenesis in three independent experiments that revealed no reduction in cells exhibiting primary cilia upon treatment (Fig. 5.10). It was therefore concluded that Nek8 activity is not essential for primary cilia assembly.

Cycling cells treated with CCT90 exhibited multiple, abnormally shaped nuclei as shown by immunofluorescence microscopy in three independent experiments, analysing 50 cells each. These data suggest a cell division defect. However, examination of the microtubule network in immunofluorescence microscope using an antibody against α -tubulin revealed no obvious defects, but no mitotic cells were detected on these slides (Fig. 5.11). Treatment of RPE1 cells with CCT32 also caused extensive multinucleation (Fig. 5.12A) as investigated in three independent experiments, analysing 15 cells each. Consistent with mitotic failure, an increase in centrosome number was observed from an average of 2.1 to 3 centrosomes per cell (Fig. 5.12B). These data suggest a division defect upon treatment of cells with either CCT90 or CCT32.

To explore a potential defect in progression through the cell cycle, immunofluorescence microscopy with the proliferation marker Ki67 was performed in three independent experiments with 50 cells each (Fig. 5.13A). Whereas 92% of untreated RPE1 cells expressed Ki67, only 30% of CCT90 treated RPE1 cells were Ki67 positive. Upon serum starvation for 48h, 28% of untreated cells expressed Ki67, whereas none of the CCT90-treated cells exhibited Ki67 staining (Fig. 5.13B). These data clearly demonstrate a significant reduction in proliferation upon treatment of cells with CCT90, which is consistent with previous data where no mitotic cells could be observed in inhibitor treated populations.

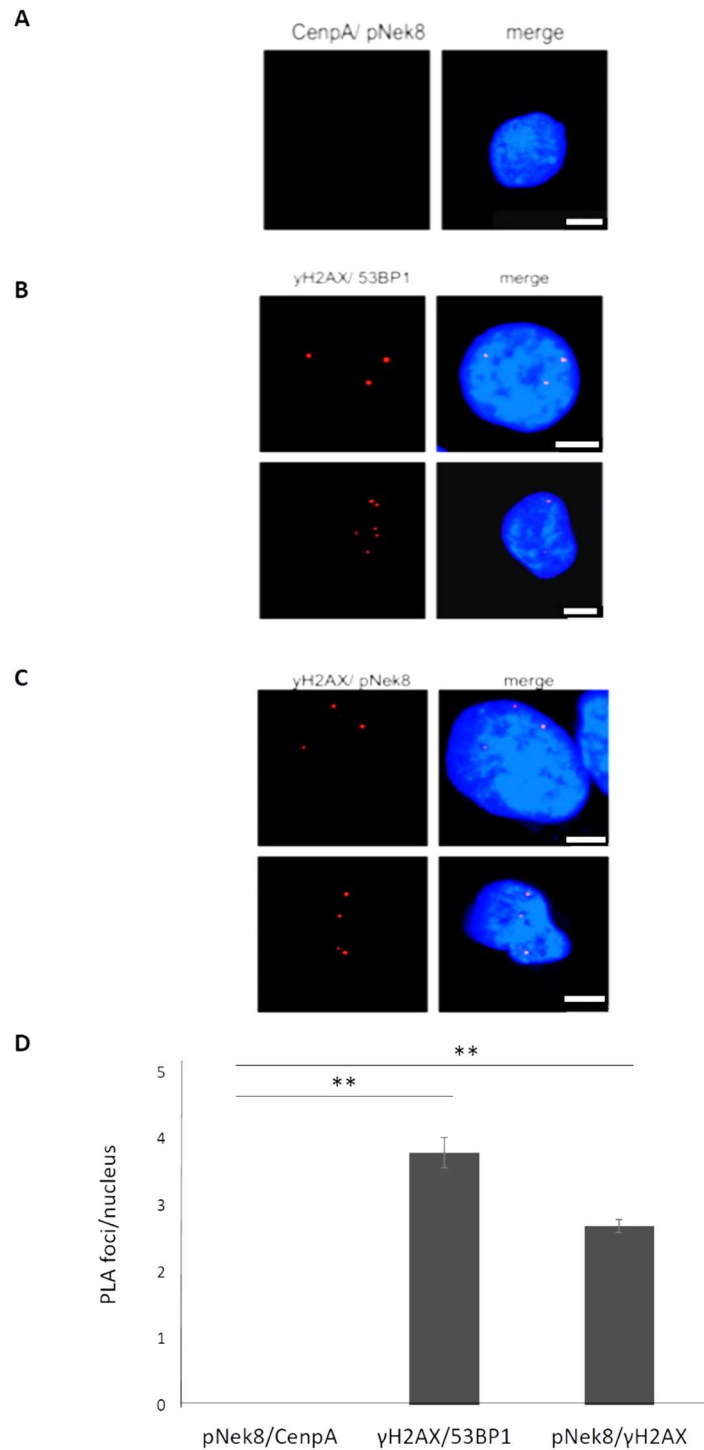


Figure 5.8 PLA assay reveals close association of active Nek8 with γH2AX foci

Proximity Ligation Assays (PLA) were performed on untreated RPE1 cells using antibodies against CenpA and pNek8 **(A)**, 53BP1 and γH2AX **(B)**, and pNek8 and γH2AX **(C)**. Red dots indicate localisation of proteins of interest in close proximity. DAPI for DNA staining (blue). Scale bars, 10 μm in top, third, and fifth panel, and 7.5 μm in second and fourth panel. **D**. Histogram shows the amount of PLA foci per nucleus from experiments in **A**, **B** and **C**, performed in triplicate, n=10, p<0.05 (**).

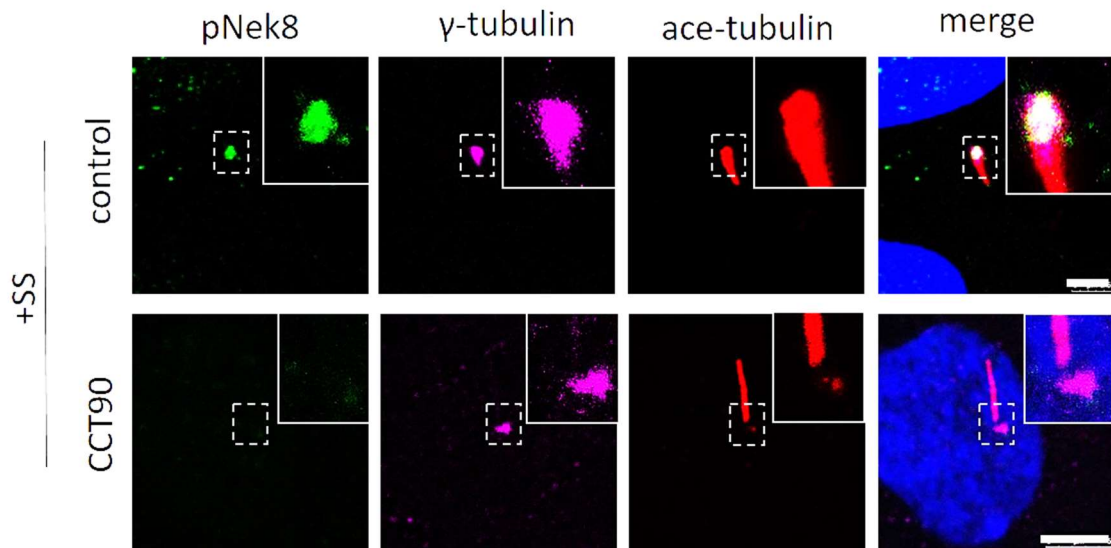


Figure 5.9 CCT90 treatment inhibits Nek8 kinase activity

Immunofluorescence microscopy of serum starved RPE1 cells that were untreated or treated with 3 μ M CCT90 for 20 h. Cells were stained with antibodies against pNek8 (green), γ -tubulin (purple), and acetylated tubulin (red). Insets show magnified images of the basal body. Shown are representative data of three independent experiments, analysing 50 cells each. DNA was stained with DAPI. Scale bars, 2.5 μ m in top row, 5 μ m in bottom row.

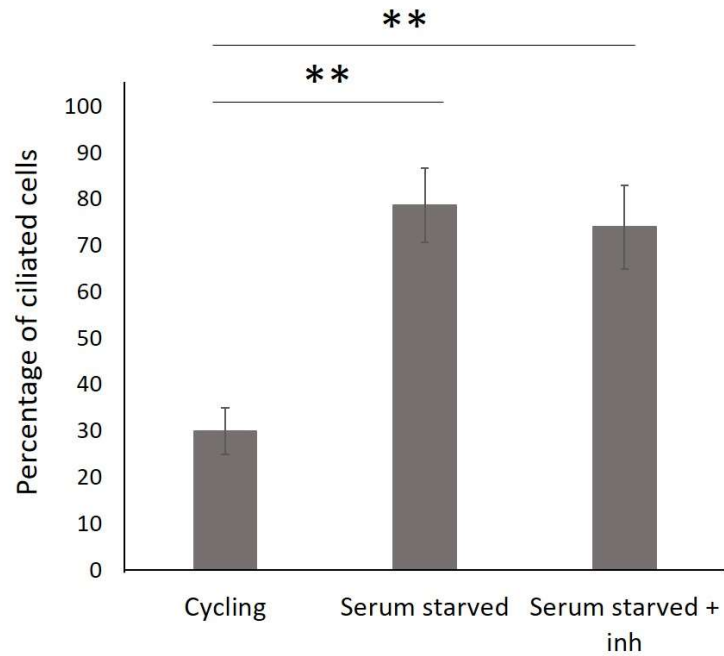


Figure 5.10 CCT90 treatment does not affect ciliogenesis

Histogram shows the percentage of ciliated cells upon treatment with 3 μ M of the CCT90 inhibitor for 20 h in the population of serum starved cells of three independent experiments, $n=50$, $p<0.05$ (**).

Finally, to investigate the effect of Nek8 inhibition on the DNA damage response, control and CCT90 inhibitor treated RPE1 cells were treated with 1.6 nM Aphidicolin for 24h in three independent experiments, analysing 20 cells each (Fig. 5.14A). Immunofluorescence microscopy with antibodies against the DNA damage marker 53BP1 showed defined DNA damage foci upon Aphidicolin treatment in control cells. However, the size of these foci in CCT90 treated cells was increased, showing a significant enrichment in large foci from an average of 1.2 in control to 3.5 in inhibitor treated cells (Fig. 5.14B). This suggests a role for Nek8 kinase activity in the DNA damage response by preventing the aggregation of DNA damage foci.

5.2.6 Generation of a gene-edited Nek8 knockout cell lines

To confirm the specificity of the pNek8 antibody, as well as eliminating concerns about off-target effects of the small molecule inhibitors, we attempted to generate RPE1 Nek8 knockout (KO) cell lines using CRISPR/Cas9-mediated gene-editing. This was done in collaboration with Prof Kouji Hirota and Koji Kobayashi at Tokyo Metropolitan University due to their recent success in generating *nek8* knock-outs in the human lymphoblast suspension cell line TK6. The vector encoding both, the Cas9 endonuclease and the guide RNA (gRNA) was designed to introduce a nick in the genomic *nek8* gene that led to a deletion of amino acids 17 to 207 in the kinase domain of the Nek8 protein (Fig. 5.15A). Two separate vectors carrying the left and right arms of a homologous sequence were designed to then introduce puromycin and neomycin resistant genes into the two alleles of the *nek8* gene in the nicked area by homology directed repair. Koji Kobayashi generated the RPE1 KO cell line by transfection of all three vectors into RPE1 cells using the Neon transfection system (Thermo Fisher). Cells were treated with 2 µg/ml puromycin and 1 mg/ml neomycin to select for knock-out cell clones, which were then individually isolated and grown to 70% confluency before using qRT-PCR to confirm knock-out of *nek8*. Initial analysis of two clones (Nek8-7 and Nek8-8) by qRT-PCR using Nek8 and ACT1 primers confirmed knockout of the clone Nek8-7 (Fig. 5.15B). This clone was then used for further studies.

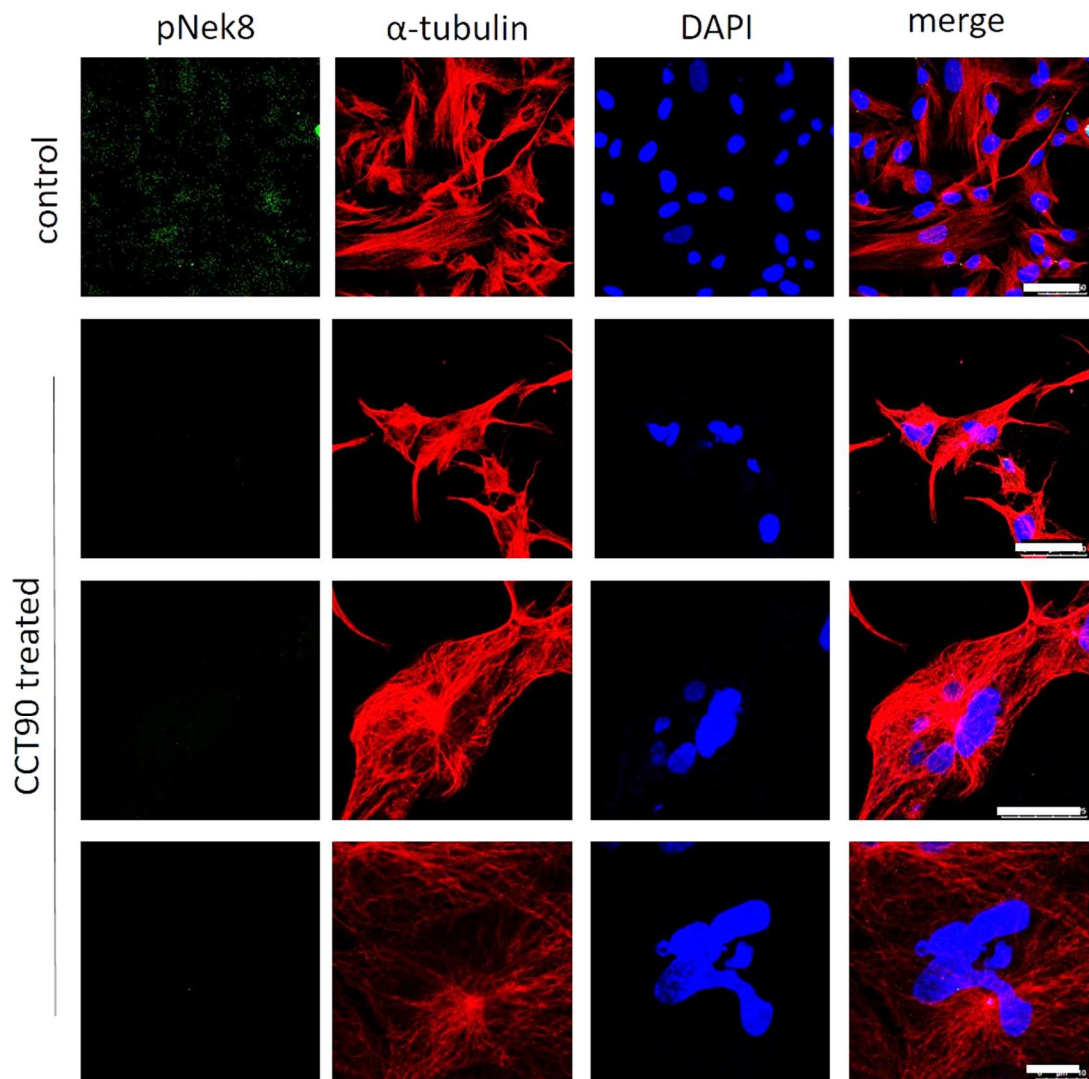


Figure 5.11 CCT90 treatment causes formation of multinucleated cells

Immunofluorescence microscopy of untreated (control) RPE1 cells and RPE1 cells treated with 3 μ M CCT90 for 20 h. Cells were stained with antibodies against pNek8 (green) and α -tubulin (red). DNA stained with DAPI (blue). Shown are representative data of three independent experiments, analysing 50 cells each. Scale bars, 50 μ m in the top two panels, 25 μ m in the third row, and 10 μ m in the bottom row.

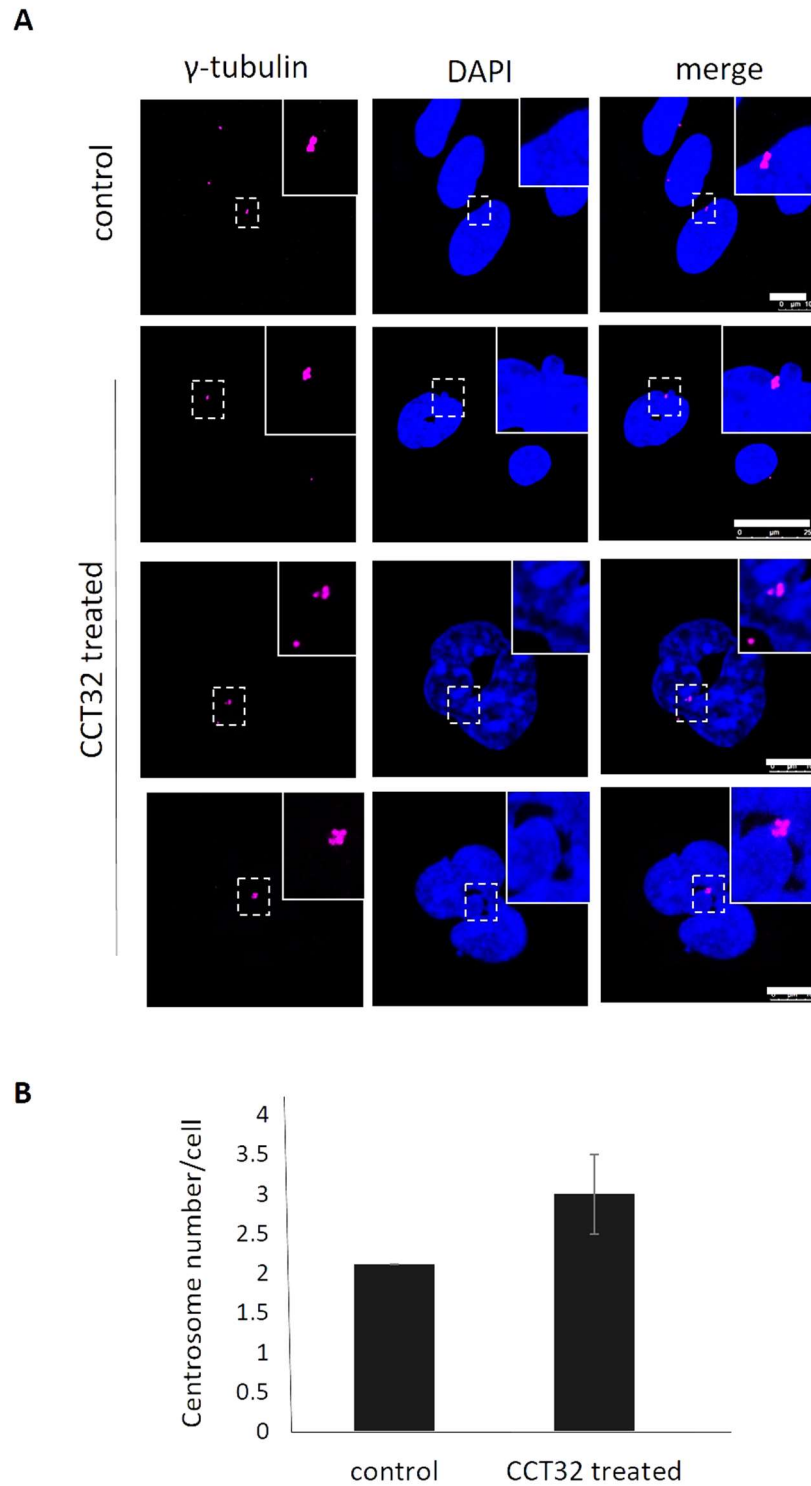


Figure 5.12 CCT32 treatment causes multinucleated cells with supernumerary centrosomes

A. Immunofluorescence microscopy of untreated (control) RPE1 cells and RPE1 cells treated with 3.2 μ M CCT90 for 20 h. Cells were stained with antibodies against γ -tubulin (purple) and DNA was stained with DAPI (blue). Insets show magnified images of centrosomes. Scale bars, 10 μ m in the top and two bottom rows, and 25 μ m in the third row. **B.** Histogram shows the centrosome number per cell in cells with and without CCT32 treatment. Experiments were performed in triplicate with n=15.

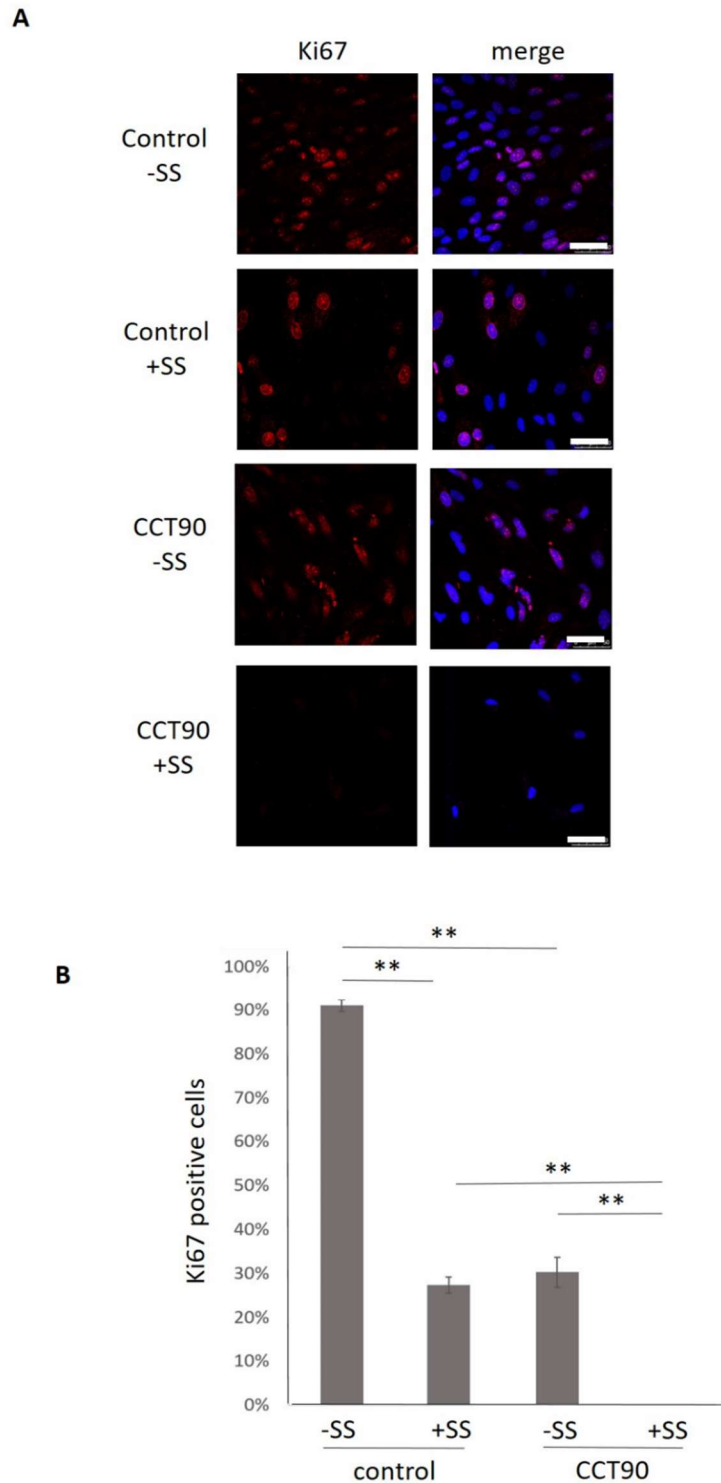


Figure 5.13 CCT90 treatment reduces proliferation in RPE1 cells

A. Immunofluorescence microscopy of cycling (-SS) and serum starved (+SS) RPE1 cells that were either untreated or treated with 3 μ M of the CCT90 inhibitor for 20 h. Cells were stained with antibodies against the proliferation marker Ki67 (red) and DNA was stained with DAPI (blue). Scale bars, 50 μ m. **B.** Histogram shows Ki67 positive cells in control and inhibitor treated cells. Experiments were performed in triplicate, n=50, p<0.05 (**).

Initial experiments, performed by Koji Kobayashi, looking at proliferation rates over a time course of 120 h showed a reduction of cell number and slower growth rates in Nek8 KO cells compared to wild-type cells. Conversely, serum starvation did not prevent cell proliferation in Nek8 KO cells (Fig. 5.16A). This observation was confirmed by analysis of Ki67 expression after 48 h of serum starvation (Fig. 5.16B). Whereas wild-type RPE1 cells exhibited a significant reduction in Ki67 positive cells from 83.7% to 4%, Nek8 KO cells showed only 42% Ki67 positive cells under normal growth conditions, which remained at 41.5% upon serum starvation. Interestingly, this is consistent with the phenotypes we observed earlier on upon treatment of RPE1 cells with the small molecule inhibitors, which led to loss of mitotic cells and reduction of Ki67 positive cells. However, when later experiments were repeated by myself with the Nek8 KO cell line, results showed no significant difference between wild-type and KO cells. Hence, qRT-PCR was undertaken to test whether the cells remained KO for Nek8, but the results indicated no loss of the Nek8 gene (Fig. 5.16C). We postulate that wild-type and Nek8 KO cells had been growing in a mixed population with the wild-type cells rapidly taking over due to the higher proliferation rates. Further attempts to separate and grow the Nek8 KO RPE1 cells as single colonies failed. Further attempts are being undertaken by Prof Kouji Hirota and his research lab in Tokyo. Nevertheless, we conclude that loss of Nek8 most likely leads to impaired proliferation of RPE1 cells making it difficult to maintain a Nek8 KO cell line.

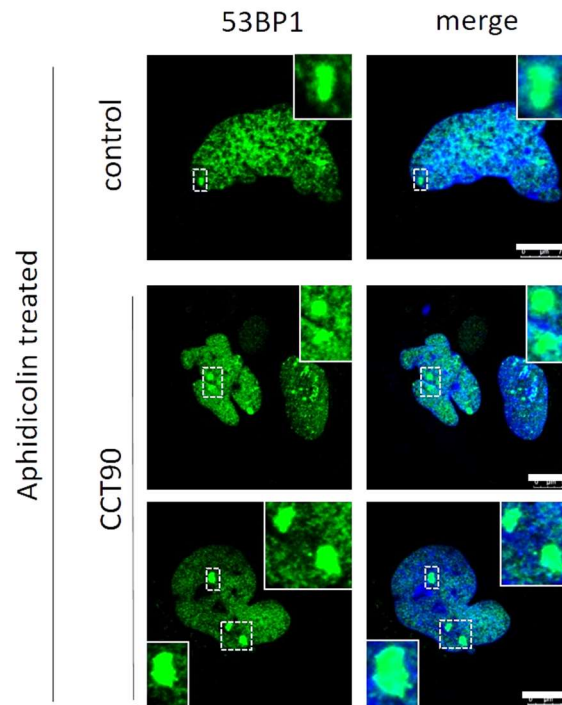
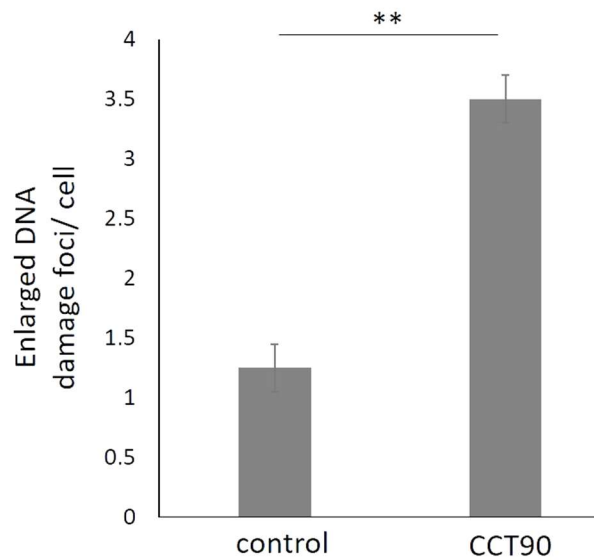
A**B**

Figure 5.14 CCT90 treatment leads to enlarged DNA damage foci in RPE1 cells

A. Immunofluorescence microscopy of RPE1 cells treated with 1.6 nM Aphidicolin for 24h in control RPE1 cells and RPE1 cells treated with 3 μ M of the CCT90 inhibitor for 20 h. Cells were stained with antibodies against the DNA damage marker 53BP1 (green) and insets show magnified views of DNA damage foci. DNA was stained with DAPI (blue). Scale bars, 7.5 μ m in top panel, and 10 μ m in bottom panels. **B.** Histogram represents the average number of DNA damage foci per cell in three independent experiments, n=20, p<0.05 (**).

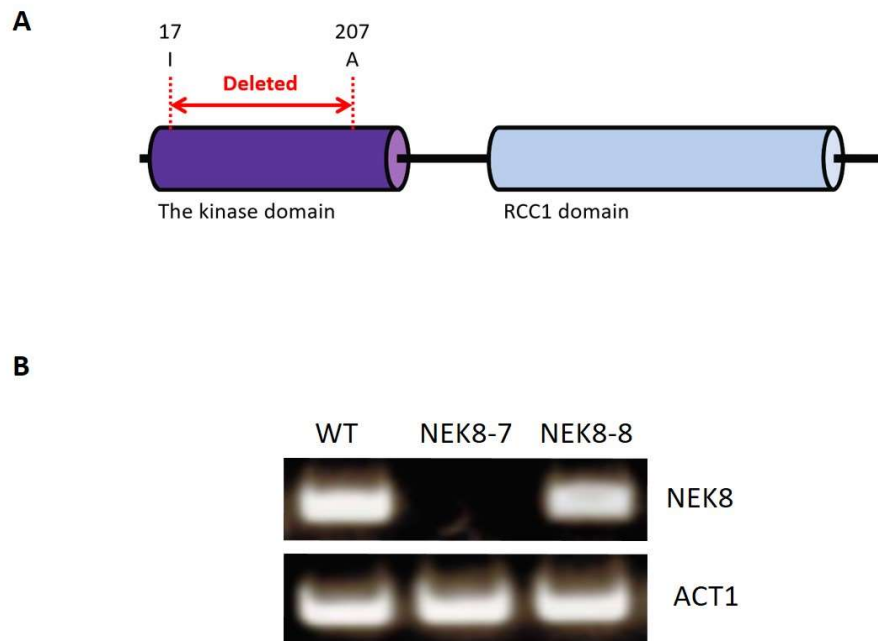


Figure 5.15 Attempting to generate RPE1 KO cells by gene editing

A. Schematic of the deleted region (amino acids 17-207) in the kinase domain of the Nek8 protein. Gene editing using CRISPR/Cas9 was performed by Koji Kobayashi (Tokyo Metropolitan University). **B.** qRT-PCR analysis of RPE1 WT and two potential Nek8 KO cell lines using primers against Nek8 and ACT1 as a control gene (data from Koji Kobayashi).

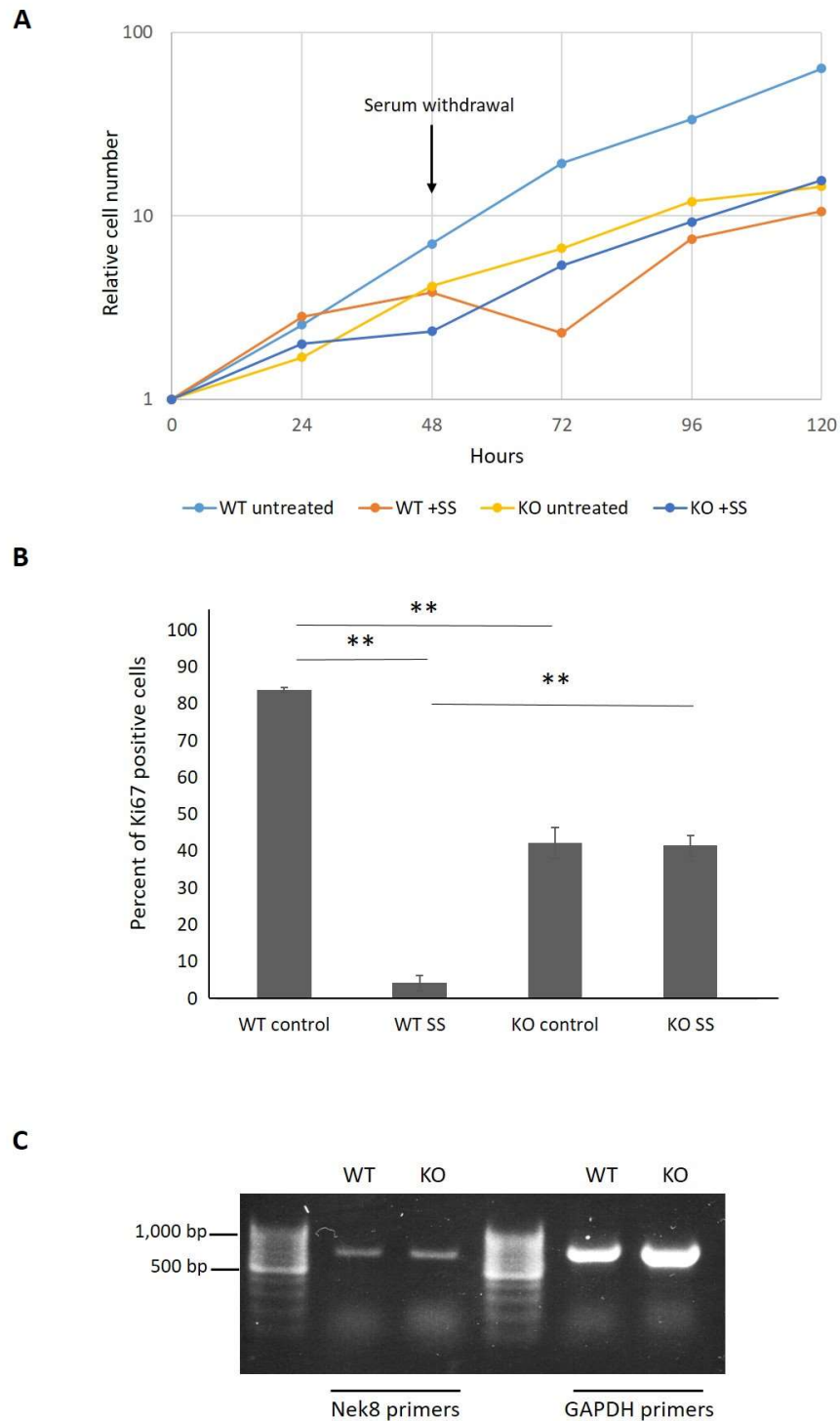


Figure 5.16 Growth studies on gene-edited RPE1 Nek8 KO cells

A. Growth curve of RPE1 WT and Nek8 KO cell lines in untreated conditions (light blue and yellow graphs) and upon serum starvation with 0% FBS after the first 48 h as indicated (orange and blue graphs). **B.** Analysis of Ki67 positive RPE1 WT and Nek8 KO cells in untreated conditions and after 48 h serum starvation. Graph shows data of two independent experiments, $n=50$, $p<0.05$ (**). **C.** qRT-PCR analysis of RPE1 WT and Nek8 KO cell lines using primers against Nek8 (amplification of a 603 bp product) and GAPDH (amplification of a 650 bp product) as a loading control. Markers are indicated on the left.

5.3 Discussion

5.3.1 Validating the pNek8 antibody

In this chapter, we have investigated the pNek8 antibody as a novel biomarker for Nek8 kinase activity. The antibody was raised against the threonine 162 residue in the activation loop of the catalytic domain. Phosphorylation at this residue has previously been shown to be essential for Nek8 activity (Zalli et al., 2011). We have shown that this antibody effectively detects Nek8 kinase activity on Western blots from kinase assays and is able to distinguish between phosphorylated and unphosphorylated protein. The pNek8 antibody was able to detect two different purified Nek8 kinase domain fragments, one generated in-house and a commercially produced protein. Furthermore, upon inhibition of Nek8 activity using the two small molecule inhibitors CCT32 and CCT90, pNek8 signal was decreased by Western blot, demonstrating high specificity of the pNek8 antibody to detect phosphorylated protein, and also confirming the ability of both inhibitors to block Nek8 phosphorylation and activation.

5.3.2 Investigation of Nek8's role in the cell

There are two Nek8 pools in the cell, one cytoplasmic and one ciliary pool and it has yet to be discovered which one is responsible for NPHP development and cyst formation in the kidney in humans (Sohara et al., 2008). However, specific localisation of Nek8 to primary cilia in kidney cells has only been described in tubule and duct cells, which is where cysts develop in NPHP patients (Manning et al., 2013). To investigate the localisation of active Nek8 *in vivo*, immunofluorescence microscopy with the pNek8 antibody was performed in cells. We observed co-localisation with centrosomes in interphase cells, spindle poles in mitotic cells, the midbody during cytokinesis, and the basal body of primary cilia in quiescent cells. Throughout the cell cycle, pNek8 also accumulated in foci in the nucleus. Nek8 has been previously described to localise to these structures (Mahjoub et al., 2005; Otto et al., 2008), indicating that the pNek8 antibody specifically detects the Nek8 protein *in vivo*. This was further confirmed by treating RPE1 cells with a Nek8 inhibitor, CCT90, and showing loss of pNek8 staining. We

conclude that the pNek8 antibody is an excellent tool for investigating Nek8 activity in cells and by Western blot of purified protein.

Using the CCT90 inhibitor to block Nek8 activity *in vivo*, we showed that ciliogenesis in serum starved RPE1 cells was not affected. This finding supports previous observations that loss-of-function Nek8 mutations did not affect ciliogenesis or cilia structure despite the fact that most of these mutants show decreased localisation to primary cilia (Otto et al., 2008). In fact, all described Nek8 NPHP mutations are located in its non-catalytic C-terminus (amino acid substitutions H425Y, L330F, A497P), suggesting interference with localisation motifs. Studies in the *jck* mouse have also shown that mutant Nek8 (G488V) still localises to primary cilia, but instead of localising only to the Inversin compartment, it localised to the whole length of the cilium. As a result, also PC-2, a calcium channel that gets recruited to the ciliary membrane by Nek8, and that we have shown to be a substrate for Nek8 kinase activity *in vitro*, heavily accumulates in the ciliary membrane (Sohara et al., 2008). Summarising, this leads to the suggestion that Nek8 might play a role in maintaining the primary cilium's function as a signal transducer by recruiting and phosphorylating components of downstream ciliary signalling cascades.

We showed that Nek8 inhibition with the small molecule inhibitors led to multinucleated, bigger cells, and caused cells to stop proliferating. Although keeping in mind that the inhibitors are known to target other kinases, they raise the prospect of a role for Nek8 in mediating cell cycle progression, potentially by interacting with and phosphorylation of Inversin and PC-2 at the cilia. The involvement of Nek8 in proliferative signalling pathways could be investigated in IMCD3 spheroids. These structures mimic a 3D collecting duct arrangement and are composed of highly polarised cells with cilia pointing inwards (see chapter 3). Disturbing pathways involved in regulating cell polarity, such as the non-canonical Wnt/PCP pathway, would lead to spheroid defects and could give an insight into Nek8's role at the cilia.

Further evidence for the involvement of Nek8 in cell cycle progression comes from analysis of the DNA damage response. Nek8 knockdown in cells still allowed for

checkpoint activation and arrest of cells in S-phase, but led to failure to repair DNA DSBs (Choi et al., 2013). Interestingly, we observed larger γ H2AX foci in cells treated with the DNA damage agent aphidicolin in the presence of the Nek8 inhibitor. This could be explained by a functional role for Nek8 in recruiting ATR and other DNA damage mediators and controlling progression through the intra-S checkpoint (Choi et al., 2013).

However, to further investigate the consequences of Nek8 inhibition, studies using siRNA-mediated depletion or gene-edited knockout cell lines will need to be done. Initial experiments with a CRISPR generated RPE1 cell line offered preliminary data for cell cycle defects upon loss of Nek8. However, this cell line proved to be a mix of WT and Nek8 KO and is still in the process of being generated anew. RPE1 cells are very difficult to grow as single cells and the initial step of isolating a Nek8 KO positive cell is therefore problematic. We have also attempted on numerous occasions to deplete Nek8 using different siRNA sequences in human RPE1 and mouse IMCD3 cells without success.

CHAPTER 6 DISCUSSION

6.1 Identifying biomarkers of Nek8 kinase activity

The aim of this thesis was to identify and generate biomarkers of Nek8 kinase activity that can be used for *in vitro* and *in vivo* analysis in cells. We therefore investigated the potential substrates of Nek8 kinase activity, Inversin and PC-2, and mapped phosphorylation sites in these proteins to generate phospho-specific antibodies. We furthermore validated a pNek8 antibody raised against a threonine residue in the activation loop of the Nek8 kinase domain to investigate Nek8 kinase activity in cells.

6.1.1 Designing Inversin phospho-antibodies as biomarkers of Nek8 kinase activity

We first investigated the known interaction partner of Nek8, Inversin, a ciliary protein involved in regulating the canonical and non-canonical Wnt pathway, that has been reported to anchor Nek8 at the cilia (Shiba et al., 2010). Mutations of both Inversin and Nek8 lead to NPHP with similar phenotypes, such as cortico-medullary cysts and *situs inversus* (Otto et al., 2002). We showed that Inversin and Nek8 exhibit multiple interaction sites, although taken together our current data suggest that the Nek8 catalytic domain favours the Inversin N-terminal ankyrin-rich domain, whereas the C-terminus of Nek8 is capable of interacting with both the Inversin N- and C-terminus. The purpose of this interaction may well be that Inversin is a substrate for Nek8 kinase activity. We therefore performed radiolabelled *in vitro* kinase assays with a purified Nek8 kinase domain fragment and purified Inversin domain proteins. Our data showed phosphorylation of all Inversin fragments with stronger signal of the Inversin N-terminus in autoradiograph analysis. Mass spectrometry of non-radiolabelled kinase assays revealed several sites along the Inversin protein that were phosphorylated by Nek8. 12 of these sites were identified consistently in several analyses, with three sites located in the N-terminus at positions T121, T324 and T359, and nine sites located in the C-terminus at positions T683, T841, T864, S865, T866, T958, S1032, S1043 and T1057.

Due to our data on stronger phosphorylation of the N-terminus of Inversin by Nek8 *in vitro* compared to the C-terminus, we decided to generate and validate phospho-specific antibodies against the three sites in the N-terminus. We showed that the Inversin-pT121 and pT359 antibodies are able to specifically detect phosphorylated Inversin protein by Western blot. This makes them an excellent tool for validating Nek8 activity without the use of radiolabelled ATP. The Inversin-pT121 and pT324 antibodies showed localisation of Inversin to the nucleus and centrosomes in the cells, which is consistent with the literature (Nurnberger et al., 2004) and indicates phosphorylation of Inversin at these structures either by Nek8 or another kinase.

The C-terminal sites appear to cluster within three distinct areas of the Inversin protein with T864, S865 and T866 located near the NLS (Lienkamp et al., 2011). These amino acids have also been described to be phosphorylated by the serine/threonine kinase Akt at the basal body of cilia (Suizo et al., 2016). Furthermore, T1032, T1043 and T1057 are located near the ninein-homology region that regulates Inversin's localisation to the cilium. We suggest that phosphorylation of Inversin by Nek8 at these residues might regulate its localisation pattern within the cell.

To further analyse the importance of each of the phosphosites, phospho-mimetic and phospho-null mutants will have to be generated and their localisation in the cell needs to be investigated. Studies with phospho-specific antibodies against the C-terminal sites will demonstrate when and where each site is phosphorylated to shed light into the function of the Nek8-Inversin complex *in vivo*. Nek8 inhibition or knockdown will then validate whether this phosphorylation is Nek8-dependent.

Once sufficiently validated, we conclude that the phospho-specific Inversin antibodies are excellent biomarkers for Nek8 activity *in vitro* and *in vivo*.

6.1.2 Investigating PC-2 as a substrate for Nek8 kinase activity

We further investigated PC-2 as a substrate for Nek8 kinase activity. PC-2 is a ciliary protein channel that allows influx and efflux of calcium upon mechano-stimulation of

the primary cilium, such as flow in the kidney tubule. Its localisation to the ciliary membrane has been shown to be Nek8-dependent and potentially phospho-dependent, as studies in *C. elegans* have shown that a phospho-null mutant of PC-2 at position S534 (serine substitution to alanine) prevents ciliary localisation (Sohara et al., 2008, Hu et al., 2006). Evidence that PC-2 might be phosphorylated by Nek8 came from studies in *jck* mice that carry the G442V substitution in the Nek8 protein, and exhibited altered localisation patterns of PC-2, as well as potential hyperphosphorylation (Sohara et al., 2008).

We showed that the intracellular C-terminal domain of PC-2 is an excellent substrate for Nek8 kinase activity *in vitro* and were able to map the following 21 sites by mass spectrometry: T683, S658, S698, S701, T721, S726, S728, T751, T771, S794, S795, S812, S492, S898, S914, S917, T931, S951, T952, S963 and S964. However, to confirm that these sites are targeted by the Nek8 kinase *in vivo*, phospho-antibodies need to be generated and the presence and localisation of these needs to be investigated upon Nek8 knockdown or inhibition. To further validate whether phosphorylation of PC-2 plays a role in its localisation to cilia, phospho-mimetic and phospho-null mutants will need to be generated and their localisation pattern investigated in cells.

6.1.3 Validation of the pNek8 antibody as a biomarker of Nek8 kinase activity

We tested a phospho-specific Nek8 antibody of the threonine 162 residue in the activation loop as a biomarker of Nek8 activity. This residue has previously been described to be a crucial mediator of Nek8 activity, as phospho-null mutants of T162 (threonine substitution with alanine) failed to phosphorylate substrates *in vitro*. *In vivo*, T162A mutants demonstrated loss of localisation to centrosomes and cilia, therefore suggesting a role for kinase activity in mediating Nek8 localisation (Zalli et al., 2011).

We were able to show that the pNek8 antibody is able to specifically detect phosphorylated and therefore activated Nek8 *in vitro* in kinase assays as we confirmed loss of signal by Western blot on purified Nek8 kinase upon treatment with Nek8 inhibitors. We also confirmed specificity of the antibody *in vivo* as Nek8 inhibition caused

loss of signal of pNek8 by IF. We showed localisation of pNek8 to centrosomes, spindle poles and γ H2AX foci in cycling cells, as well as the basal body of primary cilia in IF and confirmed a role for Nek8 kinase activity at these structures. Taken together, these data demonstrate that the pNek8 antibody is an excellent biomarker of Nek8 kinase activity *in vitro* and *in vivo*.

6.2 Analysis of the role of Nek8 in the cell

Nek8 has been described to localise to primary cilia, where it interacts with Inversin and PC-2, centrosomes in cycling cells and the nucleus, where it plays a role in the replication stress response (Zalli et al., 2011; Shiba et al., 2010; Sohara et al., 2008). However, how exactly these roles of Nek8 contribute to NPHP disease progression still remains unclear. In the second part of this thesis, we wanted to investigate the phenotype of Nek8 inhibition to shed light into its contribution to cyst formation in the kidneys of NPHP patients. For this, we used two small molecule inhibitors that can block Nek8 kinase activity *in vitro*.

We observed that inhibiting Nek8 in cells does not interfere with ciliogenesis, but leads to cell cycle and cell division defects that reduce cell proliferation and lead to multinucleated cells. We further detected the presence of larger DNA damage foci in aphidicolin-treated cells. It is possible that these defects result from loss of Nek8 activity. However, we cannot rule out that they are the consequences of inhibiting one or more other kinases in the cell.

6.2.1 A role for Nek8 at the primary cilium

PKD has been described to be a result of abnormal proliferation and differentiation (Sohara et al., 2008). Kidney cells are differentiated cells that have stopped proliferating. However, in PKD patients, these cells seem to re-enter the cell cycle. As we have shown that Nek8 is not required for ciliogenesis, we hypothesise that it might play a functional role at the primary cilium. Nek8 might be involved in regulating ciliary signalling such as the canonical Wnt pathway, that is involved in cell proliferation. A key mediator of this

pathway is Inversin, which we have shown to be a substrate for Nek8 kinase activity. Nek8 might regulate the role of Inversin targeting Dvl for degradation and switching between the canonical Wnt pathway, which is active in cycling, proliferating cells, to the non-canonical Wnt/PCP pathway, which is involved in planar cell polarity and regulates the orientation of the mitotic spindle. This pathway is favoured in quiescent cells upon Dvl degradation. Nek8 at the cilia might cause Inversin to be stabilised and mediates its interaction with other PCP components. The rapid turnover of Nek8 at the cilia would keep these pathways balanced (Zalli et al., 2011). Potentially, once Nek8 and Inversin form a complex, phosphorylation of certain Inversin residues might lead to the re-localisation of this complex to the nucleus via Inversin's NLS sequence.

PC-2, which is recruited to the ciliary membrane by Nek8 and is another substrate for Nek8 kinase activity, controls calcium concentrations in the cilium. PC-2 might also be involved in regulating Inversin, as Inversin exhibits calmodulin binding motifs, which is a calcium binding and sensing protein (Morgan et al., 2002).

6.2.2 A role for Nek8 in cell cycle progression

The fact that we observed multinucleated, bigger cells that stopped proliferating upon addition of the inhibitors, suggests a role for Nek8 in positively regulating proliferation rates and cell cycle progression. Manning et al. (2008) have described the Nek8 *jck* mutation as a gain-of-function mutation, which could explain the enhanced proliferation rates of cells and cyst formation. Further supporting this hypothesis is that Nek8 has been shown to be overexpressed in human primary breast cancer, leading to uncontrolled cell division and the development of tumours (Bowers and Boylan, 2003).

Further evidence for the involvement of Nek8 in cell cycle progression comes from studies on the DNA damage response, where Nek8 contributes to mediating the replication stress response in the intra S-phase checkpoint. Nek8 knockdown does not prevent checkpoint activation and arrest of cells in S-phase, but leads to failure in the repair of DNA DSBs (Choi et al., 2013). Interestingly, we observed larger γ H2AX foci in cells treated with the DNA damage agent aphidicolin and putative Nek8 inhibitor. This

could be explained by the proposed function of Nek8 in recruiting ATR and other DNA damage mediators to sites of damage (Choi et al., 2013). Further evidence for NPHP progression and cyst formation due to DNA damage response pathway malfunctioning comes from the description of the involvement of other NPHP disease proteins in the DNA damage response such as CEP164 and ZNF423 (Chaki et al., 2012). Further DDR proteins such as MRE11 or FAN1 have been described to play roles in ciliopathy disease progression, too (Sivasubramianam et al., 2008; Zhou et al., 2012).

6.3 A model for the role of Nek8 in the cell

As a conclusion from our data and the literature, we hypothesise the following. Nek8 gets recruited to the primary cilium by Inversin. At the cilia, the active Nek8 kinase recruits PC-2 and regulates its localisation to the ciliary membrane by phosphorylating its C-terminal domain. Once located at the ciliary membrane, PC-2 acts as a calcium channel, allowing for calcium influx upon mechano-stimulation of the primary cilium, such as urine flow in the kidney tubule. This might also regulate Inversin signalling at the base of the cilium and favours its role in targeting Dvl for proteasomal degradation, thus stimulating the non-canonical Wnt/PCP pathway involved in cell polarity. This could potentially be achieved by mediating the interaction of Inversin with the calcium-binding protein calmodulin. Nek8 is rapidly turned over at the cilia, which controls how much PC-2 protein is recruited. Upon re-entering of the cell cycle, disassembly of the primary cilium and lack of calcium-influx, Inversin stops targeting Dvl for degradation and the canonical Wnt pathway gets activated, which is involved in cell proliferation. Furthermore, Nek8 phosphorylates Inversin, which then leads to a conformation change and the re-location of the Inversin-Nek8 complex to the nucleus. We were able to detect phosphorylated Inversin in the nucleus, which could support this hypothesis. In the nucleus, Nek8 then regulates replication stress signalling and helps to maintain a healthy genome.

Inhibition or knockdown of Nek8 could potentially lead to Inversin remaining in the cytoplasm and continuing to target Dvl for degradation, thus leading to reduced proliferation as seen in our studies. Hypothesising that NPHP mutants of Nek8 are gain-

of-function mutants, Nek8 would hyper-phosphorylate Inversin and re-location of the Inversin-Nek8 complex to the nucleus would be enhanced. This would allow for an imbalance in the canonical and non-canonical Wnt/PCP pathway, favouring Dvl accumulation in the cytoplasm and over-proliferation of the cell. As Nek8 mediates the replication stress response, accumulation of Nek8 in the nucleus would lead to premature progression through the cell cycle and accumulation of DNA damage.

To test this hypothesis, IMCD3 spheroids can be used as an excellent model system as their 3D structure is a great tool to test cell integrity, proliferation and cell polarity defects. PC-2 localisation to the primary cilia will need to be analysed upon Nek8 inhibition or knockdown. Phospho-mimetic mutants of the Nek8 phosphosites in PC-2 can be used to rescue the phenotype. Furthermore, PC-2 loss from the primary cilium should lead to abnormal ciliary downstream signalling due to loss of control over Inversin. Inversin siRNA experiments can be performed to test the hypothesis of the Inversin-Nek8 complex re-locating to the nucleus. Knockdown of Inversin should then lead to abundance of Nek8 from the nucleus. Inversin disease mutants that are truncated at the C-terminus where the NLS is located can be used to further investigate this. Furthermore, *in vivo* phosphorylation assays of Inversin by Nek8 will need to be performed to pinpoint when Nek8 uses Inversin as a substrate.

6.4 Concluding remarks

In this study, we aimed to generate and validate biomarkers of Nek8 kinase activity to shed light into its yet poorly understood role in the cell.

We therefore investigated the interaction between Nek8 and Inversin *in vitro*, an approach that had not been investigated before. We showed that the Nek8 catalytic domain interacts preferably with the Inversin N-terminus, whereas the Nek8 RCC1 domain interacts with both the Inversin N- and C-terminus. Inversin was known as a substrate for Nek8 kinase activity, however, specific phosphosites had never been mapped. We therefore performed *in vitro* kinase assays and were able to map several phosphorylation sites throughout the Inversin protein, which in itself is a novelty. We

also designed and generated several antibodies against three phosphosites in the N-terminus of Inversin, T121, T324 and T359 and validated these as biomarkers of Nek8 kinase activity. Kinase assays with purified Inversin protein and the Nek8 kinase domain showed that the phospho-Inversin antibodies specifically detect purified Inversin protein *in vitro*. This makes them an excellent, novel tool for investigating Nek8 kinase activity without the need for radiolabelled material. However, their specificity and value as biomarkers of Nek8 kinase activity *in vivo* needs to be further investigated to exclude the possibility of these sites being phosphorylated by other kinases.

We furthermore demonstrated that the ciliary calcium channel PC-2 is an excellent target for Nek8 kinase activity *in vitro*. This had only been suggested before due to data obtained *in vivo*. We were able to map 21 phosphosites and propose that antibodies against these sites could be excellent biomarkers of Nek8 kinase activity, as well as great tools for investigating the role of Nek8 and PC-2 in the cell and in polycystic kidney disease progression.

A pNek8 antibody against the T162 residue in the activation loop was also validated as a biomarker of Nek8 kinase activity. This antibody has been generated by the Bayliss group and was only used for *in vitro* studies so far. We showed that this antibody specifically distinguishes between non-phosphorylated and phosphorylated and therefore active Nek8 protein *in vitro* and evaluated its specificity for Nek8 by showing loss of signal *in vitro* by Western blot and *in vivo* by IF upon treatment with Nek8 inhibitors. In cells, the pNek8 antibody demonstrates a distinct localisation pattern to centrosomes, cilia and the nucleus, which supports findings in the literature for the general Nek8 pool. However, particular studies on the localisation of active Nek8 had never been done before. Concluding, the pNek8 antibody is an excellent, novel tool to investigate Nek8's role as a kinase in the cell and is a great biomarker of Nek8 kinase activity *in vivo* and *in vitro*.

The second part of this thesis was to investigate the role of Nek8 in the cell using two small molecule inhibitors, with main focus on its role at the cilia as a signal transducer of pathways involved in proliferation and polarity, and in the replication stress response.

Nek8 knockdown cells using siRNA and the effect of Nek8 disease mutants in cells have been investigated before by several research groups, however, Nek8 inhibitors had not been used so far. Upon treatment with the inhibitors, we observed reduced proliferation rates and the formation of multinucleated cells. We also detected larger γ H2AX foci. These data match some of the findings in the literature, which supports our hopes of these inhibitors being excellent, novel tools for investigating Nek8's role in the cell and in NPHP disease progression. Taken together, these findings demonstrate a role for Nek8 in mediating cell cycle progression by linking ciliary downstream signalling and the DNA damage response.

CHAPTER 7 BIBLIOGRAPHY

Data on Breast Cancer Discussed by Researchers at Tianjin Medical University (Effect of NIMA-related kinase 2B on the sensitivity of breast cancer to paclitaxel in vitro and vivo). 2017. *Women's Health Weekly*. 149.

Abeyta, A., Castella, M., Jacquemont, C., Taniguchi, T., 2017. NEK8 regulates DNA damage-induced RAD51 foci formation and replication fork protection. *Cell Cycle*. **16**, 335-347.

Adeva, M., El-Youssef, M., Rossetti, S., Kamath, P.S., Kubly, V., Consugar, M.B., Milliner, D.M., King, B.F., Torres, V.E., Harris, P.C., 2006. Clinical and molecular characterization defines a broadened spectrum of autosomal recessive polycystic kidney disease (ARPKD). *Medicine*. **85**, 1-21.

Alexander, J., Lim, D., Joughin, B.A., Hegemann, B., Hutchins, J.R.A., Ehrenberger, T., Ivins, F., Sessa, F., Hudecz, O., Nigg, E.A., Fry, A.M., Musacchio, A., Stukenberg, P.T., Mechtler, K., Peters, J., Smerdon, S.J., Yaffe, M.B., 2011. Spatial exclusivity combined with positive and negative selection of phosphorylation motifs is the basis for context-dependent mitotic signaling. *Science Signaling*. **4**, ra42.

Avruch, J., Sdelci, S., Regué, L., Roig, J., Bertran, M.T., Caelles, C., 2011. Nek9 is a Plk1-activated kinase that controls early centrosome separation through Nek6/7 and Eg5. *The EMBO Journal*. **30**, 2634-2647.

Azvolinsky, A., Dunaway, S., Torres, J.Z., Bessler, J.B., Zakian, V.A., 2006. The *S. cerevisiae* Rrm3p DNA helicase moves with the replication fork and affects replication of all yeast chromosomes. *Genes & Development*. **20**, 3104-3116.

Bahe, S., Stierhof, Y.D., Wilkinson, C.J., Leiss, F., Nigg, E.A., 2005a. Rootletin Forms Centriole-Associated Filaments and Functions in Centrosome Cohesion. *The Journal of Cell Biology*. **171**, 27-33.

Barnum, K.J. & O'Connell, M.J., 2014. Cell cycle regulation by checkpoints. *Methods in Molecular Biology (Clifton, N.J.)*. **1170**, 29.

Bartek, J. & Jackson, S.P., 2009. The DNA-damage response in human biology and disease. *Nature*. **461**, 1071-1078.

Bavetsias, V., Crumpler, S., Sun, C., Avery, S., Atrash, B., Faisal, A., Moore, A.S., Kosmopoulou, M., Brown, N., Sheldrake, P.W., Bush, K., Henley, A., Box, G., Valenti, M., de Haven Brandon, A., Raynaud, F.I., Workman, P., Eccles, S.A., Bayliss, R., Linardopoulos, S., Blagg, J., 2012. Optimization of imidazo[4,5-b]pyridine-based kinase inhibitors: identification of a dual FLT3/Aurora kinase inhibitor as an orally bioavailable preclinical development candidate for the treatment of acute myeloid leukemia. *Journal of Medicinal Chemistry*. **55**, 8721.

Benhamouche, S., Curto, M., Saotome, I., Gladden, A.B., Liu, C., Giovannini, M., McClatchey, A.I., 2010. Nf2/Merlin controls progenitor homeostasis and tumorigenesis in the liver. *Genes & Development*. **24**, 1718-1730.

Berbari, N.F., O'Connor, A.K., Haycraft, C.J., Yoder, B.K., 2009. The Primary Cilium as a Complex Signaling Center. *Current Biology*. **19**, R535.

- Berl R. Oakley & N. Ronald Morris, 1983. A Mutation in *Aspergillus nidulans* That Blocks the Transition from Interphase to Prophase. *The Journal of Cell Biology*. **96**, 1155-1158.
- Bermejo, R., Topoisomerase I poisoning results in PARP-mediated replication fork reversal.
- Bermejo, R., Doksani, Y., Capra, T., Katou, Y., Tanaka, H., Shirahige, K., Foiani, M., 2007. Top1- and Top2-mediated topological transitions at replication forks ensure fork progression and stability and prevent DNA damage checkpoint activation. *Genes & Development*. **21**, 1921-1936.
- Bermejo, R., Lai, M.S., Foiani, M., 2012. Preventing replication stress to maintain genome stability: resolving conflicts between replication and transcription. *Molecular Cell*. **45**, 710-718.
- Bester, A., Roniger, M., Oren, Y., Im, M., Sarni, D., Chaoat, M., Bensimon, A., Zamir, G., Shewach, D., Kerem, B., 2011. Nucleotide Deficiency Promotes Genomic Instability in Early Stages of Cancer Development. *Cell*. **145**, 435-446.
- Boddy, M.N. & Russell, P., 2001. DNA replication checkpoint. *Current Biology*. **11**, R956.
- Bornens, M., 2002. Centrosome composition and microtubule anchoring mechanisms. United States: Elsevier Ltd.
- Bowers, A.J. & Boylan, J.F., 2004. Nek8, a NIMA family kinase member, is overexpressed in primary human breast tumors. *Gene*. **328**, 135-142.
- Branzei, D. & Foiani, M., 2010. Maintaining genome stability at the replication fork. *Nature Reviews Molecular Cell Biology*. **11**, 208-219.
- Cao, X., Xia, Y., Yang, J., Jiang, J., Chen, L., Ni, R., Li, L., Gu, Z., 2012. Clinical and Biological Significance of Never in Mitosis Gene A-Related Kinase 6 (NEK6) Expression in Hepatic Cell Cancer. *Pathology & Oncology Research*. **18**, 201-207.
- Casey, J.P., Brennan, K., Scheidel, N., McGettigan, P., Lavin, P.T., Carter, S., Ennis, S., Dorkins, H., Ghali, N., Blacque, O.E., Mc Gee, M.M., Murphy, H., Lynch, S.A., 2016. Recessive NEK9 mutation causes a lethal skeletal dysplasia with evidence of cell cycle and ciliary defects. *Human Molecular Genetics*. **25**, 1824-1835.
- Chaki, M., Airik, R., Ghosh, A.K., Giles, R.H., Chen, R., Slaats, G.G., Wang, H., Hurd, T.W., Zhou, W., Cluckey, A., Gee, H.Y., Ramaswami, G., Hong, C.J., Hamilton, B.A., Cervenka, I., Ganji, R.S., Bryja, V., Arts, H.H., Reeuwijk, J.v., Oud, M.M., Letteboer, S.J., Roepman, R., Husson, H., Ibraghimov-Beskrovnaya, O., Yasunaga, T., Walz, G., Eley, L., Sayer, J.A., Schermer, B., Liebau, M.C., Benzing, T., Corre, S.I., mmond, I., Janssen, S., Allen, S.J., Natarajan, S., O'Toole, J.F., Attanasio, M., Saunier, S., Antignac, C., Koenekoop, R.K., Ren, H., Lopez, I., Nayir, A., Stoetzel, C., Dollfus, H., Massoudi, R., Gleeson, J.G., Aneoli, S.P., Doherty, D.G., Lindstrad, A., Golzio, C., Katsanis, N., Pape, L., Abboud, E.B., Al-Rajhi, A.A., Lewis, R.A., Omran, H., Lee, E.Y., Wang, S., Sekiguchi, J.M., Saunders, R., Johnson, C.A., Garner, E., Vanselow, K., Andersen, J.S., Shlomei, J., Nurnberg, G., Nurnberg, P., Levy, S., Smogorzewska, A., Otto, E.A., Hildebrandt, F., 2012. Exome capture reveals ZNF423 and CEP164 mutations, linking renal ciliopathies to DNA damage response signaling. *Cell*. **150**, 533-548.
- Chan, S.W., Lim, C.J., Guo, K., Ng, C.P., Lee, I., Hunziker, W., Zeng, Q., Hong, W., 2008. A Role for TAZ in Migration, Invasion, and Tumorigenesis of Breast Cancer Cells. *Cancer Research*. **68**, 2592-2598.

- Choi, H.J.C., Lin, J., Vannier, J., Slaats, G.G., Kile, A.C., Paulsen, R.D., Manning, D.K., Beier, D.R., Giles, R.H., Boulton, S.J., Cimprich, K.A., 2013. NEK8 links the ATR-regulated replication stress response and S phase CDK activity to renal ciliopathies. *Molecular Cell*. **51**, 423.
- Christopher Belham, Joan Roig, Jennifer A. Caldwell, Yumi Aoyama, Bruce E. Kemp, Michael Comb, Joseph Avruch, 2003. A Mitotic Cascade of NIMA Family Kinases. *Journal of Biological Chemistry*. **278**, 34897.
- Ciccia, A. & Elledge, S.J., 2010. The DNA Damage Response: Making It Safe to Play with Knives. *Molecular Cell*. **40**, 179-204.
- Claude, P., 2008. Cdk1, Plks, Auroras, and Neks: The Mitotic Bodyguards. *Hormonal Carcinogenesis V*. New York, NY: Springer New York. 41-56.
- Cortez, D. & Cimprich, K.A., 2008. ATR: an essential regulator of genome integrity. *Nature Reviews Molecular Cell Biology*. **9**, 616-627.
- Cosetta Bertoli, Jan M Skotheim, Robertus A M De Bruin, 2013. Control of cell cycle transcription during G1 and S phases. *Nature Reviews. Molecular Cell Biology*. **14**, 518.
- Covell, J., Meyer, S. and Montgomery, B., 2006. *Genzyme Corporation*. [e-book].
- Dalgaard, J.Z., 2012. Causes and consequences of ribonucleotide incorporation into nuclear DNA. *Trends in Genetics : TIG*. **28**, 592-597.
- Davis, S.W., Ellsworth, B.S., Pérez Millan, M.I., Gergics, P., Schade, V., Foyouzi, N., Brinkmeier, M.L., Mortensen, A.H., Camper, S.A., 2013. Pituitary gland development and disease: from stem cell to hormone production. *Current Topics in Developmental Biology*. **106**, 1.
- De Souza, C.P.C., Osmani, A.H., Osmani, S.A., Wu, L., Spotts, J.L., 2000. Mitotic Histone H3 Phosphorylation by the NIMA Kinase in *Aspergillus nidulans*. *Cell*. **102**, 293-302.
- Deane, J.A., Cole, D.G., Seeley, E.S., Diener, D.R., Rosenbaum, J.L., 2001. Localization of intraflagellar transport protein IFT52 identifies basal body transitional fibers as the docking site for IFT particles. *Current Biology*. **11**, 1586-1590.
- Debec, A., Sullivan, W., Bettencourt-Dias, M., 2010. Centrioles: active players or passengers during mitosis? *Cellular and Molecular Life Sciences*. **67**, 2173-2194.
- Eggenchwiler, J.T. & Anderson, K.V., 2007. Cilia and Developmental Signaling. *Annual Review of Cell and Developmental Biology*. **23**, 345-373.
- Ellison, V. & Stillman, B., 2003. Biochemical characterization of DNA damage checkpoint complexes: clamp loader and clamp complexes with specificity for 5' recessed DNA. *PLoS Biology*. **1**, E33.
- Faragher, A.J. & Fry, A.M., 2003. Nek2A kinase stimulates centrosome disjunction and is required for formation of bipolar mitotic spindles. *Molecular Biology of the Cell*. **14**, 2876-2889.
- Field, S., Riley, K., Grimes, D.T., Hilton, H., Simon, M., Powles-Glover, N., Siggers, P., Bogani, D., Greenfield, A., Norris, D.P., 2011. Pkd1l1 establishes left-right asymmetry and physically interacts with Pkd2. *Development (Cambridge, England)*. **138**, 1131-1142.
- Follit, J.A., Tuft, R.A., Fogarty, K.E., Pazour, G.J., 2006. The Intraflagellar Transport Protein IFT20 Is Associated with the Golgi Complex and Is Required for Cilia Assembly. *Molecular Biology of the Cell*. **17**, 3781-3792.

Fong, C.S., Kim, M., Yang, T.T., Liao, J., Tsou, M.B., 2014. SAS-6 assembly templated by the lumen of cartwheel-less centrioles precedes centriole duplication. *Developmental Cell*. **30**, 238-245.

for preventing cancer, 2001. Genome maintenance mechanisms.

Fry, A.M., O'Regan, L., Sabir, S.R., Bayliss, R., 2012. Cell cycle regulation by the NEK family of protein kinases. *Journal of Cell Science*. **125**, 4423-4433.

Fu, J., Hagan, I.M., Glover, D.M., 2015. The centrosome and its duplication cycle. *Cold Spring Harbor Perspectives in Biology*. **7**, a015800.

Fukui, H., Shiba, D., Asakawa, K., Kawakami, K., Yokoyama, T., 2012. The ciliary protein Nek8/Nphp9 acts downstream of Inv/Nphp2 during pronephros morphogenesis and left-right establishment in zebrafish. *FEBS Letters*. **586**, 2273-2279.

Gemma Bridge, Sukaina Rashid and Sarah A Martin, 2014. DNA Mismatch Repair and Oxidative DNA Damage: Implications for Cancer Biology and Treatment. Basel: MDPI AG.

Germino, G.G., 2005. Linking cilia to Wnts. *Nature Genetics*. **37**, 455-457.

Gesteland, *et al*, FRONTIERS.

Glover, D.M. & Bettencourt-Dias, M., 2007. Centrosome biogenesis and function: centrosomics brings new understanding. *Nature Reviews Molecular Cell Biology*. **8**, 451-463.

Grallert, A. & Hagan, I.M., 2002. Schizosaccharomyces pombe NIMA-related kinase, Fin1, regulates spindle formation and an affinity of Polo for the SPB. *The EMBO Journal*. **21**, 3096-3107.

Grallert, A., Krapp, A., Bagley, S., Simanis, V., Hagan, I.M., 2004. Recruitment of NIMA kinase shows that maturation of the S. pombe spindle-pole body occurs over consecutive cell cycles and reveals a role for NIMA in modulating SIN activity. *Genes & Development*. **18**, 1007-1021.

Gregory J. Pazour, Sheila A. Baker, James A. Deane, Douglas G. Cole, Bethany L. Dickert, Joel L. Rosenbaum, George B. Witman, Joseph C. Besharse, 2002. The Intraflagellar Transport Protein, IFT88, Is Essential for Vertebrate Photoreceptor Assembly and Maintenance. *The Journal of Cell Biology*. **157**, 103-113.

Habbig, S., Bartram, M.P., Saegmueller, J.G., Griessmann, A., Franke, M., Mueller, R., Schwarz, R., Hoehne, M., Bergmann, C., Tessmer, C., Reinhardt, H., Burst, V., Benzing, T., Schermer, B., 2012. The ciliopathy disease protein NPHP9 promotes nuclear delivery and activation of the oncogenic transcriptional regulator TAZ. *Human Molecular Genetics*. **21**, 5528-5538.

Halfdan Beck, Viola Nähse-Kumpf, Marie Sofie Yoo Larsen, Karen A. O'Hanlon, Sebastian Patzke, Christian Holmberg, Jakob Mejlvang, Anja Groth, Olaf Nielsen, Randi G. Syljuåsen, Claus Storgaard Sørensen, 2012. Cyclin-Dependent Kinase Suppression by WEE1 Kinase Protects the Genome through Control of Replication Initiation and Nucleotide Consumption. *Molecular and Cellular Biology*. **32**, 4226-4236.

Hammerschmidt, M., Bitgood, M.J., McMahon, A.P., 1996. Protein kinase A is a common negative regulator of Hedgehog signaling in the vertebrate embryo. *Genes & Development*. **10**, 647-658.

Harper, J.W. & Elledge, S.J., 2007. The DNA Damage Response: Ten Years After. *Molecular Cell*. **28**, 739-745.

- Harrington, K.M. & Clevenger, C.V., 2016. Identification of NEK3 Kinase Threonine 165 as a Novel Regulatory Phosphorylation Site That Modulates Focal Adhesion Remodeling Necessary for Breast Cancer Cell Migration. *Journal of Biological Chemistry*. **291**, 21388-21406.
- Haycraft, C.J., Banizs, B., Aydin-Son, Y., Zhang, Q., Michaud, E.J., Yoder, B.K., 2005. Gli2 and Gli3 localize to cilia and require the intraflagellar transport protein polaris for processing and function. *PLoS Genetics*. **1**, e53.
- Hildebrandt, F., 2007. Nephronophthisis-associated ciliopathies. *J Am Soc Nephrol*. **18**, 1855-1871.
- Hildebrandt, F., Benzing, T., Katsanis, N., 2011. Ciliopathies. *The New England Journal of Medicine*. **364**, 1533-1543.
- Hildebrandt, F., Strahm, B., Nothwang, H., Gretz, N., Schnieders, B., Singh-Sawhney, I., Kutt, R., Vollmer, M., Brandis, M., Members of the APN Study Group, 1997. Molecular genetic identification of families with juvenile nephronophthisis type 1: Rate of progression to renal failure. *Kidney International*. **51**, 261-269.
- Hwang, H.C. & Clurman, B.E., 2005. Cyclin E in normal and neoplastic cell cycles. *Oncogene*. **24**, 2776-2786.
- Ishikawa, H. & Marshall, W.F., 2011. Ciliogenesis: building the cell's antenna. *Nature Reviews Molecular Cell Biology*. **12**, 222-234.
- Jackson, P.K., 2013. Nek8 couples renal ciliopathies to DNA damage and checkpoint control. *Molecular Cell*. **51**, 407.
- Jing Zhou, 2009. Polycystins and Primary Cilia: Primers for Cell Cycle Progression. *Annual Review of Physiology*. **71**, 83-113.
- Jirina Bartkova, Jiri Bartek, Jiri Lukas, 2007. DNA Damage Response as an Anti-Cancer Barrier: Damage Threshold and the Concept of 'Conditional Haploinsufficiency'. *Cell Cycle*. **6**, 2344-2347.
- Johnson, L.N., 2009. The regulation of protein phosphorylation. *Biochemical Society Transactions*. **37**, 627.
- Jonathan T. Lester & Neal A. DeLuca, 2011. Herpes Simplex Virus 1 ICP4 Forms Complexes with TFIID and Mediator in Virus-Infected Cells. *Journal of Virology*. **85**, 5733-5744.
- Jossen, R. & Bermejo, R., 2013. The DNA damage checkpoint response to replication stress: A Game of Forks. *Frontiers in Genetics*. **4**, 26.
- Kastan, M.B. & Bartek, J., 2004. Cell-cycle checkpoints and cancer. *Nature*. **432**, 316-323.
- Kenna, K.P., van Doormaal, Perry T C, Dekker, A.M., Ticozzi, N., Kenna, B.J., Diekstra, F.P., van Rheenen, W., van Eijk, K.R., Jones, A.R., Keagle, P., Shatunov, A., Sproviero, W., Smith, B.N., van Es, M.A., Topp, S.D., Kenna, A., Miller, J.W., Fallini, C., Tiloca, C., McLaughlin, R.L., Vance, C., Troakes, C., Colombrita, C., Mora, G., Calvo, A., Verde, F., Al-Sarraj, S., King, A., Calini, D., de Belleruche, J., Baas, F., van der Kooi, Anneke J, de Visser, M., ten Asbroek, Anneloor L M A, Sapp, P.C., McKenna-Yasek, D., Polak, M., Asress, S., Muñoz-Blanco, J.L., Strom, T.M., Meitinger, T., Morrison, K.E., Lauria, G., Williams, K.L., Leigh, P.N., Nicholson, G.A., Blair, I.P., Leblond, C.S., Dion, P.A., Rouleau, G.A., Pall, H., Shaw, P.J., Turner, M.R., Talbot, K., Taroni, F., Boylan, K.B., van Blitterswijk, M., Rademakers, R., Esteban-Pérez, J., García-Redondo, A., van Damme, P., Robberecht, W., Chio, A., Gellera, C., pper, C., Sendtner, M., Ratti, A., Glass, J.D., Mora, J.S., Basak, N.A., Hardiman, O., Ludolph, A.C., Andersen, P.M., Weishaupt, J.H., Brown,

- R.H., Al-Chalabi, A., Silani, V., Shaw, C.E., van den Berg, Leonard H, Veldink, J.H., Landers, J.E., D'alfonso, S., Mazzini, L., Comi, G.P., del Bo, R., Ceroni, M., Gagliardi, S., Querin, G., Bertolin, C., Pensato, V., Castellotti, B., Corti, S., Cereda, C., Corrado, L., Sorarù, G., 2016. NEK1 variants confer susceptibility to amyotrophic lateral sclerosis. *Nature Genetics*. **48**, 1037-1042.
- Kim, I., 2008. Fibrocystin/polyductin modulates renal tubular formation by regulating polycystin-2 expression and function. *J Am Soc Nephrol*. **19**, 455-468.
- Krien, M.J., Bugg, S.J., Palatsides, M., Asouline, G., Morimyo, M., O'Connell, M.J., 1998. A NIMA homologue promotes chromatin condensation in fission yeast. *Journal of Cell Science*. **111**, 967.
- Kumagai, A., Lee, J., Yoo, H.Y., Dunphy, W.G., 2006. TopBP1 Activates the ATR-ATRIP Complex. *Cell*. **124**, 943-955.
- Kurioka, D., Takeshita, F., Tsuta, K., Sakamoto, H., Watanabe, S., NEK9-dependant proliferation of cancer cells lacking functional p53 . *Open*.
- L Connell-Crowley, M J Solomon, N Wei, J W Harper, 1993. Phosphorylation independent activation of human cyclin-dependent kinase 2 by cyclin A in vitro. *Molecular Biology of the Cell*. **4**, 79-92.
- Lambert, S. & Carr, A., 2013. Impediments to replication fork movement: stabilisation, reactivation and genome instability. *Chromosoma*. **122**, 33-45.
- Lee Zou, Dou Liu, Stephen J. Elledge, 2003. Replication Protein A-Mediated Recruitment and Activation of Rad17 Complexes. *Proceedings of the National Academy of Sciences of the United States of America*. **100**, 13827-13832.
- Levinsohn, J., Sugarman, J., McNiff, J., Antaya, R., Choate, K., 2016. Somatic Mutations in NEK9 Cause Nevus Comedonicus. *The American Journal of Human Genetics*. **98**, 1030-1037.
- Li, G., Zhong, Y., Shen, Q., Zhou, Y., Deng, X., Li, C., Chen, J., Zhou, Y., He, M., 2017. NEK2 serves as a prognostic biomarker for hepatocellular carcinoma. *International Journal of Oncology*. **50**, 405-413.
- Lienkamp, S., Ganner, A., Walz, G., 2012. Inversin, Wnt signaling and primary cilia. *Differentiation*. **83**, S55.
- Lim, S. & Kaldis, P., 2013. Cdks, cyclins and CKIs: roles beyond cell cycle regulation. *Development (Cambridge, England)*. **140**, 3079-3093.
- Liskiewicz, T., 2015. Methods. *Anti-Corrosion Methods and Materials*. **62**, .
- LIU, X., GAO, Y., LU, Y., ZHANG, J., LI, L., YIN, F., 2014. Downregulation of NEK11 is associated with drug resistance in ovarian cancer. *International Journal of Oncology*. **45**, 1266-1274.
- Liyun Sang, *et al*, 2011. Mapping the Nephronophthisis-Joubert-Meckel-Gruber Protein Network Reveals Ciliopathy Disease Genes and Pathways.
- Mahjoub, M.R., Trapp, M.L., Quarmby, L.M., 2005. NIMA-related kinases defective in murine models of polycystic kidney diseases localize to primary cilia and centrosomes. *Journal of the American Society of Nephrology : JASN*. **16**, 3485-3489.
- Malumbres, M. & Barbacid, M., 2005. Mammalian cyclin-dependent kinases. *Trends in Biochemical Sciences*. **30**, 630-641.

- Manning, D.K., Sergeev, M., van Heesbeen, R.G., Wong, M.D., Oh, J., Liu, Y., Henkelman, R.M., Drummond, I., Shah, J.V., Beier, D.R., 2013. Loss of the ciliary kinase Nek8 causes left-right asymmetry defects. *Journal of the American Society of Nephrology : JASN*. **24**, 100-112.
- Marshall, W.F. & Nonaka, S., 2006. Cilia: Tuning in to the Cell's Antenna. *Current Biology*. **16**, R614.
- Masahide Kikkawa, Takashi Ishikawa, Takao Nakata, Takeyuki Wakabayashi, Nobutaka Hirokawa, 1994. Direct Visualization of the Microtubule Lattice Seam Both in vitro and in vivo. *The Journal of Cell Biology*. **127**, 1965-1971.
- Mayor, T., *et al*, 1999. Protein kinases in control of the centrosome cycle. NETHERLANDS: Elsevier B.V.
- McMurray, C.T., 2010. Mechanisms of trinucleotide repeat instability during human development. *Nature Reviews Genetics*. **11**, 786-799.
- Michelle K Zeman & Karlene A Cimprich, 2014. Causes and consequences of replication stress. *Nature Cell Biology*. **16**, 2-9.
- Miller, S.L., Antico, G., Raghunath, P.N., Tomaszewski, J.E., Clevenger, C.V., 2007. Nek3 kinase regulates prolactin-mediated cytoskeletal reorganization and motility of breast cancer cells. *Oncogene*. **26**, 4668-4678.
- Monroe, G.R., Kappen, I.F., Stokman, M.F., Terhal, P.A., van den Boogaard, Marie-José H, Savelberg, S.M., van der Veken, Lars T, van Es, Robert J J, Lens, S.M., Hengeveld, R.C., Creton, M.A., Janssen, N.G., Mink van der Molen, Aebele B, Ebbeling, M.B., Giles, R.H., Knoers, N.V., van Haaften, G., 2016. Compound heterozygous NEK1 variants in two siblings with oral-facial-digital syndrome type II (Mohr syndrome). *European Journal of Human Genetics*. **24**, 1760.
- Mordes, D.A. & Cortez, D., 2008. Activation of ATR and related PIKKs. *Cell Cycle*. **7**, 2809-2812.
- Morgan, D., Goodship, J., Essner, J., Vogan, K., Turnpenny, L., Yost, J., Tabin, C., Strachan, T., 2002. The left-right determinant inversin has highly conserved ankyrin repeat and IQ domains and interacts with calmodulin. *Human Genetics*. **110**, 377-384.
- Nigg, E.A., 2001. Mitotic kinases as regulators of cell division and its checkpoints. *Nature Reviews Molecular Cell Biology*. **2**, 21-32.
- Nurnberger, J., Bacallao, R.L., Phillips, C.L., 2002. Inversin Forms a Complex with Catenins and N-Cadherin in Polarized Epithelial Cells. *Molecular Biology of the Cell*. **13**, 3096-3106.
- Nürnberg, J., Kribben, A., Opazo Saez, A., Heusch, G., Philipp, T., Phillips, C.L., 2004. The Invs gene encodes a microtubule-associated protein. *Journal of the American Society of Nephrology : JASN*. **15**, 1700-1710.
- Nyberg, K.A., Michelson, R.J., Putnam, C.W., Weinert, T.A., 2002. TOWARD MAINTAINING THE GENOME: DNA Damage and Replication Checkpoints. *Annual Review of Genetics*. **36**, 617-656.
- Ogi, T., Walker, S., Stiff, T., Hobson, E., Limsirichaikul, S., Carpenter, G., Prescott, K., Suri, M., Jeggo, P.A., 2012. Identification of the First ATRIP-Deficient Patient and Novel Mutations in ATR Define a Clinical Spectrum for ATR-ATRIP Seckel Syndrome. *PLoS Genetics*. **8**, e1002945.
- Ong, A.C.M. & Harris, P.C., 2015a. A polycystin-centric view of cyst formation and disease: the polycystins revisited. *Kidney International*. **88**, 699-710.

- Ong, A.C.M. & Harris, P.C., 2015b. A polycystin-centric view of cyst formation and disease: the polycystins revisited. *Kidney International*. **88**, 699-710.
- O'regan, L., Blot, J., Fry, A.M., 2007. Mitotic regulation by NIMA-related kinases. *Cell Division*. **2**, 25.
- Osborn, A.J., Elledge, S.J. and Zou, L., 2002. Checking on the fork: the DNA-replication stress-response pathway. England: Elsevier Ltd.
- Osmani, A.H., McGuire, S.L., Osmani, S.A., 1991. Parallel activation of the NIMA and p34cdc2 cell cycle-regulated protein kinases is required to initiate mitosis in *A. nidulans*. *Cell*. **67**, 283-291.
- Osmani, S.A., Pu, R.T., Morris, N.R., 1988. Mitotic induction and maintenance by overexpression of a G2-specific gene that encodes a potential protein kinase. *Cell*. **53**, 237-244.
- Otto, E.A., 2008. NEK8 mutations affect ciliary and centrosomal localization and may cause nephronophthisis. *J Am Soc Nephrol*. **19**, 587-592.
- Pamela M. Holland, Alison Milne, Kirsten Garka, Richard S. Johnson, Cynthia Willis, John E. Sims, Charles T. Rauch, Timothy A. Bird, G. Duke Virca, 2002. Purification, Cloning, and Characterization of Nek8, a Novel NIMA-related Kinase, and Its Candidate Substrate Bicd2. *Journal of Biological Chemistry*. **277**, 16229-16240.
- Pan, D., 2010. The Hippo Signaling Pathway in Development and Cancer. *Developmental Cell*. **19**, 491-505.
- Parplys, A.C., Seelbach, J.I., Becker, S., Behr, M., Wrona, A., Jend, C., Mansour, W.Y., Joosse, S.A., Stuerzbecher, H., Pospiech, H., Petersen, C., Dikomey, E., Borgmann, K., 2015. High levels of RAD51 perturb DNA replication elongation and cause unscheduled origin firing due to impaired CHK1 activation. *Cell Cycle*. **14**, 3190-3202.
- Paulovich, A.G. & Hartwell, L.H., 1995. A checkpoint regulates the rate of progression through S phase in *S. cerevisiae* in Response to DNA damage. *Cell*. **82**, 841-847.
- Pedersen, L.B. & Rosenbaum, J.L., 2008. Intraflagellar transport (IFT) role in ciliary assembly, resorption and signalling. *Current Topics in Developmental Biology*. **85**, 23.
- Pennekamp, P., Karcher, C., Fischer, A., Schweickert, A., Skryabin, B., Horst, J., Blum, M., Dworniczak, B., 2002. The Ion Channel Polycystin-2 Is Required for Left-Right Axis Determination in Mice. *Current Biology*. **12**, 938-943.
- Peter Rellos, Frank J. Ivins, Joanne E. Baxter, Ashley Pike, Timothy J. Nott, Donna-Marie Parkinson, Sanjan Das, Steven Howell, Oleg Fedorov, Qi Yu Shen, Andrew M. Fry, Stefan Knapp, Stephen J. Smerdon, 2007. Structure and Regulation of the Human Nek2 Centrosomal Kinase. *Journal of Biological Chemistry*. **282**, 6833-6842.
- Reiter, J.F., Blacque, O.E., Leroux, M.R., 2012. The base of the cilium: roles for transition fibres and the transition zone in ciliary formation, maintenance and compartmentalization. *EMBO Reports*. **13**, 608-618.
- Roig, J., Mikhailov, A., Belham, C., Avruch, J., 2002. Nercc1, a mammalian NIMA-family kinase, binds the Ran GTPase and regulates mitotic progression. *Genes & Development*. **16**, 1640-1658.
- Ronquillo, C.C., Bernstein, P.S., Baehr, W., 2012. Senior-Løken syndrome: a syndromic form of retinal dystrophy associated with nephronophthisis. *Vision Research*. **75**, 88-97.

- Sabir, S.R., Sahota, N.K., Jones, G.D.D., Fry, A.M., 2015. Loss of Nek11 Prevents G2/M Arrest and Promotes Cell Death in HCT116 Colorectal Cancer Cells Exposed to Therapeutic DNA Damaging Agents. *PLoS One*. **10**, e0140975.
- Saitoh, S., 2001. Ocular motor apraxia, Cogan congenital type. *Ryōkibetsu Shōkōgun Shirizu*. 334.
- Salaün, P., Rannou, Y., & Prigent, C., 2008. Cdk1, Plks, Auroras, and Neks: the mitotic bodyguards. *Advances in Experimental Medicine and Biology*, 617, 41–56.
- Scholey, J.M., 2003. INTRAFLAGELLAR TRANSPORT. *Annual Review of Cell and Developmental Biology*. **19**, 423-443.
- Scott, M.P. & Rohatgi, R., 2007. Patching the gaps in Hedgehog signalling. *Nature Cell Biology*. **9**, 1005-1009.
- Sergei Sorokin, 1962. Centrioles and the Formation of Rudimentary Cilia by Fibroblasts and Smooth Muscle Cells. *The Journal of Cell Biology*. **15**, 363-377.
- Shanming Liu, Weining Lu, Tomoko Obara, Shiei Kuida, Jennifer Lehoczky, Ken Dewar, Iain A. Drummond, David R. Beier, 2002. A defect in a novel Nek-family kinase causes cystic kidney disease in the mouse and in zebrafish. *Development*. **129**, 5839-5846.
- Shen, C., Pharoah, P.D.P., Ribas, G., Schmidt, M.K., Chang-Claude, J., Bhatti, P., Vatten, L.J., Bojesen, S., Fletcher, O., Schutte, M., Milne, R.L., Sigurdson, A., Stratton, M.R., Beesley, J., Olson, J.E., Rahman, N., Mannermaa, A., dos Santos Silva, I., Antonenkova, N.N., McCarty, C.A., Broeks, A., Calle, E.E., Rajkovic, A., Kataja, V., Benitez, J., Karstens, J.H., Humphreys, M.K., Smith, L., Wang-Gohrke, S., Ghousaini, M., Doody, M., Prentice, R., González-Neira, A., Reed, M.W.R., Chanock, S.J., Bartram, C.R., Hein, R., Pooley, K.A., Bermisheva, M., Liu, J., Healey, C.S., Dunning, A.M., Chen, S., Devilee, P., Giles, G.G., Fredericksen, Z., Peplonska, B., Kraft, P., Kumle, M., Southey, M.C., Ahn, S., Andrulis, I.L., Brinton, L., Noh, D.Y., Hveem, K., Luben, R., Kang, D., Wang, X., Kosma, V., Blomqvist, C., Fedorova, S., Hopper, J.L., Curb, J.D., Ahmed, S., Hamann, U., Berg, C.D., Yoo, K., Aittomäki, K., Eccles, D., Hunter, D.J., Burwinkel, B., Hankinson, S.E., Schürmann, P., Khusnutdinova, E., van den Ouweland, Ans M W, Chenevix-Trench, G., Goode, E.L., Cox, D.G., Dörk, T., Maranian, M., Meindl, A., Yu, J., Thomas, G., Lissowska, J., Nevanlinna, H., Morrison, J., Schmutzler, R.K., Anderson, G.L., Baglietto, L., Hooning, M.J., Margolin, S., Justenhoven, C., Cox, A., Czene, K., Garcia-Closas, M., Alexander, B.H., Platte, R., Elliott, G., Hsu, G., Knight, J.A., ..., 2009. Newly discovered breast cancer susceptibility loci on 3p24 and 17q23.2. *Nature Genetics*. **41**, 585-590.
- Shiba, D., Manning, D.K., Koga, H., Beier, D.R., Yokoyama, T., 2010. Inv acts as a molecular anchor for Nphp3 and Nek8 in the proximal segment of primary cilia. *Cytoskeleton (Hoboken, N.J.)*. **67**, NA.
- Shiba, D., Yamaoka, Y., Hagiwara, H., Takamatsu, T., Hamada, H., Yokoyama, T., 2009. Localization of Inv in a distinctive intraciliary compartment requires the C-terminal ninein-homolog-containing region. *Journal of Cell Science*. **122**, 44-54.
- Siew Wee Chan, Chun Jye Lim, Li Shen Loo, Yaan Fun Chong, Caixia Huang, Wanjin Hong, 2009. TEADs Mediate Nuclear Retention of TAZ to Promote Oncogenic Transformation. *Journal of Biological Chemistry*. **284**, 14347-14358.
- Singla, V., Norman, A.R., Reiter, J.F., Aanstad, P., Corbit, K.C., Stainier, D.Y.R., 2005. Vertebrate Smoothed functions at the primary cilium. *Nature*. **437**, 1018-1021.

- Singla, V. & Reiter, J.F., 2006. The Primary Cilium as the Cell's Antenna: Signaling at a Sensory Organelle. *Science*. **313**, 629-633.
- Sivasubramaniam, S., Sun, X., Pan, Y., Wang, S., Lee, E.Y.P., 2008. Cep164 is a mediator protein required for the maintenance of genomic stability through modulation of MDC1, RPA, and CHK1. *Genes & Development*. **22**, 587-600.
- Smith, E.F. & Yang, P., 2004. The radial spokes and central apparatus: Mechano-chemical transducers that regulate flagellar motility. *Cell Motility and the Cytoskeleton*. **57**, 8-17.
- Sohara, E., 2008. Nek8 regulates the expression and localization of polycystin-1 and polycystin-2. *J Am Soc Nephrol*. **19**, 469-476.
- Spencer, M., Detwiler, P.B., Bunt-Milam, A.H., 1988. Distribution of membrane proteins in mechanically dissociated retinal rods. *Investigative Ophthalmology & Visual Science*. **29**, 1012.
- Varelas, X. & Wrana, J.L., 2012. Coordinating developmental signaling: novel roles for the Hippo pathway. *Trends in Cell Biology*. **22**, 88-96.
- Vogelstein, B. & Kinzler, K.W., 2004. Cancer genes and the pathways they control. *Nature Medicine*. **10**, 789-799.
- Wallace F. Marshall & Joel L. Rosenbaum, 2001. Intraflagellar Transport Balances Continuous Turnover of Outer Doublet Microtubules: Implications for Flagellar Length Control. *The Journal of Cell Biology*. **155**, 405-414.
- Walz, G. & Kim, E., 2007. Sensitive cilia set up the kidney. *Nature Medicine*. **13**, 1409-1411.
- Wang, Z., Horemuzova, E., Iida, A., Guo, L., Liu, Y., Matsumoto, N., Nishimura, G., Nordgren, A., Miyake, N., Tham, E., Grigelioniene, G., Ikegawa, S., 2017. Axial spondylometaphyseal dysplasia is also caused by NEK1 mutations. *Journal of Human Genetics*. **62**, 503.
- Wogan, G.N., Hecht, S.S., Felton, J.S., Conney, A.H., Loeb, L.A., 2004. Environmental and chemical carcinogenesis. *Seminars in Cancer Biology*. **14**, 473-486.
- Wolf, M.T.F., 2015. Nephronophthisis and related syndromes. *Current Opinion in Pediatrics*. **27**, 201.
- Wu, L., Osmani, S.A., Mirabito, P.M., 1998. A Role for NIMA in the Nuclear Localization of Cyclin B in *Aspergillus nidulans*. *The Journal of Cell Biology*. **141**, 1575-1587.
- Yang, J., Adamian, M., Li, T., 2006. Rootletin Interacts with C-Nap1 and May Function as a Physical Linker between the Pair of Centrioles/Basal Bodies in Cells. *Molecular Biology of the Cell*. **17**, 1033-1040.
- Yang, Y., Keeler, C., Kuo, I.Y., Lolis, E.J., Ehrlich, B.E., Hodsdon, M.E., 2015. Oligomerization of the polycystin-2 C-terminal tail and effects on its Ca²⁺-binding properties. *The Journal of Biological Chemistry*. **290**, 10544-10554.
- Yoder, B.K. & Davenport, J.R., 2005. An incredible decade for the primary cilium: a look at a once-forgotten organelle. *The American Journal of Physiology*. **289**, F1159.
- Zalli, D., Bayliss, R., Fry, A.M., 2012. The Nek8 protein kinase, mutated in the human cystic kidney disease nephronophthisis, is both activated and degraded during ciliogenesis. *Human Molecular Genetics*. **21**, 1155-1171.
- Zegerman, P. & Diffley, J.F.X., 2010. Checkpoint-dependent inhibition of DNA replication initiation by Sld3 and Dbf4 phosphorylation. *Nature*. **467**, 474-478.

- Zhou, B.S. & Elledge, S.J., 2000. The DNA damage response: putting checkpoints in perspective. *Nature*. **408**, 433-439.
- Zhou, Z., Hao, Y., Liu, N., Raptis, L., Tsao, M., Yang, X., 2011. TAZ is a novel oncogene in non-small cell lung cancer. *Oncogene*. **30**, 2181-2186.
- Zhou, W., Otto, E.A, Cluckey, A., Airik, R., Hurd, T.W., Chaki, M., Diaz, K., Lach, F.P., Hildebrandt, 2012. FAN1 mutations cause karyomegalic interstitial nephritis, linking chronic kidney failure to defective DNA damage repair. *Nature Genetics*. **44**, 910.